TOWARDS THE SYNTHESIS OF MODEL PEROXIDASES

Thesis submitted in accordance with the requirements of the University of Liverpool for the degree of Doctor in Philosophy by Jorge Manuel Tavares Branco Varejão

November 2000

To my family

ACKNOWLEDGEMENTS

I wish to express my sincere acknowledgement to:

Prof. R. A. W. Johnstone for his kind invitation to do a PhD degree at The University of Liverpool and for all guidance, help and support given in the different steps of this work.

To Prof. A. M. d'A. Rocha Gonsalves of the University of Coimbra (Portugal) for the help and support given at the Organic Chemistry Laboratory of The University of Coimbra, where some of the compounds described in the present work were prepared.

To Prof. Maria da Conceição Cruz Costa of Escola Superior Agrária de Coimbra for the incentive and enthusiasm that always had given to the realisation of this work. Without them, this work would never have been realised.

To all staff of The Department of Chemistry of the University of Liverpool for their kindness and effort in the analytical characterisation of the compounds prepared in this work.

To "Junta Nacional de Investigação Científica e Tecnológica" (JNICT, now "Fundação para a Ciência e Tecnologia", FCT, Portugal) for the financial support (DB/2853/93-RM).

TOWARDS THE SYNTHESIS OF MODEL PEROXIDASES

Abstract

Peroxidases are an important class of haem containing enzymes, involved in natural biosynthesis of compounds such as lignin. In this work, a synthetic peroxidase model, formed by association of amphiphilic polymers such as co-poly(4-styrenesulphonic acid, sodium salt; 2-vinylnaphthalene; PSSS-VN) and metalloporphyrins was studied. The polymers form, when dissolved in water, hydrophobic microdomains that are able to "dissolve" hydrophobic molecules. If a metalloporphyrin is added to a amphiphilic polymer solution, it is inserted in the polymer microdomains, forming a rugged model "enzyme". These systems were assayed for peroxidase-like activity using 2,2'-azino-*bis*(3-ethylbenzthiazoline-6-sulfonic acid) (ABTS) as substrate and hydrogen peroxide as oxygen donor in phosphate buffer solutions. Different types of polymers were prepared having phenyl, naphthyl and anthranyl units as the hydrophobic group and different metalloporphyrins were assayed in searching for a system showing higher peroxidase-like activity. Assay of other heterogeneous systems, based on Merrifield and Chitin resins, was further carried out. The incorporation in the reaction medium of nitrogen bases was tested to check for activity increase. Use of iron(III) *tetrakis*(2,6-dichlorophenyl)porphyrin (FeTDCPP) on PSSS-VN polymers in the presence of added exogenous 2-methylimidazole resulted in the gain of the highest peroxidase-like activity.

The results obtained in the above systems, where a metalloporphyrin should be in a close position to the microdomain "wall" naphthyl rings, led to the synthetic preparation of porphyrin ligands having an aromatic ring (tolyl, naphthyl and anthranyl) in a close proximity of the porphyrin macrocycle. An example of such compound is 5-(2-[2-oxycarbonylnaphthalene]-phenyl)-10,15,20-*tris*-heptylporphyrin. Other compounds series substituted with two aromatic rings and both with *meso*-phenyl and *meso*-heptyl groups were prepared. These porphyrins revealed to adopt a folded conformation in chloroform solutions, in which the aromatic ring stays in a close position to porphyrin. This result was evident from ^{1}H NMR studies, where some of the protons of the aromatic rings suffer a considerable upfield shift. The highest upfield shifts were obtained when the aromatic ring was the anthranyl group, and diminishes with naphthyl and further with tolyl groups, both on *meso*-heptyl and *meso*-phenyl substituted porphyrins. The metal complexes (Fe and Mn) of these

porphyrins were prepared and, at least from UV/visible spectra, the results suggests that they adopt a partially folded conformation.

When the metalloporphyrins substituted with aromatic rings were assayed in a modified peroxidase-like activity assay, the metalloporphyrins having one and two aromatic rings showed smaller activities relative to unsubstituted porphyrins. This effect was observed both in *meso*- heptyl and *meso*-phenyl porphyrins and both with ABTS and guaiacol as substrate. This apparently, makes that having aromatic rings close to the macrocyclic porphyrin is not a factor favouring the peroxidase-like activity of such compounds.

Most of the porphyrins prepared throughout this work were prepared by a modified Rothemund/Adler method, using nitrobenzene as a co-solvent in the reaction medium. This method gives generally better results than the classical methods and a study was made on finding the effects of nitroarene addition in the Rothemund reaction and in the oxidation of porphyrinogens to porphyrins. The results allowed a discussion relative to the reaction intermediates and the origin of chlorin. Nitroarenes were found to assist the oxidation of porphyrinogen and other reaction intermediates to porphyrins, by interfering with reducing reaction intermediates and oxygen to form superoxide, which is converted quickly in the acidic solvent to hydrogen peroxide. This specie was proved to form when nitroarenes are present in reaction medium and suggest that its presence led to better yields on porphyrin formation.

The low aerial stability of porphyrins such as 5-(2,6-dihydroxyphenyl)-10,15,20-*tris*-heptylporphyrin and 5-(2,6-dihydroxyphenyl)-10,15,20-*tris*-phenyl-porphyrin in dichloro-methane solutions was observed. It was possible to isolate and characterise by mass, ^{1}H NMR and visible spectroscopy one of the compounds formed and a proposal for its structure was made.

TABLE OF CONTENTS

PORPHYRIN NOMENCLATURE

In this Thesis, the basic porphyrin ring carbon atoms are numbered from 1 to 20 as shown below.

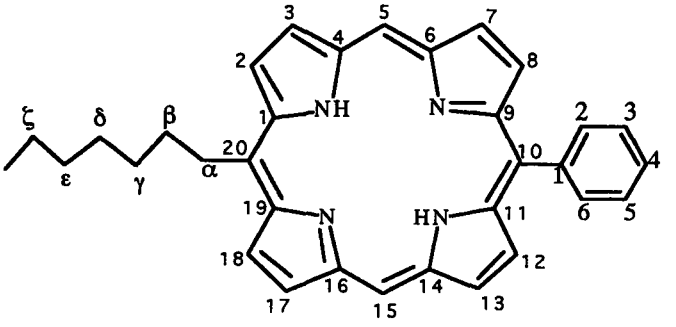

Occasionally, the pyrrolic positions 2,3,7,8,12,13,17 and 18 are called the β-pyrrolic positions and frequently, the 5, 10, 15 and 20 positions are called the *meso* positions. For the phenyl groups in 5,10,15,20-positions, the numbering of the carbons was made as showed. For the heptyl groups in the 5,10,15,20-positions, the carbon atoms were referred with the Greek alphabet letters as showed.

CHAPTER 1: INTRODUCTION

I. Introduction

1. Metalloporphyrins as successful natural enzyme active centres

Nature makes use of porphyrins as a metal ligand for building the active centre of a number of important enzymes, which consist of the metalloporphyrin itself and its accompanying apoprotein. In such enzymes, the metalloporphyrin structure is invariable, but the accompanying apoprotein has the required structural characteristics to promote selective activity. Remarkable examples are exemplified by haemoglobin, myoglobin, catalase, cytochrome P450 and peroxidases, which all have a common iron(III) complex of protoporphyrin IX in the active centre.[1] Such achievements by Nature have stimulated enormous interest in understanding the mechanisms of action of such versatility. The comprehension of their modes of action will certainly bring benefits in other fields, one such being the design of new efficient and powerful oxidation catalysts. This is one major reason for the growing number of research studies on porphyrins and related systems and in trying to mimic several types of enzymic activity.[2]

The research described here concerns the study of one enzyme, *viz.*, a peroxidase, so as to relate its structure and mode of action with improved simpler artificial systems that show similar peroxidase activity.

2. Peroxidases

Peroxidases (P) are found in all living organisms and are involved in essential aspects of their metabolism. Depending on the living organism, in which a peroxidase is found, so is their type or class assortment: Class I for animals, Class II for fungi and Class III for those found in higher plants. An example of their action includes involvement in biosynthesis and degradation of lignin,[3] an abundant natural polymer. The intervention of peroxidases in different important biosynthetic processes has been considered. Stress induced in plants by accumulation of transition metals as Al or Cd induces changes in isozymes profiles

that are correlated with xenobiotic activity.[4] Viruses disrupt peroxidase levels and modify normal isozyme patterns.[5] Plant injury has the same effect and this is thought to be related with defence through cell wall reinforcing by plants.[6] Organisms scrupulously control enzyme activity by having a complete set (complex) of different peroxidase enzymes, the so-called isozyme clusters. Peroxidases having special characteristics are expressed (activated) for action in particular situations.

2.1. Structures of peroxidases

The structural characteristics of peroxidases have been revealed by the contribution of a great number of authors, using a panoply of analytical techniques such as X-ray crystallography, NMR spectroscopy and so on. X-Ray crystal structures have been determined for the following peroxidases: Lignin peroxidase (Lip),[7] Manganese peroxidase (MnP)[8], Cytochrome C peroxidase (CcP)[9], *Arthromyces Ramosus* peroxidase (RAP)[10] and, recently, Horseradish peroxidase (HRP)[11]. Depending on the peroxidase, the apoprotein has a characteristic number of amino acids (for HRP, the polypeptidic chain consist of 308 amino acids), with sequences that can be surprisingly different. The apoprotein can be described as formed by two domains, in which different numbers of helical segments have been identified.[8] The apoprotein folding is such that it forms a crevice where the haem group (iron complex of protoporphyrin IX) resides. Other important structural characteristics include the presence of disulphide bridges (4 in LiP[7], 5 in MnP[8]) and the presence of co-ordinated Ca^{2+} ions (two in HRP, to which stabilising effects have been attributed[12]). Peroxidases are among the most stable enzymes and can withstand temperatures as high as 80°C.[12b] Peroxidases also exhibit several sites of glycosylation, which have been shown to make peroxidases more soluble in aqueous solutions.[13]

An important feature found in all known peroxidases is that some amino acids are systematically found in all structures, *i. e.*, they are highly conserved.[1] These particular amino acids have been found to be involved in essential steps of enzyme reactivity. Their location is near to that of haem. One of these amino acids is a histidine (in HRP it is His 170; see Figure 1) co-ordinated with haem iron(III) as a so-called *proximal* histidine. Close to this amino acid there is another, belonging to this group, an aspartic acid (in HRP it is Asp 242). On the other side of the haem there are two more amino acids with similar characteristics, *viz.*, a histidine and an arginine (in HRP they are His 42 and Arg 38; see Figure 1). These residues are not coordinated with the central iron (haem is *penta*coordinated) and are located slightly apart from haem (*distal* position). It is

thought that with others amino acids they form a channel accessible to H_2O_2 and to small alkyl hydroperoxides.[14] Monooxygenase activity showed by peroxidases suggests that small molecules, with appropriate shape, can also gain access to this region as, for example, with I^- and R_1SR_2.[1,15] But this region is essentially inaccessible to most substrates. Close to the haem there are several phenylalanine units (in Figure 1 some of these are shown). Their relevance will be discussed later.

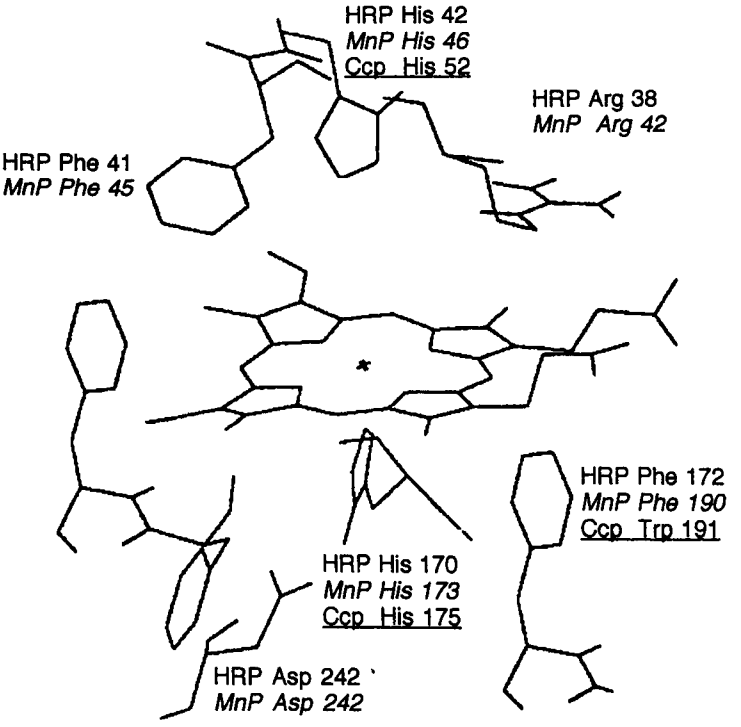

Figure 1. Picture showing the haem group and the highly conserved amino acids for HRP, *MnP* and CcP.

2.2. Peroxidase reactivity.

After activation with H_2O_2, peroxidases (P) catalyse two one-electron oxidations of substrate (S), as shown in reaction 1.

$$P + H_2O_2 + 2S \rightarrow P + 2H_2O + 2S\cdot \qquad (1)$$

An important feature of equation (1) is that, in peroxidases, there is *no* formal oxygen atom transfer. Depending on the peroxidase, the substrate (S) may be an aromatic molecule (such as a phenol or an aromatic amine as in HRP), a protein (as with Cytochrome C in CcP) or an ion or small molecule that can act as

a carrier of an oxidant equivalent (as with Mn^{2+} or veratryl alcohol in Manganese peroxidase). With particular substrates, peroxidases are able to catalyse monooxygenase oxidation, in which an oxygen atom from H_2O_2 is added to the substrate (S) to form an oxidised version (SO), as shown in reaction 2. This type of reactivity is more characteristic of enzymes of the cytochrome P450 family (see also Section 4, in this chapter).

$$P + H_2O_2 + S \rightarrow P + SO + H_2O \qquad (2)$$

2.3. Mechanism of peroxidative reaction[1]

The peroxidative reaction of HRP can be formulated in the following three steps, to give the overall reaction (3) shown below:

$$\begin{array}{ll} \text{(i)} & HRP + H_2O_2 \rightarrow HRP\text{-}I + H_2O \\ \text{(ii)} & HRP\text{-}I + SH \rightarrow HRP\text{-}II + S\cdot \\ \text{(iii)} & HRP\text{-}II + SH \rightarrow HRP + S\cdot + H_2O \\ \hline & HRP + H_2O_2 + 2\,SH \rightarrow HRP + 2\,S\cdot + 2\,H_2O \end{array} \qquad (3)$$

In step (i), oxidation of the ferric haem by H_2O_2 leads to an oxyferryl porphyrin complex, known as *Compound I.* Compound I is two oxidation units above the Fe(III) and is generally recognised as having a radical-cationic structure. Reaction of Compound I with a substrate converts it into *Compound II*, with release of a one-electron oxidised substrate. Subsequent reaction of Compound II with another substrate molecule regenerates peroxidase in its former (III) state and releases the second oxidised substrate molecule.

This reaction has been particularly well studied and most of its characteristics are known. The cycle is initiated (see Figure 2) by the access of H_2O_2 to the distal site of the peroxidase (Figure 2, a). Hydrogen bonding of Arg 38 is thought to be important in directing and conducting H_2O_2 to this position.[16] When H_2O_2 is close to the haem iron, histidine 42 plays an essential role, acting as an acid/base catalyst, by accepting a proton from H_2O_2 with the concomitant formation of an OOH^- anion. This hydroperoxide anion then coordinates with the haem iron, forming a transitory peroxo iron(III) complex (Figure 2, b and c). The O–O bond is cleaved rapidly in a heterolytic process, which is assisted by the proximal histidine (His170) and the distal His 42 and Arg 38. The protonated histidine releases its proton, probably through Arg 38 to a OOH oxygen,[10] to form water and Compound I (See Figure 2, d and e).

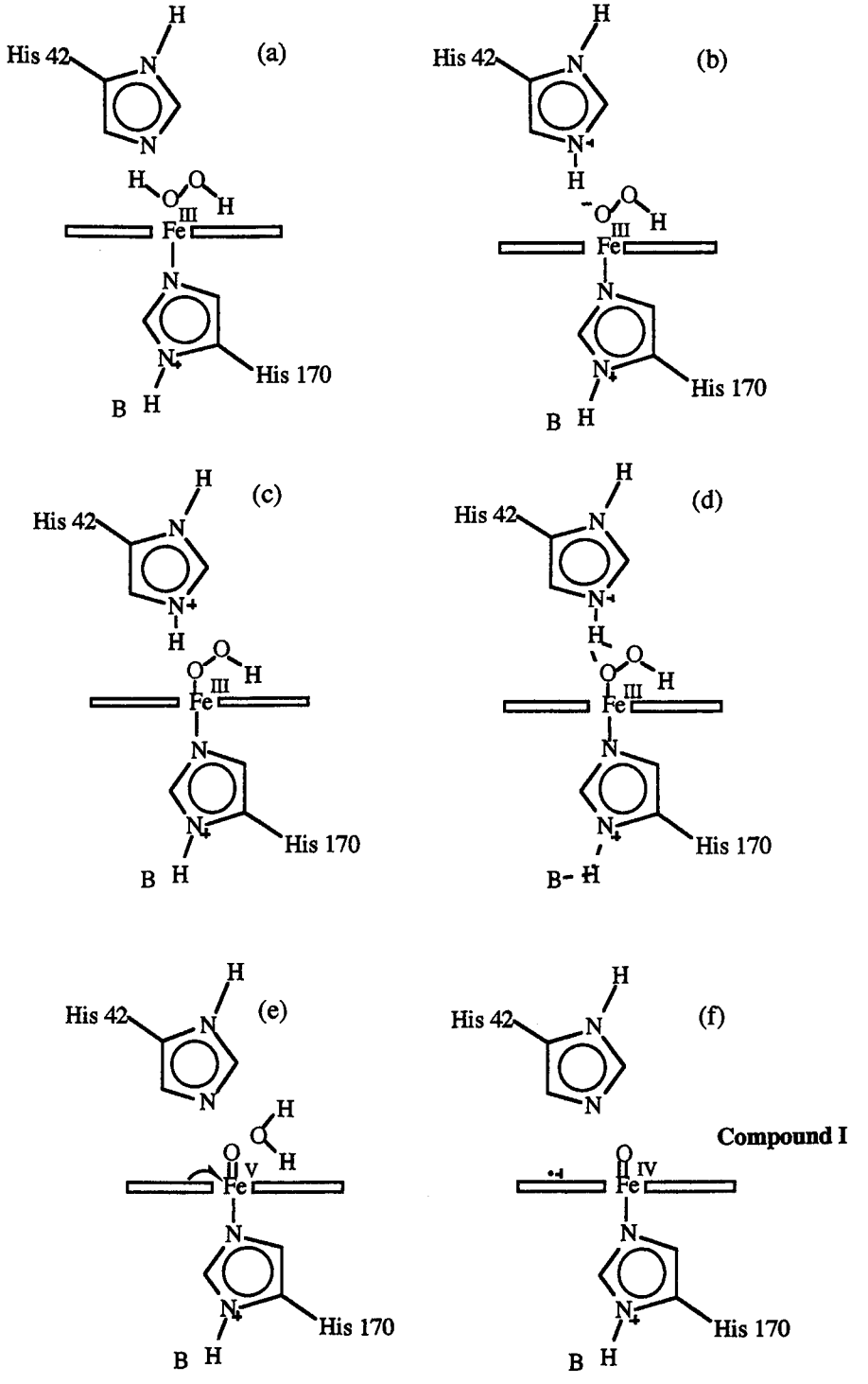

Figure 2. Mechanism steps leading to the formation of Compound I in HRP peroxidase (for further details, see text).

Compound I has been proved to have a radical character (ESR spectroscopy), which indicates that at least in HRP, the haem porphyrin reduces

Fe(V)=O to Fe(IV)=O (Figure 2, e and f). The next step involves the approach of a substrate molecule to a region known to have some aromatic donor binding ability (see Section 3 for further details). Studies with radicals and molecules showing suicide enzyme inactivation have partially identified this reaction site.[17-19] The active site involves an edge portion of haem, namely a *meso* position and an adjacent β-pyrrolic methyl group. The relevance of the nearby amino acids residues will be discussed later. In this edge region of the porphyrin, electron transfer occurs, with reduction of Compound I to Compound II (see Figure 3, a and b) and with the concomitant release of a one-electron oxidised substrate. A substrate proton is accepted by the distal histidine, forming a hydrogen bond with Fe=O. It was shown that, if histidine is unprotonated, Compound II is essentially inactive.[20] This, together with the necessity for having an unprotonated distal histidine for Compound I formation, is the origin of the well known bell-shaped activity profile relationship with pH and highlights the acid/base catalytic properties of the distal histidine, which is essential for peroxidase activity. The proposed mechanism for the one-electron reduction of Compound II to the native HRP is of oxidation of substrate with transfer of $H^{\cdot}$ to ferryl oxygen, forming water with the second histidine proton and releasing HRP in its original state (Figure 3, c, d and e).

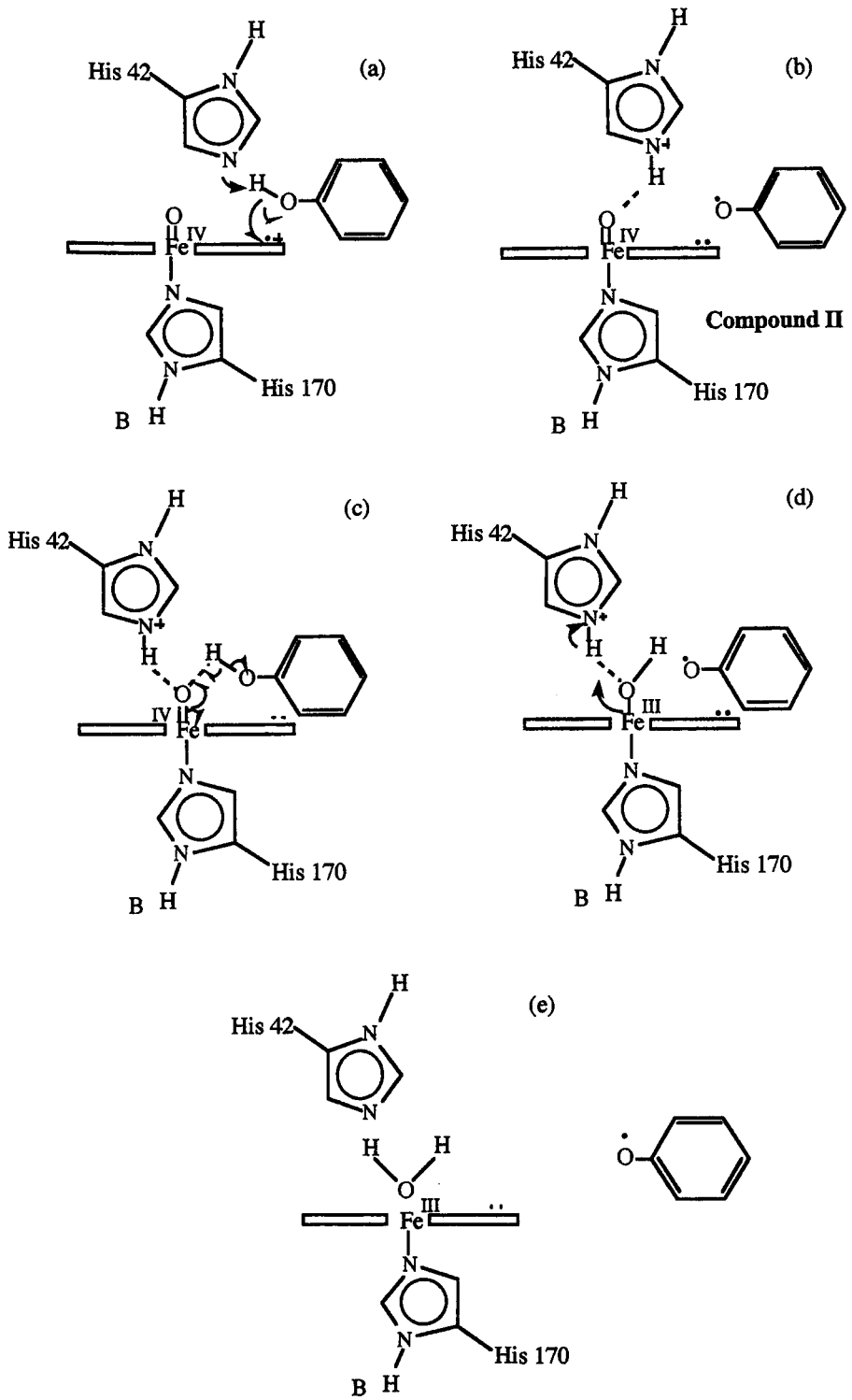

Figure 3. Mechanism steps converting Compound I in Compound II, for HRP peroxidase (for further details, see text).

3. Structure-function relationship of peroxidases

Knowledge of peroxidase structure and its mode of action does not answer a basic question: "Why such a structure, this central metal, these amino acids and no others?". Peroxidases work quite well with the prescribed amino acids, but if these are changed, for example by replacing the proximal histidine with glutamic acid, what result should be expected? In fact, this sort of question would be answered in Nature, which could be expected to choose the most competent structural element for a particular transformation. It would be very helpful if all the implications of making such structural changes could be understood.

3.1. The central metal ligated to the porphyrin

Iron is exclusive in complexing haem complexed with peroxidases and other related enzymes. Replacement of central metal in HRP and CcP was carried out by their enzymic denaturation followed by haem extraction. Posterior protein refolding and insertion of a metal-modified haem gave artificially modified enzymes. In Table 1, the initial rates of formation of Compound I for manganese-modified HRP and CcP are given.

Table 1. Initial rates of formation of Compound I comparison for native and manganese modified haem in HRP and CcP.

Enzyme	**Rate of formation of Compound I[a]** **K** ($mol^{-1}.L.\ s^{-1}$)	**Reference**
HRP		
Native HRP	1.8×10^7	21
Mn HRP	1.7×10^3	21
CcP		
Native CcP	1.4×10^8	14
Mn CcP	7.5×10^5	14

a. Apparent second order rate constant for the enzyme reaction with H_2O_2.

In both cases, the manganese-substituted enzymes exhibited a considerable decrease in the rate of Compound I formation. This may explain natural preference for iron. More detailed analysis of the Mn-replacement enzyme shows

that, contrary to iron, Mn-complexed enzymes have a positive enthalpy change when reacting with H_2O_2,[21] making them less favourable for use in haem.

3.2. The primary structure of the polypeptide chains in enzymes

Recently, development of molecular biology techniques has allowed manipulation of the genes holding the information for protein synthesis. This has brought with it the possibility of changing a particular amino acid in an enzyme to produce an artificially modified protein or enzyme. In other words, the method requires, (i) identification of the gene that encodes the protein amino acids, (ii) cutting and changing of the codon that encodes a particular amino acid, and (iii) DNA recombination in a bacterial plasmid. The modified bacteria are allowed to produce the required protein, which can be isolated and purified. The isolated apoprotein is left in conditions that allow for its refolding, which allows the introduction of the haem group by solubilization of haem together with the apoprotein. Recent progress and development in peroxidase chemistry has increased enormously by application of such techniques. In Table 2, some single point mutation experiments are listed together with the effects these changes conferred on the enzyme.

Table 2. Single point mutations experiments in peroxidases, in amino acids close to the haem centre with the resulting effect on their activity.

Peroxidase	Exp. No.[a]	Replaced amino acid	Described effects	Ref. No.
CcP	1	His 175 → Gln	The enzyme show about the same wild rate on Compound I formation	22
	2	His 175 → Glu	Enhanced activity (by a factor of 7)	22
	3	His 175 → Cys	Activity lost (to only 7%)	22
	4	His 52 → Leu	Rate of Compound I formation lowers to 1/5	23
	5	His 175 → Gln +Trp 191→ Phe[b]	Activity completely lost. Gives a long lived porphyrin pi cation radical.	22
HRP	6	His 170 → Ala	Possibility of distal co-ordination with iron. Hydrogen peroxide bond (O–O) breaking difficult.	24
	7	His 42 → Ala	Decrease in the rate of Comp. I formation by a 10e6 factor. Better thioanisole and styrene epoxidation.	26,36
	8	His 42 → Ala + Phe 41 → His *b*	Compound I formation equal to 3 x 10e4 mol-1.L.s-1 (the value for wild is 0.7 x 10e7 mol-1.L.s-1)	27
	9	His 42 → Ala	Rate of Compound I formation greatly decreased (10e6). Compound II not detected. Rate in thioanisole sulfoxidation 100 times higher.	26,36
	10	His 42 → Val		
	11	His 42 → Leu	Lowers apparent k with H2O2 by 5 orders of magnitude.	28
	12	Asn 70 → Val	Hydrogen bonding with distal histidine.	25,26
	13	Asn 70 → Asp	Rate of formation of Compound I lowers from 1.6 x 10e7 to 6 x 10e5. Regulates the pKa of distal Hist.	
	14	Arg 38 → Leu	Decrease 3 times the rate constant with H2O2.	28
	15	Arg 38 → Lys	Decrease 6 times the rate of H2O2 bond breaking.	16
	16	Arg 38 → Ser	Suppress the formation of Fe(II)–O2, as in myoglobins.	29
	17	Arg 38 → Gly		
	18	Phe 143 → Glu	Very low catalytic activity. Affect haem entrapment.	31
	19	Phe 143 → Glu	Create a charge at the entrance of the haem binding pocket and protects the latter from substrates and radicals	32
	20	Phe 41→ Leu	Monooxygenase activity increases.	15
	21	Phe 41→ Thr	Monooxygenase activity increase (styrene epoxidation possible).	15
	22	Phe 41 → His	Reduce peroxidase activity (more than 400 times).	33
	23	Phe 41 → Trp	Decrease peroxidative activity 8 times.	31
	24	Phe 41 → Val	Decrease peroxidative activity 8 times.	
	25	Phe 41 → His	Rate of Compound I formation decreased by 2. Lowers slightly the peroxidase activity.	34
	26	Phe 41 → Hist	Unstable enzyme. Haem binding difficult.	35
	27	Phe 41 → Ala	Catalyses thioanisole sulfoxidation with a rate 100 times higher.	36
	28	Phe 172→ Tyr	The radical of Compound I is located in the protein. Compound I decays very rapidly to Compound II, in other words Tyr 172 is immediately oxidised.	30

a. Experiment number.
b. Double point mutation experiments, in which two amino acids were replaced.

The data compiled in Table 2 allows a discussion about the function of each of the highly conserved amino acids surrounding haem.

Proximal histidine (Table 2, experiments number 1-3, 5, 6). This is the first highly conserved amino acid occurring in peroxidases. Its main role, together with the nearby Asn has been associated as a "push-pull" electron activity, which facilitates the formation of Compound I and Compound II[1] and as a means of stabilising Compound I. Single-point mutation studies showed that a complementary action of this histidyl residue is to be axially complexed with haem iron(III), so as the distal histidine site unco-ordinated (Table 2, experiment number 6 and references therein). There is also evidence that others amino acids can substitute for histidine. Replacing histidine by glutamine has no observable effect on CcP activity (Table 2, experiment number 1), but its replacement by glutamic acid enhances peroxidase activity by a factor of seven (Table 1, experiment number 2).

Distal histidine (Table 2, experiments number 4, 7-11). This residue is found in all known peroxidases. It plays an important role in directing H_2O_2 towards haem and is also involved in O-O bond breaking. Peroxidase activity is lost by a factor of 10^6 when this amino acid is changed to a non-polar one.[26,36] Other changes in this amino acid lead to the same activity decrease, with a concomitant increase in the mono-oxygenative activity. Studies with *Arthromyces Ramosus* peroxidase have shown that conformational flexibility appears to help proton translocation from one oxygen to the other, in HOO, so as to facilitate the formation of Compound I.[10] Chloroperoxidase, an enzyme that shows both peroxidase and mono-oxygenase activity (Section 5), has a glutamic acid residue[37] in the distal position, supporting the idea that other functions can substitute for this residue.

Distal arginine (Table 2, experiments number 14-17). This is another highly conserved peroxidase amino acid. Single-point mutagenesis of this residue suggests that it occupies a position in the hydrogen bonding sphere of the NH group of the distal His 42 and contributes both to access of H_2O_2 to the active site and to hydrogen transposition in the O-O bond breaking process.

Phe 41 (Table 2, experiments number 20-27). This residue helps to form the docking site for haem and stabilises and confines the pi cation-radical of Compound I in the porphyrin structure. Its replacement by His, Trip or Val led to a decrease in the enzyme peroxidative activity, while changing it to a small hydrocarbon amino acid (Ala, Leu and Thr) improves the mono-oxygenase activity of the mutants.

Phe 172 (Table 2, experiments number 5 and 28). This residue has proved to be important in differentiating peroxidase reactivity between HRP and CcP. In CcP this residue is replaced by tryptophan 191 and it is now known that the first oxidation equivalent is located in the protein instead of being positioned at the haem cation-radical; this feature is essential for CcP activity.[22] For MnP, LiP, and HRP the presence of the less oxidizable amino acid (Phe) stabilises the cation-radical located in haem. In fact, changing this amino acid in HRP to tyrosine, results in a radical-cation located in the protein.[30]

Substrate binding site. For some time, this area remained the most obscure part of peroxidases, namely, in identifying the amino acids involved. Part of the site was known from studies on molecules acting as structural probes, *i.e.*, phenylhydrazine and benzhydroxamic acid. Inhibition of HRP activity by phenylhydrazine led to a phenyl group covalently linked to a C20 *meso* carbon on haem or to a position near C18 methyl group; the compound does not interfere with the action of haem.[17,19] There is a consensus that the C20 *meso* position in haem blocks electron transfer and that the adjacent methyl on C18 is involved with the site.[17,18,19] This C18-position is the closest that a substrate can approach to central iron. NMR Spectroscopy techniques show that two phenylalanine residues (Phe A and Phe B) are involved.[18,19] These two amino acids are thought to be Phe 142 and Phe 143. Others studies, argued against these residues and suggested Phe 179 and Phe 221 as the best possible candidates.[38] Amino acid, Phe 142, has some indirect effects but it seems that other residues are also involved. This structural dilemma was definitely resolved by X-ray on a crystal of HRP, the first for a class III peroxidase. The three phenylalanine residues involved in forming the aromatic binding region for the substrate are Phe 142, 68 and 179.[11]

4. Mono-oxygenases of the P450 family and Chloroperoxidase. Differentiating mono-oxygenase from peroxidase activity

The mono-oxygenases of the P450 family are able to use H_2O_2 as oxygen donor to transfer oxygen to a range of substrates (reaction 4, in which P is a mono-oxygenase, S the substrate and SO the oxidation product).[39]

$$P + H_2O_2 + S \rightarrow P + SO + H_2O \qquad (4)$$

The catalytic cycle of cytochromes P450 is summarised in Figure 4.[40] The enzyme resting state involves a water molecule complexed to ferric haem, which is

released on insertion of substrate. This step is accomplished with a redox potential decrease from -212mV to -313mV, thereby enabling the subsequent reduction of the ferric state by putadorodixin and the docking of oxygen. Posterior reduction of the complex so formed and scission of the O-O bond catalysed by H^+ yields a complex equivalent to Compound I in peroxidases. The exact location of the oxidation equivalents remains hypothetical but analogy with peroxidases points to a cation-radical type of haem-centred species. By reaction of this complex with substrate, a hydrocarbon radical forms together with a hydroxy haem complex. Rearrangement results in the hydroxylation and release of the substrate, returning the enzyme to its former state.

An interesting feature of P450 cytochromes is their ability to form the high-valent ferryl complexes (represented as $Fe^V=O$ in Figure 4) from reduced oxygen molecules, e.g., from H_2O_2 or hydroperoxides. In such cases the similarities with the earlier steps of peroxidase mechanisms are more evident. The active centre of these enzymes has a haem coordinated in the proximal position by a cysteine thiolate anion, leaving the distal position free for co-ordination. The polypeptidic chain forms a cage on this side of the haem, which allows access of substrate close to ferric iron. The characteristics of the cage are essentially hydrophobic but, in some cases, amino acids guide the entrance of particular substrates. There is evidence of a channel involving proton transfer as required to the catalytic cycle.

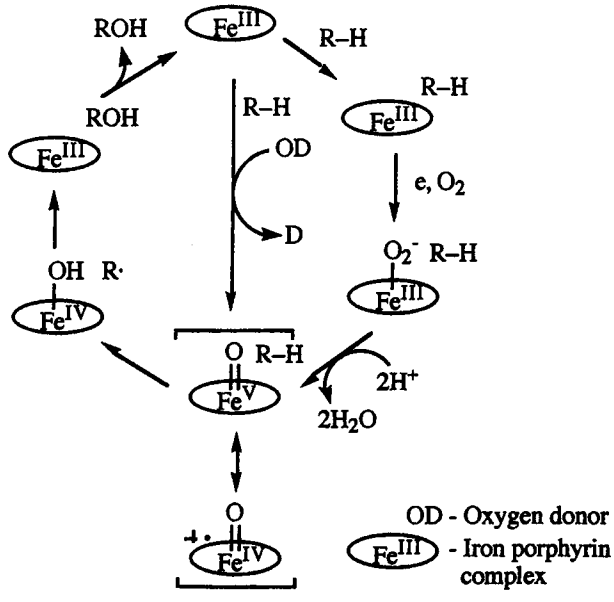

Figure 4. The accepted mechanistic cycle for the P450 enzymes family. The shunt pathway is represented in the centre of the diagram, and converts directly the resting enzyme in the active ferryl intermediate, by action of oxygen donors (OD) like H_2O_2 or OCl^-.

Chloroperoxidase is an interesting enzyme, which shows catalase, peroxidase and mono-oxygenase activity. The availability of the crystal structure for this enzyme[41] shows that the proximal position for haem is occupied by a cysteine residue, that in the distal position there is a hydrophobic patch and that a glutamic acid residue acts as the catalytic base required for the peroxidative mechanism. Small organic substrates can gain access to the ferryl complex (Compound I), which enables P450-type activity.

These findings, together with results from mutation experiments, highlight the possibility of altering the catalytic activity of these enzymes by strictly controlling the immediate environment of the central haem. A lack of space surrounding haem in peroxidases prohibits the entry of small substrate molecules from entering the active centre and disfavouring mono-oxygenase activity. Contrariwise, this activity seems to need a close approach of substrate to the haem iron.

5. Synthetic models of peroxidases

In the presence of an oxygen donor and a substrate metalloporphyrins mimic peroxidase activity. This has been known for a long time and such model systems have helped in the mechanistic elucidation of peroxidase action.[1] When using simple metalloporphyrins as peroxidase models, new aspects arose from the properties of porphyrins themselves. One such is the finding that porphyrins and metalloporphyrins have a natural tendency to form aggregates in aqueous media;[42] are easily oxidised by powerful oxidising compounds or reaction intermediates (such as Compound I and Compound II) leading to their rapid depletion;[43] form easily and irreversibly, specially under basic conditions, the μ-oxo complex, which is unreactive towards peroxidative (and mono-oxygenative) reactions.[44,53] For these reasons, use of special substrates having very high reactivities with Compound I and Compound II are required in order to prevent depletion of catalyst and other side reactions. Such substance is ABTS (2,2'-azino-*bis*-3-ethylbenz-thiazoline-6-sulfonic acid).[45]

The development of synthetic porphyrins having groups at *meso*-positions and carrying substituents at the 2,6-phenyl-positions has opened up the possibility of a more convenient study of these model systems because such porphyrin/metal complexes do not aggregate, do not form μ-oxo complexes and are stable over a very wide pH range.[46] One remarkable example of such compound is iron(III) *tetrakis*(2,6-dichloro-3-sulfonatophenyl)porphyrin,[47]

prepared by sulfonation of TDCPP.[48] Porphyrins with such characteristics provide better catalysts for reactions that mimic natural peroxidase systems and the *in situ* preparation of stable Compound I and Compound II species.[49]

The main characteristics of the reaction of ABTS with an oxygen donor (OD), such as hydrogen peroxide, in the presence of metalloporphyins are [46, 50-52, 53]:

(i) The substrate is oxidised through a reaction that obeys second order kinetics (dependence in ABTS oxidation in the concentrations of both metalloporphyrin and oxygen donor and independence of substrate concentration, as shown in equation 5). As a consequence, the rate–determining step involves reaction of oxygen donor with metalloporphyrin, and is suggested to be the breaking of the O-O peroxo bond.

$$V = \frac{d[ABTS^{+\cdot}]}{dt} = -2\frac{d[OD]}{dt} = k\,[Mporph]^1\,[OD]^1\,[ABTS]^0 \qquad (5)$$

(ii) The observed initial rate of ABTS oxidation with respect to pH shows a complex profile, which may be rationalised as the superimposition of two bell-shaped curves (Figure 5).

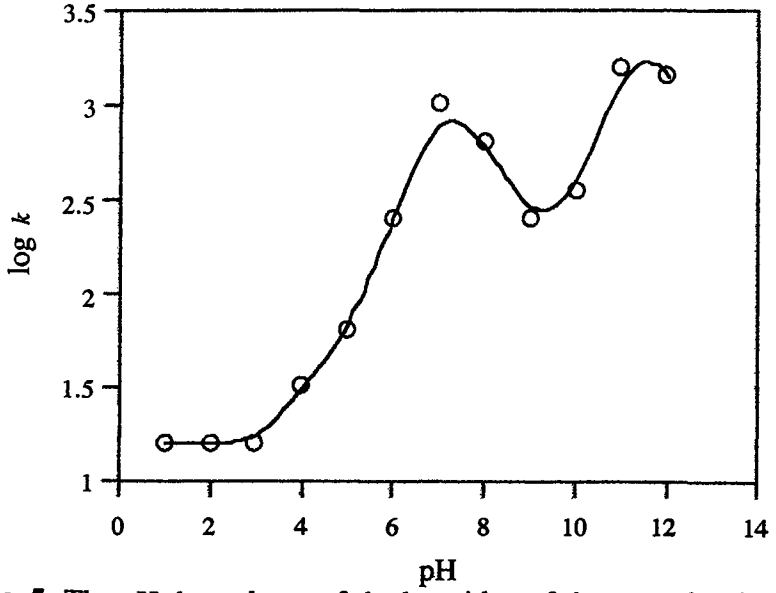

Figure 5. The pH dependence of the logarithm of the second order rate constant (k) for the reaction of Fe^{III}TDCPPS with t-ButOOH in the presence of ABTS (adapt. from ref. 52).

(iii) Typical second order rate constants for ABTS oxidation account in the range of 10-20 $mol^{-1}.L.s^{-1}$.[50-52]

(iv) When using H_2O_2 as an oxygen donor, competition between substrate oxidation (equation 6) and H_2O_2 oxidation to O_2 (catalase like activity, equation 7) occurs. This activity can be surprisingly high, particularly at high pH values.[52]

$$Fe^{III}TDCPPS + 2H_2O_2 + 2ABTS + 2H^+ \rightarrow Fe^{III}TDCPPS + 2H_2O + 2ABTS^{\cdot+} \quad (6)$$

$$Fe^{III}TDCPPS + 2H_2O_2 \rightarrow Fe^{III}TDPPS + 2H_2O + O_2 \quad (7)$$

The mechanism of peroxidase-like activity parallels that of natural systems. In the first step, the accepted scheme involves binding of the oxygen donor (e. g., H_2O_2, peracids or hydroperoxides). Since synthetic systems do not have a formal distal ligand, it is not clear if the binding species is RO_2^- or RO_2H,[1] as occurs in the natural system. Breaking of the O-O bond, a process that in the natural systems is assisted by axial ligands (e.g., histidine and a nearby asparagine); in artificial systems it is assisted by general acid/base catalysis. This assistance is essential for peroxidase activity; it has been known for some time that anhydrous H_2O_2 is unable to react with iron metalloporphyrins to give Compound I or Compound II.[49] Much discussion has arisen about the mechanism of O-O breaking. Both homolytic,[46, 50-52] and heterolytic[54] bond breaking has been suggested, depending on the oxygen donor used. For example, acyl hydroperoxides favour heterolytic bond-breaking but alkyl hydroperoxides favour homolytic processes. Interaction of Compound I with the substrate results in its one-electron oxidation and in the concomitant reduction of Compound I to form Compound II.

It is recognised that Compound I possesses a greater reactivity relative to Compound II. Since electron transfer from the substrate seems to occur at the outer sphere of the porphyrin, the higher reactivity of Compound I can be rationalised in terms of electron-tunnelling, the path is shorter in Compound I relative to Compound II (electron transfer from the porphyrin outer sphere closer than electron transfer from the central metal).[55] Besides this, Compound I has the ability to epoxidize alkenes but Compound II is much less reactive towards them.[49]

Both Compound I and Compound II models have been prepared and fully characterised.[49] Compound I can be prepared by reaction of 3-chloro-peroxybenzoic acid with iron (III) *tetrakis*(2,6-dichloro-3-sulfonatophenyl) porphyrin chlorate, in acetonitrile at -35°C. It is a green compound, for which the

visible spectrum is shown in Figure 6. Addition of one equivalent of tetrabutyl ammonium hydroxide to a Compound I solution at -35°C in acetonitrile yields a red complex, for which the visible spectrum is also shown in Figure 6. This complex has the same properties as does Compound II.

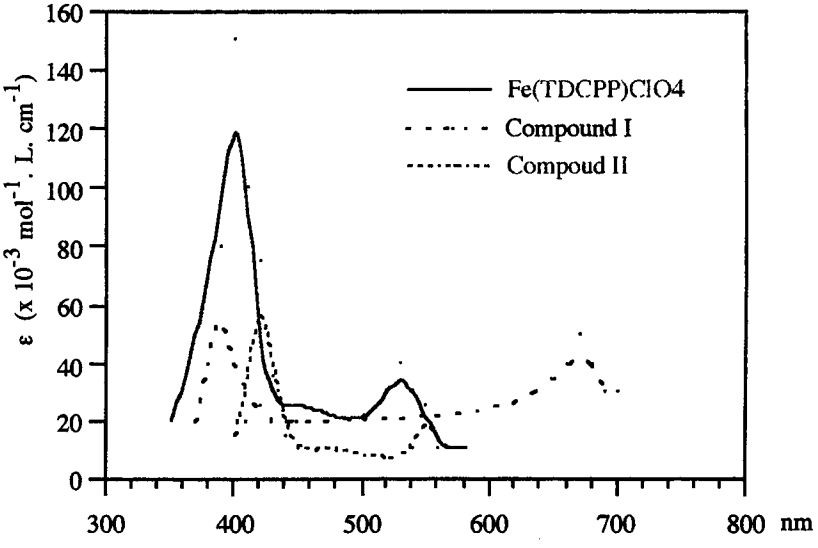

Figure 6. Visible spectra of iron(III) *tetrakis*(2,6-dichloro-3-sulfonatophenyl) porphyrin chlorate solution in acetonitrile, its reaction product with 3-chloroperoxybenzoic acid in acetonitrile (Compound I) and this solution after reaction with tetrabutylammoniumhydroxide (Compound II) (adapted from ref. 49).

5.1. Effect of axial ligands

Experiments done with single-point mutated HRP, in which the distal ligand (His 42) is absent, leads to major loss of enzyme activity (from 8.9 x 10^6 to 19.4 $mol^{-1}.L.s^{-1}$ for initial rate of formation of Compound I). This loss of activity can be partially recovered by addition of exogenous 2-substituted imidazoles to the reaction system.[26] In synthetic systems made with metalloporphyrins, the presence of such heterocyclic nitrogen bases is also beneficial to the peroxidative reaction. Simple addition of 2,4,6-trimethylpyridine in the ABTS oxidation with a metalloporphyrin increases the rate of reaction and makes possible the observation of Compound II.[51] In Table 3, values for the second order rate

Table 3. Second order rate constant for the reaction of Fe(TDCPPS) with ABTS and H_2O_2, using different buffers (Adapted from ref. 51).

Buffer	**[Buffer]** $\times 10^3$ **mol.L^{-1}**	***k*** **mol^{-1}.L.s^{-1}**
Phosphate (pH=6.7)	5	263
	50	256
2,6-dimethylpyridine (pH=6.9)	5	460
	50	1060
2,4,6-dimethylpyridine (pH=7.5)	5	883
	50	1700

constant are presented for the oxidation of ABTS with Fe^{III}(TDCPPS) and with H_2O_2, in the presence of several buffers. It is clear that catalytic effects are present when an amine buffer is employed.

In Table 3, values for the second order rate constant are presented for the oxidation of ABTS with Fe^{III}(TDCPPS) and with H_2O_2, in the presence of several buffers. It is clear that catalytic effects are present when an amine buffer is employed.

6. The system PSSS-VN polymer/metalloporphyrin

When developing artificial systems as peroxidase mimics it would be desirable if the maximum number of natural peroxidase characteristics could be included. While the construction of polypeptidic chains is not easily achieved, a new interesting system can be used as an artificial apoprotein. It uses amphiphilic polymers, *viz.*, co-poly(4-styrenesulfonic acid, sodium salt; 2-vinyl-naphthalene; PSSS-VN), which forms stable hydrophobic domains in aqueous media.[56] Their association with the metalloporphyrins provides an assembly of a metalloporphyrin in a hydrophobic domain (Scheme 1). The amphiphilic polymer faces outward with its $-SO_3Na$ groups at the water interface, leaving a hydrophobic interior. Molecules that are formally insoluble in water will dissolve in aqueous solutions containing the amphiphilic polymer. In the case of porphyrins, there is evidence that the porphyrins lie sandwiched between naphthalene residues of the PSSS-VN polymers.

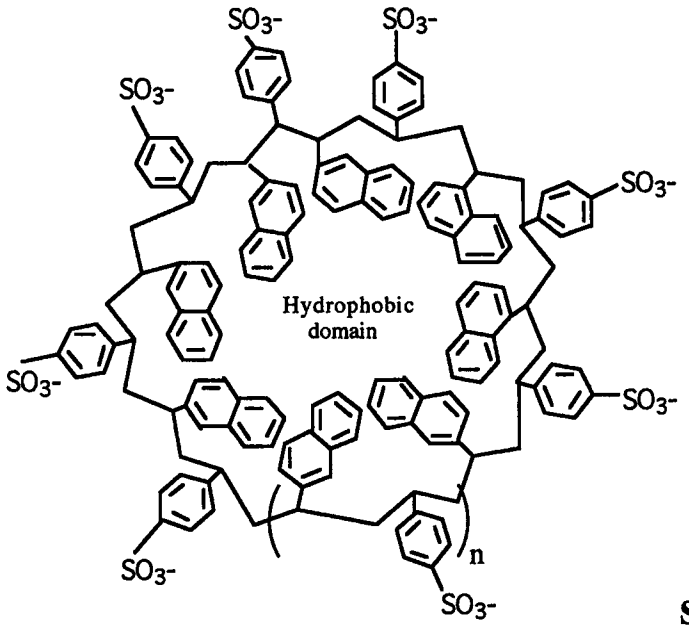

Scheme 1

These systems were tested against peroxidase activity tests using ABTS.[45] The results were very promising, in that the systems exhibited an ability to oxidise several water-soluble dyes and small molecules with very high efficiencies.[57]

The main goal of the work described in this thesis was to continue research on the PSSS-VN/metalloporphyrin system, as an artificial analogue of a peroxidase. The activity was checked under one set of conditions with various substrates. The synthesis of model structures to mimic the metalloporphyrin/aromatic interaction in the polymer system was also tested. These are the subjects of the next chapters.

II. Notes and references

1. H. B. Dunford in, *Peroxidases in Chemistry and Biology*, Eds. J. Everse, K. E. Everse and M. B. Grisham, CRC Press, Boca Raton, 1991.

2. A search in BIDS (Bath Information Data Services) database for *peroxidase*, retrieved the following number of "hits" in five years: 451 (1994), 480 (1995), 590 (1996), 537 (1997), 585 (1998).

3. G. Labat, B. Meunier, *Bull. Soc. Chim. Fr.*, 1990, **127**, 553.

4. B. Ezaki, S. Tsugita and H. Matsumoto, *Plant Physiol.*, 1996, **96**, 21; S. L. Chen, C. H. Kao, *Plant Growth Regul.*, 1995, **17**, 67.

5. P. Montalbini , R. Buonaurio, N. N. U. Kumar, *J. Phytopath.*, 1995, **143**, 295.

6. M. D. Brownleader, N. Ahmed, M. Trevan, M. F. Chaplin, P. M. Dey, *Plant Physiol.*, 1995, **109**, 1115.

7. D. Ping , J. R.Collins and G. H. Loew, *Prot. Engin.*, 1992, **5**, 679.

8. M. Sundaramoorthyt, K. Kishi, M. H. Gold, and T. L. Poulos, *J. Biol. Chem.*, 1994, **269**, 32759.

9. X. D. Su , T. Yonetani, U. Skoglund, *FEBS Lett.*, 1994, **351**, 437.

10. K. Fukuyama, H. Matsubara, H. Hatanaka, Y. Shibano, T. Amachi, *J. Mol. Biol.*, 1994, **235**, 331; K. Fukuyama, *J. Biol. Chem.*, 1995, **270**, 21884.

11. M. Gajhede, D. J. Schuller, A. Henriksen, A. T. Smith, T. L. Poulos, *Nature Strut. Biol.*, 1997, **4**, 1032.

12 (a) H. S. Pappa and A. Cass, *Europ. J. Biochem.*, 1993, **212**, 227; S. L. Timofeevski, S. D. Aust, *Arch. Biochem. Biophys.*, 1997, **342**, 169; (b) B. C. Nwanguma, M. O. Eze, *J. Instit. Brew.*, 1995, **101**, 4.

13. J. W. Tams, K. G. Welinder, *Anal. Biochem.*, 1995, **228**, 48.

14. T. Yonetani and T. Asakura, *J. Biol. Chem.*, 1969, **244**, 4580.

15. S. Ozachi and P. R. O. de Montelano, *J. Am. Chem. Soc.,* 1995, **117**, 7056.

16. J. N. RodriguezLopez, A. T. Smith, R. N. F. Thorneley, *J. Biol. Chem.*, 1996, **271**, 4023.

17. M. A. Ator, P. R. O. de Montelano, *J. Biol. Chem.*, 1987, **262**, 1542.

18. N. C. Veitch and R. J. P. Williams, *Eur. J. Biochem.,* 1995, **229**, 629.

19. D. J. Gilfoyle, J. N. Rodriguez-Lopez and A. T. Smith, *Eur. J. Biochem.*, 1996, **236**, 714.

20. H. B. Dunford and J. S. Stillman, *Coord. Chem. Rev.*, 1976, **19**, 187.

21. K. K. Khan, M. S. Mondal and S. Mitra, *J. Chem. Soc., Dalton Trans.*, 1996,1059.

22. K. Choudhury, M. Sundaramoorthy, A. Hickmanilii, T. Yonetani, E. Woehl, M. F. Dunnt, and T. L. Poulos, *J. Biol. Chem.*, 1994, **269**,20239.

23. J. E. Erman, L. B. Vitello, M. A. Miller, A. Shaw, K. A. Brown, J. Kraut, *Biochem.*, 1993, **32**, 9798.

24. S. L. Newmyer, J. Sun, T. M. Loehr, P. R. O. Demontellano, *Biochem.*, 1996, **35**, 12788.

25. M. Mukai, S. Nagano, M. Tanaka, K. Ishimori, I. Morishima, T. Ogura, Y. Watanabe, T. Kitagawa, *J. Am. Chem. Soc.,* 1997, **119**, 1758.

26. S. L. Newmyer, P. R. O. Demontellano, *J. Biol. Chem.*, 1996, **271**, 14891.

27. M. I. Savenkova, S. L. Newmyer, P. R. O. Demontellano, *J. Biol. Chem.*, 1996, **271**, 24598.

28. J. N. Rodriguez Lopez, A. T. Smith, R. N. F. Thorneley, *J. Biol. Inorg. Chem.*, 1996, **1**, 136.

29. J. N. RodriguezLopez, A. T. Smith, R. N. F. Thorneley, *J. Biol. Chem.*, 1997, **272**, 389.

30. V. P. Miller, D. B. Goodin, A. E. Friedman, C. Hartmann and P. Demontellano, *J. Biol. Chem.*, 1995, **270**, 18413.

31. I. G. Gazaryan, V. V. Doseeva, A. G. Galkin, V. L. Tishkov, *FEBS Lett.*, 1994, **354**, 248.

32. E. A. Mareeva, M. A. Orlova, V. V. Doseeva, D. B. Loginov, A. G. Galkin, I. G. Gazarian, V. I. Tishkov, *Appl. Biochem. Biotechn.*, 1996, **61**, 13.

33. I. G. Gazaryan, A. G. Galkin, V. V. Doseeva, V. I. Tishkov, *Biochemistry-Moscow*, 1995, **60**, 1187.

34. D. B. Loginov, I. G. Gazaryan, V. V. Doseeva, A. G. Galkin, V. I. Tishkov, E. A. Mareeva and M. A. Orlova, *Russ. Chem. Bull.*, 1994, **43**, 1923.

35. E. A. Mareeva, M. A. Orlova, V. V. Doseeva, D. B. Loginov, A. G. Galkin, I. G. Gazarian, V. I. Tishkov, *Appl. Biochem. Biotech.*, 1996, **61**, 13.

36. S. L. Newmyer, P. R. O. Demontellano, *J. Biol. Chem.*, 1995, **270**, 19430.

37. M. Sundaramoorthy, J. Terner, T. L. Poulos, *Structure*, 1995, **3**, 1367.

38. N. C. Veitch, R. J. P. Williams, N. M. Bone, J. F. Burke and A. T. Smith, *Eur. J. Biochem.*, 1995, **233**, 650.

39. F. P. Guengerich and T. L. Macdonald, *Acc. Chem. Res.*, 1984, **17**, 9; M. J. Coon, X. Ding, S. J. Pernecky and D. N. Vaz, *FASEB J.*, 1992, **6**, 669.

40. T. L. Poulos and R. Raag, *FASEB J.*, 1992, **6**, 674.

41. M. Sundaramoorthy, J. Terner, T. L. Poulos, *Structure*, 1995, **3**, 1367.

42. R. F. Pasternack, P. R. Huber, P. Boyd, G. Engasser, L. Francesconi, E. Gibbs, P. Fasella, C. Venturo and L. de C. Hinds, *J. Am. Chem. Soc.*, 1972, **94**, 13.

43. J. A. S. Cavaleiro, M. J. E. Hewlins, A. H. Jackson and G. P. M. S. Neves, *J. Chem. Soc., Chem. Commun.*, 1986, 1311.

44. J. A. Smegal, B. C. Schardt, C. L. Hill, *J. Am. Chem. Soc.*, 1983, **105**, 3510.

45. J. Putter and R. Becker in, *Methods of Enzymatic Analysis*, Vol. 3, Eds. H. U. Bergmeyer, VCH Publications, Weinheim, 1985, pages 286 *et seq.*

46. M. F. Zipplies, W. A. Lee, and T. C. Bruice, *J. Am. Chem. Soc.*, 1986, **108**, 4433.

47. A. M. d'A. Gonsalves, R. A. W. Johnstone, M. M. Pereira, A. M. D. deSantana, A. C. Serra, A. J. F. N. Sobral, P. A. Stocks, *Heterocycles*, 1996, **43**, 829.

48. A. M. d'A. Rocha Gonsalves, J. M. T. B. Varejao and M. M. Pereira, *J. Heter. Chem.*, 1991, **28**, 635.

49. H. Sugimoto, H. Tung, and D. T. Sawyer, *J. Am. Chem. Soc.*, 1988, **110**, 2465.

50. T. C. Bruice, *Aldrichim. Acta,* 1988, **21**, 87.

51. R. Panicucci and T. C. Bruice, *J. Am. Chem. Soc.*, 1990, **112**, 6063.

52. K. Murata, R. Panicucci, E. Gopinath, and T. C. Bruice, *J. Am. Chem. Soc.*, 1990, **112**, 6072.

53. N. Colclough and J. R. Lindsay Smith, *J. Chem. Soc. Perkin Trans. 2*, 1995, 235.

54. T. G. Traylor and J. P. Ciccone, *J. Am. Chem. Soc.*, 1989, **111**, 8413.

55. B. He, R. Sinclair, B. R. Copeland, R. Makino, L. S. Powers, I. Yamazaki, *Biochemistry*, 1996, **35**, 2413.

56. M. Nowakowska and J. E. Guillet, *Chem. Britain,* 1991, **27**, 327-330.

57. R.A. W. Johnstone, A. J. Simpson, P. A. Stocks, *Chem. Comm.*, 1997, 2277.

CHAPTER 2: THE PSSS-VN/METALLOPORPHYRIN SYSTEMS

I. Introduction

1. PSSS-VN polymers

The polymers, which are the subject of this present study, form hydrophobic domains when dissolved in aqueous solutions. This characteristic requires that the polymer synthesis should use the condensation of two monomers having different properties. Typically, one is hydrophobic and usually possesses an aromatic moiety (e.g. vinylnaphthalene) and the other contains a highly polar functionality (e.g. styrenesulfonic acid, sodium salt). The equimolar copolymerization of such monomers can be performed easily by radical initiation, (e.g. by using azoisobutyronitrile, AIBN) and gives a water-soluble polymer, *viz.*, co-poly(4-styrenesulfonic acid, sodium salt, 2-vinylnaphthalene) (PSSS-VN). The synthetic reaction scheme and conditions are outlined in Scheme 1, in which the co-polymer is shown in idealised form.[1,2]

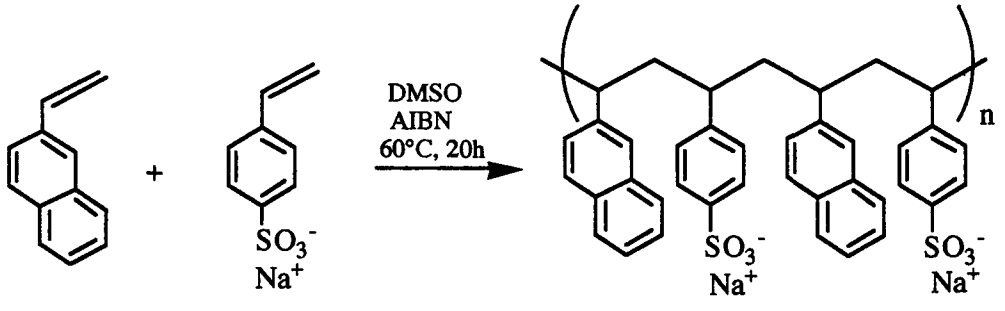

Scheme 1

The polymer structure in aqueous media has been partially characterised and can be described as one having a pseudo-micellar conformation leading to hydrophobic regions or pockets in the interior of the macromolecule.[3] This view is consistent with experimental evidence: sedimentation-velocity studies showed

that the "micelles" exist as single molecular coils and not as an aggregate in aqueous solutions;[4] viscosity and light scattering measurements suggest that the polymer is made-up of mostly short SSS segments connected by longer VN sequences; depolarisation ratio measurements indicate that the shape of the macromolecular coil is symmetric.[5] From these and other observations it is assumed that the polymer forms a rigid random coil with flexible VN-rich sections and is more expanded than any neutral analogue of similar molecular mass in a good solvent.[5]

The PSSS-VN type polymers have been shown to dissolve hydrophobic molecules in aqueous media, inside the hydrophobic domains (Scheme 2). They can solubilize at least eight molecules of 9-methylanthracene without any change in sedimentation coefficients.[4]

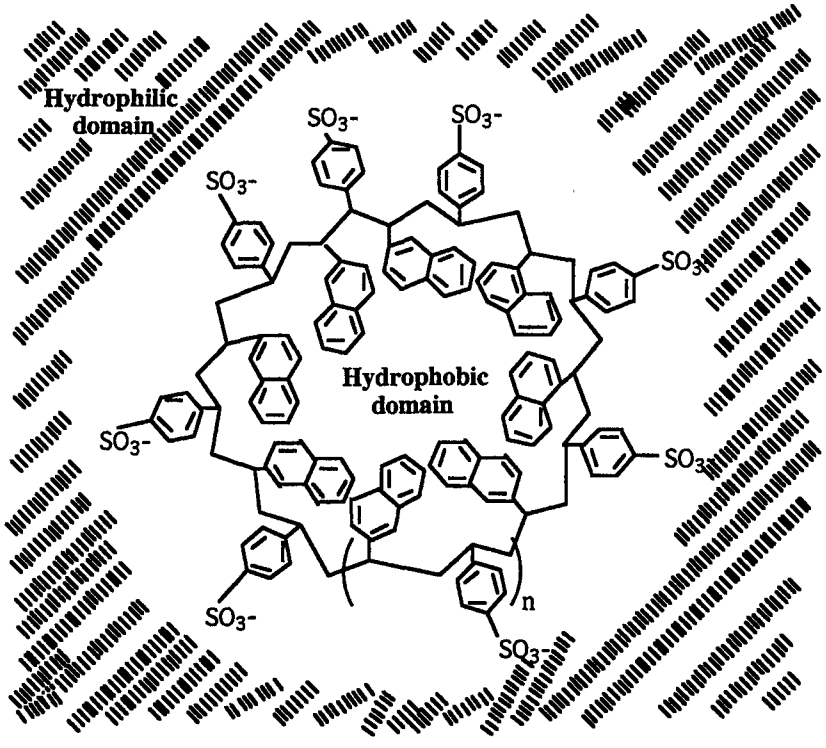

Scheme 2

A characterisation of the solubilization of some polycyclic aromatic hydrocarbons (PAHs) in a PSSS-VN aqueous solution was described.[2] It considers the PSSS-VN aqueous solution as consisting of two phases, the aqueous and the polymer "pseudo" phase, and as parameters the total PAH concentration, PAH concentration in the aqueous phase, PAH concentration in the polymer

"pseudo" phase and a partition coefficient. The value of these parameters for some PAH solubilization are shown in Table 1.

Table 1. Values of parameters[a] characterising the solubilization of some PAH compounds in aqueous solutions of PSSS-VN at pH = 7 (ref. 2).

PAH sample	$[PAH]_T$ x 10^6 mol.L^{-1}	$[PAH]_{PP}$ x 10^2 mol.L^{-1}	$[PAH]_{aq}$ x 10^6 mol.L^{-1}	**D** x 10^{-7}
Anthracene	18.6	3.6	0.4	12.7
9, 10-Dimethylanthracene	11.1	2.2	0.3	15.8
9, 10-Diphenylanthracene	6.4	1.3	0.1	36.7
9-Methylanthracene	35.2	6.8	1.4	0.4
Perylene	2.2	0.4	0.0012	1870

a. $[PAH]_T$ = total sample concentration in the polymer solution; $[PAH]_{PP}$ = total sample concentration in the polymer pseudo phase; $[PAH]_{aq}$ = total sample concentration in the saturated aqueous phase; D = Sample molar fraction distribution coefficient between polymer "pseudo" phase and aqueous phase (adapted from reference 2).

The use of the PSSS-VN polymers provides an 1.9 x 10^9-fold increase in perylene concentration in an aqueous solution. The concentration of such molecules in the polymer "pseudo" phase attains concentrations up to about 7 x 10^{-2} mol.L^{-1} for 9-methylanthracene.

Interesting applications described for these polymers explore their ability to concentrate hydrophobic molecules in their microdomains; irradiation with light of the correct wavelength generates excited states of the naphthyl moieties, which by subsequent oxygen quenching generate singlet oxygen. This last reactive species promotes several types of oxidation in the inserted species. Along with this process the molecules become considerably more polar, facilitating their release in aqueous media. An obvious potential application for such a system is the extraction and oxidation of organic pollutants in ground waters.[6] Considering the mechanistic resemblance with an enzyme together with a photochemical fuelling process these systems have been called "photozymes".[7]

2. The system PSSS-VN polymer with metalloporphyrins

A very promising development made through the use of these polymers has been microdomain dissolution of metalloporphyrins into water. Metalloporphyrins constitute the central group in several enzymes, such as

peroxidases and cytochromes (see the Introduction section in this thesis) and their association with amphiphilic polymers can be described as rugged enzyme models. Leading studies with PSSS-VN/metalloporphyrin systems have revealed them to have high peroxidase activity.[8] The results were very encouraging in that the quasi-enzymes were shown to bleach (catalytically oxidise) several industrial dyes and small molecules with hydrogen peroxide as oxygen donor.[9] Unlike simple water-soluble porphyrins, which auto-oxidise rapidly with hydrogen peroxide, the PSSS-VN/metalloporphyrin systems were found to be remarkably stable.

II. Results

1. Preliminary discussion

1.1. PSSS-VN/metalloporphyrin system and rate measurements.

The present study began with the PSSS-VN polymer system containing metalloporphyrins, using oxidative experimental conditions already described[8] and based on a published test for assaying peroxidase activity.[10] After preparation of the required aqueous solution of PSSS-VN/metalloporphyrin polymer, as described in the experimental section, peroxidase activity was measured by using the recently introduced one-electron oxidation screening substrate, 2,2'-azino-*bis*-3-ethylbenz-thiazoline-6-sulfonic acid (ABTS, see Introduction to this thesis). The oxygen donor used was hydrogen peroxide. Oxidation of ABTS leads to a stable cation-radical ($ABTS^{\cdot+}$) having strong UV/VIS absorption bands at 420 and 660 nm, making the course of oxidation easy to follow by UV/VIS spectrophotometry. This test constitutes the peroxidase activity detection system used here and extensively referred to in later sections (see Figure 1 and, for full details, see the experimental section).

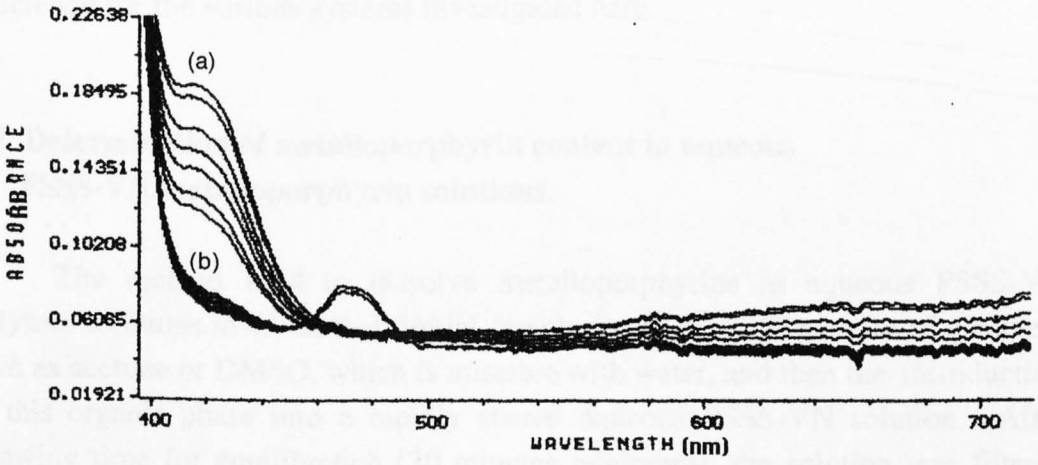

Figure 1. Visible absorption spectral sequence for oxidation of ABTS (1.7×10^{-3} $mol.L^{-1}$) by (a): pH 6 buffered FeTDCPPS (3×10^{-6} $mol.L^{-1}$) after 15 seconds, 1, 2, 3, 4, 6 and 7 minutes of H_2O_2 addition and (b): for MnTDCPPS under the same conditions. In the first experiment, the increase in $ABTS^{\cdot+}$ concentration is clearly visible from its characteristic absorption bands at 420 and 660 nm.

The rate law for ABTS oxidation with synthetic simple metalloporphyrins follows second order kinetics (Equation 1).[11]

$$\text{rate (V)} = \frac{d[ABTS^{\cdot+}]}{dt} = -2\frac{d[H_2O_2]}{dt} = k\,[\text{Mporph}]^1\,[H_2O_2]^1\,[\text{ABTS}]^0 \qquad (1)$$

Mporph is any metalloporphyrin complex. Under *pseudo* first order conditions, [Mporph]<[H_2O_2]<<[ABTS], and the value of the rate constant (k) is almost constant for different H_2O_2 concentrations. In the present research, the evaluation of peroxidase-like activity was made by measuring the observed initial rate constant for ABTS oxidation. This was done by plotting the amount of $ABTS^{\cdot+}$ formed *versus* time (minutes). At the beginning of reaction, the resulting line is approximately straight and these points were set to a linear fit. The slope of the line obtained from the linear fit is recorded as the observed rate (k_{obs}). From (1), the value of k_{obs} is dependent on metalloporphyrin concentration, and therefore,

$$k_{obs} = k'\,[\text{Mporph}]$$

and $$k' = \frac{k_{obs}}{[\text{Mporph}]}$$

in which k' is the normalised initial observed rate for ABTS oxidation. This experimental value (k') was selected for comparison purposes of peroxidative efficiency for the various systems investigated here.

1.2 Determination of metalloporphyrin content in aqueous PSSS-VN/metalloporphyrin solutions.

The method used to dissolve metalloporphyrins in aqueous PSSS-VN polymer solutions involves their initial dissolution in a small quantity of a solvent such as acetone or DMSO, which is miscible with water, and then the introduction of this organic phase into a rapidly stirred aqueous PSSS-VN solution. After allowing time for equilibration (30 minutes minimum), the solution was filtered through an 0.22μm teflon membrane filter, where any "undissolved" metalloporphyrin was retained. The resulting filtrate remained slightly coloured and its visible spectrum exhibited the characteristic metalloporphyrin "Soret" band. Based on known molar absorption coefficients (ε), the metalloporphyrin content in the aqueous polymer solution was easily calculated, assuming that the ε value for metalloporphyrin inserted into the hydrophobic domain was approximately that found for solution in organic solvents. In order to verify this

assumption, the porphyrin content was determined for a number of PSSS-VN/metalloporphyrin aqueous solutions by using a different analytical technique. Metal determination by atomic absorption spectroscopy (AA) was selected. Figure 2 provides a graph of the results for estimation of metalloporphyrin by VIS spectrophotometry plotted against those obtained by AA determination, for different PSSS-VN/metalloporphyrin solutions.

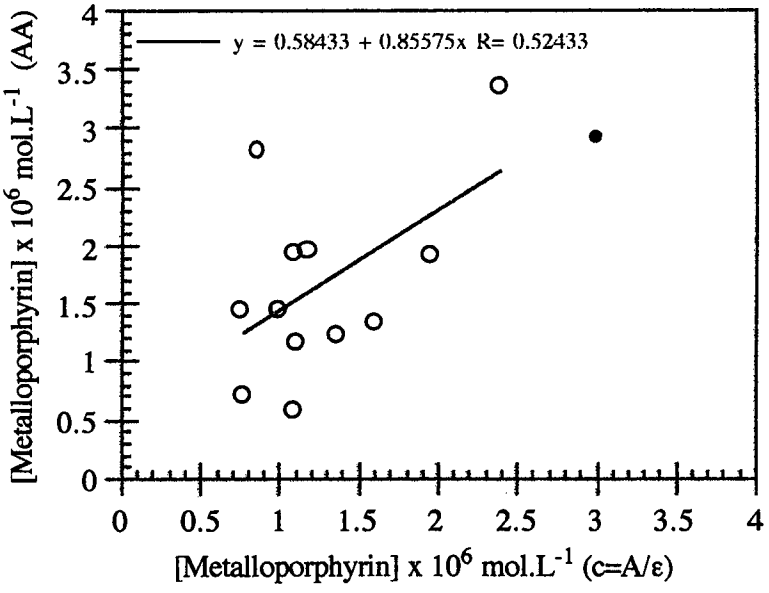

Figure 2. Plot of the metalloporphyrin quantification in PSSS-VN/ metalloporphyrin solutions by the visible spectrophotometric technique against those determined by atomic absorption spectrophotometry. The black dot represent the theoretical amount of porphyrin added to the system. A linear fit was applied to the dataset, the evaluated equation being shown together with the calculated correlation coefficient (R).

The plot and the scatter follow an approximate linear fit (slope = 0.86) showing that the VIS spectrophotometric technique results in a slightly lower metalloporphyrin estimation. The average difference between the two analytical techniques is about 12%. Taking into consideration the experimental simplicity of the VIS spectrophotometric technique, it was decided to use this as a standard for all subsequent work.

2. Reference assays

2.1. Assay of Horseradish peroxidase (HRP) activity

As a reference to compare the activity of metalloporphyrins and PSSS-VN/metalloporphyrin systems, a commercial sample of peroxidase (Horseradish; Fluka) was first examined for rate constant under the system conditions referred to above. The result for the *pseudo* first order rate of ABTS oxidation (k') was 4.24×10^5 min^{-1} (see details in the experimental section of Chapter 6).

2.2. Peroxidase activity of water soluble metalloporphyrins.

Fe, Mn, Co and Mo complexes of the water-soluble *tetrakis*(2,6-dichloro-3-sulfonatophenyl)porphyrin (TDCPPS)[12] were prepared. These were examined by the ABTS test oxidation under the conditions given above. The results are shown in Table 2.

Table 2. Normalised initial observed rate of $ABTS^{\cdot+}$ formation (k'), for different metalloporphyrins in aqueous solution.[a]

Metalloporphyrin	k' $min.^{-1}$
Fe(TDCPPS) (**1a**)	5.11
Mn(TDCPPS) (**1b**)	0.28
Co(TDCPPS) (**1c**)	0.10
Mo(TDCPPS) (**1d**)	0.06

a. Conditions: [metalloporphyrin] $\approx 3.0 \times 10^{-6}$ $mol.L^{-1}$; $[H_2O_2] = 0.83 \times 10^{-3}$ $mol.L^{-1}$; [ABTS] = 1.7×10^{-3} $mol.L^{-1}$. For further details, see experimental section of Chapter 6.

The results obtained seem to mimic Nature; iron complexes confer to the model kinetics the highest rate ($k' = 5.11$ min^{-1}), followed by manganese ($k' = 0.28$ min^{-1}, see Figure 1 of this Chapter). Use of either cobalt or molybdenum resulted only in very small rates ($k' = 0.099$ and 0.058 min^{-1} respectively).

3. Peroxidase activity of PSSS-VN/metalloporphyrin systems

3.1. Effects of metalloporphyrin structure: the central metal

Natural peroxidases exclusively use iron as the prosthetic metal centre. The degree of similarity of the present synthetic model relative to the natural enzyme is very small. In these circumstances, it is not obvious that use of iron as central metal should result in high peroxidase activity. For this reason, the present research began by determining the peroxidase-like catalytic activity of several sample metalloporphyrins (complexes of Fe, Mn, and Co with *tetrakis*(2,6-dichlorophenyl) porphyrin solubilized in co-poly(4-styrenesulfonic acid, sodium salt/2-vinylnaphthalene), which had been prepared from equal molar ratios of each monomer (PSSS-VN 50/50). The reason for testing these metals was determined by their capability for assuming different stable oxidation states. The results obtained are shown in Table 3.

Table 3. Normalised initial observed rate for $ABTS^{\cdot+}$ formation (k'), in aqueous PSSS-VN/ metalloporphyrin solutions.[a]

Metalloporphyrin	k' x 10 min^{-1}
Fe(TDCPP) (**2a**)	4.36
Mn(TDCPP) (**2b**)	0.52
Co(TDCPP) (**2c**)	0.51

a. Conditions: [metalloporphyrin] = 1.5 - 2.5 x 10^{-6} $mol.L^{-1}$; [H_2O_2] = 0.83 x 10^{-3} $mol.L^{-1}$; [ABTS] = 1.7 x 10^{-3} $mol.L^{-1}$. For further details, see the experimental section of Chapter 6.

The results show that peroxidase specific activities are one order of magnitude less than those of the water-soluble metalloporphyrins, ranging from 0.51 to 4.4 x 10^{-1} min^{-1}. Furthermore, the dependence of observed rates of substrate oxidation on metal type follows the order iron > manganese > cobalt (see Table 2). From these results, it was decided that subsequent experimentation should be restricted to Mn and Fe complexes because of the low activities found for Co porphyrin complexes.

3.2. Effects of metalloporphyrin structure: the ligand

An important difference between the present system and most others peroxidase models[13] centres on characteristics of the porphyrin ligand. Natural enzymic porphyrins possess substituents in the β-pyrrolic positions, whereas synthetic *meso*-phenyl substituted ligands are more common in synthetic models. The great use of the latter arises because of their relatively greater ease of synthesis and because of the beneficial shielding effect of phenyl groups, which prevent the rapid annihilation of porphyrin.[14] In PSSS-VN/metalloporphyrin systems the hydrophobic pockets form a sort of rugged enzyme domain. It is not certain under these conditions what are the best choices of ligands. In this present work, manganese and iron complexes of both *meso*-alkyl and -aryl porphyrins were prepared in order to test them with the system referred to above. Mixed alkyl/aryl *meso*-substituted porphyrins were synthesised and are included in the present study. Table 4 shows the results of using the Mn and Fe complexes of these different porphyrins on ABTS oxidation. The activity was also examined for different amphiphilic polymers, as indicated.

Table 4. Normalised initial observed rate of $ABTS^{\cdot+}$ formation (k'), in aqueous PSSS-VN/metalloporphyrin solutions.[a]

Polymer	PSSS-VN 50/50 (**6a**)		PSSS-VN 66/33 (**6b**)		PSSS-S[c] 66/33 (**7a**)	
Metal	Mn	Fe	Mn	Fe	Mn	Fe
Porphyrin	k' x 100 min^{-1}					
TDCPP (**2**)	4.28	43.60	23.20	*b*	1.05	8.20
TPP (**3**)	0.67	1.99	14.40	*b*	*b*	0.54
T(n-heptyl)P (**4**)[d]	7.32	4.77	*b*	2.10	*b*	2.70
(**5**)[e]	2.55	*b*	*b*	2.33	*b*	5.37

a. Conditions: [metalloporphyrin] = 1.5-2.5 x 10^{-6} $mol.L^{-1}$; [H_2O_2] = 0.83 x 10^{-3} $mol.L^{-1}$; [ABTS] = 1.7 x 10^{-3} $mol.L^{-1}$. For further details, see experimental section, Chapter 6; *b.* Not evaluated; *c.* PSSS-VN: co-poly(sodium 4-styrenesulfonic acid, sodium salt, 2-vinyl naphthalene), (50/50; initial molar ratios of hydrophilic monomer to hydrophobic monomer used in the preparation of the co-polymer); PSSS-S: co-poly(sodium 4-styrenesulfonic acid, sodium salt, styrene); *d.* 5,10,15,20-tetrakis-heptylporphyrin; *e.* 5-(2,6-dimethoxyphenyl)-10,15,20-*tris*-heptylporphyrin.

The behaviour of these different porphyrin ligand suggests the following (see Table 4). Use of TDCPP appears to produce greater activities but, in some cases, *meso*-alkyl porphyrins give better results than does simple TPP. TDCPP proved to be one of the best ligands in mimicing Cytochrome P450 activity with regard to its excellent stability towards oxidation.[15] The complex pattern shown

by the alkyl/aryl porphyrins, suggests that several activity/stability effects could be acting together.

3.3. Polymer structure

3.3.1. Relative monomer content

The first experiments on the PSSS-VN system used a polymer prepared from equal amounts of the hydrophobic and hydrophilic monomers. To investigate the effects of changing the ratio of the monomers on the peroxidase reaction model, a small number of polymers was prepared from different initial molar ratios of monomers. In each case, only the water-soluble polymer fractions were investigated. The results are shown in Table 5.

Table 5. Normalised initial observed rate for $ABTS^{\cdot+}$ formation (k'), using different aqueous PSSS-VN polymer/metalloporphyrin solutions.[a]

Initial molar ratio of monomers SSS/VN	Molar ratio of monomers in final polymer[b]	FeTDCPP (**2a**)	MnTDCPP (**2b**)
		k' x 100 min^{-1}	
80/20 (**6c**)	82/18	3.23	1.57
66/33 (**6a**)	76/24	4.90	3.76
50/50 (**6b**)	53/47	43.60	5.16
33/66 (**6d**)	31/69	*c*	23.20

a. Conditions: [metalloporphyrin] = 1.5-2.5 x 10^{-6} $mol.L^{-1}$; [H_2O_2] = 0.83 x 10^{-3} $mol.L^{-1}$; [ABTS] = 1.7 x 10^{-3} $mol.L^{-1}$. For further details, see the experimental section of Chapter 6; *b.* Determined by C, H, S elemental analysis; *c.* Not evaluated.

The results (Table 5) show that, as the vinyl naphathalene content increases, the specific peroxidase activity also increases, from to 1.57 to 23.2 x 10^{-3} min^{-1} when using MnTDCPP and from 3.23 to 43.6 x 10^{-3} min^{-1} for FeTDCPP. Even without characterising such composition changes in terms of structural modifications, it seems reasonable to expect a higher internal diameter of the hydrophobic micro domains as the initial proportion of vinyl naphthalene monomer increases. However, there is a problem associated with the use of polymers having large proportions of hydrophobic domains in that they become increasingly less soluble in water, which tends to off-set the increased inherent catalytic activity.

3.3.2. Use of other monomers for amphiphilic polymer synthesis

The above results were obtained using 4-vinylnaphthalene as the hydrophobic monomer in polymer preparation. This present section deals with the replacement of the naphthalene moiety by other hydrophobic structures.

3.3.2.1. Replacement of vinylnaphthalene by styrene

Replacement of naphthalene by phenyl was done by substituting vinyl-naphthalene for styrene in the polymer preparation. Use of styrene is particularly interesting because of its availability and low cost.

The results obtained with the use of different initial ratios of both monomers and the effects on peroxidase activity are displayed in Table 6.

Table 6. Normalised initial observed rate of $ABTS^{\cdot+}$ formation (k'), in co-poly(4-styrenesulfonic acid, sodium salt, styrene) polymers (PSSS-S)/metalloporphyrins aqueous solutions.[a]

Initial molar ratio of monomers SSS/S	Molar ratio of monomers in final polymer[b]	FeTDCPP (**2a**)	MnTDCPP (**2b**)
		k' x 100 min^{-1}	
66/33 (**7b**)	70/30	8.20	1.05
50/50 (**7a**)	50/50	5.54	1.22
33/66 (**7c**)	83/17	7.67	2.36

a. Conditions: [metalloporphyrin] = 1.5-2.5 x 10^{-6} $mol.L^{-1}$; [H_2O_2] = 0.83 x 10^{-3} $mol.L^{-1}$; [ABTS] = 1.7 x 10^{-3} $mol.L^{-1}$. For further details, see the experimental section of Chapter 6; *b.* Determined by C, H, S elemental analysis.

These styrene polymers lead to lower peroxidase activities, in the range of 5-8 x 10^{-2} min^{-1} for FeTDCPP and 1-2 x 10^{-2} min^{-1} for MnTDCPP. There is little variation in activity as the monomer ratio is changed, unlike the results shown in Table 5.

These polymers may have longer term stability, compared with the PSSS-VN polymers (see Section 6, in this Chapter).

3.3.2.2. Replacement of vinylnaphthalene by 9-vinylanthracene (VA)

Table 7 lists the peroxidase activities for the test reactions made with PSSS-VA polymers, prepared from different initial ratios of both monomers.

Table 7. Normalised initial observed rate of $ABTS^{\cdot+}$ formation (k'), in different PSSS-VA polymers/ Fe(TDCPP) aqueous solutions.[a]

Initial molar ratio of monomers SSS/VA	Molar ratio of monomers in final polymer[b]	FeTDCPP (**2a**)
		k' x 100 min^{-1}
66/33 (**8b**)	95/5	5.01
50/50 (**8a**)	92/8	4.93
33/66 (**8c**)	91/9	15.00

a. Conditions: [metalloporphyrin] = 1.5-2.5 x 10^{-6} $mol.L^{-1}$; [H_2O_2] = 0.83 x 10^{-3} $mol.L^{-1}$; [ABTS] = 1.7 x 10^{-3} $mol.L^{-1}$. For further details, see the experimental section of Chapter 6; *b.* Determined by C, H, S elemental analysis.

Table 7 shows that, in the preparation of these polymers, there is only a small hydrophobic monomer incorporation, in the range of 5-9%. In this situation, it is not certain if hydrophobic domains form, at least with the properties discussed in the Introduction of this Chapter. The results show lower specific peroxidase-like activities but, when the hydrophobic moiety content increases, there is a clear increase in peroxidase-like activity. Due to lack of time, the study was restricted to the use of iron porphyrins (see Table 7).

4. PSSS-VN polymers with covalently-linked metalloporphyrins

In terms of absolute peroxidase activities obtained with the use of PSSS-VN polymers, in some cases they are quite low (as, for example, when the polymer is soluble sparingly in water). One reason for this trend is probably the relatively small content of porphyrin in solution by the dissolution procedure (see experimental section of chapter 6). While the water soluble metalloporphyrins were used at concentration of 2-3 x 10^{-6} $mol.L^{-1}$ (for practical reasons), when using the PSSS-VN polymers, typical porphyrin concentrations are in the range of 2-9 x 10^{-7} $mol.L^{-1}$. Possibly modification of experimental methodology for

porphyrin dissolution will eventually increase that amount. One method to cincumvent this is to covalently link a metalloporphyrin to the PSSS-VN polymer. To accomplish this, suitable vinyl metalloporphyrins were prepared so that they could be incorporated in the polymerisation reaction (see experimental section of Chapter 6). The main results for peroxidase activity in the ABTS test are shown here in Table 8.

Table 8. Normalised initial observed rate for $ABTS^{\cdot+}$ formation (k'), in aqueous PSSS-VN/metalloporphyrin polymers.[a]

Covalently linked metalloporphyrin[b]	k' **x 100** min^{-1}
FeTPP (**9a**)	36.50
MnTPP (**9b**)	0.93

a Conditions: [metalloporphyrin] = 3.0 - 7.0 x 10^{-6} $mol.L^{-1}$; $[H_2O_2]$ = 0.83 x 10^{-3} $mol.L^{-1}$; [ABTS] = 1.7 x 10^{-3} $mol.L^{-1}$. For further details, see the experimental section of Chapter 6; *b*. Vinyl derivatives.

The specific peroxidase activity found in these systems, is about 15 times higher for FeTPP , and slightly better for MnTPP, when comparing with the same held in solution by PSSS-VN polymer (see Table 4). It must be highlighted that, with these polymers, very high absolute peroxidase activities can be reached because of the high metalloporphyrin content in the polymer.

5. Effects of the presence of nitrogenated bases

Discussion of peroxidase activity in terms of addition of nitrogen bases such as pyridine or imidazole to model systems has been covered in the Chapter 1. The use of amines improves peroxidase activity in several systems containing metalloporphyrins. The present study examined the same effects under two different sets of experimental conditions. The first was to use a covalent insertion of pyridine units in the amphiphilic polymer structure and the other was the simple addition to the reaction medium of exogenous substituted imidazoles.

5.1 Incorporation of covalently linked pyridyl groups into the polymer

Pyridyl groups were inserted in the amphiphilic polymer by synthesizing PSSS-VN polymer in the added presence of vinyl pyridine. Different proportions of pyridyl units in the amphiphilic polymer were examined in order to check for activity changes in the peroxidase model. The results are shown in Table 9.

Table 9. Normalised initial observed rate for $ABTS^{\cdot+}$ formation (k'), using pyridine containing PSSS-VN polymers/metalloporphyrin.[a]

Initial proportion of vinylpyridine % weight	FeTDCPP (**2a**)	MnTDCPP (**2b**)
	k' x 100 min^{-1}	
0.0 (**6b**)	4.90	3.76
4.3 (**10a**)	14.00	3.10
7.5 (**10b**)	5.78	2.63

a. Conditions: [metalloporphyrin] = 1.5-2.5 x 10^{-6} $mol.L^{-1}$; $[H_2O_2]$ = 0.83 x 10^{-3} $mol.L^{-1}$; [ABTS] = 1.7 x 10^{-3} $mol.L^{-1}$. Initial molar ratios of hydrophilic monomer to hydrophobic monomer used in the preparation of the co-polymer was approximately 33/66% molar. For further details, see the experimental section of Chapter 6.

The results show that, with FeTDCPP, use of 3% weight of vinyl pyridine in the polymer leads to an increase of about 3 times in activity, whilst use of a greater proportion of pyridine (7.5%) reduces the observed initial rate of oxidation of ABTS. For MnTDCPP, the presence of pyridine units clearly inhibits peroxidase activity. Probably, these results can be rationalised by considering two different factors: the possible double (*bis*) coordination of metalloporphyrins with imidazole or pyridyl ligands which would result in an catalytically inactive complex;[16] the presence of more soluble monomers (*viz.*, pyridine) may interfere with the stability of the polymer micro-domains, sizes or hydrophobicity (see also Section 6 in this Chapter).

5.2. Addition of exogenous imidazoles to PSSS-VN/metalloporphyrin peroxidase system

It was also decided to examine the effects of adding non-covalently bound imidazole to the reaction medium. In a preliminary test, a small quantity of 2-methylimidazole was added into a diluted PSSS-VN/MnTPP solution, for which the peroxidase activity is almost zero (Figure 3).

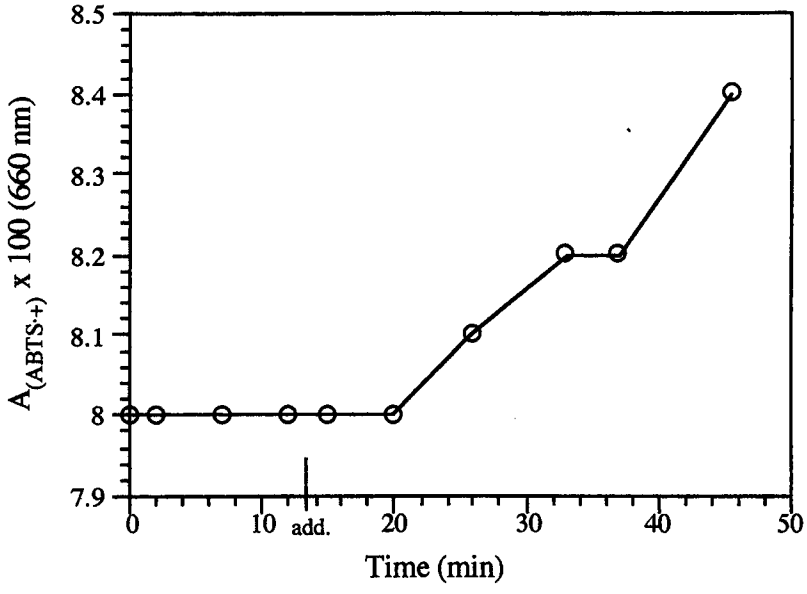

Figure 3. Plot of the characteristic 660 nm absorption band of $ABTS^{\cdot+}$ *versus* time, during a peroxidase assay of a dilute PSSS-VN/MnTPP solution, using H_2O_2. The plot shows the effect of adding 200μL of 2-methylimidazole solution (25 mg/100 mL; time = 13 min.). A pronounced increase in peroxidase activity is observed.

It is clear that from the point of addition of 2-methylimidazole, the peroxidase activity undergoes a big increase. This result prompted the investigation in a quantitative manner of the effects of the addition of increasing quantities of 1- and 2-methylimidazoles to the reaction medium. Both 1-methyl and 2-methylimidazoles were tested since work done with peroxidases and metalloporphyrins highlighted the better properties of the second base because it can coordinate but not to form a stable complex with the metalloporphyrin.[17]

Table 10 shows the effect of adding increasing quantities of 1-methylimidazole to the reaction medium, using covalently-linked metalloporphyrin/PSSS-VN polymers as peroxidase mimics.

Table 10. Normalised initial observed rate for $ABTS^{\cdot+}$ formation (k'), in PSSS-VN-metalloporphyrin aqueous solutions with increasing quantities of 1-methylimidazole.[a]

Final concentration of 1-methylimidazole mol.L^{-1} x 10^4	FeTPP in polymer (**9a**) k' x 100 min^{-1}	Final concentration of 1-methylimidazole mol.L^{-1} x 10^4	MnTPP in polymer (**9b**) k' x 100 min^{-1}
0.0	37	0.0	0.93
0.5	78	0.5	1.01
1.5	87	17	1.40
2.5	100	*b*	*b*
7.2	98		

a. Conditions: [metalloporphyrin] = 3.0-7.0 x 10^{-6} mol.L^{-1}; [H_2O_2] ≈ 0.83 x 10^{-3} mol.L^{-1}; [ABTS] ≈ 1.7 x 10^{-3} mol.L^{-1}. For further details, see the experimental section of Chapter 6.
b. Further values were not evaluated.

Table 11 is represents a similar study but with increasing concentrations of the isomeric 2-methylimidazole.

Figure 4 and 5 show the graphs representing initial observed rate constants for ABTS oxidation, plotted against the concentration of 1- or 2-methyl imidazole added, for polymers identified in Table 10 and 11.

Table 11. Normalised initial observed rate of $ABTS^{\cdot+}$ formation (k'), in PSSS-VN-metalloporphyrin aqueous solutions to which increasing quantities of 2-methylimidazole were added.[a]

Final concentration of 2-methylimidazole mol.L^{-1} x 10^4	FeTPP in polymer (**9a**) k' x 100 min^{-1}	Final concentration of 2-methylimidazole mol.L^{-1} x 10^4	MnTPP in polymer (**9b**) k' x 100 min^{-1}
0.0	37	0.0	0.93
0.4	78	2.1	1.43
1.3	87	6.0	2.53
2.1	100	7.9	2.00
6.0	112		
7.9	136		
11.4	160	*b*	*b*
14.6	157		
20.5	168		

a. Conditions: [metalloporphyrin] = 3.0-7.0 x 10^{-6} mol.L^{-1}; [H_2O_2] ≈ 0.83 x 10^{-3} mol.L^{-1}; [ABTS] ≈ 1.7 x 10^{-3} mol.L^{-1}. For further details, see the experimental section of Chapter 6;
b. Further determinations were not evaluated.

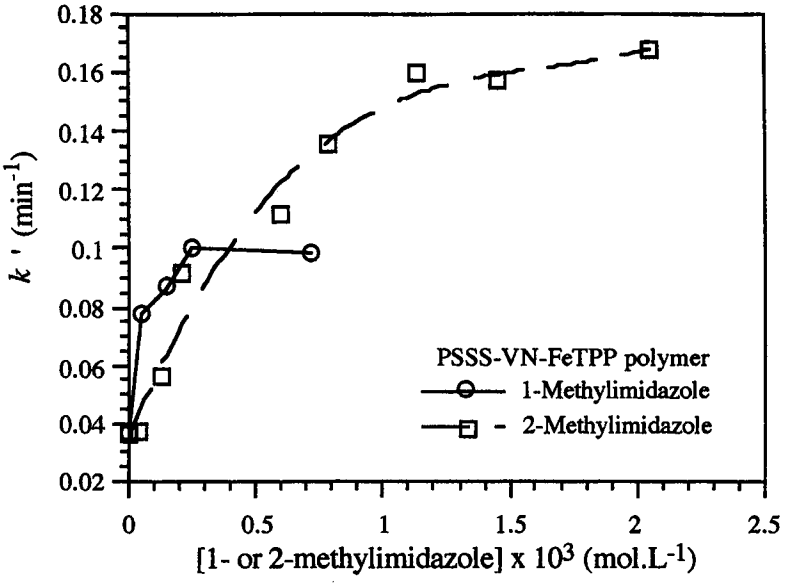

Figure 4. Graph of normalised initial observed rate (k') of ABTS oxidation for the PSSS-VN-FeTPP polymer (Table 10, 11) in the presence of increasing concentrations of 1- and 2-methylimidazole.

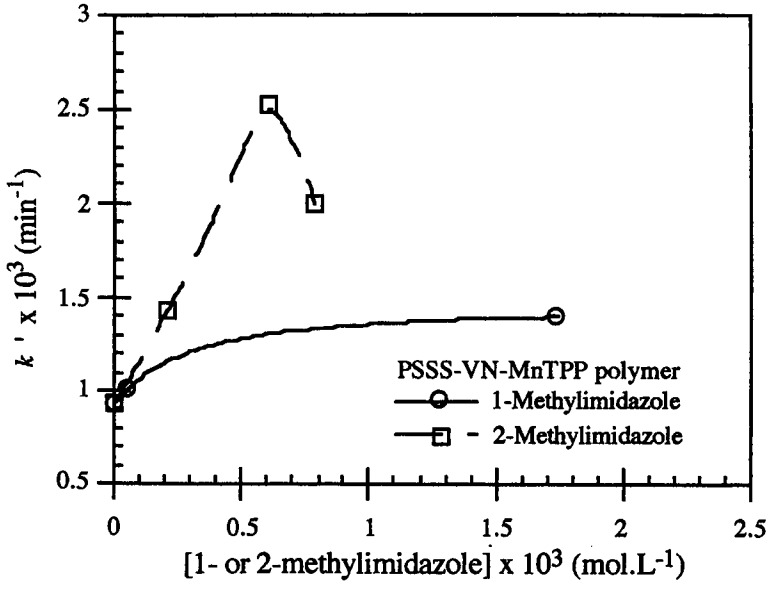

Figure 5. Graph of normalised initial observed rate (k') of ABTS oxidation for the PSSS-VN-MnTPP polymer (Table 10, 11) in the presence of increasing concentrations of 1- and 2-methyl imidazole.

These results are informative. With 1-methylimidazole, the rate of the peroxidase-like activity increases both with iron and manganese porphyrins but the beneficial effect is most pronounced for iron as the central metal of the porphyrin complex. In this last case, there seems to exist a maximum in the increase in activity relative to the amount of 1-methylimidazole added at about of 3×10^{-4} mol.L^{-1} (Figure 4). This maximum probably reflects the start of formation of the *bis*-imidazolyl metal complex, which is inactive toward peroxidase reaction (see earlier section and references therein).

The use of 2-methylimidazole imparts a big increase in the peroxidase activity, for both the Fe and Mn metalloporphyrins. While the benefiticial effect of 2-methylimidazole with the MnTPP polymer has a maximum at 5.2×10^{-3} mol.L^{-1}, the addition of further quantities of 2-methylimidazole to Fe porphyrin-polymer continues to increase the rate, reaching eventually a 5 fold increase. This increase in the rate observed with the FeTPP-polymer tends to diminish at concentrations of 2-methylimidazole greater than 1×10^{-3} mol.L^{-1}, probably due to the onset of formation of the *bis*-complex.

6. Stability of PSSS-VN polymers

The measured activity for a specific peroxidase system involving a PSSS-VN polymer has a tendency to decrease with increasing polymer shelf life. It is not difficult to accept that PSSS-VN polymers left in the light and in the presence of oxygen suffer oxidation reactions that eventually lead to major structural modifications. These may have drastic consequences in terms of hydrophobic microdomain structure and system activity for aqueous polymer solutions. Evidence of such polymer degradation was obtained by recording the infrared spectra of both a freshly made sample and one that was a year old. Partial spectra are presented in Figure 6.

The spectra are similar but the one-year old sample has an extra sharp absorption band at 3760 cm^{-1}. IR Tables suggest that this sort of band is caused by non-hydrogen bonding -OH groups. This is the sort of result expected for aerial oxidation.

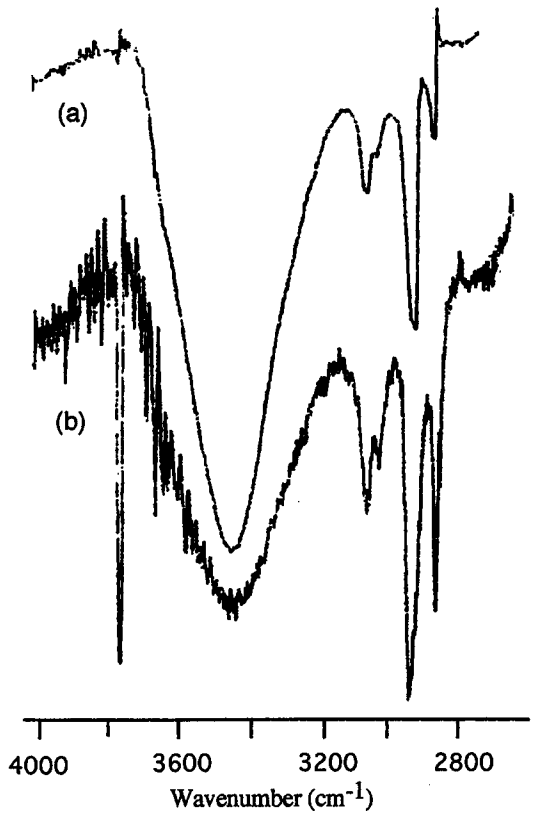

Figure 6. Partial IR spectra (2800-4000 cm^{-1}) of (a): a freshly prepared sample of co-poly-(4-styrenesulfonic acid, sodium salt, 2-vinyl naphthalene), prepared from an equal molar ratio of the monomers (PSSS-VN 50/50) and (b) a one-year old sample of the same polymer. This last sample has a sharp absorption band at 3760 cm^{-1}, which does not exist in the freshly made sample.

7. PSSS-VN/metalloporphyrins related heterogeneous systems.

This study includes a search for systems having close similarities with the initial PSSS-VN systems but made so as to be heterogeneous. Thus, the chosen polymer would not be amphiphilic but would contain naphthyl residues, similar to those in the PSSS-VN polymers. The first approach was based on a modification of a Merrifield polymer by using naphthyl units. The latter, if appropriately spaced, could form hydrophobic microdomains able to intercalate metalloporphyrins. The other approach takes advantage of an abundant, cheap, natural polymer (Chitin), which possesses free hydroxyl groups and secondary amidic groups that can co-ordinate with a metalloporphyrin, thus providing a method for anchoring them.

7.1 Modified Merrifield type polymers

Poly(4-chloromethyl)styrene (Merrifield resins) are extensively used to attach different funtional groups or molecules to the main resin backbone.[16] In the present work, Merrifield resins were modified by attaching 2-naphthoxy groups, as illustrated in Scheme 3, in which the chloromethyl groups are shown reacting with sodium 2-naphthoxide to give a polymer that might hold metalloporphyrins. The resulting polynaphthoxy material (PN) was insoluble in water and other organic solvents. Therefore, PN was stirred overnight with a concentrated solution of either iron or manganese TDCPP. The polymer was then filtered off and was washed exhaustively with dichloromethane until no more colour of porphyrin appeared in the filtrate. At this stage, the resin was highly coloured and clearly had strongly adsorbed a lot of metalloporphyrin. This material was used in tests for peroxidase activity, for which results which are listed in Table 12.

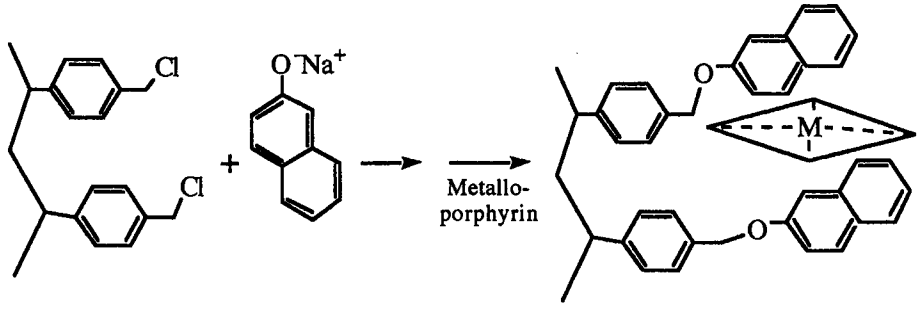

Scheme 3

Table 12. Normalised initial observed rate of $ABTS^{\cdot+}$ formation (k'), in aqueous solutions containing modified Merrifield resin/metallo-porphyrin.[a]

Metalloporphyrin in Merrifield resin	k' x 10^{6}[b] min^{-1}
FeTDCPP (**11a**)	2.36
MnTDCPP (**11b**)	2.14

a. Conditions: 10 mg/mL of metalloporphyrin modified Merrifield resin; $[H_2O_2]$ = 0.83 x 10^{-3} mol.L-1; [ABTS] = 1.7 x 10^{-3} mol.L-1. Total volume = 2.4 mL. For further details, see the experimental section of Chapter 6; *b.* The amount of metalloporphyrin was measured by atomic absorption spectroscopy for Fe and Mn on samples which had been calcinated at 500°C. (see experimental section).

The results obtained with this heterogeneous PN system resin/metalloporphyrins showed much smaller peroxidase activities (by a factor of 1000) when compared with the previous homogeneous amphiphilic polymers. The normalised initial rate constants obtained for both Mn and FeTDCPP oxidation of ABTS are about 2 x 10^{-6} min^{-1}. The iron complex is slightly better than that of manganese (Table 12).

7.2. Chitin based polymers

Chitin is an abundant natural polymer obtained from the exoskeletons of shellfish, in which the polymer repeat unit is an acetylated (β)-D-glucosamine (**1**) connected through β(1→4) linkages.[18] Chitin is known for its excellent absorption and adsorption properties. Most transition metals bind to chitin to form very stable complexes.[19] This property must be related to the presence of free hydroxyl groups and the amidic nitrogens that are able to coordinate to metal ions. If these groups were able to co-ordinate with the central metal of a metalloporphyrin, then chitin could be a convenient means to "immobilise" the porphyrins in a heterogeneous system. In the present study, chitin complexes were formed with iron, manganese and cobalt bound TDCPP (see experimental section for further details, Chapter 6).

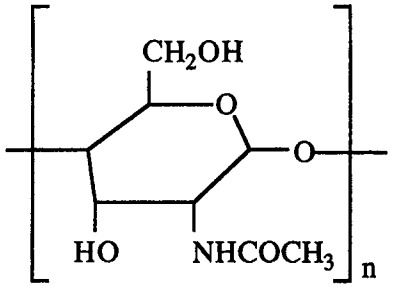

(**1**)

In Table 13 the peroxidase activities for three chitin "immobilised" iron, manganese and cobalt complexes of TDCPP are shown.

Table 13. Normalised initial observed rate of $ABTS^{\cdot+}$ formation (k'), in aqueous solutions of metalloporphyrins "immobilised" in chitin.[a]

Metalloporphyrin on chitin	k' **x** 10^4 [b] **min^{-1}**
FeTDCPP (**12a**)	2.41
MnTDCPP (**12b**)	1.74
CoTDCPP (**12c**)	2.03

a. Conditions: 5 mg/2.4 mL of chitin with adsorbed metalloporphyrin; $[H_2O_2]$ = 0.83×10^{-3} mol.L^{-1}; [ABTS] = 1.7×10^{-3} mol.L^{-1}. Total volume = 2.4 mL. For further details, see the experimental section of Chapter 6; *b.* Quantification of metalloporphyrin on chitin was carried out by visible spectrophotometry after extraction with methanol, see the experimental section, Chapter 6.

The chitin based metalloporphyrin heterogeneous polymers show peroxidase activities in the range of $k' = 1.7\text{-}2.4 \times 10^{-4}$ min^{-1}, *viz.*, better than those obtained with the modified Merrifield polymers but less than those obtained with PSSS-VN systems. As in the previous cases, iron metalloporphyrins attain the greatest activities. The activities obtained by using Co complexes with chitin are very close to the activity obtained by the use of iron porphyrins (Table 13), but there is not much difference for any of them.

III. Final discussion

The peroxidase mimic catalytic systems formed from the association of different amphiphilic polymers and metalloporphyrins has been introduced in this chapter. Others systems that have resemblance with these in terms of the close proximity of aryl rings to the metalloporphyrins were also made.

A comparison of the best relative rate constants for ABTS oxidation obtained in the different system-types assayed is presented in Table 14.

Table 14. Comparison of normalised initial observed rate constants for $ABTS^{\cdot+}$ formation (k') using best values for the different system-types studied in the present work.

Catalyst in system[a]	k' min^{-1}
Horseradish peroxidase (Fluka)[b]	4.2×10^5
FeTDCPPS[c]	5.1
FeTDCPP in PSSS/VN 50/50[d]	0.4
PSSS-VN-FeTPP in the presence of 2-imidazole[e]	1.7
FeTPP on chitin[f]	2.4×10^{-4}

a. See Section II, 1.1; *b.* See Section II, 2.1; *c.* See Section II, 2.2; *d.* See Section II, 3.1; *e.* See Section II, 5.2; *f.* See Section II, 7.2.

The work began with peroxidase-like activity assay of references, namely a peroxidase enzyme and water soluble metalloporphyrins. The natural peroxidase enzyme (HRP) gave the highest activity ($k' = 4.24 \times 10^5$ min^{-1}). The water-soluble metalloporphyrins as sulfonic acid derivatives of *tetrakis*-2,6-(dichlorophenyl) porphyrin, mimic this activity but with a 10^5 fold decrease in rate. There is a maximum activity for use of iron as central metal, as in FeTDCPPS ($k'_{FeTDCPPS}$ = 5.1 min^{-1}). Use of manganese, cobalt and molybdenum produces smaller activities, with normalised initial rate for ABTS oxidation of k'= 0.3, 0.1 and 0.06 min^{-1}, respectively. Besides this apparently tremendous activity gap, the simplicity of these compounds relative to the natural enzyme together with their facile synthesis made them some of the best catalysts found for peroxidase-like activity mimics. Their use has a major disadvantage, in the lack of good selectivity between peroxidase and mono-oxygenase activity.

Use of PSSS-VN polymers in aqueous solutions allows the inclusion of hydrophobic metalloporphyrins in hydrophobic micro-domains and the system does show peroxidase-like activity, with smaller but similar activities relatively to

the water soluble metalloporphyrins referred to above (k' = 0.52-4.4 x 10 min^{-1}). Different aspects of such systems were studied in the present work.

Use of Fe, Mn, Co and Mo as the central metal in the metalloporphyrins showed that iron gave consistently the best results, a behaviour that mimics that observed with the water-soluble metalloporphyrins models and with the natural enzyme (see Introduction, Section 3.1). In all cases, for which comparison can be made, manganese complexes gave peroxidase activities about ten times less than that of iron. For other transition metals such as Co and Mo, all systems gave very small oxidation rates in the peroxidase-like activity tests.

The structural characteristics of the ligand in the metalloporphyrins were also investigated, since their most suited requirements for high catalytic activity are not known for this system. *meso*-Phenyl, *meso*-heptyl and mixed *meso*-phenyl/heptyl substituents were tested. The results (Table 4) indicate that *meso*-dichlorophenyl complexes gave the best peroxidase activities. This suggests that phenyl groups bearing electron withdrawing substituents (as with Cl in TDCPP) enhance peroxidase-like activity. This result parallels others obtained for mono-oxygenase-like mimics, in which this ligand has proved to give the best results.[21] Comparison of the activities found for heptyl and mixed phenyl/heptyl *meso*-substituted porphyrins, reveals a pattern, which is difficult to interpret. The presence of a heptyl chain in the ligand led to smaller catalytic properties than for TDCPP but were generally better than those obtained with TPP alone. Use of mixed phenyl/heptyl substituents led to opposite results (see Table 4), suggesting the influence of others effects.

The polymer characteristics necessary for high catalytic activities were also studied. The first objective of study was the use of different proportions of hydrophobic/hydrophilic monomers used in preparation of the polymer and the effects of these different proportions on peroxidase-like activity. From these studies (Table 5, 6, and 7), it appears that increasing the proportion of hydrophobic monomer in the polymer favours higher activities. However, an associated difficulty is the increasing insolubility of the polymer in water as the hydrophobic monomer content is increased. In the present study, a proportion of 66/33 (percentage molar) for the respective hydrophobic/hydrophilic monomers was found to be best because there was a gain in terms of peroxidase activity without any significant reduction in the aqueous solubility of the polymer.

Other monomers than vinylnaphthalene were tested as the hydrophobic part of the amphiphilic polymer, namely styrene and 9-vinylanthracene. Use of these last yields PSSS-S and PSSS-VA polymers, respectively (see Section 3.3.2). In the case of PSSS-VA polymers, C, H, N and S analysis suggest that a very low degree of vinylanthracene had been incorporated. The peroxidase-like activities

found when using these last polymers, follows a trend PSSS-VN>PSSS-S>PSSS-VA (the initial proportions of the monomer were equimolar in each case). Changes in microdomain characteristics probably occur so as to lead to the observed results. Further investigations on the causes of such effects were not made.

The above discussion allows a summary of the different characteristics of amphiphilic polymer/metalloporphyrin systems required to obtain higher peroxidative activities: (i) use of iron metalloporphyrins, (ii) use of TDCPP as a ligand in the metal complex, (iii) as between phenyl, naphthyl or anthranyl in the polymer as hydrophobic components, naphthyl is the best choice, (iv) a higher ratio of hydrophobic to hydrophilic monomers in the polymer structure (such as 66/33 % molar) is recommended, (v) the addition of exogenous imidazoles (those that do not form stable complexes with metalloporphyrins such as 2-methylimidazole) is beneficial, as discussed below. Systems which incorporate the above requisites, exhibit very good peroxidative properties, which coupled with the intrinsic PSSS-VN polymer characteristics, make a potential system for use in applications where hydrophobic molecule concentration and peroxidase-like activity are required.

Two experimental observations were not completely studied in this work but deserve attention in future developments. One was the apparently low stability of the PSSS-VN polymer, as revealed by IR spectra recorded on a one year old sample in comparison to an other which was freshly made. The first sample shows a new band, attributed to the presence of non-hydrogen bonding -OH groups. Taking in consideration the presence of aromatic groups in the polymer capable of absorbing light and transferring this energy to species such as oxygen, the observation of oxidation is not surprising. This may be related with the other aspect observed in this work, *viz.*, a lack of good reproducible activity measurements in the peroxidase-like tests when using PSSS-VN polymers, especially if their preparation was spaced by relatively long periods of time or if different batches of the same polymer were used. However, these are relatively minor drawbacks affecting how the polymer should be stored and a need for precise control of reaction conditions during their preparation.

The preparation of amphiphic polymers to which metalloporphyrin were covalently linked was also considered, through the synthesis of vinylmetalloporphyrins such as iron(III)- and manganese(III) 5-(4-vinylphenyl)-10,15,20-*tris*-phenylporphyrin chloride. The specific peroxidase activities found in these systems (e. g., $k'_{FeTPP} = 0.4$ min^{-1}) are similar to the highest obtained with PSSS-VN/FeTDCPP but are significantly better than for FeTPP and MnTPP simply held in solution by the PSSS-VN polymers through non-bonded interactions. This fact suggests that use of porphyrins bearing electron withdrawing substituents in

the polymer may even reach higher peroxidase-like activities than those obtained with the polymers used here. An important fact in this case is the amount of metalloporphyrin that can be incorporated in these polymers. This can reach very high concentrations, leading to the attainment of very high absolute peroxidase activities, which were the highest obtained throughout this work with exception of Horseradish Peroxidase itself.

Another factor found to give even greater peroxidase-like activities was the addition of N-blocked imidazoles to the reaction medium, both for PSSS-VN polymers with dissolved metalloporphyrins or for the metalloporphyrin covalently linked to amphiphilic polymers. These ligands have a close resemblance to those in the natural system (see Introduction to this thesis) and recover activity in mutated enzymes, which do not possess a distal histidine.[20] In this present study, addition of 1-methylimidazole to the PSSS-VN-metalloporphyrin system proved to be beneficial to a limited extent, probably due to its ability to form a stable and inactive *bis* complex with the metalloporphyrins metal. Much more efficient was the use of 2-methylimidazole, which gave a 4 to 5-fold increase in peroxidative-like activity rate obtained with the PSSS-VN-FeTPP polymer (k' increased from 0.4 min^{-1} to 1.7 min^{-1}; Table 11). Less successful was the incorporation of pyridyl groups in the PSSS-VN polymer backbone, which even in a small concentration appeared to interfere with the aqueous structure of the polymer, thereby interfering with the peroxidase activity.

The heterogeneous catalysts prepared in the present studies, revealed small activities when tested in the ABTS peroxidase test. For modified Merrifield resins containing metalloporphyrins $k' = 2 \times 10^{-6}$ min^{-1} and, $k' = 1.7\text{-}2.4 \times 10^{-4}$ min^{-1} for chitin-based polymers. These results certainly reflect the presence, of a solid/liquid interface, in which the surface area of the solid controls the rate, as against the homogeneous systems in solution, where reactant encounter is controlled by diffusion. It should be stressed that no characterisation was made of the superficial specific surface area in the prepared resins. However, it was clear that the particle size of the resins used were high and no attempts were made to increase this area, by grinding the powder for example. This fact strengthens the relevance of these results, especially in the case of the chitin-based polymers. Other potential advantages of these systems are the probability of better long-term storage stability and their ease of use and recovery in the catalytic activity. Chitin is particularly cheap as a support, being the second most abundant organic substance after cellulose.

IV. References

1. M. Nowakowska, B. White and J. E. Guillet, *Macromolecules*, 1988, **21**, 3430.

2. M. Nowakowska, B. White, and J. E. Guillet, *Macromolecules* , 1989, **22**, 2317.

3. P. M. Macdonald, D. Staring and Y. Yue, *Langmuir*, 1993, **9**, 381.

4. B. White, P. Johnson and J. E. Guillet, *Polym. Int.*, 1993, **30**, 401.

5. G. J. Vancso, B. R. White and J. E. Guillet, *Eur. Polym. J.*, 1993, **29**, 751.

6. E. Sustar, M. Nowakowska and J. E. Guillet, *J. Photochem. Photobiol.*, 1992, **63**, 357.

7. M. Nowakowska and J. E. Guillet, *Chem. Britain*, 1991, **27**, 327-330.

8. Paul Stocks, PhD Dissertation, The University of Liverpool, 1995.

9. R. A. W. Johnstone, A. J. Simpson, P. A. Stocks, *Chem. Comm.*, 1997, 2277.

10. J. Putter and R. Becker in, *Methods of Enzymatic Analysis*, 1985, Vol. 3. Eds. H. U. Bergmeyer, VCH Publications, Weinheim, page 286 *et seq.*

11. R. Panicucci and T. C. Bruice, *J. Am. Chem.Soc.*, 1990, **112**, 6063.

12. A. M. d'A. Gonsalves, R. A. W. Johnstone, M. M. Pereira, A. M. D. deSantana, A. C. Serra, A. J. F. N. Sobral, P. A. Stocks, *Heterocycles*, 1996, **43**, 829.

13. R. J. Cheng, L. Latos-Grazynski, A. L. Balch, *Inorg. Chem.*, 1982, **21**, 2412.

14. M. F. Zipplies, W. A. Lee, and T. C. Bruice, *J. Am. Chem. Soc.*, 1986, **108**, 4433.

15. B. Meunier, *Chem. Rev.*, 1992, **92**, 1411.

16. P. R. Cooke, J. R. L. Smith., *J. Chem. Soc., Perk. Trans.*, 1994, 1913.

17. T. Uno, A. Takeda, S. Shimabayashi, *Inorg. Chem.*, 1995, **34**, 1599.

18. M. Poulicek, F.Gaill, G. Goffinet, *ACS Symposium Series*, 1998, **707**, 163.

19. See for example: H. Minamisawa, H. Iwanami, N. Arai, T. Okutani, *Anal. Chim. Acta*, 1999, **378**, 279; L. Zhang, L. Zhao, Y.T. Yu, C. Z. Chen, *Water Res.* 1998, **32**, 1437; M. T. S. D. Vasconcelos, C. A. R. Gomes, *Eur. Polym. J.*, 1997, **33**, 631.

20. S. L. Newmyer, P. R. O. Demontellano, *J. Biol. Chem.*, 1996, **271**, 14891.

21. A. M. d'A. Gonsalves, M. M. Pereira, *J. Mol. Cat. A. Chem.*, 1996, **113**, 209.

CHAPTER 3: SYNTHESIS AND CHARACTERIZATION OF MODEL PORPHYRINS

I. Introduction

The PSSS-VN polymers, when dissolved in aqueous solutions form hydrophobic domains, in which metalloporphyrins can be inserted. Such an assembly establishes a system that shows good peroxidase activity (Chapter 2). The metalloporphyrin in a polymer domain is in a region of hydrophobicity, *viz.*, close to the naphthyl polymer groups. This close proximity may facilitate the peroxidase mechanistic pathway through assisting electron transfer steps involved in Compound I and Compound II formation (Chapter 1). Following on from this possibility, a main goal of the present study was the formation of synthetic model porphyrins, possessing an aromatic section such as phenyl or naphthyl, linked by a covalent bond to the porphyrin ring and in such a position as to allow some interference with the macrocyclic part of the porphyrin itself, *viz.*, to attempt to synthesize "sandwich" mimics of the polymer system (see Scheme 1)

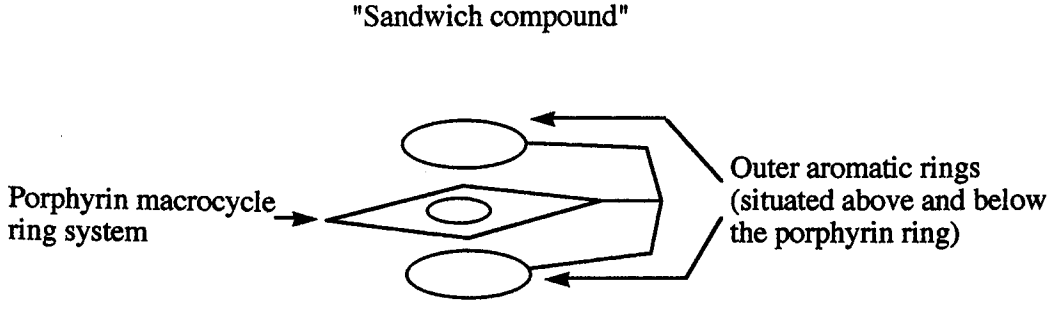

Scheme 1

This chapter describes the preparation and characterisation of such "sandwich" compounds. Subsequent chapter describe their use in peroxidase-like catalytic models.

Structures possessing planar aromatic parts in close proximity to each other are known, both in natural and in synthetic systems. For example, floral coloration

is attributed to planar molecules (anthocyanidins) that are known to be stacked with others planar structures.[1] Electron donor/acceptor complexes are formed when some organic molecules are allowed to interact. Thus, picric acid and aromatic hydrocarbons[2] and porphyrin with covalently-linked aromatic elements are well documented.[3-7] Special properties arise for the compounds having such characteristics.

II. Results and Discussion

1. Strategy in designing porphyrins having covalently-linked aromatic sections

The objective of incorporating in the same molecule both a porphyrin macrocycle and another aromatic structure, was targeted after taking into account various possible covalent linkages between the sections. In an attempt to simplify the synthesis of such relatively large molecules, some readily available porphyrins, namely substituted 5,10,15,20-*tetrakis*arylporphyrins were selected as starting points. These were used to incorporate the necessary structural functions that would allow subsequent attachment of suitable aromatic elements. A study with computer models[8] suggested that *meso*-2-hydroxy- or 2,6-dihydroxyphenyl-porphyrins could be esterified with several aromatic acids to providing an anchorage that would position the aromatic group in the desired proximity to the porphyrin ring. This approach was developed in the present work. Scheme 2 depicts the approach diagrammatically. The starting point for the preparation of such compounds was an asymmetric *meso*-substituted porphyrin, in which R could be phenyl or heptyl and R' a hydroxyphenyl group (Scheme 2a). This last shows the linkage after reaction of the hydroxy compounds with acyl chlorides, in which R" is tolyl, naphthyl or the anthranyl. For example, this led to the preparation of the tolyl-substituted porphyrin (R = phenyl) or the *bis* naphthyl-substituted porphyrin (R = heptyl). In all following descriptions where reference is made to substituents located above or below the plane of the porphyrin macrocycle, the designation *aromatic ring* is used through this work, even though the porphyrin itself could be considered aromatic.

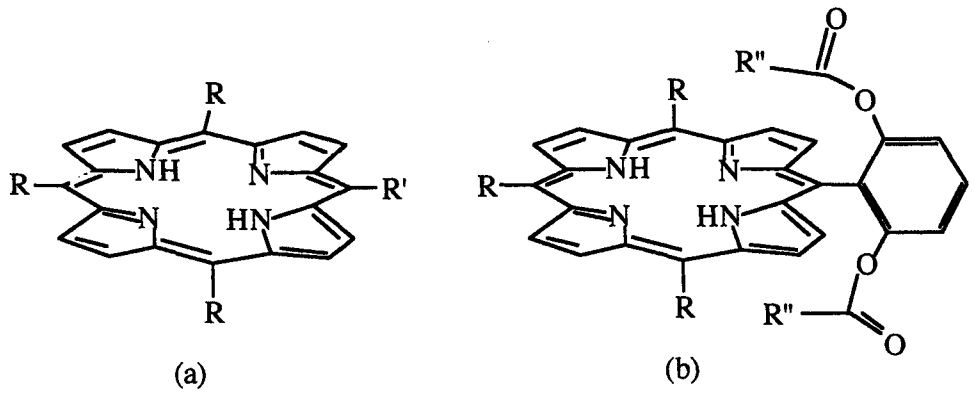

R = Phenyl or heptyl groups
R' = Substituted phenyl (2-hydroxy or 2,6-dihydroxyphenyl)
R" = Covalently linked aromatic rings (tolyl, naphthyl or anthranyl)

Scheme 2

The aromatic rings selected to be incorporated in the porphyrins were 4-tolyl, 2-naphthyl and 9-anthranyl. The selection of these groups parallels the monomers used for the preparation of the amphiphilic polymers, described in Chapter 2.

The presence of aromatic rings in the aryl-substituted porphyrins forms a steric barrier around the porphyrin macrocycle. As a means of diminishing this effect, porphyrins possessing the smaller *meso*-heptyl groups were also prepared (Scheme 2). The types of compounds prepared are shown in Table 1.

Table 1. Structures of porphyrins prepared in the present work.

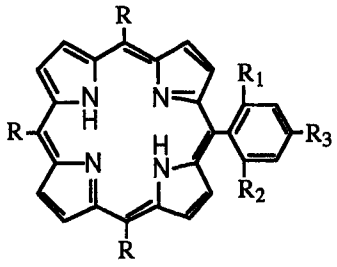

Compound number	R	"Aromatic group"		
		R_1	R_2	R_3
(1)	heptyl	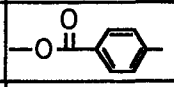	H	H
(2)	heptyl	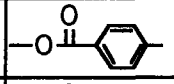	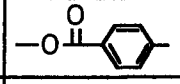	H
(3)	phenyl	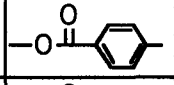	H	H
(4)	phenyl	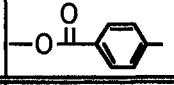	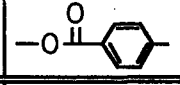	H
(5)	heptyl	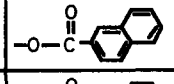	H	H
(6)	heptyl	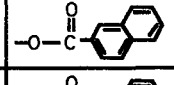	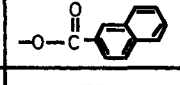	H
(7)	phenyl	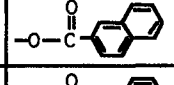	H	H
(8)	phenyl	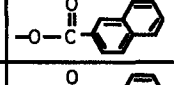	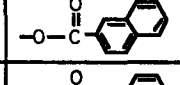	H
(9)	phenyl	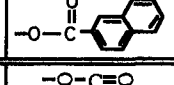	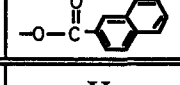	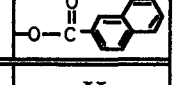
(10)	heptyl	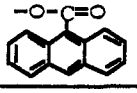	H	H
(11)	heptyl	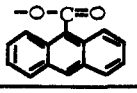	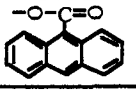	H
(12)	phenyl	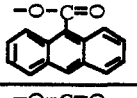	H	H
(13)	phenyl	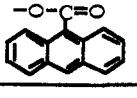	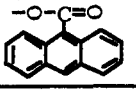	H

2. Porphyrin synthesis

Scheme 3 shows the stepwise method used to prepare the compounds shown in Table 1, with 5-(2,6-*bis*-[2-oxycarbonylnaphthalene]phenyl)-10,15,20-*tris*-phenylporphyrin (**8**) chosen to illustrate the synthesis. Complete details are presented in the experimental section of Chapter 6. Because of their ease of preparation and greater stability, the required hydroxyphenyl porphyrins were made *via* the corresponding 2-methoxy- or 2,6-dimethoxyphenylporphyrin (Scheme 3). The simple Rothemund-Adler method[9] or the method recently introduced with nitrobenzene/acetic acid as solvent were used to make such porphyrins.[10] The need of start with an asymmetrically *meso* substituted porphyrin required the use of a mixture of two different aldehydes as reactants. Such a reaction gives a product, which is a "statistical" mixture of porphyrins, from which the desired compound may be separated by application of flash chromatography or preparative TLC (only for some difficult separations). Subsequently, these initial methoxy compounds were demethylated with hydrobromic acid to give the mono- or dihydroxyphenylporphyrins, which were purified and then reacted with the required acid chloride, so as to form the compounds (**1-13**) shown in Table 1.

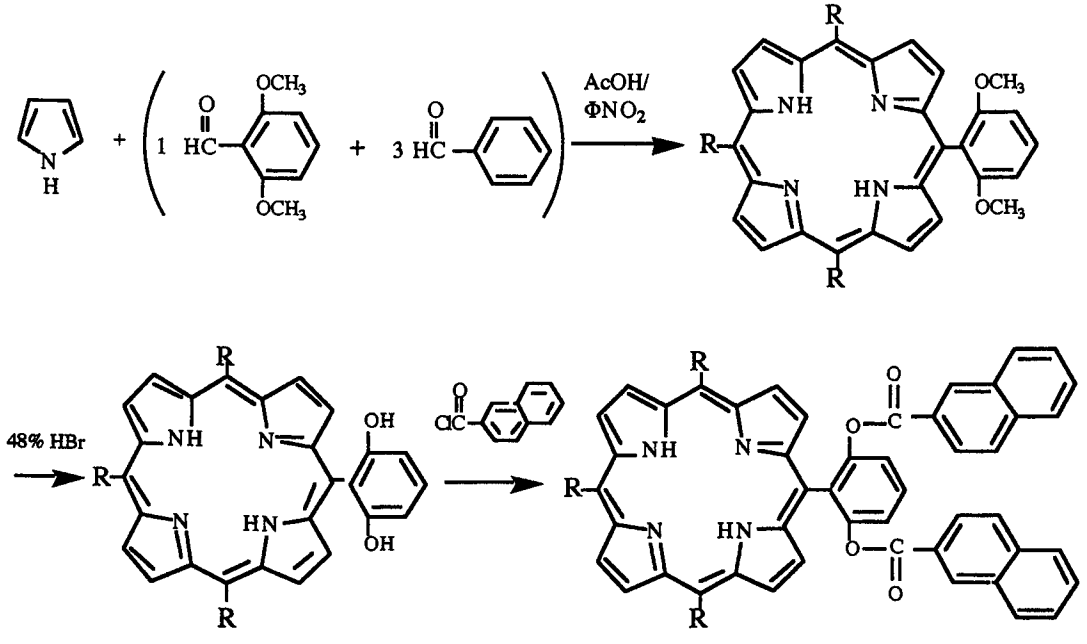

Scheme 3

3. Conformational aspects of porphyrins

Porphyrins having similar structural characteristics to those selected for preparation in this present work have been synthesised and characterised.[3-7] A series of 5,15-diaryl-2,3,7,8,12,13,17,18-octamethylporphyrins substituted with sulphonyloxyanthraquinonyl and dimethylaminophenyl groups has been described.[3,4] When dissolved in solvents such as chloroform, these substances assume a folded conformation (exemplified in Scheme 4a), in which the aromatic ring adopts a position close to the porphyrin macrocycle, instead of the extended conformation (Scheme 4b) that might have been expected.

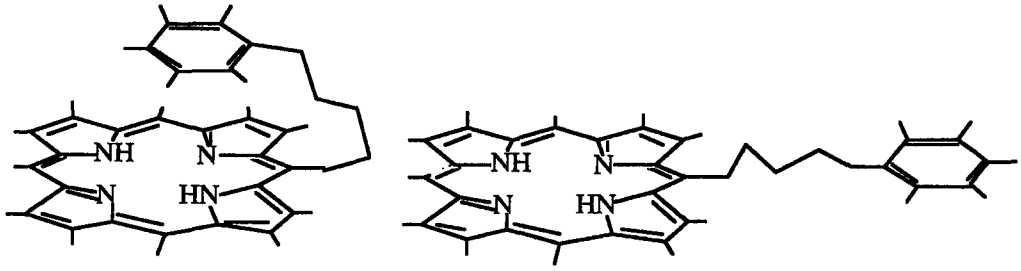

(a) (b)

Scheme 4

The folded conformation was deduced from ^1H NMR measurements, in which the protons of the aromatic ring show upfield shifts, demonstrating their close positioning relative to the porphyrin macrocycle. Porphyrin aggregation and stacking was ruled out through dilution experiments. The effect was seen with both electron-donating and electron-withdrawing aromatic rings, and is especially important when the link between the porphyrin and an aromatic ring is made through a sulphonyloxy group (-SO_2O-).[3] This preference was observed also in other compounds, such as in benzyl phenyl sulphones, N-[(arylsulphonyl)-methyl]-N-methyl carbamates and p-toluenesulfonic esters of aromatic hydrocarbons.[3,4]

4. Characterisation of porphyrins by ^{1}H NMR

4.1. 5-[4-Oxycarbonyltoluene]phenylporphyrins series

Scheme 5 shows the structure and the ^{1}H NMR spectrum of (a) 5-(2,6-*bis*-[4-oxycarbonyltoluene]phenyl)-10,15,20-*tris*-heptylporphyrin (**2**) in $CDCl_3$ and (b) shows the same compound in a mixture of $CDCl_3/CF_3CO_2H$ (1/1). The corresponding COSY spectra were obtained in order to assist in the assignment of proton signals (see Experimental Section).

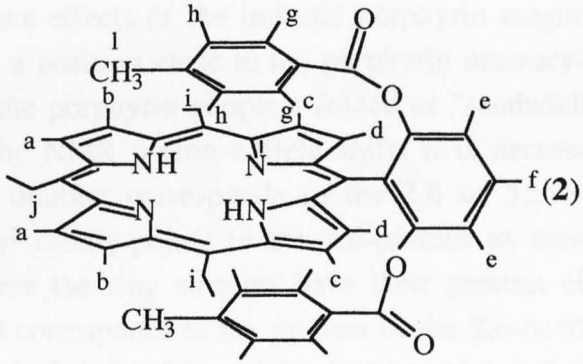

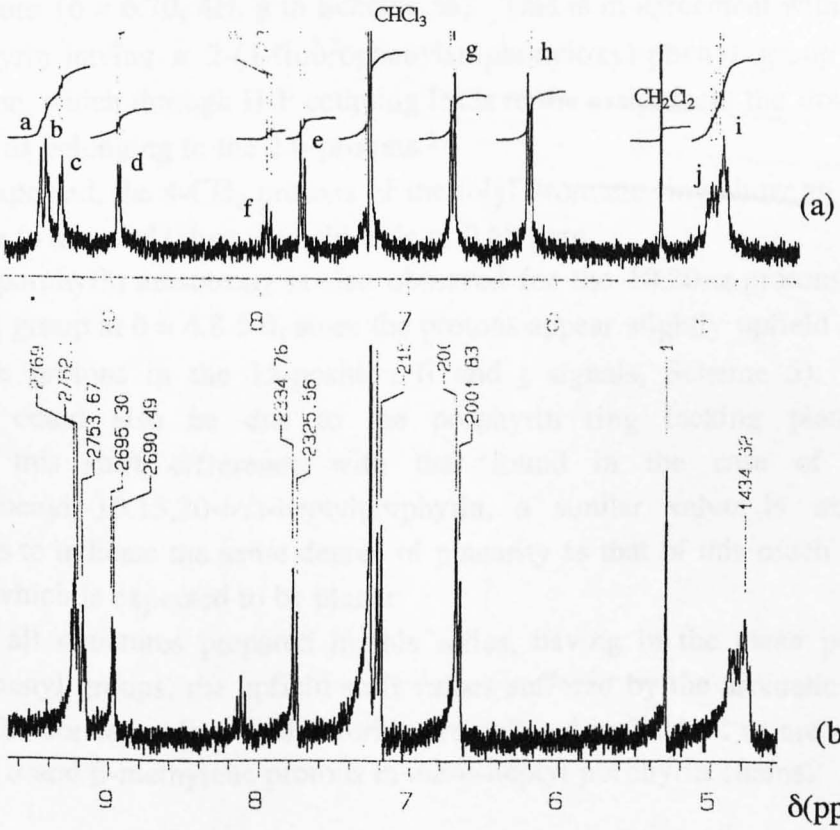

Scheme 5

The β-pyrrolic protons are clearly identified as low field peaks a, b, c, d in Scheme 5 (δ = 8.8-9.4, 4 x 2H), showing the expected four doublets reflecting the two-fold symmetry of the compound. At δ = 7.8-8.0 there is a triplet (f, 1H) and a doublet (e, 2H), due to the single *meso*-phenyl group. At higher field, two pairs of doublets appear, clearly assignable to the 4-tolyl aromatic ring attached as an ester substituent on the phenyl in the *meso* position. These signals are shifted to high field relative to the normal resonances in the free acid. For example, 4-toluic acid chloride has ^{1}H signals at δ = 7.28 and δ = 7.97. The NMR spectrum is invariant if taken at different porphyrin concentrations, thereby negating any possibility of aggregate formation. In these circumstances, the observed shifts indicate that the 4-tolyl groups suffer the effects of the induced porphyrin magnetic field. Thus, this group must be in a position close to the porphyrin macrocycle, which is the situation expected if the porphyrin adopts a folded or "sandwich" conformation. In order to quantify the NMR proton upfield shifts it is necessary to determine unequivocally which doublet corresponds to the 2,6 or 3,5 tolyl protons. A computer model study[8] clearly points to the 2,6-protons as being closest to the porphyrin centre, where the ring currents have their greatest effect. Thus, the doublet at higher field corresponds to the protons in the 2,6-positions of the tolyl group (δ = 6.19, 4H, h in Scheme 5a), and the doublet at lower field corresponds to the 3,5-protons (δ = 6.70, 4H, g in Scheme 5a). This is in agreement with results for a porphyrin having a 2-(4-fluorophenylsulphonyloxy)-phenyl group at the *meso* position, which through H-F coupling leads to the assignment the doublet at higher field as belonging to the 2,6-protons.[5]

As expected, the 4-CH_3 protons of the tolyl aromatic ring show an upfield shift relative to those of toluic acid chloride of 0.68 ppm.

The porphyrin anisotropy is also observed for the 10,20-α-protons in the *meso* heptyl group at δ = 4.8-5.0, since the protons appear slightly upfield relative to the same protons in the 15-position (i and j signals, Scheme 5). These differences could also be due to the porphyrin ring lacking planarity.[11] Comparing this shift difference with that found in the case of 5-(2,6-dimethoxyphenyl)-10,15,20-*tris*-heptylporphyrin, a similar value is observed, which seems to indicate the same degree of planarity as that of this much simpler porphyrin, which is expected to be planar.

For all structures prepared in this series, having in the *meso* positions heptyl or phenyl groups, the upfield shift values suffered by the aromatic ring(s), relative to the corresponding acid chloride are collated in Table 2 as are also the splits of the α and β-methylene protons in *meso*-heptyl porphyrin chains.

Table 2. ^{1}H NMR upfield shifts in aromatic ring protons[a] and α/α'- and β/β'-heptyl methylene protons shift difference in 5-(4-oxycarbonyltoluenephenyl)-porphyrins.

Compound	(1)	(2)	(3)	(4)
R[b]	Heptyl	Heptyl	Phenyl	Phenyl
Aromatic ring(s)	Tolyl	*bis*-Tolyl	Tolyl	*bis*-Tolyl
Protons	^{1}H NMR shifts (Δδ)			
3,5-Tolyl	0.99	1.09	0.93	1.03
2,6-Tolyl	1.11	1.29	1.08	1.22
1-CH_3 (Tolyl)	0.68	0.73	0.62	0.67
α_{CH_2}, α'_{CH_2}[c]	0.07	0.08	—	—
β_{CH_2}, β'_{CH_2}[c]	≈ 0	0.03	—	—

a. Upfield shifts relative to 4-toluic acid chloride; b. *meso*-10,15,20 substituents (see Section 1 of this Chapter); c. Protons in α/β (10,20-porphyrin positions) and in α'/β' (15-porphyrin position) carbons of the *meso*-heptyl chains.

Table 2 shows the upfield shifts in the tolyl ring protons and those in the 1-methyl group. The respective values are very similar both in the *meso*-heptyl and *meso*-phenyl substituted porphyrins, but being slightly greater in the former. This suggests that all of these compounds adopt a folded conformation, when dissolved in $CHCl_3$. The other result shown in Table 2 is that porphyrins having double aromatic ring substitution (one at each face of the porphyrin ring) give greater upfield chemical shifts for their protons. This effect is observed both in the *meso*-heptyl and *meso*-phenyl substituted porphyrins.

4.1.1. The effect of addition of acid to porphyrins (1-4) in $CDCl_3$ solution

The ^{1}H NMR spectrum of a solution of (2) in $CHCl_3/CF_3CO_2H$, in which the porphyrin is in the dication form ($PorphH_2^{2+}$) is also shown in Scheme 5. As can be seen, the signals corresponding to the 2,6- and 3,5-tolyl protons show a significant downfield shift, relatively to the spectra taken in $CDCl_3$, to a position slightly upfield relative to these protons in toluic acid chloride. A similar effect is observed for the 1-methyl of the tolyl group. This behaviour has been observed earlier with related compounds[3-6] and indicates that, in these species, the aryl rings have been shifted from facing the macrocyclic porphyrin ring to a more distant position. For the *meso*-phenyl substituted porphyrins, this same effect was observed. The α- and β-methylene protons of the *meso*-alkyl substituents (R), appear to be little modified relative to free-base ^{1}H NMR spectra.

An asymmetric positioning of the two aromatic rings was observed in the spectrum of the 5-(2,6-*bis*[4-oxycarbonyltoluene]phenyl)-10,15,20-*tris*-phenyl-porphyrin (**4**), taken in $CHCl_3/CF_3CO_2H$ solution (Scheme 6).

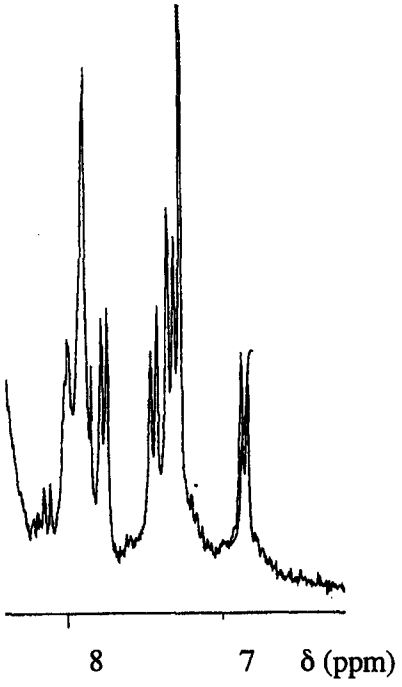

Scheme 6

The spectrum show four pairs of doublets, assigned to the 2,6- and 3,5-protons of the tolyl group. This sort of spectrum is to be expected if the tolyl groups in compound (**4**) are positioned at different distances from the porphyrin ring. The reason for the observed spectrum is not clear but is discussed at the end of this Chapter.

^1H NMR spectral data are collated in Table 3. The small upfield shift in the *bis*-aryl substituted porphyrins relative to the mono-substituted porphyrins has been found before (Table 1) and is also observed in the dication form.

Table 3. ^{1}H NMR upfield shifts in aromatic ring protons[a] and α/α'- and β/β'-heptyl methylene protons shift difference in 5-[4-oxycarbonyltoluene]phenyl porphyrins dications.

Compound	(1)	(2)	(3)	(4)
R[b]	Heptyl	Heptyl	Phenyl	Phenyl
Aromatic ring(s)	Tolyl	*bis*-Tolyl	Tolyl	*bis*-Tolyl
Protons	^{1}H NMR shifts (Δδ)			
3,5-Tolyl	0.47	0.59	*d*	*e*
2,6-Tolyl	0.70	0.76	*d*	*e*
1-CH_3 (Tolyl)	0.31	0.40	*d*	*e*
α_{CH_2}, α'_{CH_2}[c]	—	0.04	—	—
β_{CH_2}, β'_{CH_2}[c]	—	0.09	—	—

a. Upfield shifts relative to 4-toluic acid chloride; b. *meso*-10.15,20 substituents (see Section 1 of this Chapter); c. Protons in α/β (10,20-porphyrin positions) and in α'/β' (15-porphyrin position) carbons of the *meso*-heptyl chains; d. Data not evaluated; e. Data dependent of the correct proton assignment (see text and Scheme 6).

4.1.2 Low temperature ^{1}H NMR spectra

Several times during this work, the NMR spectra of compounds (**1-4**) showed duplicate proton signals from the aromatic rings suffering the effects of porphyrin induced field, with different chemical shifts and usually small areas. Such effect, is expected if different position (conformers) of the aromatic rings above (or below) the porphyrin macrocyclic occurs. This observation suggests a rapid movement of the aromatic rings between different low energy positions. In these circumstances, it is pertinent to measure NMR spectra at different temperatures. In this work, samples were selected for low temperature (-60°C) measurement of ^{1}H NMR spectra. Scheme 7 shows the ^{1}H NMR spectrum for compound (**2**), in $CDCl_3$ at -60°C.

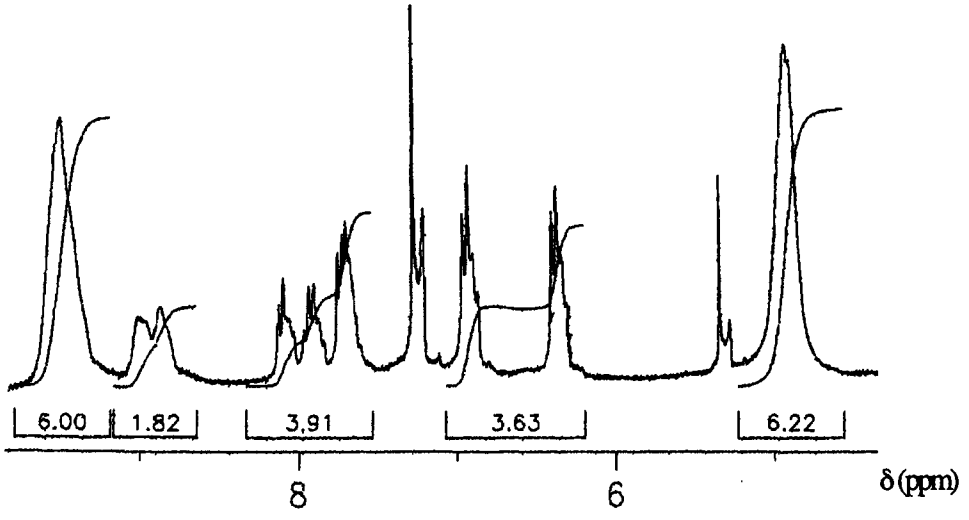

Scheme 7

As can be seen by comparing this spectrum with that in Scheme 5 taken at room temperature, the overall appearance is similar, but there is a considerable enlargement in peak width. Tolyl protons suffer a small shift downfield but, more importantly, the pair of doublets on the tolyl ring now show two pairs of doublets. which indicates the existence of two conformers, similar to each other and in the proportion of approximately 70:30.

4.2. 5-[2-Oxycarbonylnaphthalene]phenylporphyrins series

The upfield shifts of the protons in the tolyl rings attached to the porphyrin seen above are observed again in the naphthyl-substituted porphyrins. However, the aromatic structure in this case is more complex and so are the NMR spectra. The simplest compound prepared in this series was the 5-(2-[2-oxycarbonylnaphthalene]phenyl)-10,15,20-*tris*-heptylporphyrin (**5**), for which the structure and its ^{1}H NMR spectrum are shown in Scheme 8.

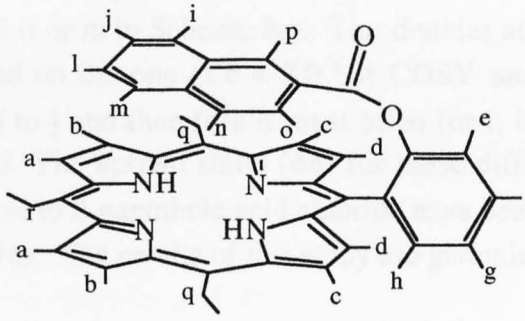

(a)

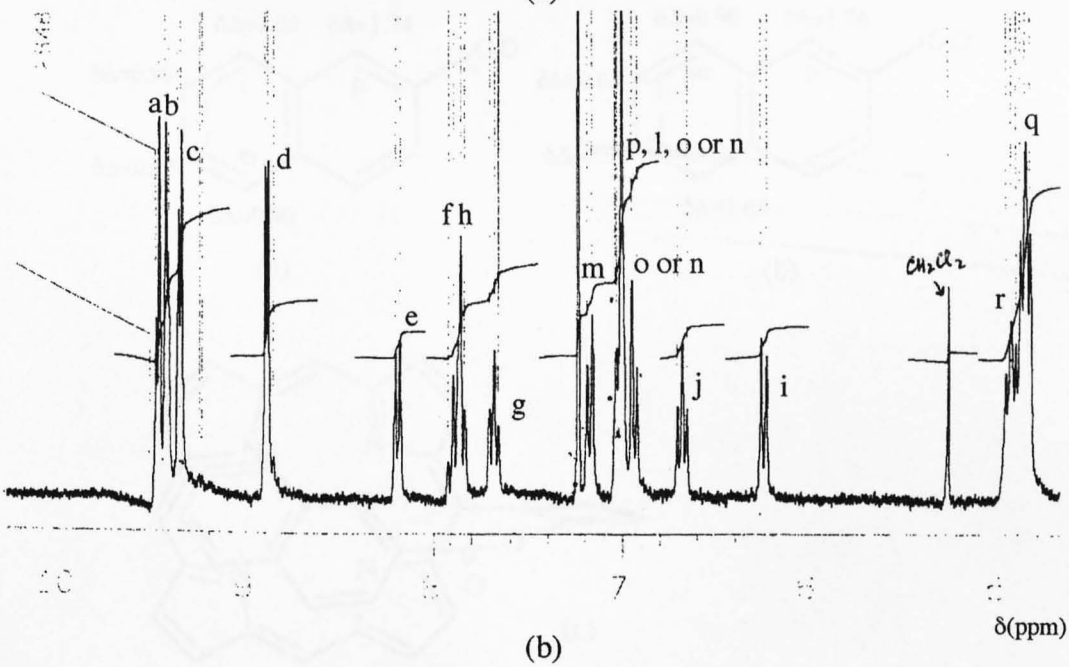

(b)

Scheme 8

The spectrum in Scheme 8 shows a relatively well resolved set of signals, which facilitate the assignment of the major structural molecular units. At δ = 8.9-9.5 there appear the β-pyrrolic protons, with the expected four doublets (4 x 2H,

a, b, c and d signals). At δ = 7.6-8.2, the *meso* substituted phenyl protons can be observed (4H, e, f, g and h signals) and, at higher field, the protons corresponding to the *meso*-heptyl chains (α-methylene protons q and r in Scheme 8b). The signals for δ = 6.2-7.2, with a total area value of 7, are undoubtedly those due to the naphthyl protons. Careful analysis of COSY spectra allows a partial identification of these signals: the singlet corresponding to the 1-position of the naphthyl group (p in Scheme 8a) is seen at δ = 7.0. The doublet found at δ = 7.1 corresponds to one of protons at position 3 or 4 (o or n), the other being superimposed on the singlet at δ = 7.0. The signal with a chemical shift of δ = 6.7 is a triplet, corresponding either to proton 6 or 7 of naphthyl group (l or j, see Scheme 8a). This proton couples with the doublet at δ = 6.2, which corresponds either to proton 5 or 8 (i or m in Scheme 8a). The doublet at δ = 6.9 is coupled to a signal superimposed on the one at δ = 7.0 but COSY analysis shows that this last signal is coupled to j and therefore it must be m (or i, by symmetry). Which assignment is correct? The upfield shifts (Δδ) for these different proton positions (i, j, l, m and p) relative to 2-naphthoic acid chloride have been calculated, for both assignment possibilities. The results of this study are given in Scheme 9.

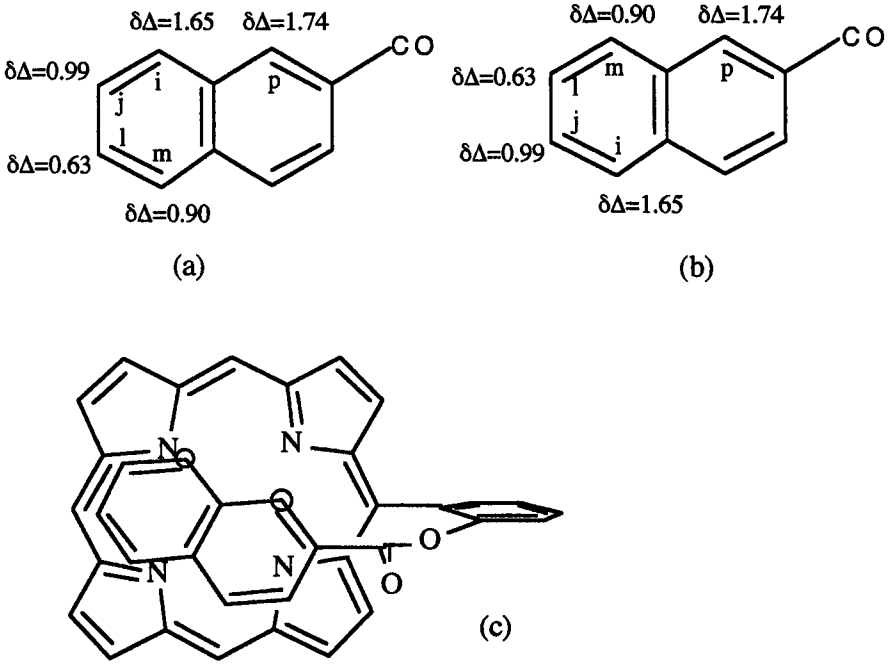

Scheme 9

Bearing in mind that the upfield shifts originate because of the naphthyl position over the porphyrin macrocycle, it would be expected that the protons located close to the centre of the field should suffer the biggest upfield shifts and

that these should diminish as the distance to the centre increases. The assignment made in Scheme 9a led to upfield shifts that diminishes when the distance from naphthyl carbon 1 increases (1 > 8 > 7 > 6 > 5). Those calculated for assignment (b) in Scheme 9 show the biggest upfield shifts at positions 1 and 5, *viz.*, at opposite positions relative to the naphthyl centre. Studies with computer models,[8] indicate the impossibility of finding these two positions simultaneously close to the porphyrin centre (see Scheme 9c), and therefore the assignment presented in Scheme 9b is not feasible. Based on these observations, it is proposed that the proton assignments should be as illustrated in Scheme 9a.

^{1}H NMR spectra of porphyrins having *meso*-phenyl instead heptyl groups show most of the characteristics of the latter, except for observation of more NMR signals, particularly a triplet and a doublet, close to the naphthyl ring protons (see Scheme 10). COSY analysis shows that these signals are coupled and, taking their chemical shift values, they should belong to the naphthyl protons at positions 5 and 6 (or 7 and 8). Assuming the earlier assignment for the naphthyl protons, the reverse order means that, in this case, proton 6 and 7 (or 7 and 8) change their positions relative to the field centre. This may indicate that the naphthyl group moves between two conformations, with a relative weight given by the ratio of the areas peak (approximately 2:1).

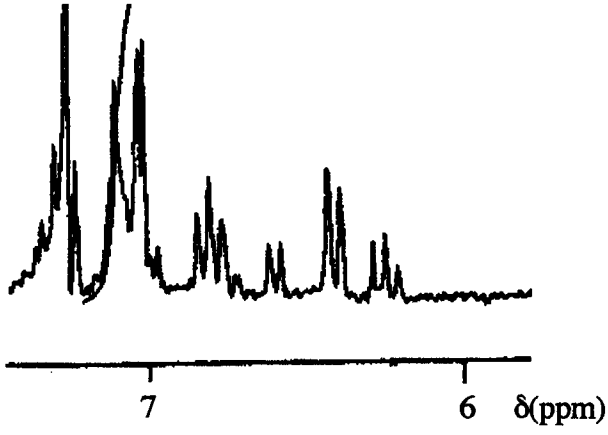

Scheme 10

This and all ^{1}H NMR data for compounds (**5-9**) prepared in this series are collated in Table 4.

Table 4. ^{1}H NMR upfield shifts in aromatic ring protons[a] and α/α'- and β/β'-heptyl methylene protons shift difference in 5-[2-oxycarbonylnaphthalene]phenyl-porphyrins.

Compound.	(**5**)	(**6**)	(**7**)[d]	(**8**)[d]	(**9**)[d]
R[b]	Heptyl	Heptyl	Phenyl	Phenyl	Phenyl
Aromatic ring(s)	Naphthyl	*bis*-Naphthyl	Naphthyl	*bis*-Naphthyl	*tris*-Naphthyl
Protons	^{1}H NMR shifts (Δδ)				
1H-Naphthyl	1.74	1.80	1.64	1.78	1.69
8H-Naphthyl	1.65	1.84	1.51	1.67	1.71
7H-Naphthyl	0.99	1.02	0.83	0.89	0.91
αCH_2, $\alpha' CH_2$[c]	0.08	0.11	—	—	—
βCH_2, $\beta' CH_2$[c]	0.09	0.15	—	—	—

a. Upfield shifts relative to 2-naphthoic acid chloride; b. *meso*-10,15,20 substituents (see Section 1 of this Chapter); c. Protons in α/β (10,20-porphyrin positions) and in α'/β' (15-porphyrin position) carbons of the *meso*-heptyl chains; d. Only major conformation signals were taken in account.

The proton assignments for the naphthyl group indicate that they suffer the biggest upfield shifts in position 1, followed by the shift for the proton in position 8. For porphyrins containing two aromatic rings (one above and one below the porphyrin ring), the upfield shifts for all naphthyl protons are slightly greater than those observed in the corresponding singly substituted porphyrins, a similar effect to that observed earlier for the tolyl-substituted porphyrins.

Comparing the porphyrins with regard to different *meso*-substitutions, the protons of the naphthyl ring in the *meso*-heptyl-substituted compounds have bigger upfield shifts than to the *meso*-phenyl-substituted porphyrins.

The NMR chemical shift difference between α and α' and β and β' *meso*-heptyl protons are measurable in this case and even more so in the double aromatic ring-substituted porphyrins. This effect may be a sign of some degree of porphyrin macrocycle distortion.

4.2.1. Effect of addition of acid to solutions of porphyrins in $CDCl_3$

When obtaining the NMR spectrum of 5-(2-[2-oxycarbonylnaphthalene]-phenyl)-10,15,20-*tris*-heptylporphyrin (**5**) in a mixture of $CDCl_3$/TFA a downfield shift of all naphthyl protons was observed, since these signals are found at δ = 7.3-8.3. Assignments are difficult to make due to superimposition of the signals from *meso*-substituted phenyl group. As before with tolyl rings, in these porphyrins it seems that the naphthyl group has moved away from the face of the porphyrin macrocyclic on protonation.

A characteristic observation in the ^{1}H-NMR spectra of the porphyrin dications (**5**) and (**6**) is the big chemical shift difference between α and α' and β and β' methylene protons in the heptyl chains, due to increased anisotropy relative to free base. The results are presented in Table 5.

Table 5. Chemical shift difference in α/α'and in β/β' protons of the *meso*-heptyl chains in 5-[2-oxycarbonylnaphthalene]-phenyl-10,15,20-*tris*-heptylporphyrins dications.

Compound.	(**5**)	(**6**)
R[a]	Heptyl	Heptyl
Aromatic ring(s)	Naphthyl	*bis*-Naphthyl
Protons	^{1}H NMR shifts (Δδ)	
α_{CH_2}, α'_{CH_2}[b]	0.18	0.27
β_{CH_2}, β'_{CH_2}[b]	0.23	0.37

a. *meso*-10,15,20 substituents (see Section 1 of this Chapter); b. Protons in α/β (10,20-porphyrin positions) and in α'/β' (15-porphyrin position) carbons of the *meso*-heptyl chains.

4.2.2. Low temperature ^{1}H NMR measurements

Scheme 11 shows a 400 MHz ^{1}H NMR spectrum of 5-(2,6-*bis*-[2-oxycarbonylnaphthalene]phenyl-10,15,20-*tris*-phenylporphyrin (**8**) taken in $CDCl_3$ at room temperature (Scheme 11a) and at -60°C (Scheme 11b).

At room temperature the shifts for protons in the naphthyl ring are approximately the same as those described for 5-(2-[2-oxycarbonylnaphthalene]-phenyl)-10,15,20-*tris*-heptyl-porphyrin (**5**), with a characteristic doublet and a triplet shifted upfield (δ = 6.3 and 6.7, respectively). At -60°C all the naphthyl signals are shifted downfield by about 0.4 ppm to δ = 6.7-7.4, indicating a greater distance between naphthyl and porphyrin rings. There is evidently a change in chemical shift relative to the position of the naphthalene protons and this indicates a clear conformational change when reducing the temperature. This is also clear for the β-pyrrolic protons near δ = 9 which show changes in signals shape and pattern, probably due to the movement of the naphthyl group. This result contradicts some earlier observations with compounds related to the present ones[4-7] and observations made in this work for "sandwich" compounds having as aromatic, rings tolyl and anthranyl groups, in which the decrease of the temperature have not significantly changed the NMR spectra signals pattern (see Sections 4.1.2 and 4.3.1, in this chapter).

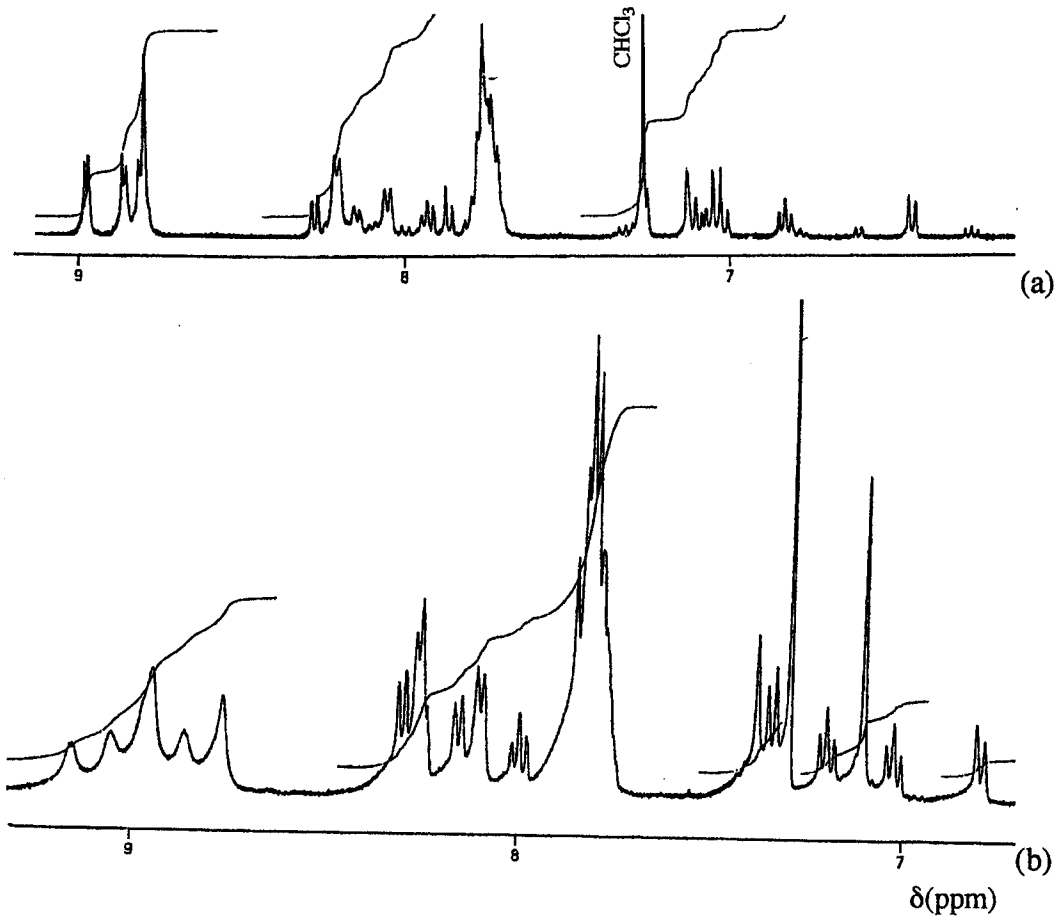

Scheme 11

4.3. 5-[9-Oxycarbonylanthracene]phenylporphyrin series

Scheme 12 shows the ^1H NMR spectrum of 5-(2-(9-oxycarbonyl-anthracene)-10,15,20-*tris*-heptylporphyrin (**10**), taken in $CDCl_3$. The corresponding COSY spectrum is also shown, to assist in identification and assignment of proton resonances.

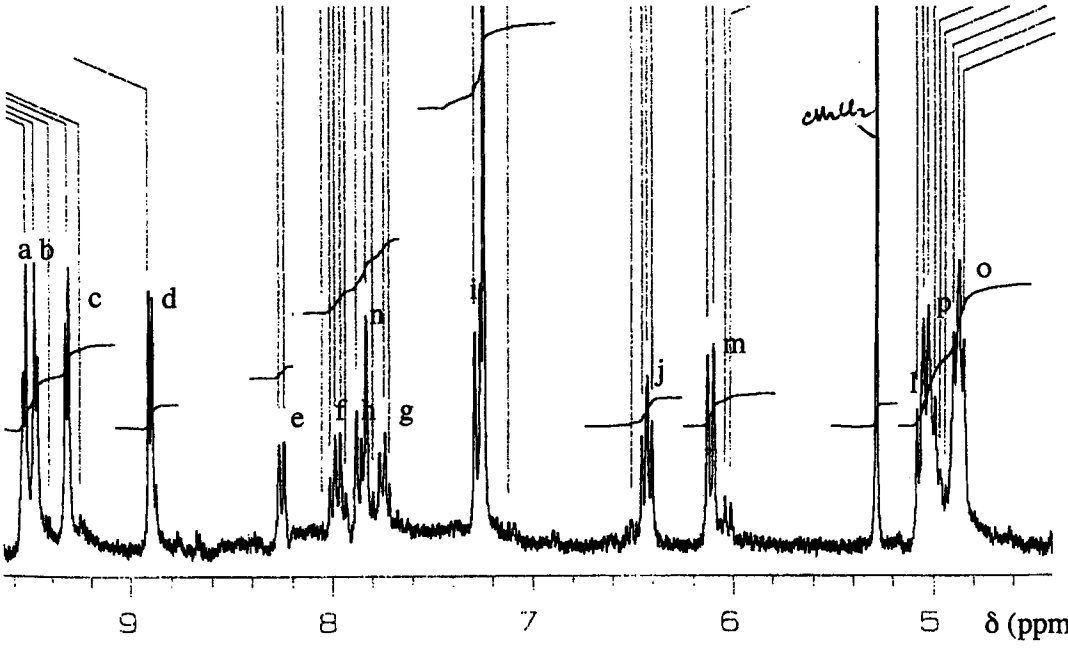

(a)

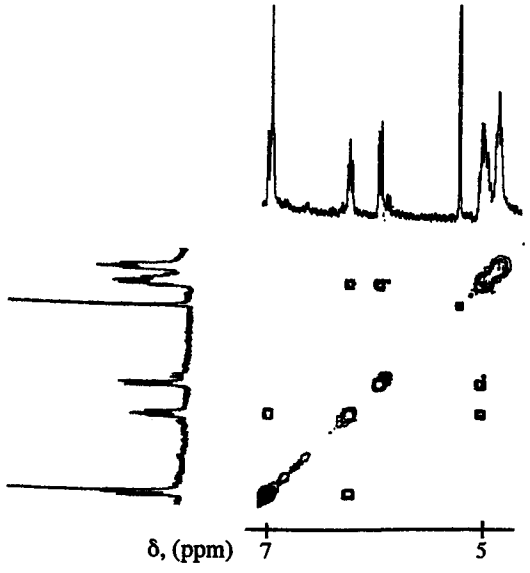

(b)

(c)

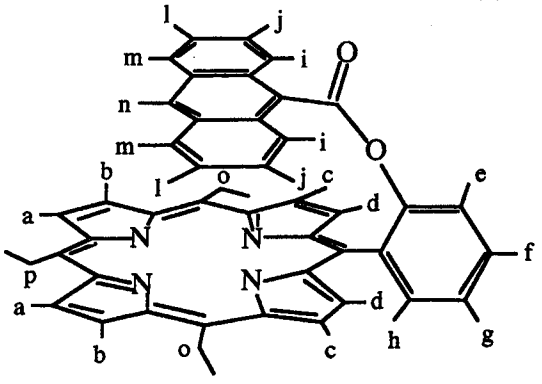

(10)

Scheme 12

At δ = 8.9-9.5 ppm there are the β-pyrrolic protons, with the familiar four doublets (4 x 2H, a, b, c and d). The proton resonances between δ = 7.7 and 8.3

correspond to the four protons of the *meso*-substituted phenyl group (4H; e, f, h and g respectively in Scheme 12c) with the exception of a singlet at $\delta = 7.8$ (see below). Two more signals are seen clearly at $\delta = 6.1$ (2H, d) and at $\delta = 6{,}4$ (2H, t). COSY spectral analysis allows the identification of yet two more signals, coupled with the last named (Scheme 12b), one at $\delta = 7.25$ just superimposed on the $CHCl_3$ signal (a careful magnification shows it to be a doublet) and another at $\delta = 5.0$, which is superimposed on the α-methylene of the heptyl *meso*-substituent. To identify the multiplicity of this last signal, the equivalent NMR spectrum of 5-(2-[9-oxycarbonylanthracene]-10,15,20-*tris*-phenylporphyrin (**11**) was inspected (Scheme 13 shows the relevant part of the spectrum). This last compound does

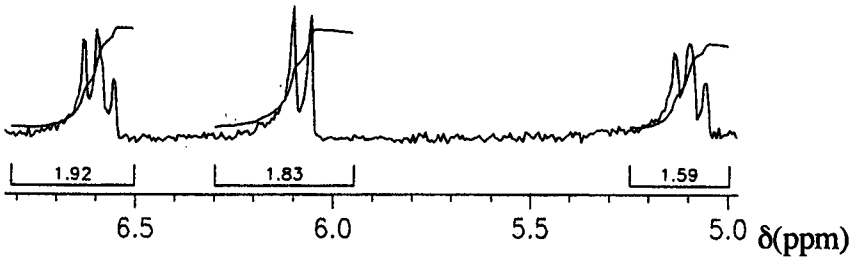

Scheme 13

not possess *meso*-alkyl substituents and therefore does not show any signals at these chemical shift values. As can be seen in Scheme 13 the anthranyl proton signals appear at approximately the same chemical shifts as in the equivalent *meso*-heptyl compound (**10**). At $\delta = 5.1$ (**11**) has a triplet, corresponding to two protons which are coupled with both of the protons centred at $\delta = 6.1$ and $\delta = 6.6$. These protons show the expected pattern for the anthranyl protons i, j, l and m (anthranyl carbon positions 1, 2, 3, and 4). Thus, the triplet must represent a proton with a considerable upfield shift. Computer modelling studies[8] locate the 1,8-anthranyl protons at a greater distance from the porphyrin macrocycle centre, where the induced magnetic field has its greatest intensity. This result, together with the pattern shown by the COSY spectrum shown in Scheme 12, supports the following assignment: $\delta = 5.0$ (protons 3,6; l in Scheme 12c); $\delta = 6.1$ (protons 4,5; m); $\delta = 6.3$ (protons 2, 7; j); $\delta = 7.2$ (protons 1,8; i in Scheme 12c). The proton at anthranyl position 10, which is not expected to show any strong coupling with any of these others protons, is not easily located in the spectrum; a good candidate for it is the singlet at $\delta = 7.8$.

The chemical shift differences for α/α' and β/β' heptyl protons in compound (**10**) have the biggest values of all the compounds prepared (approximately 0.16 ppm). This difference is also clearly observed for the γ/γ' heptyl methylene protons and this may be due to a lack of planarity in the macrocycle ring. However, this supposition is not supported by UV/visible spectroscopy (see later). It is more likely that the greater ring size of the anthracene residue means that its magnetic field effect is felt more strongly at the α, β, γ protons than would be the case for the smaller naphthyl or tolyl ring systems.

The other compounds prepared in this series (**11-13**) show very similar chemical shifts for anthranyl protons as do those of compound (**10**) (see Table 6). In the case of the *meso*-phenyl-substituted porphyrins (**12, 13**), this observation is most surprising, considering the presence of a steric block between the anthranyl and the *meso*-phenyl substituents.

Table 6. ^{1}H NMR upfield shifts in aromatic ring protons[a] and α- and β-heptyl methylene protons shift difference in 5-[9-oxycarbonylanthracene]phenylporphyrins.

Compound	(**10**)	(**11**)	(**12**)	(**13**)
R[b]	Heptyl	Heptyl	Phenyl	Phenyl
Aromatic ring(s)	Anthranyl	*bis*-Anthranyl	Anthranyl	*bis*-Anthranyl
Protons	^{1}H NMR shifts (Δδ)			
1,8-Anthranyl	0.86	*d*	0.86	0.78
2,7-Anthranyl	1.12		0.95	0.92
3,6-Anthranyl	2.56		2.52	2.51
4,5-Anthranyl	1.94		1.98	1.98
α_{CH_2}, α'_{CH_2}[c]	0.16		—	—
β_{CH_2}, β'_{CH_2}[c]	0.16		—	—

a. Upfield shifts relative to 9-anthranoic acid chloride; b. *meso*-10,15,20 substituents (see Section 1 of this Chapter); c. Protons in α/β (10,20-porphyrin positions) and in α'/β' (15-porphyrin position) carbons of the *meso*-heptyl chains; d. Data not evaluated (see the Experimental Section of Chapter 6).

4.3.1 Effect of addition of acid and low temperatures on ^{1}H NMR measurements on porphyrins (10-13)

The spectrum of compound (**10**) in a mixture of $CDCl_3$/TFA shows a shift of about 2.1 ppm downfield for the 3,6-anthranyl proton signals, indicating an increase in the distance of the anthracene ring from the porphyrin macrocycle. The α-methylene protons of the heptyl groups, have about the same chemical shift difference as those of the free base.

The low temperature (-60°C) NMR spectrum of compound (**10**) shows almost the same chemical shifts as when taken at room temperature, with the exception of some peak broadening.

4.4. Metal complexes of porphyrins containing aromatic rings

The molecular characteristics of the porphyrins containing aromatic rings can be deduced from the NMR data described above (see the final discussion in this chapter). A major challenge to this work was to try to determine what conformational changes occur (if any) when their metal complexes are prepared. For Fe and Mn porphyrins, the position of attached aromatic rings is not certain and NMR analysis is difficult for these paramagnetic metals. Despite the possibility of obtaining NMR spectra of simple iron porphyrin complexes (high spin complexes) their analysis is not straightforward and the chemical shifts are spread through a large range of values. Usually low spin metal complexes, which can be prepared conveniently by chelation to cyanide, are easier to interpret.[13] However, this approach has as a serious drawback in that spectra of *bis*-cyanide complexes are not necessarily the same as those of the uncomplexed metalloporphyrins. In the present work, only one attempt was made to check for different positioning of aryl rings by using ^{1}H NMR spectral analysis of a metalloporphyrin. The structure chosen for this work was a compound having aromatic rings in positions for which folded conformations are possible (as the 2,6-positions of the 5-*meso*-substituted phenyl group) and one aromatic ring in such a position for which the folding is not possible (as the 4-position of the 5-*meso* substituted phenyl group). A compound with such characteristics is the iron(III) *bis*-cyanide complex of 5-(2,4,6-*tris*-[2-oxycarbonylnaphthalene]phenyl)-10,15, 20-*tris*-phenylporphyrin (**9**), shown in Scheme 14.

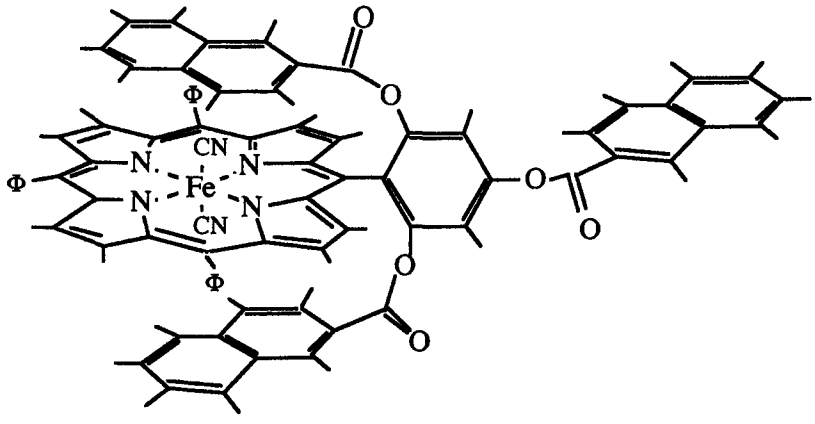

Scheme 14

The 400 MHz ^{1}H NMR spectrum of the iron(III) *bis*-cyanide complex of porphyrin (**9**) is shown in Scheme 15. Proton assignments proved to be difficult, even with the aid of COSY analysis. This may reflect a structural complexity and

the known sensitivity for this kind of spectrum to reflect minor structural differences in the porphyrins.[12] A search of the literature for ^{1}H NMR spectra of iron/porphyrin complexes led to the expectation of finding the β-pyrrolic protons upfield ($0 > \delta > -14$)[13], but it was not possible to observe any resonances at those positions. The *meso*-phenyl protons would be expected at δ = 6-8, where the recorded spectra exhibit well defined peaks.

The lack of ready interpretation from this spectrum and shortage of time meant that this aspect of the research was not taken further.

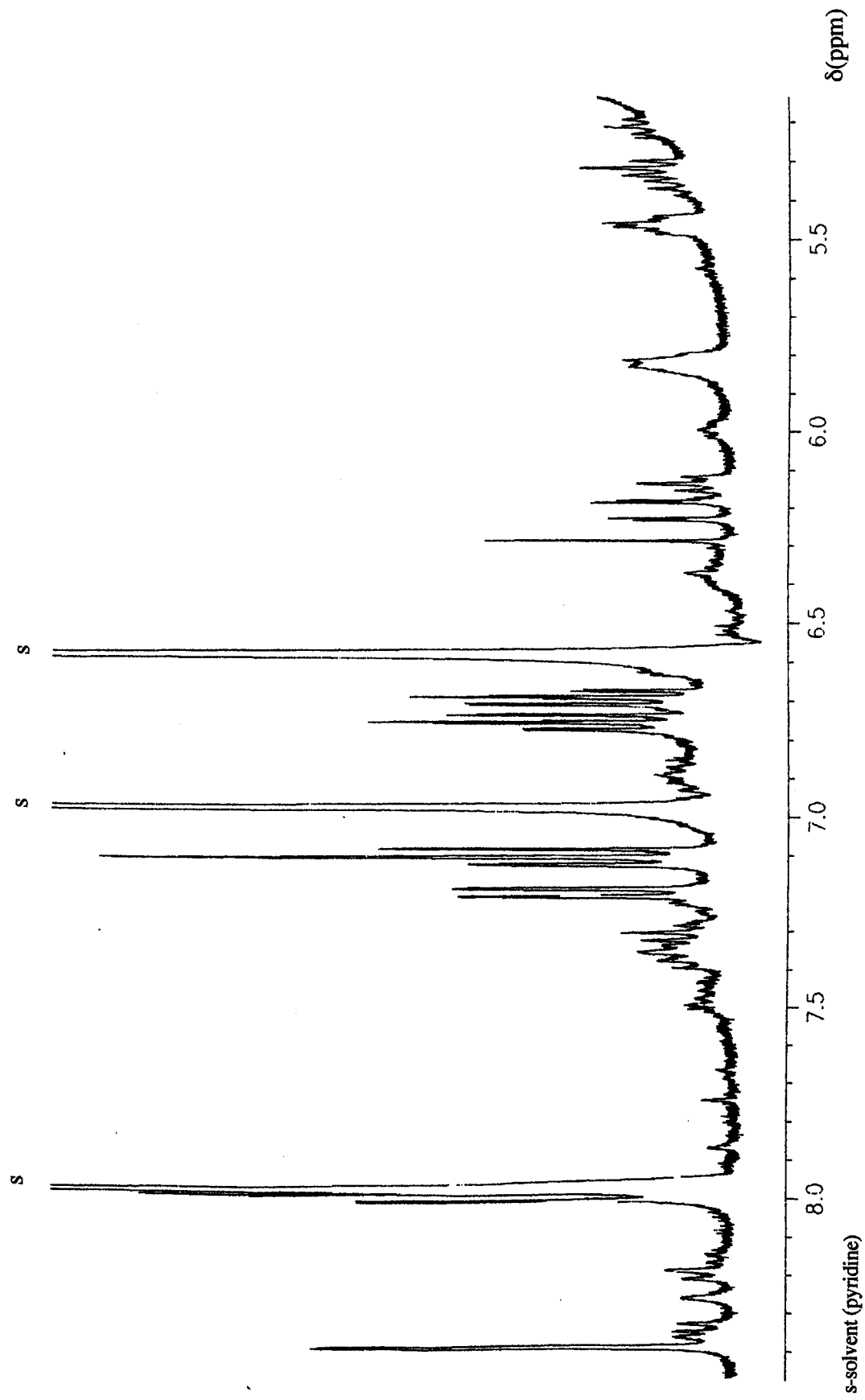

Scheme 15

5. Characterisation of free base porphyrins by UV-VIS spectrometry

The tendency for porphyrins containing aromatic rings such as those described in this work to assume a folded conformation may originate from electrostatic interaction between the porphyrin macrocycle and the aromatic ring (see Final Discussion in this chapter). It might be expected that these electrostatic effects would alter the energy levels in the π-molecular orbitals of the molecule. If this is correct then their UV/VIS spectra should reflect these small charge/energy modifications in shifts for π-π* transitions. The method has a potential for providing information about the occurrence of conformational effects. Table 7 lists the major UV/VIS bands observed for the free base porphyrins (**1-10, 12** and **13**).

The major absorptions are, (a) the Soret band at 418 nm and, (b) for longer wavelengths in the range of 520 to 660 nm, the characteristic porphyrin Q bands. Another set of bands appears between 240 to 400 nm and arise from the aromatic rings linked to the porphyrin. At about 240-250 nm, there is a band normally found with phenyl groups.

Analysis of the spectra from for the series of compounds (**1-4**), (**5-9**) and (**10-13**) makes it possible to account for a number of regularities. The first of these is the characteristic absorptions of any porphyrin macrocycle ring (the Soret and Q bands). These are scarcely changed throughout the series (**1-4**), (**5-9**) and (**10-13**) when compared with compounds in which aromatic rings are absent (see references in Table 7). This indicates that the porphyrin macrocycle ring remains planar throughout. The only significant differences arise from the various *meso*-substitutions, *viz.*, whether or not phenyl or heptyl groups are present. Relative to the normal absorptions of any of the aromatic rings, for example for compounds (**4**), (**8**), and (**13**), especially in the naphthyl and anthranyl porphyrin series, a band shift of these occurs towards the red region of the spectrum. For porphyrins substituted with naphthyl ring(s) the observed red shifts relative to the 2-naphthoic acid spectrum are of 4 nm for the 280 nm band and 7 nm for the 335 nm absorption (Table 7). In the anthranyl substituted porphyrin (**10**) and (**12**) there appear to be a red shift of up to 2 nm in the 346 nm band and of 2-4 nm for the 368 nm absorption. A further band appear at 398-400 nm in compounds (**10**), (**12**) and (**13**), which may correspond to the 384 nm band of 9-anthranoic acid chloride. These shifts are almost certainly due to π-π interactions between the outer orbitals of the porphyrin macrocycle and the outer orbitals of the aromatic rings.

Table 7. Observed absorption bands in the UV/visible region for free base porphyrins (**1-13**)[a]

Compound		Aromatic ring bands					Soret band	Q bands			
		λ, nm (ε x 10^{-3}, $mol^{-1}.L.cm^{-1}$)									
References[b,c]											
5,10,15,20-*Tetrakis*heptylporphyrin							418 (305)	520 (11)	556 (8)	600 (4)	658 (6)
5,10,15,20-*Tetrakis*phenylporphyrin		240					418 (357)	514 (23)	546 (12)	586 (11)	644 (9)
5-[4-oxycarbonyltoluene]phenylporphyrins											
5-(2-[4-oxycarbonyltoluene]phenyl)-10,15,20-*tris*-heptylporphyrin	**(1)**	244 (3)	284 (10)	304 (10)	350 (14)	366 (17)	418 (305)	518 (12)	552 (7)	596 (4)	654 (4)
5-(2,6-*bis*-[4-oxycarbonyltoluene]phenyl)-10,15,20-*tris*-heptylporphyrin	**(2)**	246 (5)		304 (14)	350 (18)	366 (21)	418 (279)	518 (16)	552 (9)	596 (6)	654 (7)
5-(2-[4-oxycarbonyltoluene]phenyl)-10,15,20-*tris*-phenylporphyrin	**(3)**	244 (30)		308 (13)	348 (17)	368 (23)	418 (410)	514 (17)	548 (7)	590 (5)	644 (3)
5-(2,6-*bis*-[4-oxycarbonyltoluene]phenyl)-10,15,20-*tris*-phenylporphyrin	**(4)**	244 (35)		308 (10)		370 (16)	418 (287)	514 (12)	548 (5)	590 (4)	644 (2)
5-[2-oxycarbonylnaphthalene]phenylporphyrins											
5-(2-[2-oxycarbonylnaphthalene]phenyl)-10,15,20-*tris*-heptylporphyrin	**(5)**			*d*			418 (404)	514 (9)	554 (7)	596 (4)	656 (5)
5-(2,6-*bis*-[2-oxycarbonylnaphthalene]phenyl)-10,15,20-*tris*-heptylporphyrin	**(6)**	274 (16)	284 (16)	294 (16)	342 (14)	370 (15)	418 (257)	518 (11)	554 (7)	596 (4)	656 (4)
5-(2-[2-oxycarbonylnaphthalene]phenyl)-10,15,20-*tris*-phenylporphyrin	**(7)**	272 (18)	284 (19)	294 (17)		370 (19)	418 (321)	514 (14)	548 (6)	590 (4)	646 (3)
5-(2,6-*bis*-[2-oxycarbonylnaphthalene]phenyl)-10,15,20-*tris*-phenylporphyrin	**(8)**		283 (34)			374 (23)	418 (217)	515 (19)	548 (9)	590 (8)	646 (6)

Table 7. Continuation

Compound		Aromatic ring bands					Soret band		Q bands			
		λ, nm (ε x 10^{-3}, $mol^{-1}.L.cm^{-1}$)										
5-(2,4,6-*tris*-[2-oxycarbonylnaphthalene]phenyl)-10,15,20-*tris*-phenylporphyrin	(**9**)	274 (42)	284 (46)	294 (40)	342 (22)	370 (25)	420 (462)		514 (19)	548 (8)	590 (6)	644 (3)
5-[9-oxycarbonylanthracene]phenylporphyrins												
5-(2-[9-oxycarbonylanthracene]phenyl)-10,15,20-*tris*-heptylporphyrin	(**10**)	308 (8)		346 (12)	368 (17)	398 (18)	418 (235)	484 (2)	518 (9)	552 (5)	596 (3)	654 (3)
5-(2-[9-oxycarbonylanthracene]phenyl)-10,15,20-*tris*-phenylporphyrin	(**12**)	256	332 (9)	350 (14)	366 (18)	400	418 (162)	446 (5)	514 (9)	546 (4)	590 (3)	642 (2)
5-(2,6-*bis*-[9-oxycarbonylanthracene]phenyl)-10,15,20-*tris*-phenylporphyrin	(**13**)	262	340	358	376	400	418		512	546	586	642

e

a. Dichloromethane solution; *b.* 2-Naphthoic acid spectrum, (λ, nm), 235, 280, 335[14]; *c.* 9-Anthranoic acid chloride spectrum, (λ, nm), 316, 332, 346, 364, 384; *d.* Peak observation difficult; *e.* No satisfactory CHN analysis was obtained for this compound.

6. Characterisation of metalloporphyrins by UV-VIS spectrometry

Table 8 lists observed bands for the UV/VIS spectra of metalloporphyrin prepared from porphyrin ligands (**1-8, 10-12** and **13**). These are the well known bands for such metallo-compounds, *viz.*, the Soret and α- and β-bands. Additionally, bands corresponding to the aromatic substituents are expected and these are often observable. However, it was found that some of these last bands have very small absorption coefficients, making their detection difficult. The observed bands for the aromatic rings show the same red shifts as those described above for the free base porphyrins. For metalloporphyrins substituted with naphthyl ring(s) the observed red shifts relative to the 2-naphthoic acid spectrum are of 3-7 nm for the 235 nm band and of 2-4 nm for the 280 nm absorption band (Table 8). For the iron(III) complexes of the anthranyl substituted porphyrins (**10**), (**12**) and (**13**) the observed red shift in the 332 nm band is of 2 to 4 nm.

Table 8. Observed absorption bands in the UV/visible region for porphyrins (**1-13**) metal complexes[a]

Ligand		Metal	Aromatic ring bands						Soret band		α, β bands	
			λ, nm (ε x 10^{-3}, $mol^{-1}.L.cm^{-1}$)									
References[b,c]												
5,10,15,20-*Tetrakis*heptylporphyrin		Fe						332 (24)	416 (116)	536 (11)		
5,10,15,20-*Tetrakis*phenylporphyrin		Fe						332	416 (166)	530 (10)		
5-[4-oxycarbonyltoluene]phenylporphyrins												
5-(2-[4-oxycarbonyltoluene]phenyl)-10,15,20-*tris*-heptylporphyrin	(1)	Fe	244 (36)					334 (28)	416 (111)	536 (8)		648 (4)
5-(2,6-*bis*-[4-oxycarbonyltoluene]phenyl)-10,15,20-*tris*-heptylporphyrin	(2)	Fe	244 (38)				324 (17)		394,414[d] (87)	534 (7)		
5-(2-[4-oxycarbonyltoluene]phenyl)-10,15,20-*tris*-phenylporphyrin	(3)	Fe	244 (59)					336 (20)	412 (210)			
5-(2,6-*bis*-[4-oxycarbonyltoluene]phenyl)-10,15,20-*tris*-phenylporphyrin	(4)	Fe	246 (43)					336 (25)	394,414[d] (205)		488 (10)	598 (5)
5-[2-oxycarbonylnaphthalene]phenylporphyrins												
5-(2-[2-oxycarbonylnaphthalene]phenyl)-10,15,20-*tris*-heptylporphyrin	(5)	Fe	238 (20)	270 (20)	282 (21)	292 (20)	328 (20)		416 (97)	532 (8)		
5-(2,6-*bis*-[2-oxycarbonylnaphthalene]phenyl)-10,15,20-*tris*-heptylporphyrin	(6)	Fe		272 (21)	284 (24)	294 (20)	322 (16)	338 (15)	416 (85)	532 (7)		
5-(2-[2-oxycarbonylnaphthalene]phenyl)-10,15,20-*tris*-phenylporphyrin	(7)	Fe	242 (64)	276 (16)	282 (26)			336 (15)	414 (101)		570 (6)	
5-(2,6-*bis*-[2-oxycarbonylnaphthalene]phenyl)-10,15,20-*tris*-phenylporphyrin	(8)	Fe	242 (5)	272 (26)	284 (27)	292 (24)		336 (24)	416 (99)	532 (6)		

Table 8. Continuation

Ligand			Aromatic ring bands								Soret band		α, β bands	
			λ, nm (ε x 10^{-3}, $mol^{-1}.L.cm^{-1}$)											
5-(2,4,6-*tris*-[2-oxycarbonylnaphthalene]phenyl)-10,15,20-*tris*-phenylporphyrin	(**9**)	Fe	242 (309)	272 (88)	282 (97)	294 (82)	336 (77)				416 (194)		580 (18)	
5-(2,6-*bis*-[2-oxycarbonylnaphthalene]phenyl)-10,15,20-*tris*-heptylporphyrin	(**6**)	Mn		270 (38)	284 (40)	294 (35)	340 (33)	380 (43)	402 (42)	422 (38)	470 (87)		568 (12)	608 (11)
5-(2,6-*bis*-[2-oxycarbonylnaphthalene]phenyl)-10,15,20-*tris*-phenylporphyrin	(**8**)	Mn	242	270	282 (76)	294		380 (78)	400 (80)	422 (65)	468 (143)		558 (31)	
5-[9-oxycarbonylanthracene]phenylporphyrins														
5-(2-[9-oxycarbonylanthracene]phenyl)-10,15,20-*tris*-heptylporphyrin	(**10**)	Fe	254 (91)				334 (24)				416 (67)	504 (6)	634 (2)	
5-(2-[9-oxycarbonylanthracene]phenyl)-10,15,20-*tris*-phenylporphyrin	(**12**)	Fe	254 (36)				336 (16)				414 (41)	548 (17)	614 (2)	
5-(2-[9-oxycarbonylanthracene]phenyl)-10,15,20-*tris*-heptylporphyrin	(**13**)	Fe	254				336				414 (48)[e]	548	614	

a. Methanolic solution; *b.* 2-Naphthoic acid spectrum, (λ, nm), 235, 280, 335[14]; *c.* 9-Anthranoic acid chloride spectrum, (λ, nm), 316, 332, 346, 364, 384; *d.* "Double" Soret band; *e.* No satisfactory CHN analysis was obtained for the free base porphyrin ligand.

III. Final Discussion

When characterised by ^1H NMR spectroscopy in $CDCl_3$, the porphyrinic compounds (**1-13**) prepared in the present work, which possess a hydroxyl substituted phenyl coupled to an aromatic ring via an ester linkage (tolyl, naphthyl or anthranyl), show noticeable upfield shifts of the signals for the protons on the aromatic ring(s). In the previous sections of this Chapter, suggestions were made for the various proton assignments. Comparison of the upfield shifts in the series of compounds (**1-13**), show that they increase in the order 4-tolyl < 2-naphthyl < 9-anthranyl (Tables 2, 4 and 6). The large upfield-shift of the protons at the 3,6-positions in the anthranyl group are the biggest of all the compounds synthesised. This is not only valid for *meso*-alkyl substituted porphyrins but, more interestingly, also for *meso*-phenyl substituted porphyrins, for which modelling studies[8] suggest the presence of steric constraints. Apart from compounds for which a preference for folded conformations have been described,[3-7] there are none having steric blocks. The chemical shifts for the two homologous series of the *meso*-substituted compounds (heptyl and phenyl) are very similar, with a somewhat smaller upfield shift for *meso*-alkyl-substituted porphyrins. Comparison of singly-substituted and doubly-substituted aromatic groups in porphyrins, reveals a consistently larger upfield shift for the latter.

These results may indicate a preference for a folded conformation in which the aromatic ring occupies a position relatively near to centre of the porphyrin macrocyclic. This preference is found although the different *meso*-substitution between alkyl and aryl groups, since aromatic ring chemical shifts are very similar in the *meso* phenyl and heptyl substituted porphyrins.

One observation that may be important in discussing the molecular dynamics of these compounds is that, for *meso*-phenyl substituted porphyrins, the ^1H NMR signals of specific protons of the aromatic groups appear in more than one chemical shift position (Section 4.1.2). This indicates that, on the NMR time scale, the aromatic groups "oscillate" between two (or more) low energy positions (conformations). This effect arises especially in compounds in which steric constrains are more evident (the *meso*-phenyl-substituted porphyrin series). This oscillation allows the positioning of the aromatic groups close to one face of the porphyrin ring (in such a position they strongly experience induced ring currents on the NMR time scale) and may constitute a way for the molecule avoid the worst steric effects.

When measuring NMR spectra for compounds (**1-13**) in a mixture of $CDCl_3$/TFA, a pronounced downfield shift of the aromatic ring protons was observed. This effect was found in all compounds (**1-13**) and suggests that the distance of the aromatic groups from the centre of the porphyrin macrocycle had increased significantly. A similar effect had been observed earlier in compounds having somewhat similar structures.[4-7] It has been proposed that protonation of the free base porphyrin yields the corresponding porphyrin dication ($PorfH_2^{2+}$) that should contain two counter ions close by. These last species may be responsible for pushing away the aryl rings. Further evidence for such a mechanism can be inferred from the observation that, in the doubly-substituted aromatic ring porphyrins (**2, 4, 6, 8,** and **13**), each of aromatic rings can assume a different disposition from the other (see Scheme 6). This effect can be accommodated with special counter ion arrangements or the mono-cation porphyrin state.

Low temperature ^1H NMR measurements gave different results for the three sets of compounds (**1-4**; **5-9**; **10-13**). With the 4-tolyl-substituted porphyrins (**1-4**), a slight downfield shift of the tolyl protons occurred but, more importantly, the 2,6 and 3,5 tolyl protons signals split. This may mean that, on the NMR time scale, there are two conformations possible. If this effect is observed on reducing the measurement temperature to -60°C then, at higher temperatures, the tolyl group should be oscillating between these conformations at a much greater rate, giving a spectrum of averaged shifts. The naphthyl-substituted porphyrins at -60°C exhibit a downfield shift for all naphthyl protons, compared with similar spectra taken at room temperature. At the same time, the signal pattern appear changed. Taken together, these alterations indicate a change in the position of the naphthyl group to a point more distant relative from the macrocyclic ring than is the case at lower temperatures. Surprisingly, the anthranyl compound at low temperature showed no significant changes, with the exception of some signal broadening. This may simply mean that the anthranyl group(s) have more difficulty in "oscillating" and that there is only one stable conformation at both room temperature and at -60°C.

The results presented here provide some insights into the problem of how the preference for folded conformations shown by the compounds (**1-13**) and to the involvement of π–π interactions. Earlier explanations for such folding were discussed in terms of van der Walls interactions, with suspected contributions of charge-transfer complex effects through HOMO-LUMO donor-acceptor pairs.[4,5] Compounds, in which these effects have been proved to occur show charge-

transfer transitions in their UV-visible spectra or have broadened absorption bands.[2] The UV-visible spectra for all free-base porphyrins (**1-13**) reveal no differences from the characteristic absorptions of standard porphyrins. However, the characteristic absorptions of the aromatic ring(s), at least for naphthalene and anthracene, are shifted to longer wavelengths (red shift). This observation parallels a recent result from a fluorescence study of an anthracene-linked protoporphyrin, which had a folded conformation.[15] In that case, fluorescence quenching of the anthracene group was observed but not of the porphyrin core. The unchanged UV-visible spectral characteristics of the porphyrin ring, indicate that HOMO-LUMO energy levels in the macrocyclic are almost the same in the porphyrin with or without any aromatic ring or with a folded structure, disfavouring possible charge-transfer explanations. The observation that aromatic ring(s) absorption bands suffer a red shift indicate that the energy difference between π-π^* orbitals decreases (Scheme 16a). One possibility is that the ground state porphyrin electronic charge distribution stabilizes the π^* level of the aromatic ring in the folded porphyrins, through electrostatic interactions (see Scheme 16b). In such a case, the energy level of the π^* orbital of aromatic ring would decrease, giving the observed red shift. This would occur without significantly changing the π-π energy levels in porphyrin macrocycle. This electrostatic stabilization may have some contribution for the observed preference for a folded conformation and may constitute an alternative explanation for the effects found on protonation of porphyrin, in which the aromatic ring(s) seem to move apart. The effects may arise from modified charge-densities in the porphyrin ring.

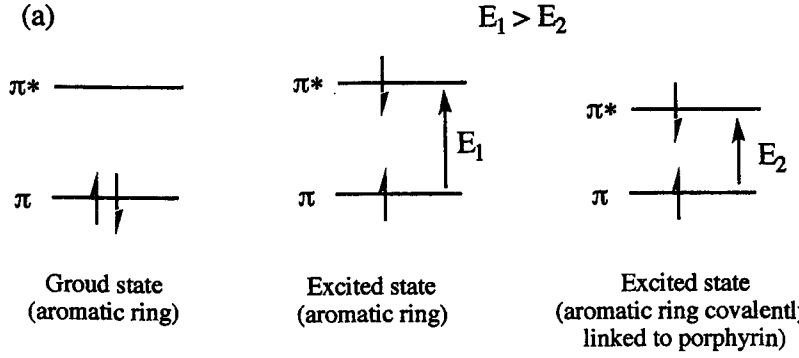

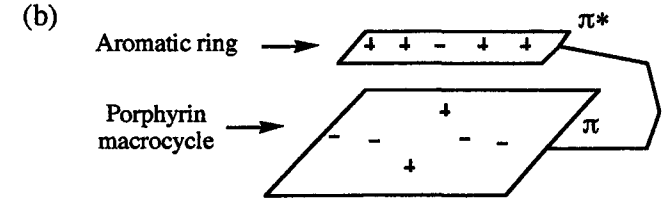

Scheme 16

The results observed disfavour possible explanations involving charge-transfer complexes for the folded conformation shown by compounds (**1-13**). An alternative interpretation for the preference observed in such compounds has been made. This involves simple electrostatic attraction through the σ–π electron framework of both porphyrin macrocycle and aromatic ring.[16] Mathematical modelling using this description explains quite well the observed folding. Recently, a set of porphyrins synthesised with alkyloxy groups substituted on phenyl at the *meso* positions revealed upfield shifts for -CH_2 protons, showing that even alkyl chains may adopt a folded conformation.[17] These results tend to confirm (at least partially) the reality of weak π–π interactions and the importance of σ–π electrostatic effects.

Full clarification of these aspects is outside the goals of this work but the general conclusions are useful for interpretation of results.

The present work on peroxidase-like activity required metallation of compounds (**1-13**) in order to use them in peroxidase experiments. Therefore, it is pertinent to try to understand the conformations assumed for the aromatic ring(s) in such metallated compounds. Attempts to identify their conformations through NMR were unsuccessful due to difficulties in making the correct proton

assignments (see Section 5 of this Chapter). The results with porphyrin dications suggest that, if a central metal be coordinated to a ligand, then the aromatic rings should move away. From the results obtained in the analysis of UV-visible spectra (see above), an inspection of the red shift suffered by the aromatic groups may give indications about the presence of folded conformations. The observed bands for the aromatic ring(s) in metal complexes of porphyrins (**8**, **9** and **13**) reveal red shifts of the same or greater magnitude as those of the free bases.

The main goal of this part of the present work was the preparation of porphyrins having aromatic rings (tolyl, naphthyl or anthranyl) attached through a covalent link in such a way that these groups could lie above and below the plane of the porphyrin ring. Their preparation was successful and their characterization and dynamic description have been partially uncovered by ^{1}H NMR spectroscopy. The relation of these model porphyrins to the environment that occurs inside the PSSS-VN polymers is uncertain, despite the fact that there is a superficial similarity. An important observation linking these different systems is that the effects described in this chapter are observed intramolecularly, while a intermolecular effect, where separate aromatic rings adopt a position close to each other, has not yet been documented.[6] This makes the relevance and applicability of these observations in the PSSS-VN/metalloporphyrins systems uncertain but the special characteristics of the latter systems, do not rule out this possibility. The next chapter, which discusses the behaviour of these compounds in peroxidase-like reactions, gives some indications.

IV. Notes and References

1. E. Haslam, *Chem. Britain*, 1993, 875.

2. J. March in, "*Advanced Organic Chemistry, Reactions, Mechanisms and Structure*", 3rd Ed., Wiley, 1985, New York.

3. G. M. Sanders, M. van Dijk, G. P. Koning, A. van Veldhuizen and H. C. van der Plas, *Rec. Trav. Chim. Pays-Bas,* 1985, **104**, 243.

4. G. M. Sanders, M. van Dijk, A. van Veldhuizen, and H. C. van der Plas, *J. Chem. Soc., Chem. Commun.*, 1986, 1311.

5. G. M. Sanders, M. van Dijk, A. van Veldhuizen, H. C. van der Plas, U. Hofstra and T. J. Schaafsma, *J. Org. Chem.*, 1988, **53**, 5272.

6. R. Schrijvers, M. van Dijk, G. M. Sanders, E. J. R. Sudholter, *Rec. Trav. Chim. Pays-Bas,* 1994, **113**, 351.

7. C. Colominas, L. Eixarch, P. Fors, K. Lang, S. Nonell, J. Teixidó and F. R. Trull, *J. Chem. Soc., Perkin Trans. 2,* 1996, 997.

8. Software from Hyper Chem, Hypercube Inc., 1998, Gainsville, Florida, USA.

9. P. Rothemund, *J. Am. Chem. Soc.,* 1935, **57,** 2010; *ibid.,* 1939, **61,** 2912; A. D. Adler, F. R. Longo, J. D. Finarelli, J. Goldmacher and L. Korsakoff, *J. Org. Chem.,* 1967, **32,** 476.

10. A. M. d'A. Rocha Gonsalves, J. M. T. B. Varejão, and M. M. Pereira, *J. Het. Chem.,* 1991, **28,** 635; R. A.W. Johnstone, M. L. P. G. Nunes, M. M. Pereira, A. M. d'A. Rocha Gonsalves and A. C. Serra, *Heterocycles*, 1996, **43**,1423.

11. A. M. d'A. Rocha Gonsalves, personal communication.

12. A. M. d'A. Rocha Gonsalves, *Tetrahedron Lett.*, 1974, **42**, 3711.

13. J. Wojaczyúski, L. Latos-Graiyúski, W. Lirycyk, E. Pacholska, K. Rachlewicz, and L. Szterenherg, *Inorg. Chem.,* 1996, **35**, 6861.

14. The Merck Index, *An Encyclopedia of Chemicals, Drugs, and Biologicals*, Ed.s M. Windholz, S. Budarani, R. F. Blunetti, 10th Ed., Rathway, 1983, N. J., USA.

15. L. Giribabu, B. G. Maiya, *Res. Chem. Interm.*, 1999, **25**, 769.

16. C. A. Hunter and J. K. M. Sanders, *J. Am. Chem. Soc.*, 1990. **112**, 5525.

17. Q. M. Wang and D. W. Bruce, *J. Chem. Soc., Chem. Commun.*, 1996, 2505.

CHAPTER 4: PEROXIDASE-LIKE ACTIVITY OF MODEL PORPHYRINS

I. Introduction

The different iron and manganese porphyrin complexes prepared in the preceding chapter of the present work were assayed in a peroxidase like-system so as to compare their activity with that of natural Horseradish peroxidase. The results may aid understanding of the molecular dynamics of metal porphyrin complexes having aromatic ring(s) above (or below) the porphyrin macrocycle, an aspect that was not totally uncovered in the previous chapter (see Chapter 3). The interpretation of the results obtained may assist the rationalisation of the observed effects in terms of those results obtained with the PSSS-VN/metalloporphyrin systems, discussed in Chapter 2.

The first problem detected in the peroxidase-like assay of the metalloporphyrins was their small solubility in aqueous solutions which made difficult the use of the system employed with the PSSS-VN polymers. To overcome this, verification of alternative mediums was made in order to establish an adequate system for metalloporphyrins assay, if possible the most similar with that used with the amphiphilic polymers.

II. Results and Discussion

1. Development of a system for assay of peroxidase-like activity of various metalloporphyrins

1.1. System and rate measurements

The system developed to test the aptitude of combined metalloporphyrin/ PSSS-VN polymers as a peroxidase-like catalysts uses 2,2'-azino-*bis*-3-ethylbenzo-thiazoline-6-sulfonic acid (ABTS) as an oxidisable substrate and H_2O_2 as an oxidiser. An aqueous phosphate buffer solution of pH 6 was used as the solvent medium. Oxidation of ABTS leads to a stable cation-radical ($ABTS^{\cdot+}$) which has large visible absorption bands at 420 and 660 nm. These make the course of oxidation of ABTS easy to monitor by UV/VIS spectrophotometry because ABTS itself does not absorb at these wavelengths. The main problem of applying this reaction to metalloporphyrins was their low solubility in the aqueous buffer. This led to several modifications to the system in order to circumvent the difficulty. The various approaches that were examined, relied basically on trying out other reaction media, while maintaining both ABTS and H_2O_2. Reaction rate measurements were carried out by the same procedure (Chapter 2, Section II. 1.1) as for water soluble metalloporphyrins, i.e. measurement of the observed initial rate of formation of the oxidised product, $ABTS^{\cdot+}$, and then normalization of the result, on dividing the initial rate constant by the porphyrin concentration.

1.2. Use of a simple phosphate buffer

Dissolution of metalloporphyrin samples in simple phosphate buffer gives a clear solution with the characteristic colour of a metalloporphyrin. Careful inspection of such systems showed that most of metalloporphyrin was present as a colloidal dispersion, since most of its colour disappeared if the solution was filtered through a 20μm Teflon membrane filter. The activities of both filtered and unfiltered solutions towards ABTS oxidation were determined, but very low or even zero rates were observed.

1.3. Use of a phosphate buffer/methanol mixture

A modification of the above system was the substitution of the aqueous phosphate buffer by a mixture of aqueous phosphate buffer and methanol (60/40 v/v). Before measurement, the metalloporphyrin was dissolved in the methanol and then diluted with the buffer; at the mixture composition chosen, both buffer salts and porphyrin remained in solution. This was thought to avoid the solubility problems found in purely aqueous media but, even in this case, the metalloporphyrin was shown to be present as a colloidal dispersion. The results obtained under these conditions are presented in Table 1.

Table 1. Normalised initial observed rate for $ABTS^{\cdot+}$ formation (k'), in a phosphate buffer/methanol (60/40) solution, using metalloporphyrins.[a]

Metalloporphyrin	k' **x** 10^3 **min**$^{-1}$
FeTPPCl	1.27
Iron(III) 5-(2-[2-oxycarbonylnaphthalene]phenyl)-10,15,20-*tris*-phenylporphyrin chloride	1.78
Iron(III) 5-(2,6-*bis*-(2-oxycarbonyl-naphthalene)phenyl)-10,15,20-*tris*-phenyl-porphyrin chloride	9.03

a. Concentration of reactants: [metalloporphyrin] = 3-27 x 10^{-6} mol.L^{-1}; [H_2O_2] = 0.83 x 10^{-3} mol.L^{-1}; [ABTS]=1.7 x 10^{-3} mol.L^{-1}.

The results, when compared with those obtained with the water soluble metalloporphyrins (Chapter 2, Section II. 2.2) were disappointing and no further experiments were done with this system.

1.4. Use of pure methanol

In a third attempt, methanol alone was used as the reaction medium, in which both the metalloporphyrins and the oxygen donor (H_2O_2) were soluble. In the first experiments, use of guaiacol as substrate was selected in order to avoid any difficulties in solubility of the oxidisable substrate. However, in the later work, it was found that ABTS was soluble in methanol. Therefore, in this part of the work, an assay of guaiacol oxidation was included as well as ABTS. Despite

the fact that this system is unbuffered, an assessment of the peroxidase-like activity was carried out. Figure 1 shows a plot of the measured concentration of $ABTS^{+\cdot}$ absorbance at 660 nm against time for an assay of the effectiveness of FeTPP, FeTDCPP and iron (III) 5,10,15,20-*tetrakis*heptylporphyrin chloride (FeT(heptyl)P) as catalysts in methanol.

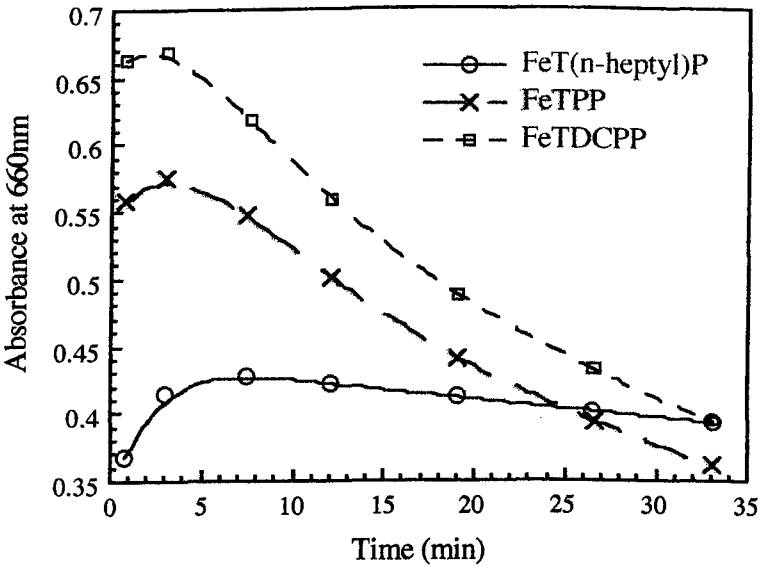

Figure 1. Plot of the 660 nm absorption band of $ABTS^{+\cdot}$ *versus* time, in a peroxidase-like activity test of FeT(heptyl)P, FeTPP and FeTDCPP in methanol, using H_2O_2 as oxygen donor.

The plots show that there is a small transient increase in the 660 nm absorption band, followed by its steady and pronounced decrease, interestingly when using FeTPP or FeTDCPP for even lower values than its residual starting value. This sort of behaviour is not readily understood. Measurement of the pH of the reaction medium indicated that its value increased during the course of reaction, and there is a possibility that ABTS began to precipitate. This result illustrates the convenience of methanol as a medium for its solubility properties but, at the same time, a system failure, due to the unbuffered nature of methanol alone.

1.5. Use of "buffered" methanol

The last result suggested another assay, in which methanol is "buffered". To do this, a methanolic solution of sodium acetate (1 mg/mL) was prepared. An electrode calibrated for pH with a pH-meter was then placed in the solution. The applicability of the normal pH scale in this case is ambiguous but to a certain extent it resembles aqueous systems. Acetic acid was added to this methanolic solution with stirring until the pH reached the value of 6. A preliminary test using this reaction medium in a peroxidase-like system with ABTS as substrate and H_2O_2 as oxygen donor and FeTPP and FeTDCPP as catalysts revealed excellent peroxidase-like activities. These experiments were repeated and the results were found to be reproducible. Therefore, this system was used as a standard for all subsequent tests of catalytic activity of metalloporphyrins.

2. Peroxidase-like activity of metalloporphyrins in "buffered" methanol

In Table 2 are presented the results of the peroxidase-like activity assay using guaiacol as substrate, with all metalloporphyrins prepared in this work, in buffered (pH 6) methanolic solution.

Table 2. Normalised initial observed rate constants (k') for oxidation of guaiacol in methanol/sodium acetate/acetic acid metalloporphyrin solutions.[a]

Porphyrin	**Metal**	k' [b] min^{-1}
"Horseradish peroxidase" (Fluka)[c]		3121.65
5,10,15,20-*Tetrakis*(2,6-dichlorophenyl)porphyrin	Fe	0.41
5,10,15,20-*Tetrakis*phenylporphyrin	Fe	0.45
5,10,15,20-*Tetrakis*heptylporphyrin	Fe	0.50
5-(2-[4-Oxycarbonyltoluene]phenyl)-10,15,20-*tris*-heptylporphyrin (**1**)	Fe	0.37
5-(2,6-*bis*-[4-Oxycarbonyltoluene]phenyl)-10,15,20-*tris*-heptylporphyrin (**2**)	Fe	0.14
5-(2-[2-Oxycarbonylnaphthalene]phenyl)-10,15,20-*tris*-heptylporphyrin (**5**)	Fe	0.32
5-(2,6-*bis*-[2-Oxycarbonylnaphthalene]phenyl)-10,15,20-*tris*-heptylporphyrin (**6**)	Fe	0.11
5-(2-[9-Oxycarbonylanthracene]phenyl)-10,15,20-*tris*-heptylporphyrin (**10**)	Fe	0.10
5-(2-[4-Oxycarbonyltoluene]phenyl)-10,15,20-*tris*-phenylporphyrin (**3**)	Fe	0.24
5-(2,6-*bis*-[4-Oxycarbonyltoluene]phenyl)-10,15,20-*tris*-phenylporphyrin (**4**)	Fe	0.06
5-(2-[2-Oxycarbonylnaphthalene]phenyl)-10,15,20-*tris*-phenylporphyrin (**7**)	Fe	0.16
5-(2,6-*bis*-[2-Oxycarbonylnaphthalene]phenyl)-10,15,20-*tris*-phenylporphyrin (**8**)	Fe	0.08
5-(2-[9-Oxycarbonylanthracene]phenyl)-10,15,20-*tris*-phenylporphyrin (**12**)	Fe	0.06
5-(2,6-*bis*-[9-Oxycarbonylanthracene]phenyl)-10,15,20-*tris*-phenylporphyrin (**13**)	Fe	0.05
5,10,15,20-*Tetrakis*phenylporphyrin	Mn	0.01
5,10,15,20-*Tetrakis*(2,6-dichlorophenyl)porphyrin	Mn	0.003
5-(2,6-*bis*-[2-Oxycarbonylnaphthalene]phenyl)-10,15,20-*tris*-heptylporphyrin (**6**)	Mn	0.001

a. Conditions used: Medium: 2 mL of methanol containing 1 mg/mL of sodium acetate, pH adjusted to 6 by addition of acetic acid; [metalloporphyrin] = 3.4-18.3 x 10^{-6} mol.L^{-1}; [H_2O_2] = 0.83 x 10^{-3} mol.L^{-1}; [Guaiacol] = 4.2 x 10^{-4} mol.L^{-1}. For further details, see experimental section, Chapter 6; b. Rate measurement done according to Chapter 2, Section II. 1.1; c. Reaction carried out in aqueous phosphate buffer, [HRP] = 9.3 x 10^{-9} mol.L^{-1}.

In Table 3 are presented the results of promoting the same reaction but using ABTS as substrate in the same buffer system as for Table 2.

Table 3. Normalised initial observed rate constants (k') for formation $ABTS^{\cdot+}$ in methanol/sodium acetate/acetic acid metalloporphyrin solutions.[a]

Porphyrin	**Metal**	**k '[b] min^{-1}**
"Horseradish peroxidase" (Fluka)[c]		42425
5,10,15,20-*Tetrakis*(2,6-dichlorophenyl)porphyrin	Fe	0.99
5,10,15,20-*Tetrakis*phenylporphyrin	Fe	4.62
5,10,15,20-*Tetrakis*heptylporphyrin	Fe	1.11
5-(2-[4-Oxycarbonyltoluene]phenyl)-10,15,20-*tris*-heptylporphyrin (**1**)	Fe	2.09
5-(2,6-*bis*-[4-Oxycarbonyltoluene]phenyl)-10,15,20-*tris*-heptylporphyrin (**2**)	Fe	1.75
5-(2-[2-Oxycarbonylnaphthalene]phenyl)-10,15,20-*tris*-heptylporphyrin (**5**)	Fe	1.18
5-(2,6-*bis*-[2-Oxycarbonylnaphthalene]phenyl)-10,15,20-*tris*-heptylporphyrin (**6**)	Fe	1.07
5-(2-[9-Oxycarbonylanthracene]phenyl)-10,15,20-*tris*-heptylporphyrin (**10**)	Fe	0.80
5-(2-[4-Oxycarbonyltoluene]phenyl)-10,15,20-*tris*-phenylporphyrin (**3**)	Fe	2.58
5-(2,6-*bis*-[4-Oxycarbonyltoluene]phenyl)-10,15,20-*tris*-phenylporphyrin (**4**)	Fe	1.42
5-(2-[2-Oxycarbonylnaphthalene]phenyl)-10,15,20-*tris*-phenylporphyrin (**7**)	Fe	2.62
5-(2,6-*bis*-[2-Oxycarbonylnaphthalene]phenyl)-10,15,20-*tris*-phenylporphyrin (**8**)	Fe	1.69
5-(2-[9-Oxycarbonylanthracene]phenyl)-10,15,20-*tris*-phenylporphyrin (**12**)	Fe	0.67
5-(2,6-*bis*-[9-Oxycarbonylanthracene]phenyl)-10,15,20-*tris*-phenylporphyrin (**13**)	Fe	0.74
5,10,15,20-*Tetrakis*phenylporphyrin	Mn	0.07
5,10,15,20-*Tetrakis*(2,6-dichlorophenyl)porphyrin	Mn	0.03
5-(2,6-*bis*-[2-Oxycarbonylnaphthalene]phenyl)-10,15,20-*tris*-heptylporphyrin (**6**)	Mn	0.06
5-(2,6-*bis*-[2-Oxycarbonylnaphthalene]phenyl)-10,15,20-*tris*-phenylporphyrin (**8**)	Mn	0.03

a. Conditions used: Medium: 2 mL of methanol containing 1 mg/mL of sodium acetate, pH adjusted to 6 by addition of acetic acid; [metalloporphyrin] = 2-22 x 10^{-6} mol.L^{-1}; [H_2O_2] = 0.83 x 10^{-3} mol.L^{-1}; [ABTS] = 1.7 x 10^{-3} mol.L^{-1}. For further details, see experimental section, Chapter 6; b. Rate measurement done according to Chapter 2, section 1.1; c. Reaction carried out in aqueous phosphate buffer, [HRP] = 9.3 x 10^{-9} mol.L^{-1}.

Table 2 results reveal the exceptional catalytic properties of the HRP enzyme, and show them to be approximately 6000 times better than the best metalloporphyrin based system, when comparing peroxidase activity per metal centre. The values found, can appear disappointing considering their disparity relative to HRP enzyme use. However, significant catalytic activities were obtained with metalloporphyrin systems. The discrepancy observed means that in

HRP catalysis, very low concentrations of the enzyme are required (as 9.3 x 10^{-9} mol.L^{-1}, used in the assays shown in Table 2 and 3) but, with metalloporphyrins concentrations of about 10^{-6} mol.L^{-1} are experimentally more adequate, to give approximately the same absolute peroxidase activity.

Small activities were found for manganese porphyrin complexes and guaiacol oxidation ranging from 0.003 to 0.01 min^{-1}. These values are 10-40 times lower, relative to iron.

For iron complexes the greater peroxidative activities were found to be obtained with porphyrins that do not bear any aromatic ring attached to the porphyrin macrocycle, namely TDCPP, TPP and T(heptyl)P. For these, the activity follows the order T(heptyl)P > TPP > TDCPP.

The results obtained with the metal complexes of porphyrins bearing aromatic ring(s) (**1-13**), show the following pattern: the peroxidase activity is less when the aromatic ring changes from 4-tolyl to 2-naphthyl and even more if changed to 9-anthranyl (see Chapter 3, Section II. 1). For these compounds, double aromatic ring substitution gives even lower rates of guaiacol oxidation. This behaviour is repeated in both *meso*-aryl and *meso*-alkyl substituted metalloporphyrins. If these two series of compounds are compared, it is evident that with guaiacol, there is a decrease in peroxidase activity for the *meso* phenyl-substituted porphyrins compared with the corresponding alkyl substituted porphyrins.

The results shown in Table 3, on the peroxidase-like activity assay of metalloporphyrins with ABTS, gives rate constants similar to those obtained for guaiacol, the exception being with FeTPP, which showed an activity 4-5 times greater than the other metalloporphyrins having no linked aromatic rings. The observed k' values are higher than those found for guaiacol and there is a closing of the gap between the activities found for these synthetic systems and for natural HRP enzyme (the natural system gave normalised initial rates of oxidation 1800 some times greater than the best metalloporphyrin). In these cases, the *meso*-phenylporphyrins have greater peroxidase-like activities than do the *meso*-heptylporphyrins.

3. Peroxidase *versus* mono-oxygenase activity of model catalysts

A small number of iron(III) porphyrin complexes, selected from the prepared compounds, were tested for their activity in a typical mono-oxygenase system. The later was developed by changing the substrate (ABTS or guaiacol) to an

an alkene (cyclooctene, see Scheme 1), while maintaining unaltered the others conditions. The results obtained are shown in Table 4.

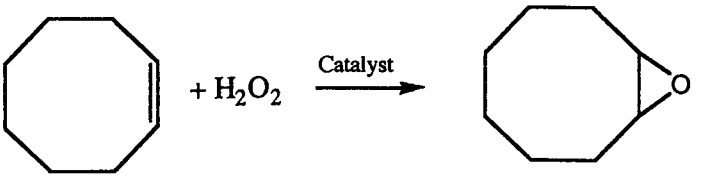

Scheme 1

A big difference between peroxidase-like and monooxygenase-like activity was observed, reaching rates some 1000 times greater for the peroxidase catalysis. This indicates that under, these experimental conditions, simple porphyrins perform more efficiently in the peroxidase pathway, relative to the monooxygenase reaction. When comparing the effects of having aromatic ring(s) in the porphyrin catalysts, opposite effects were found. The peroxidase activity decreased for metalloporphyrins having one or two naphthyl rings, but the same substitution pattern led to an increase in monoxygenase-like activity. However, at no time was monooxygenase activity close to that of peroxidase activity (approximately 1000:1).

Table 4. Normalised initial observed rate constants (k') for oxidation of ABTS and cyclooctene, in methanol/sodium acetate/acetic acid metalloporphyrin solutions.[a]

Metalloporphyrin	**Peroxidase test** k' (min^{-1})[b]	**Monooxygenase test** $k' \times 10^3$ (min^{-1})[c]
FeTPPCl	4.62	3.77
Iron 5-(2-[2-oxycarbonylnaphthalene]phenyl)-10,15,20-*tris*-phenylporphyrin chloride	2.62	4.09
Iron 5-(2,6-*bis*-[2-oxycarbonylnaphthalene]phenyl)-10,15,20-*tris*-phenylporphyrin chloride	1.69	4.76

a. Conditions: Medium: 2mL of methanol containing 1mg/mL of sodium acetate, pH adjusted to 6 by addition of acetic acid; [metalloporphyrin] = 3-5 x 10^{-6} $mol.L^{-1}$; [H_2O_2] = 0.83 x 10^{-3} $mol.L^{-1}$; [ABTS] = 1.7 x 10^{-3} $mol.L^{-1}$; [cyclooctene] = 6x 10^{-1} $mol.L^{-1}$. For further details, see the experimental section of Chapter 6; b. Rate measurement done according to Chapter 2, Section II. 1.1; c. Cyclooctene oxide formation measured by gas-liquid chromatography (see the experimental section of Chapter 6).

III. Final Discussion

The results obtained in the assay for peroxidase-like activity of the metalloporphyrins towards guaiacol as oxidisable substrate, reveal that greater activities were found when using iron as the central metal and with no extra attached aromatic rings (see Introduction and Section II.1 of Chapter 3 for structure elucidation). Manganese complexes gave lower activities, a result found previously with the metalloporphyrins embedded in PSSS-VN polymers. These observations are in accord with reported results achieved with HRP and CcP enzymes, in which replacement of the haem iron by manganese led to a fall in activity of 10^3 to 10^4 times, in Compound I formation (Chapter 1, Section I. 3.1).[1] For this reason, all subsequent discussion here refers only to the iron porphyrin complexes.

The test of the iron complexes of porphyrins without any aromatic ring(s) but with different *meso*-substituents, gives observed activities in the order, heptyl > phenyl > 2,6-dichlorophenyl. However, the activities are almost the same in the three cases, varying from 0.4 to 0.5 min^{-1}. Using the same conditions and metalloporphyrins for oxidation of ABTS, FeTPP gave the greatest peroxidase-like activity, being some 5 times better than that obtained with FeTDCPP or FeT(heptyl)P. It should be stressed that the normalised initial rate constants for ABTS oxidation (in the range of 1-5 min^{-1}) are of the same magnitude as those obtained with simple water soluble metalloporphyrins, which reach up to 5 min^{-1} for FeTDCPPS (See Chapter 2).

The observed activity using Horseradish peroxidase enzyme in aqueous buffer relative to metalloporphyrins is approximately 6000 and 1800 times greater, for oxidation of guaiacol and ABTS, respectively. Considering the simplicity of the artificial system, the observed difference is not as great as it might appear. For reference purposes, single point mutated enzymes, in which the distal histidine residue near the metal centre was changed to alanine, led to a decrease in peroxidase activity of 10^6,[2] making it a much worse catalyst than the systems studied here. In view of the low degree of refinement of these synthetic systems, the results can be considered excellent. Furthermore, the facile increase the porphyrin content in such systems and the predictable activity increase that the addition of nitrogenated bases can impart to the system, indicate the possibility of attaining even better absolute peroxidase-like activities.

For all these reasons, the developed methanolic buffered system can be used as a substitute, with advantage in terms of simplicity, to the use of water-soluble metalloporphyrins to implement peroxidase-like reactions with H_2O_2.

Use of porphyrin ligands having aromatic ring(s) covalently linked to the porphyrin macrocyclic, gives activities towards guaiacol oxidation, which are always lower than when simple porphyrins are used. When the oxidisable substrate is ABTS, this is valid only for FeTPP, since the iron complexes of the singly and doubly-aromatic ring(s) substituted porphyrins ligands have greater peroxidase-like activities than do FeTDCPP or FeT(heptyl)P. The exception to this behaviour was observed with porphyrins possessing as the aromatic ring(s) the anthranyl group (see Table 4).

Dependence on actual structure of the aromatic ring(s) linked to the porphyrin macrocycle was observed. Both in the guaiacol and ABTS tests, the normalised initial rate constants follow the order 4-tolyl > 2-naphthyl > 9-anthranyl. This result is true both in the *meso*-phenyl or -heptyl porphyrin series. Comparing singly *versus* doubly aromatic ring(s) substituted metalloporphyrins, the normalised initial rates are always less in the double substitution. These results seems to indicate that the aromatic ring proximity to the central metal in the porphyrin macrocycle led to smaller peroxidase-like activities.

1. The relation of the results with peroxidase/mono-oxygenase mechanisms

The peroxidase activity found with synthetic metalloporphyrin-based systems is less than that obtained with the natural Horseradish peroxidase system. This indicates a lower efficiency in one or more steps in the peroxidase mechanism. Possibilities are the approach of the oxygen donor to the central metal and the formation of Compound I and Compound II, and the electron transfer to substrate, necessary for continuity in the peroxidase cycle. Apparently, aromatic ring(s) such as 4-tolyl, 2-naphthyl or 9-anthranyl in a close proximity to the porphyrin macrocyclic lead to a decrease in peroxidase-like activity. This may be due to steric effects of approach of H_2O_2 to the metal centre or electronic effects due to interaction of π-orbitals on the aromatic rings and orbitals on the central metal. Other different crucial steps in the mechanism of peroxidase reaction may suffer interference by that structural characteristic, as the block of general acid-base catalysis step (see Chapter 1).

The results obtained on comparing mono-oxygenase/peroxidase preference show evidence that the system is much more better for peroxidase catalysis. Having one or two aromatic ring(s) covalently linked to porphyrin decreases the peroxidase-like activity but the same substitution improves slightly the monooxygenative properties of the complexes. A similar decrease in peroxidase-like activity with a concomitant increase in monooxygenative activity has been

observed in single point mutation experiments on enzymes, in which the distal histidine was replaced by alanine.[2] These results may signify that the presence of aromatic ring(s) immediately above and below the porphyrin macrocyclic can facilitate the approach of the substrate to the metal where the mono-oxygenase reactions takes place. This system would have some resemblance to the hydrophobic domain found in the P450 enzymes.

2. Conformation of metalloporphyrins having covalently-linked aromatic rings

Analysis of conformational aspects of the metalloporphyrins having aromatic ring(s) above or below the porphyrin macrocyclic, suggest two possibilities; there may be folded or the open conformations (See Chapter 3) and even alternation between them. It can expected that, if the metalloporphyrins adopt an extended conformation, their peroxidase-like activity should be comparable to that found in metalloporphyrins which do not possess any attached aromatic ring. However, if the conformation is a folded one, most probably interferences would be felt in the reaction steps that could lead to improvement or blocking of the reaction. The results obtained with ABTS (Table 3) are in some cases, better than those obtained with FeTDCPP or FeT(heptyl)P but not FeTPP; those obtained with guaiacol (Table 2) indicate a reaction blocking, which suggest a folded conformation.

3. Relation of the results to those observed in peroxidase-like activity of PSSS-VN/metalloporphyrin systems

The comparability of the model metalloporphyrins to the environment of metalloporphyrin embedded inside PSSS-VN polymers is uncertain. A porphyrin macrocycle with covalently-linked aromatic rings shows a marked preference for a folded conformation, which is never obtained with the same separated structural elements, *viz.*, a porphyrin and an aromatic ring.[3] However, as far as the system reflects a model of the PSSS-VN microdomains in the polymer, apparently the proximity between a porphyrinic core and an aromatic structure in the polymer is not a structural element that is essential in favouring peroxidase-like activity.

IV. References

1. T. Yonetani and T. Asakura, *J. Biol. Chem.*, 1969, **244**, 4580; K. K. Khan, M. S. Mondal and S. Mitra, *J. Chem. Soc., Dalton Trans.*, 1996, 1059.

2. S. L. Newmyer, P. R. O. Demontellano, *J. Biol. Chem.*, 1995, **270**, 19430; M. I. Savenkova, S. L. Newmyer, P. R. O. Demontellano, *J. Biol. Chem.*,1996, **271**, 24598.

3. R. Schrijvers, M. van Dijk, G. M. Sanders, E. J. R. Sudholter, *Rec. Trav. Chim. Pays-Bas*, 1994, **113**, 351.

CHAPTER 5: NEW ASPECTS IN PORPHYRIN SYNTHESIS

I. Introduction

The work described in the preceding chapters involved the synthesis, purification and characterisation of different types of porphyrins and metalloporphyrins. One of the methodologies utilised in preparing such compounds was a variant of the classical one-step Rothemund porphyrin synthesis, in which the reaction is done in a mixture of acetic acid and nitrobenzene.[1] The author of the present work took part in the earlier steps of the development of this new synthetic method. Additionally, further studies in this new method have been carried out in an attempt to comprehend the effects of the addition of nitrobenzene to the reaction medium.

In this present Chapter, the results of studies on this last aspect have been carried out, together with some interesting results concerning the low stability of 5-(2,6-dihydroxyphenyl)-10,15,20-*tris*-heptylporphyrins and 5-(2,6-dihydroxyphenyl)-10,15,20-*tris*-phenylporphyrins, two intermediates required for the preparation of some substituted porphyrins used in this work.

II. Results and Discussion

1. Use of substituted nitrobenzenes as oxidants in a "one-pot" synthesis of 5,10,15,20-*tetrakis*arylporphyrins.

1.1 Methods for preparing *meso*-substituted porphyrins

The classical general method for the synthesis of *tetrakis*aryl- or *tetrakis*alkyl-porphyrins was introduced a long time ago (the Rothemund reaction)[2] and was later improved.[3,4] This improvement consisted of reacting pyrrole with an aldehyde in refluxing acetic or propionic acid, under aerobic conditions.[4] In one or two favourable cases as, for example, with *tetrakis*phenylporphyrin (TPP) the required porphyrin crystallises in fair yield (20-25%).[4] Where this crystallization does not occur, a lengthy work-up procedure is then necessary and usually with small yields. Later, a two-step synthesis was developed,[5] in which a porphyrinogen is first formed in a non-oxidative medium and this is then oxidised to the required porphyrin in a separate step. More recently, this procedure has been adapted[6] and it was found to give better results for sterically hindered *tetrakis*arylporphyrins. However, this strategy often still gives only modest yields.[7]

Comparison of these various methods[4-7] shows that, whilst the earlier method[4] is simple and convenient, the more recent two-step synthesis is laborious, requires critical laboratory control, needs long reaction times and requires expensive reagents for the oxidation stage. It would be convenient if more porphyrins could be synthesised in high yield through a one-step, one-pot procedure.[4] One improvement has been reported and this greatly enhanced the ease synthesis and isolation of a large number of *tetrakis*arylporphyrins.[1] Further improvements, together with a comparison of the various methods have appeared.[8] The crucial difference between the later and earlier versions of the Rothemund single step method lies in the presence of nitrobenzene in the reaction medium. In the presence of this nitro compound, porphyrins are obtained in yields two or three times better than without. For example, in the case of *tetrakis*(4-methoxyphenyl)porphyrin, one of the highest yields (78%) ever obtained for a one-pot preparation of such compounds has been reported.[8,9] For some of the more difficult syntheses, as, for example, with *tetrakis*-(2,6-dichorophenyl)porphyrin (TDCPP), the increase in yield is about seven fold, rising from 0.7%[10] to 5%[1]. For the preparation of a specific porphyrin, this method gives better yields than the two-step synthesis;[6,7] examples include *tetrakis*-(4-

nitrophenyl)porphyrin and *tetrakis*-(4-methoxyphenyl)porphyrin[1] and the recently reported *tetrakis*pyrazolylporphyrins.[11] This same method allows the preparation of *tetrakis*alkylporphyrins in one step.[1,9] A specific advantage in the use of nitrobenzene as a component of the reaction is the (usually) easy isolation of porphyrins by simple filtration because they crystallize directly from the reaction medium or will do so after addition of a small amount of methanol.[1] Because of the marked beneficial effect of nitrobenzene on the synthesis of porphyrins, this procedure was the method of choice for several of the porphyrins prepared in the present research.

In the following sections are described the effects of variously substituted nitroarenes on the synthesis of porphyrins.

1.2. Effects of the addition of nitroarenes on the Rothemund porphyrin one-pot synthesis

The strategy designed to study the effects of nitroarenes on porphyrin synthesis included a determination of initial rates of porphyrin formation, the detection of intermediates in the reaction pathway and the study of the reaction product distributions.

1.2.1. Effect of addition of nitrobenzene on the isolated yield of *tetrakis*(2,6-dichlorophenyl) porphyrin (TDCPP)

The synthesis of *tetrakis*(2,6-dichlorophenyl)porphyrin (TDCPP) in the classical Rothemund/Adler conditions in the presence of nitrobenzene is an example of the beneficial effects of the presence of this mild oxidant and allows convenient preparation in yields of about 5%. A detailed analysis of the yield of isolated porphyrin was made during the course of reaction, with or without the addition of nitrobenzene. The results are depicted in Figure 1, in which it can be seen that the initial rate and the amount of isolated porphyrin are significantly higher in the presence of nitrobenzene. This result rules out the possibility that nitrobenzene acts simply as a mean of ensuring precipitation of the porphyrin during reaction and thereby preventing it from suffering deleterious degradation. Reaction is both quicker and higher yielding in the presence of nitrobenzene. No precautions were taken to eliminate air from the system and it is likely that, in the absence or presence of nitrobenzene some of the oxidation may be due to oxygen.

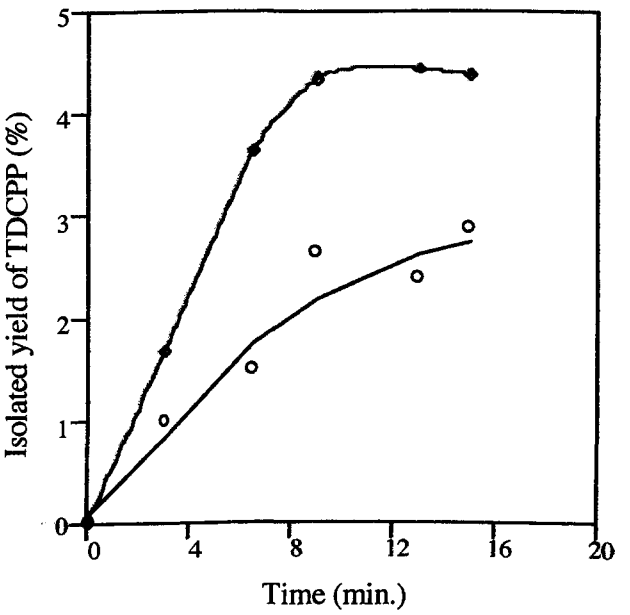

Figure 1. Yield of isolated TDCPP formed in a Rothemund/Adler reaction plotted against time, in the presence (◊) or absence (o) of nitrobenzene in the reaction medium (details appear in the experimental section).

1.2.2. Effects of substituted nitrobenzenes on the kinetics of porphyrinogen oxidation

Rates of formation of porphyrin concern the reaction of pyrrole and an aldehyde to give intermediate formation of a porphyrinogen. In one-pot Rothemund reactions, the step being monitored is the initial rate of porphyrin formation following oxidation of porphyrinogen, which last is known to be the rate determining step (Scheme 1).[12] For this reason and to avoid unnecessary interference from the pyrrole/aldehyde condensation steps, a porphyrinogen was prepared separately and the effects of oxidants on the conversion of porphyrinogen to porphyrin were examined (Scheme 1). The experiments were carried out on the porphyrinogen (I) prepared from *tetrakis*-(4-methoxyphenyl)porphyrin, which is known to exhibit a pronounced solvent effect.[1] This porphyrinogen (I) was prepared *in situ* and was then oxidised in the presence of various substituted nitroarenes under both aerobic and non-aerobic conditions. Initial rates of reaction were monitored by UV/visible spectroscopy in the region of 380-560 nm.

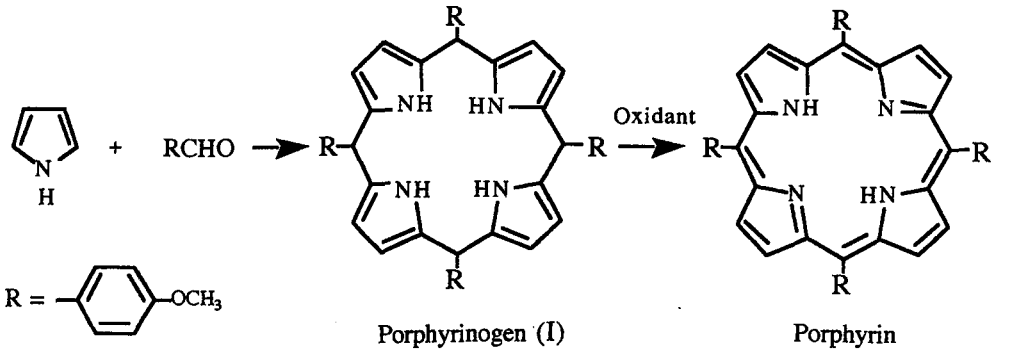

Scheme 1

To examine the effects of electron-withdrawing and electron-donating substituents, the following nitroarenes were used: nitrobenzene (**1**), 1,4-dinitrobenzene (**2**), 4-nitroaniline (**3**), 4-nitrobenzoic acid (**4**), and 4-nitroanisole (**5**). The modified Rothemund/Adler synthesis uses nitrobenzene at fairy high concentration ($\approx$ 3 mol.L^{-1})[1] but the other nitroarenes (**2-5**) are solids and, at a concentration of 3 mol.L^{-1} would raise problems in workup of reaction mixtures. Therefore, lower concentrations (0.15 mol.L^{-1}) of the nitro compounds (**1-5**) were used. Comparative blank reactions were carried out by replacing nitrobenzene by an molar equivalent of toluene.

The formation of porphyrin was monitored by measuring its characteristic Soret band at 424 nm. Porphyrin synthesis is known to generate also other species such as chlorins[4] and porphyrin isomers that have one pyrrole ring inverted relative to the centre of the macrocycle.[14] All such compounds also have a Soret band in their visible spectra. In this section of the present work, for oxidation of porphyrinogen, spectroscopic determinations of porphyrin were made without correction for all the other compounds. In a later section, a method is described for physically separating the desired porphyrin from these other compounds.

On studying porphyrinogen oxidation to porphyrin a typical spectral time sequence is shown in Figure 2.

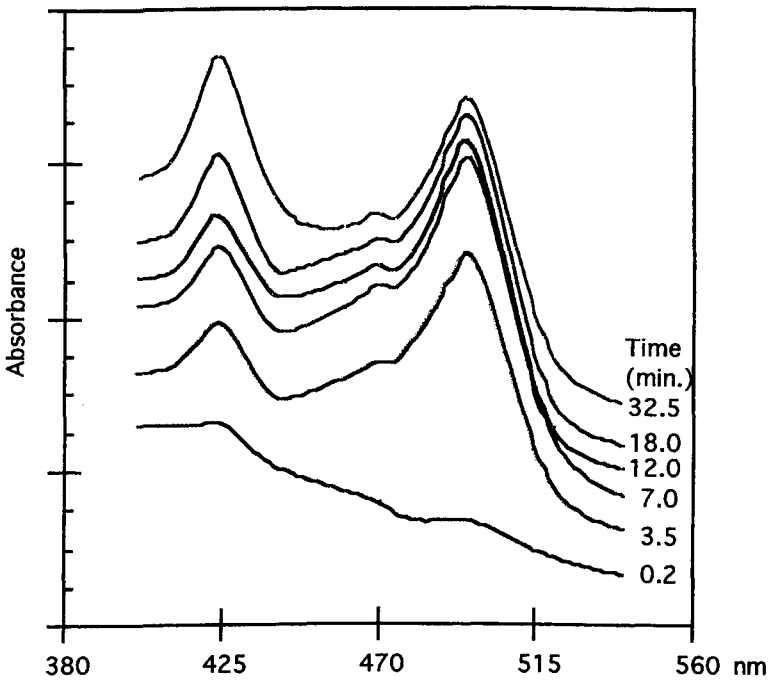

Figure 2. Time sequence for formation of *tetrakis*(4-methoxyphenyl)porphyrin in porphyrinogen oxidation, in acetic acid containing 0.15 mol.L^{-1} of dinitrobenzene, under aerobic conditions. The band at 424 nm is indicative of porphyrin or porphyrin-like compounds but the band at 495 nm is characteristic of porphodimethenes and the small band at 465 nm indicates the presence of another reaction intermediate.

As expected, *tetrakis*(4-methoxyphenyl)porphyrinogen had no absorption in the visible region. On oxidation, it generates species having a large absorption band at 495 nm, a smaller band at about 465 nm and the characteristic Soret band at 424 nm. The 495 nm band corresponds to the presence of porphodimethenes.[13] The observation of a band at 465 nm has not previously been reported in porphyrin synthesis.

Initial rates of formation of 4-methoxyphenylporphyrin were obtained from the absorption at 424 nm. In the presence of a large excess of oxidant(s), these zero order[3b] rates are shown in Table 1, which includes results for various nitroarenes as oxidants, with or without the simultaneous presence of oxygen.

Table 1. Initial rates of formation of *tetrakis* (4-methoxyphenyl)porphyrin, in the oxidation of the corresponding porphyrinogen.[a]

Nitroarene (**1-5**)	$k_{anaerobic}$	$k_{aerobic}$	$k_{aerobic}$[b] (calculated)	$k_{aerobic(obs.)}$-$k_{aerobic(cal.)}$
	all x 10^6 (mol .L^{-1}.min^{-1})			
Nitrobenzene	0.45	2.86	2.28	+0.58
1,4-Dinitrobenzene	2.26	3.98	4.09	-0.11
4-Nitroaniline	0.86	5.89	2.69	+3.20
4-Nitrobenzoic acid	0.98	2.90	2.81	+0.09
4-Nitroanisole	0.31	1.59	2.14	-0.55
No nitroarene[c]	-	1.83	-	-

a. For zero order reactions, the rate is equal to the rate constant, *k*. Reaction conditions: see the experimental section of Chapter 6; b. Sum of oxygen initial rate (1.83 x10^{-6} mol.L^{-1}.min^{-1}) and anaerobic nitroarenes initial rates; c. One molar equivalent of toluene was used instead of nitroarene.

The use of 1,4-dinitrobenzene (**2**) for oxidation of porphyrinogen resulted in the highest initial rate with the other nitro compounds following in the order, 1,4-dinitrobenzene > 4-nitrobenzoic acid > 4-nitroaniline > nitrobenzene > nitroanisole. In contrast, nitroarenes (**1-5**) in the presence of oxygen form compounds having a Soret band with initial rates in the range 2.90-5.89 x 10^{-6} mol. L^{-1}.min^{-1} and with 4-nitroaniline > 1,4-dinitrobenzene > 4-nitrobenzoic acid > nitrobenzene > nitroanisole. These rates are greater than that observed when oxygen alone is used as the oxidant (k = 1.83 x 10^{-6} mol. L^{-1}.min^{-1}). Thus, in the presence of oxygen, 4-nitroaniline is particularly efficient but 4-nitroanisole even appears to suppress formation of porphyrin. A similar but greater porphyrin formation suppression was observed when making one-step porphyrin synthesis in the presence of nitrosobenzene (0.15 mol.L^{-1} in acetic acid).

Estimated values for expected initial rates obtained by the addition of the individual rates to the rate in air are shown in Table 1 (column 4). It can be seen that nitrobenzene and 4-nitroaniline, under aerobic conditions, generate porphyrin at rates that are very different from the sums of individual rates (column 5, Table 1). For 1,4-dinitrobenzene and 4-nitrobenzoic acid, these additive rates are close to the observed values.

The logarithms of initial rates of porphyrin formation (log k, see Table 1) in the presence of nitroarenes (**1-5**) were plotted against half-wave reduction potentials ($E^{1/2}$) of nitroarene and against Hammett σ^+ constants (Figure 3).

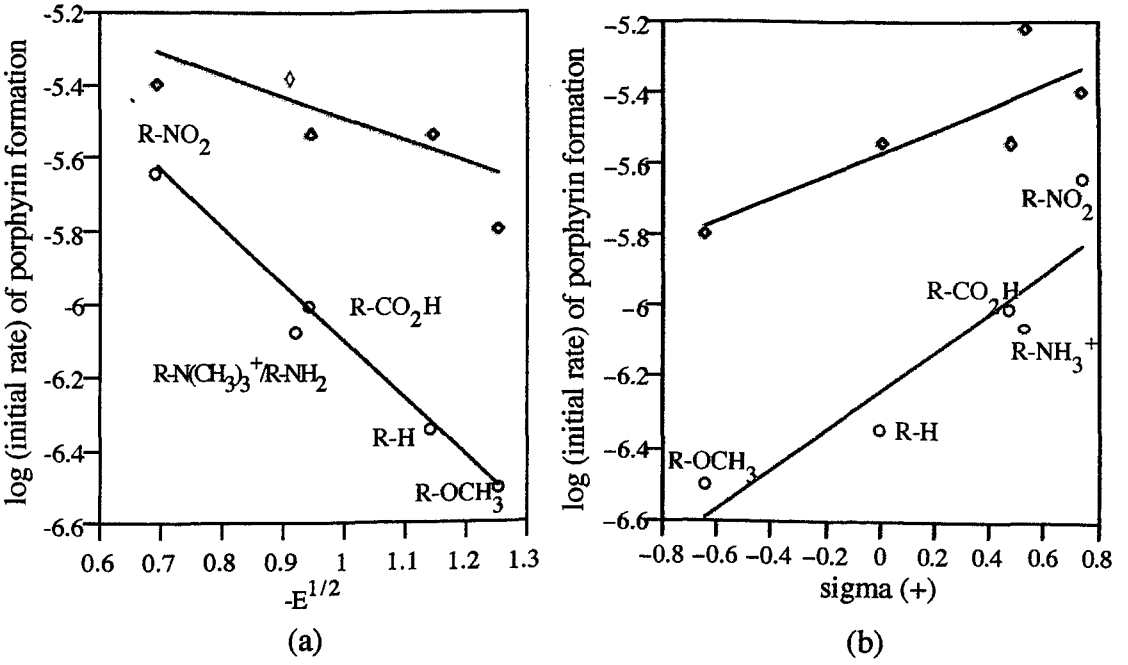

Figure 3. (a) Plots of the logarithm of the initial rate of formation of *tetrakis*(4-methoxyphenyl)porphyrin, under anaerobic (o) and aerobic (◊) conditions, against half-wave reduction potentials (half-wave polarographic reduction potentials *versus* aqueous saturated calomel electrode)[15] of nitroarenes; (b) Plots of the logarithm of the initial rate of formation of porphyrin, under anaerobic (o) and aerobic (◊) conditions against Hammett σ+ constants.

For anaerobic oxidation of porphyrinogen, a good correlation is obtained for the logarithm of the initial rate *versus* half-wave reduction potentials ($-E^{1/2}$) of the nitroarenes (**1**,**2**,**4**,**5**). $E^{1/2}$ values for 4-nitroaniline ($E^{1/2}$ = -1.35V) and 4-nitroanilinium cation ($E^{1/2}$ = -0.74V) do not correlate with the observed initial rate of porphyrin formation. Under the experimental conditions used, 4-nitroaniline should be partially protonated and have an apparent half wave reduction potential between the above values. The calculated value accounting this is $E^{1/2}$ = -0.92V, which is approximately the value expected from interpolation from the plot in Figure 3a. The σ+ Hammett plot show good correlation with anaerobic initial rates, with a ρ value of c.a. +0.5. Under aerobic conditions correlation is observed both in the plots with nitroarenes half-wave reduction potentials and with Hammett σ+ data, but the data show more scatter.

1.2.3. Reaction intermediates in porphyrinogen conversion to porphyrin

The first stage in the oxidation of porphyrinogen (I, see Scheme 2) to porphyrin involves conversion into a porphomethene (II) and, subsequently, into a porphodimethene (III).

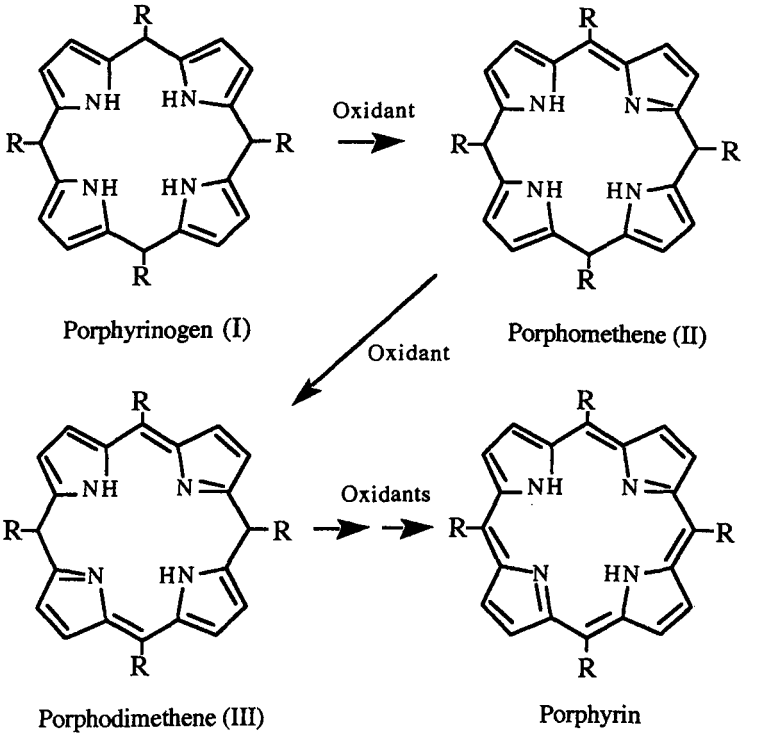

Scheme 2

Porphodimethenes are easily identified and quantified by visible spectroscopy because of their characteristic absorption band near 500 nm.[13] In the results presented here, the appearance of an absorption band at 495 nm is interpreted as intermediate formation of a porphodimethene. By using a reported ε value for a porphodimethene,[16] it is possible to quantify approximately the amount of porphodimethene being formed. Its concentration with time of reaction is shown in Figure 4, both under anaerobic and aerobic conditions in the presence of nitroarenes. Oxidation with oxygen alone has been included for comparison.

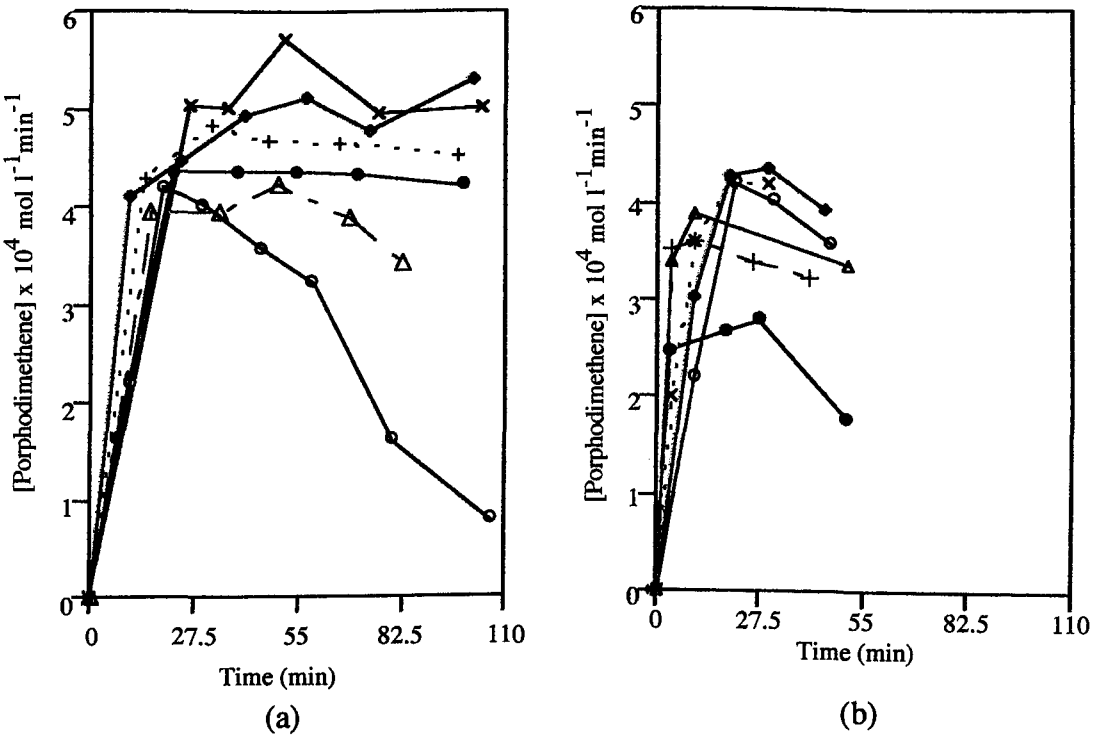

Figure 4. (a) Plots of porphodimethene concentration against time during the oxidation of *tetrakis*(4-methoxyphenyl)porphyrinogen under anaerobic conditions in the presence of 0.15 mol.L^{-1} of nitrobenzene (◊), 4-nitroaniline (•), 4-nitroanisole (x), 4-nitrobenzoic acid (+) and 1,4-dinitrobenzene (Δ). (b) The same plots but under aerobic conditions. In both sets aerobic oxidation is included as (o), for comparison purposes.

The rapid development of a 495 nm band, during oxidation of porphyrinogen under anaerobic conditions in the presence of nitroarenes (**1-5**), indicates that all of these nitro compounds convert porphyrinogen efficiently into porphodimethenes. Measured initial (zero) order rates for oxidation with nitroarenes are in the range of 2.3 to 8 x 10^{-5} mol.L^{-1}.min^{-1}. For oxidation with oxygen (air) alone the value is 2.5 x 10^{-5} mol.L^{-1}.min^{-1}. All of the nitroarenes are less efficient in oxidising porphodimethene to porphyrin or chlorin in the absence of oxygen. Only 1,4-dinitrobenzene appears to oxidise porphodimethenes further at a similar but smaller rate than oxygen. By itself, oxygen causes the 495 nm band to decrease. However, in the presence of air, 4-nitroaniline, 4-nitrobenzoic acid and 1,4-dinitrobenzene do aid oxidation of porphodimethenes since the rates of consumption of porphodimethenes is markedly increased (Figure 4b). In contrast to its oxidising ability in the absence of air (Figure 4a), 4-nitroaniline with air causes rapid removal of the porphodimethene. This synergistic effect decreases in the order 4-nitroaniline > 4-nitrobenzoic acid > 1,4-dinitrobenzene > nitrobenzene > 4-nitroanisole. It may be noted at this stage that the yields of

intermediate porphodimethenes are similar to these of the final product (porphyrin).

1.2.4. The different yield in chlorin in porphyrinogen to porphyrin oxidation in the presence of nitroarenes

Porphodimethenes are consumed, leading to the formation of porphyrin, chlorin and other products. The concomitant generation of chlorin in porphyrin synthesis can potentially give information on reaction mechanism. Recently, it was found that, for some porphyrin syntheses carried out with the two-step method, the final product was strongly contaminated with chlorin.[9] The reaction conditions involve the oxidation of porphyrinogen to porphyrin in acetic acid under aerobic conditions but in the presence of nitrobenzene. To study this effect in greater detail the oxidation of the porphyrinogen derived from TDCPP was investigated. The results are presented in Table 2.

Table 2. Yield and product distribution from oxidation of the porphyrinogen from TDCPP by nitroarenes under aerobic conditions.[a]

Nitroarene	Isolated Yield (%)[c]	[Porphyrin]/[Chlorin] (%)[b]
Nitrobenzene (**1**)	24.4	43 / 57
1,4-Dinitrobenzene (**2**)	26.5	75 / 25
4-Nitroaniline (**3**)	26.3	74 / 26
4-Nitroanisole (**4**)	19.1	45 / 55
Air alone	20.0	49 / 51

a. Reaction conditions: porphyrinogen (TDCPP) was oxidised in acetic acid, containing the nitroarenes (**1-4**) in the presence of air (see the experimental section, Chapter 6); b. Determined from the ratio of the signals for NH in ^{1}H NMR spectra of the products after column chromatography (see experimental section); c. Sum of porphyrin and chlorin.

The highest yields (porphyrin plus chlorin) are obtained during oxidation with either 1,4-dinitrobenzene or 4-nitroaniline in the presence of air (Table 2), with a ratio of porphyrin to chlorin of about 3:1. However, with nitrobenzene, 4-nitrobenzoic acid or air alone the yields are slightly smaller but the proportion of chlorin increases significantly, reaching 57% in the case of nitrobenzene itself.

A correlation of the amount of chlorin formed with the half-wave potentials for the nitroarenes is shown in Figure 5.

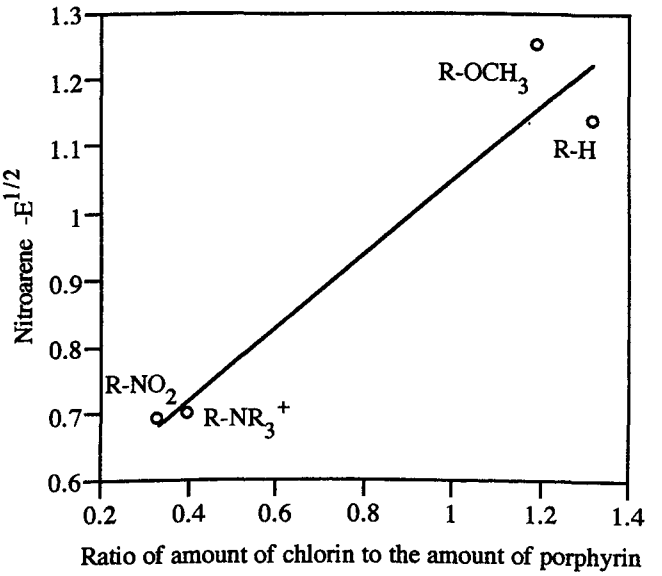

Figure 5. Plots of the ratio of chlorin to porphyrin formed from the oxidation of porphyrinogen of TDCPP *versus* half-wave reduction potentials of the nitroarenes (**1**-**4**). Reactions were carried in the presence of air and the ratio of chlorin to porphyrin was determined by ^{1}H NMR.

The graph indicates that as the nitroarenes become less efficient oxidising agents, more of the chlorin is formed.

1.2.5. Oxidants and reductants in nitroarene modified Rothemund reaction medium.

The above results suggest that nitroarenes are involved in the actual oxidation leading to porphyrin. If this is the case, it would be expected that reduction products of nitroarenes should be detectable. During two Rothemund syntheses of TDCPP in the presence of nitrobenzene under aerobic and anaerobic conditions the products of reaction were analysed by GC-MS for the presence of aniline or phenylhydroxylamine, both well-known products of reduction of nitrobenzene. Under aerobic conditions, after 30 minutes reaction, only traces of nitroaniline and acetanilide were found. Under anaerobic reaction, the same compounds were detected in a slightly greater amount, together with products derived from the reduction of the aldehyde (benzylic alcohol) and pyrrole oxidation (2,4-pyrrolidone). In both cases, the amounts were only tiny compared with the quantity of nitrobenzene used.

The results show that nitrobenzene is not significantly consumed during reaction and its involvement appears to be catalytic. This suggests that other

species could be formed in the presence of nitroarene and oxygen. If nitroarenes are reduced to a radical-anion, this might react with oxygen to form superoxide ($O_2^{\cdot -}$), which would be a powerful oxidant. In a small-scale test experiment, *tetrakis*-(4-methoxyphenyl)porphyrinogen was treated with potassium superoxide in acetic acid/water. Only traces of porphodimethene intermediate were detected but the rate of production of porphyrin (6.7×10^{-5} mol.L^{-1}.min^{-1}) was about forty times the rate usually observed in air (Table 1). It is known that $O_2^{\cdot -}$, under acidic conditions, dismutes rapidly to hydrogen peroxide and oxygen.[17] Because of this, an attempt was made to detect and quantify the presence of hydrogen peroxide during oxidation of *tetrakis*(2,6-dichlorophenyl)porphyrinogen, when the oxidising species was either oxygen or oxygen in the presence of an nitroarene. The procedure used the luminescent detection of H_2O_2 by luminol catalysed by peroxidase.[18] Figure 5 shows a graph of the amount of hydrogen peroxide detected in the presence or absence of nitrobenzene.

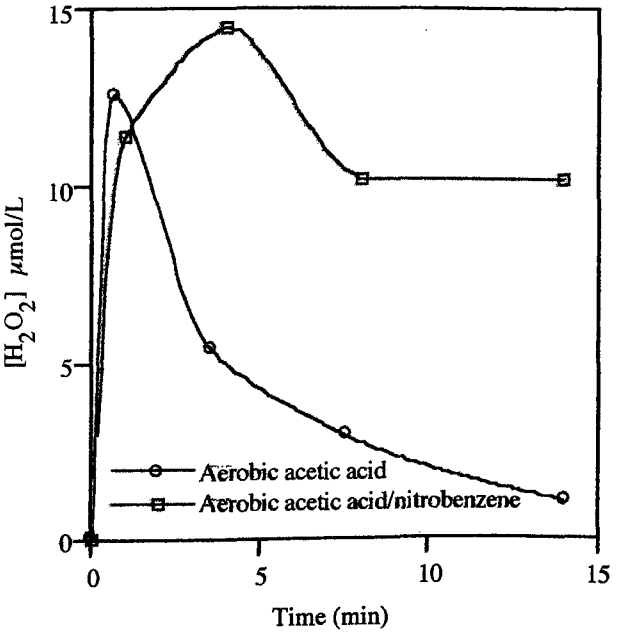

Figure 6. Variation in hydrogen peroxide concentration with time on oxidising *tetrakis*(2,6-dichlorophenyl)porphyrinogen in acetic acid in air (o) or with 0.15 mol.L^{-1} of nitrobenzene in air (□).

During oxidation of porphyrinogen with air alone, there was an immediate increase in hydrogen peroxide concentration but this decayed rapidly to very low values (Figure 6). However, with nitrobenzene present under aerobic conditions, the same rapid increase in H_2O_2 concentration was also observed but its decay was much slower and appeared to reach a steady state concentration of about

10 μmol.L^{-1} after 7-8 minutes. The result indicates that nitrobenzene promotes the formation of hydrogen peroxide in the presence of air.

2. Discussion

2.1. Intermediates in the conversion of porphyrinogen to porphyrin

The steps in porphyrinogen conversion to porphyrin have been suggested to involve firstly the oxidation of two porphyrinogen methyne positions to form a porphodimethene,[13] and that the latter might be the origin of phlorin (Scheme 3).[3b]

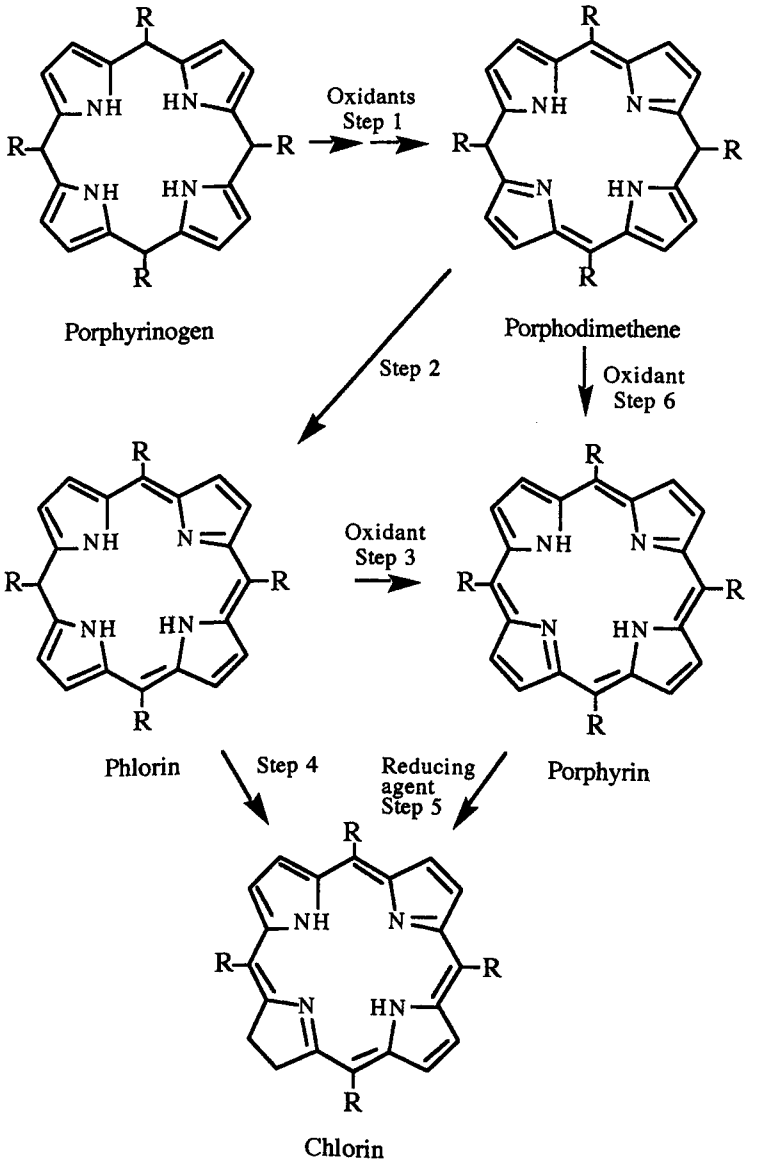

Scheme 3

Porphodimethenes detected on synthesis of TPP absorb at 480 nm[3b,5,13] and, in the present study, would correspond to the observation of a 495 nm band on oxidation of *tetrakis*(4-methoxyphenyl) porphyrinogen. In the case of

*tetrakis*arylporphyrins, phlorins were never reported, probably due to their great instability towards oxidation.[16] In reduction of uroporphyrin and coproporphyrin, an intermediate phlorin has been observed; UV/visible spectra show a characteristic main absorption band at 440 nm, together with a small broad band at about 730-740 nm.[16b] During the oxidation of *tetrakis*(4-methoxyphenyl)porphyrinogen, development of an absorption band at 465 nm was observed (see Figure 2). The band cannot be the porphyrin dication, since the spectra were recorded in alkaline medium (see experimental section of Chapter 6) and the band should represent an intermediate in the stepwise formation of porphyrin (Figure 2). The wavelength (465 nm) lying between that for porphodimethenes at 495 nm and that for porphyrin at 424 nm indicates an intermediate chromophore of structure between porphyrins and porphodimethenes. A phlorin is clearly a possibility for this intermediate. Previous work on oxidising *tetrakis*arylporphyrinogens has produced no spectroscopic evidence for such an intermediate.[13] However, in reactions carried out in one pot, the visible spectra of the reaction mixture are poorly resolved due to the presence of great number of absorbing species and also a large band with its maximum value centred at the Soret value is observed.

2.2. The origin of chlorin in porphyrin synthesis

Phlorin has been suggested to be an intermediate in stepwise formation of porphyrin and that it could be oxidised either to porphyrin or be isomerized to chlorin[3b] (Step 4, Scheme 3), which is one of the best-known sideproducts of the Rothemund reaction. The origin of chlorin in the Rothemund reaction is not completely understood. Evidence of chlorin formation in porphodimethene oxidation to porphyrin has never been produced. Instead, Dolphin proved that chlorin is formed by porphyrin reduction on normal Rothemund reaction conditions[13] (Step 5-Scheme 3).

Reactions carried out in one pot with acetic or propionic acid in the presence of nitrobenzene generally does not generate any detectable quantity of chlorin but, in the absence of nitrobenzene, the reaction is known to give small quantities of chlorin.[4] However, porphyrinogen oxidation in a mixture of acetic acid and nitrobenzene, under the same conditions as those for the one-pot reactions, resulted in the formation of large amounts of chlorin.[9] The main difference between these two systems lies in the separation of the initial condensation steps that precede porphyrinogen formation from the subsequent reaction steps to form porphyrin. There is the possibility that oxidation of porphyrinogen requires the availability of large excesses of oxidant and, if this is

not so, the products or intermediates of reaction may themselves be reduced. This would explain the observed formation of chlorin, through porphyrin reduction. Such effect is not observed in one-pot Rothemund reactions, because some of the great number of reaction intermediates present in reaction medium can themselves provide the required oxidant. The old methods of porphyrin preparation through the reaction of an aldehyde and pyrrole in a sealed tube, which generate low yields of porphyrins illustrate the oxidative ability of the reaction intermediates.[4] Such oxidation is undesirable because some of intermediates are used up in oxidising other intermediates in more advanced stages of reaction, thereby diminishing the overall yield of porphyrin. Figure 5 shows that oxidation of *tetrakis*(2,6-dichlorophenyl)porphyrinogen results in smaller amounts of chlorin when nitroarenes having small negative half-wave potentials ($E^{1/2}$) are present in the reaction medium. These same nitroarenes led to faster formation of porphyrin (Table 1). Clearly, the presence of other oxidative species in the medium of either the Rothemund reaction or in porphyrinogen solutions is a key factor, on which depends the amount of chlorin formed. If chlorin forms from phlorin, this would be an isomerization and should be independent of the presence of oxidants and approximately the same levels of phlorin as chlorin might be expected. If chlorin forms by reduction of porphyrin, the presence of a strong oxidising medium should result in a smaller amount of chlorin, as is observed.

In the development of a synthetic two-step procedure, by which porphyrinogens are produced initially and later oxidised, the above experiments show that nitroarenes alone are useful but that they also lead to formation of large proportions of chlorins and, indeed, these conditions are often suitable for preparing chlorins rather than porphyrins.

Observation of an absorption band at 465 nm in the oxidation of *tetrakis*(4-methoxyphenyl)porphyrinogen suggests that more than one synthetic path is possible in the conversion of porphyrinogen to porphyrin. This path may involve a phlorin intermediate and one such possibility is the sequence shown in Scheme 3 (step 2 and then step 3), *viz.*, porphodimethene conversion to phlorin, which is then oxidised to porphyrin.

2.3. The rate determining step in the conversion of porphyrinogen into porphyrin

The overall process, by which porphyrinogens are converted to porphyrins, is the rate determining step in Rothemund reaction.[3b] This can be attributed at least to two steps: the conversion of porphyrinogen into porphodimethenes or the conversion of porphodimethenes into porphyrin (step 1 and 6; Scheme 3).

conversion of porphodimethenes into porphyrin (step 1 and 6; Scheme 3). Measurement of rates of porphodimethene formation are about a hundred times greater than the overall values for porphyrin formation (2.5-8 x 10^{-4} and 2-6 x 10^{-6} $mol.L^{-1}.min^{-1}$ respectively) and therefore they exclude step 1 as the rate determining step. This suggests that the rate determining reaction may be step 6 (Scheme 3). The importance of a different path for converting porphyrinogens into porphyrins must be await future developments.

2.4. Effects of nitroarenes on the synthesis of porphyrins

The observations described in Section 1 support a hypothesis that nitrobenzene and oxygen work together in promoting oxidation of porphyrinogen. Following this last oxidation, with respect to the appearance of intermediates and reaction products, a number of conclusions may be drawn: (a) nitroarenes in the absence of air effect almost no conversion of porphyrinogen to porphyrin, with the exception of 1,4-dinitrobenzene; (b) the presence of both a nitroarene *and* oxygen leads to the conversion of porphyrinogen into porphyrin with greater efficiency than does air alone, although there is an exception with 4-nitroanisole; (c) nitroarenes having small negative $E^{1/2}$ are better than those with large negative $E^{1/2}$; (d) reasonable linear correlations are observed on plotting the rate constant for formation of porphyrin (log k) against "Hammet" σ^+ constants and against $E^{1/2}$; (e) during oxidation, two intermediates are observed, one absorbing at 495 nm clearly assignable to porphodimethene formation; (f) aerobic oxidation of porphodimethenes is catalysed by nitroarenes (Figure 3b) and the presence of nitroarenes leads to higher initial rates and better yields of porphyrins. The nitroarenes that are more readily reduced work best.

It is proposed that nitroarenes act by transferring electrons to oxygen, which then becomes a powerful oxidant (superoxide; $O_2^{\cdot -}$) and implies that, in acidic media as used in these experiments, hydrogen peroxide must form rapidly and that this is probably involved in the oxidation steps of converting porphyrinogen into porphyrin (Scheme 4).

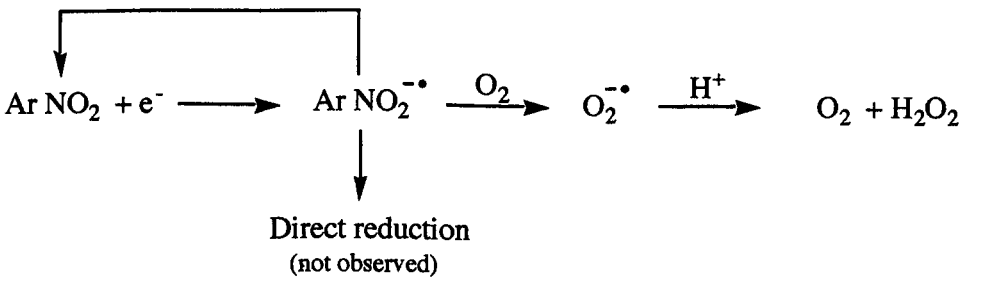

Scheme 4

Evidence for this suggestion comes from the fact that nitroarenes are not reduced to amines (anilines) or hydroxylamine in significant amounts and the presence of hydrogen peroxide has been demonstrated when nitroarenes are used but is observed only fleetingly when nitroarenes are absent (Figure 5). These observations indicate there must be a reducing agent causing initial reduction of the nitroarene by electron transfer. For the initial rates of reaction measured here, this must be the porphyrinogen which is known to be a good reducing agent.[13]

Use of hydrogen peroxide in oxidising porphyrinogens to porphyrins was assayed in the two-step synthesis of porphyrins after this observation.[8] The method proved to give good results, being used in the preparation of some porphyrins described in this work (see Chapter 6, Section III. 1., Method b).

Based on these observations the oxidation of 9,10-dihydroanthracene (DHA) to anthracene has been examined as a follow-up model for the porphyrinogen to porphyrin transformation. Acidity, the type of nitroarene and air were all found to play important roles. Thus nitrobenzene with trifluoromethyl sulfonic acid (molar equivalent), caused oxidation of dihydroanthracene very rapidly. The suggested mechanism is shown in Scheme 5.

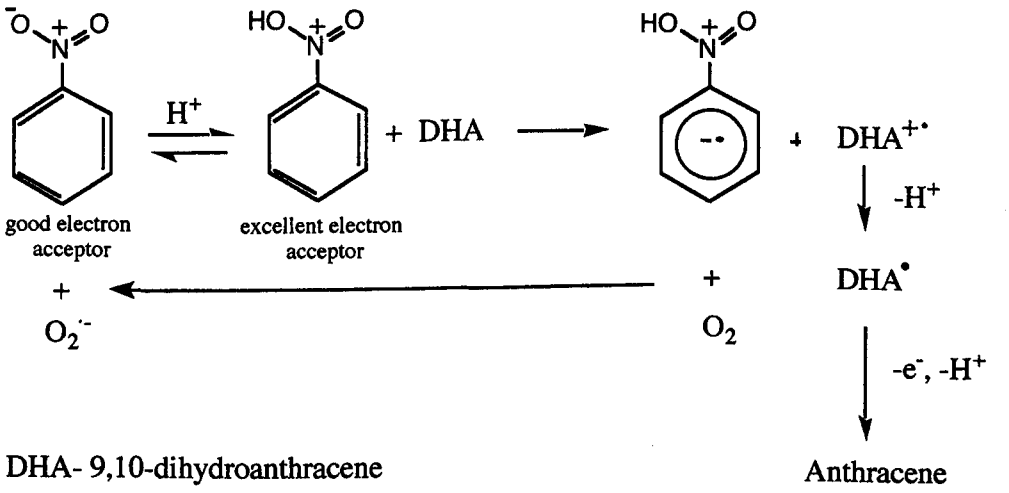

Scheme 5

Use of nitrobenzene/trifluoromethyl sulfonic acid equimolar mixture at 90°C was assayed in the oxidation of *tetrakis*phenylporphyrinogen, to give yields of porphyrin in the range of 7-9%. These relatively low yield values may indicate loss of porphyrinogen through decomposition catalysed by the strong acid.

3. The low stability of 5-(2,6-dihydroxyphenyl)-10,15,20-*tris*-heptylporphyrin and5-(2,6-dihydroxyphenyl)-10,15,20-*tris*-phenylporphyrin to air exposure

3.1. Isolation and chemical characterisation of the reaction products from exposure to air of dichloromethane solutions of 5-(2,6-dihydroxyphenyl)-10,15,20-*tris*-heptyl- and 5-(2,6-dihydroxyphenyl)-10,15,20-*tris*-phenyl-porphyrins

In the preparation of *meso*-asymmetric porphyrinic ligands such as 5-(2,6-*bis*-[4-oxycarbonyltoluene]phenyl)-10,15,20-*tris*-heptylporphyrin, discussed in Chapter 3, the stepwise synthesis required the preparation of porphyrins (**6**) and (**7**) (Scheme 6).

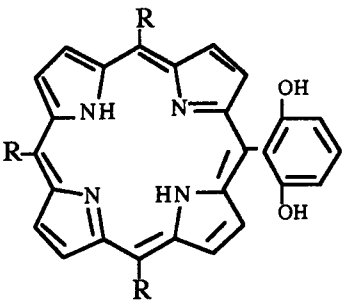

(**6**) R -C_6H_5
(**7**) R -$(CH_2)_6CH_3$

Scheme 6

When allowed to stand in chloroform or dichloromethane solution for a week at room temperature on air, these porphyrins changed from their original brown-cyan colour to a light violet, suggesting some reaction had occurred. Thin layer chromatographic analysis on silica with chloroform as eluant indicated the formation of a new compound, having lesser polarity than the original 2,6-dihydroxyphenylporphyrin (**6**, **7**; Scheme 6). Several attempts were made to isolate this new compound through silica-gel column chromatography in both the *meso*-phenyl and *meso*-alkylporphyrin series. In the *meso*-phenylporphyrin series, the chromatographic bands corresponding to the compound were always broad and poorly resolved, indicating a gross mixture. Furthermore, ^{1}H NMR spectra of these fractions lacked any clarity due to a superposition of many proton signals over the *meso*-phenyl signals. However, in the *meso*-heptylporphyrin series, it was possible to isolate chromatographically, a small quantity of a newly-formed compound (**8**), which was characterised by mass, ^{1}H NMR and visible spectroscopy. The resulting data are shown in Figure 7, in which the NMR spectrum of 5-(2,6-dimethoxyphenyl)-10,15,20-*tris*-heptyl-porphyrin (**7**) is included for comparison purposes.

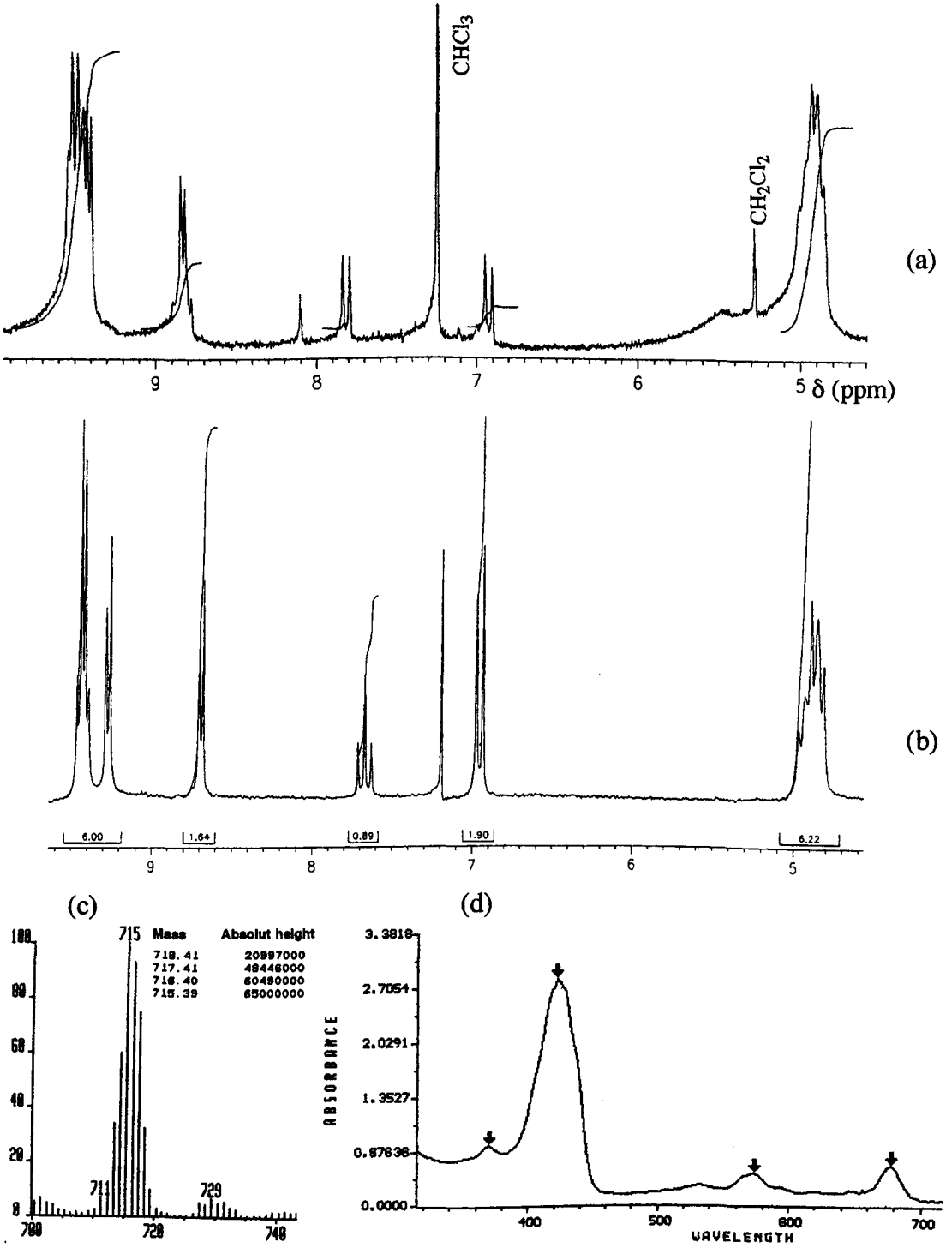

Figure 7. (a) 200 MHz ^{1}H NMR spectrum of the compound (designated here as **8**) obtained by column chromatography following exposure to air for one week of a solution of 5-(2,6-dihydroxyphenyl)-10,15,20-*tris*-heptylporphyrin; (b) ^{1}H NMR spectrum of 5-(2,6-dimethoxyphenyl)-10,15,20-*tris*-heptylporphyrin, shown for comparison; (c) Molecular ion region in the mass spectrum of (**8**); (d) Visible spectrum of (**8**).

The main NMR observations on the new compound show that, (a) the normally upfield shifted nitrogen pyrrolic protons disappear or suffer a downfield shift that makes them superimposed on the CH_2 of the alkyl chains (not shown); (b) the triplet and coupled doublet expected for the *meso*-phenyl protons, which can be seen in the spectrum of 5-(2,6-dimethoxyphenyl)-10,15,20-*tris*-heptylporphyrin (Figure 7b), are changed into two coupled doublets with an area corresponding to one proton, at about the same chemical shifts (δ = 6.92 and δ = 7.82; Figure 7a); (c) a further signal, a singlet, at δ = 8.1 (Figure 7a) can be seen; (d) a downfield shift occurs with the 3,7 β-pyrrolic porphyrin protons together with some loss of resolution in the signals for the 2,8,12,13,17,18 protons.

The mass spectral information shows two groups of peaks, one at m/z between 712 and 719 (there being a maximum at m/z = 715/716) the other, having smaller size is found at m/z between 727 and 732, with a maximum at m/z = 729 (see Figure 7c). The calculated mass for 5-(2,6-dihydroxyphenyl)-10,15,20-*tris*-heptylporphyrin ($C_{47}H_{60}N_4O_2$) is 712.47. This means that its M-H^+ peaks (FAB) should be found at m/z = 713/714. The observed peaks at m/z = 712-719 and at m/z = 727/732 indicate the occurrence of structural modifications and probable insertion of oxygen.

The UV-visible spectra show the characteristic Soret band at 420 nm but significantly broadened. The characteristic Q porphyrinic bands have changed into two bands, one at 575 and another at 680 nm (Figure 7d).

4. Discussion

The chemistry of compounds related to (**6**) and (**7**) has been studied extensively for porphyrins substituted in the *meso* positions with 3,5-di-t-butyl-4-hydroxyphenyl.[19-22] In this last compound, aerial oxidation[19] or conproportion[20] leads to the formation of an oxidised compound in which aromatic conjugation is extended to the *meso*-phenyl groups. The product is formed by stepwise aerial oxidation *via* an intermediate formation of a radical species, which is stabilized by resonance.[19] In Scheme 7, is shown a possible oxidative pathway for these species.

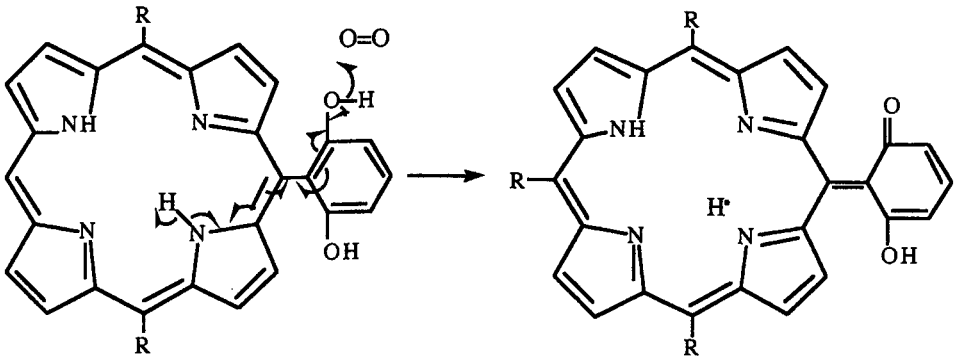

Scheme 7

These compounds show in their ^1H NMR spectra a pronounced downfield shift of the pyrrolic NH protons and, in their visible spectra, a large band between 450-750 nm, centred at 480 nm.[19] For unsymmetrical *meso*-tetraarylporphyrins with 3,5-di-t-butyl-4-hydroxyphenyl and 4-hydroxyphenyl substituents their visible spectra show broadened Soret bands and the collapse of the Q bands into 2 or 3 bands, one centred at about 680 nm.[21]

The compound isolated in the present work, showed some of the characteristics described for asymmetric *meso*-tetraarylporphyrins with 3,5-di-t-butyl-4-hydroxyphenyl and 4-hydroxyphenyl substituents, namely the 680 nm visible spectral band and the modification in the NH resonance pattern in NMR spectrum. However, mass and NMR spectra observations suggest the occurrence of further modifications. If the molecular ion peaks are those at m/z = 715/716, most probably the new compound is reduced relatively to the original compound (**6** or **7**) but, if the molecular ion peaks are those found at m/z = 728/729, most probably an atom insertion occurred. An important observation arises from the *meso*-phenyl proton signals. The coupled doublets at $\delta = 6.9$ and $\delta = 7.8$, clearly indicate that one of the *meso*-phenyl group protons, either at position 3 or 5, is absent. This result strengthens the idea of an atom insertion in one of the 3 or 5 *meso*-phenyl position. Since the solutions of (**6**) and (**7**) were exposed to air during some time, it is not difficult to think in oxygen insertion at that position (Scheme 8).

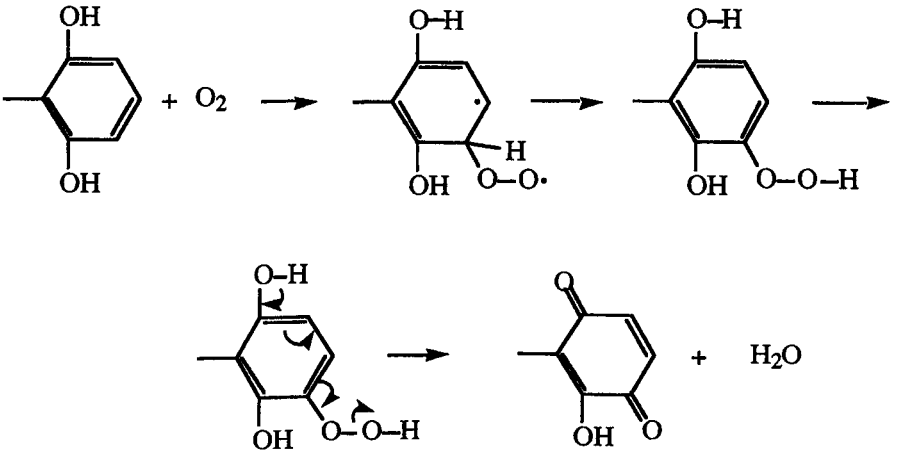

Scheme 8

Initially, oxygen should react in one of such positions to give an hydroperoxide. However the mass spectral peaks at about m/z = 729 suggest that only one oxygen was added, because that value is in accord with a compound with a formula $C_{47}H_{60}N_4O_3$ (molecular ion expected at m/z = 729/730). The conversion of a hydroperoxide to an alcohol or a ketone are reactions known for long time (Scheme 8). The visible spectrum, the β-pyrrolic and (N)H NMR proton spectral pattern changes indicate that not only modifications occurred in the *meso*-phenyl group, but also in the porphyrin ring. This is the result expected for the oxidation similar to that depicted in Scheme 7 and verified by earlier studies.[19-22] In these cases, the expected formula for the reaction product is $C_{47}H_{58}N_4O_3$ (molecular ion at m/z = 727/728), which is close to the value observed. The concomitant formation of a reduced compound plus some oxidized compound suggest that one acts as an H acceptor and the other reacts with oxygen . This would lead to the formation of two compounds, one oxidised with a mass of 726 and another with a mass of 714, which is the result observed in the mass spectrum (Scheme 9).

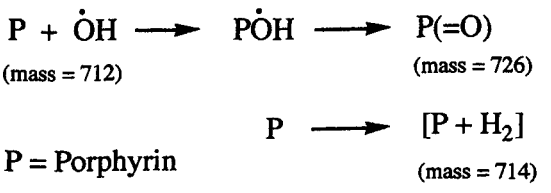

Scheme 9

The structure of the oxidized compound is proposed to be one of that showed in Scheme 10.

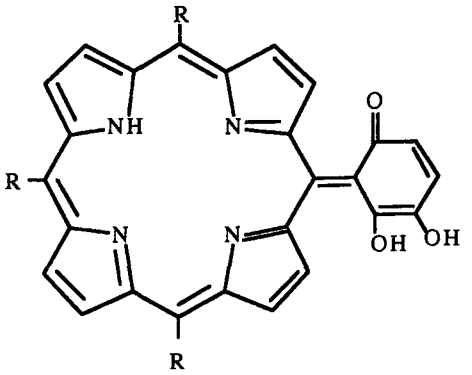

(9)

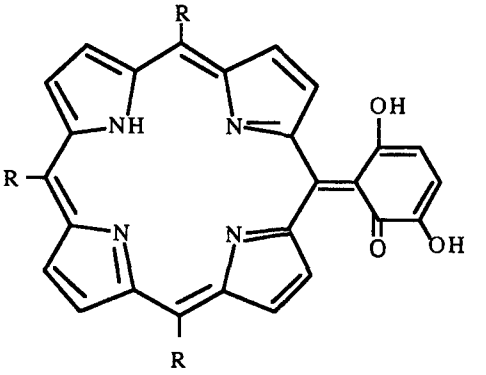

(10)

Scheme 10

III. References

1. (a) J. M. T. B. Varejão, M.Sc. Thesis, Universidade de Coimbra, Coimbra, 1990; (b) A. M. d'A. Rocha Gonsalves, J. M. T. B. Varejão and M. M. Pereira, *J. Het. Chem.*, 1991, **28**, 635 .

2. (a) P. Rothemund; *J. Am. Chem. Soc.*, 1935, **57**, 1810; (b) P. Rothemund; *J. Am. Chem. Soc.*, 1935, **61**, 2912.

3. a) A. D. Adler, F. R. Longo and W. Shergalis; *J. Am. Chem. Soc.*, 1964, **86**, 3154; b) A. D. Adler, L. Skar, F. R. Longo, J. D. Finarelli and M. G. Finarelli; *J. Het. Chem.*, 1968, **5**, 669.

4. A. D. Adler, L. Skar, F. R. Longo, J. D. Finarelli, J. Goldmacher, J. Assour and L. Korsakoff; *J. Org. Chem.*, 1967, **32**, 476.

5. A. M. d'A. Rocha Gonsalves and M. M. Pereira, *J. Het. Chem.*, 1985, **22**, 931.

6. a) J. S. Lindsey, H. C. Hsu and I. C. Schreiman, *Tetrahedron Lett.*, 1986, **41**, 4969; b) J. S. Lindsey, I. C. Schreiman, H. C. Hsu, P. C. Kearney, and A. M. Marguerettaz; *J. Org. Chem.*, 1987, **52**, 827.

7. J. S. Lindsey and R. W. Wagner, *J. Org. Chem.*, 1989, **54**, 828.

8. R. A. W. Johnstone, M L. P. G. Nunes, M. M. Pereira, A. M. d'A. Rocha Gonsalves and A. C. Serra, *Heterocycles*, 1996, **43**, 1423.

9. M. L. P. G. Nunes, PhD Thesis, University of Liverpool, 1995.

10. C. L. Hill and M. M. Williamson, *J. Chem. Soc. Chem. Commun*; 1985, 1228.

11. M. Bruix, J. Elguero and W. Meutermans, *J. Chem. Research (S)*, 1992, 370.

12. Jean B. King, Jonh J. Leonard, and Frederick R. Longo; *J. Am. Chem. Soc.*, 1972, **94**, 3986.

13. D. Dolphin, *J. Het. Chem.*, 1970, **7**, 275.

14. P. J. Chmieelewski, L. Latos-Grazynski, K. Rachlewicz, and T. Glowiah, *Angew. Chem. Int. Ed. Engl.*, 1994, **33**, 779.

15. (a) M. R. Rifi and Frank H. Covitz in, "*Introduction to Organic Electrochemistry*", New York, Marcel Dekker, 1974, p. 183; (b) August H. Maki and David H. Geske, *J. Am. Chem. Soc.*, 1961, **83**, 1852; (c) M. E. Peover, *Trans. Faraday Soc.*, 1964, **60**, 479.

16. (a) "*Porphyrins and Metalloporphyrins*", Ed. K. M. Smith, Elsevier, Amsterdam, 1975; (b) J. E. Falk in, *Porphyrins and Metalloporphyrins*,Vol. 2, Elsevier, New York, 1964, pag. 12.

17. M. A. J. Rodgers, E. L. Powers in, "*Oxygen and Oxy Radicals in Chemistry and Biology*", Academic Press, New York, 1981.

18. R. B. Herhert, F.G. Holliman and J. D. Kynnerley, *Tetrahedron Lett.*, 1980, **16**, 1907.

19. (a) L. R. Milgrom, J. P. Hill, G. Yahioglu, *J. Het. Chem.*, 1995, **32**, 97; (b) R. Milgrom, J. P. Hill, P. J. F. Dempsey, *Tetrahedron*, 1994, **50**, 13477 (c) R. Milgrom, J. P. Hill, W. D. Flitter, *J. Chem. Soc., Perk. Trans.*, 1994, 2,521; (d) R. Milgrom, J. P. Hill, *J. Het. Chem.*, 1993, **30**, 1629; (e) R. Milgrom, W. D. Flitter, *Tetrahedron*, 1993, **49**, 507; (f) R. Milgrom, J. P. Hill, W. D. Flitter, *J. Chem. Soc., Chem. Comm.*, 1992, 773; (g) R. Milgrom, W. D. Flitter, *Tetrahedron*, 1992, **48**, 2951; (h) R. Milgrom, W. D. Flitter, *Tetrahedron*, 1991, **47**, 7683; (i) R. Milgrom, W. D. Flitter, E. L. Short, *J. Chem. Soc., Chem. Comm.*, 1991, 788; (j) A. J. Golder, L. R. Milgrom, K. B. Nolan, D. C. Povey, *J. Chem. Soc.,Chem. Comm.*, 1989, 1751; (l) R. L. Milgrom, C. C. Jones, A. Harriman, *J. Chem. Soc., Perk. Trans.*, 1988, 2, 71; (m) W. J. Albery, P. N. Bartlett, C. C. Jones, L. R. Milgrom, *J. Chem. Research.-S*, 1985, 364.

20. R. Milgrom, W. D. Flitter, *J. Chem. Soc., Chem. Comm.*, 1991, 1492.

21. (a) R. L. Milgrom, N. Mofidi, C. C. Jones, A. Harriman, *J. Chem. Soc., Perk. Trans.*, 1989, 2,301; (b) R. L. Milgrom, N. Mofidi, A. Harriman, *J. Chem. Soc., Perk. Trans., 2*, 1989, 805.

22. R. L. Milgrom, C. Palmer, *J. Chem. Research-S*, 1990, 66.

23. M. McCarron, Univ. Liverpool, 1998/9, (Private Communication).

CHAPTER 6: EXPERIMENTAL SECTION

I. Introduction

In this chapter are described the experimental details concerning the preparation and analytical characterization of the compounds used in the present work, together with experimental system conditions used to determine their peroxidase-like activity.

The organisation of this experiment description follow the chapter division of the present thesis.

II. General considerations

1. Chemicals

All chemicals were used as received, unless otherwise stated. Chloroform and dichloromethane used in visible spectra recording were previously passed through an alumina column (5 x 5 cm).

2. Analytical methods

Analytical thin layer chromatography (TLC) was carried out on Merck 60 silica gel plates (20 x 20 cm; 0.3 mm layer). Flash chromatography was performed in silica-gel 60 (230-400 mesh, pore diameter = 60Å, surface area = 550m^2/g) or alumina (Woelm, activity grade I), in conditions described in text. UV/visible spectra were measured on a Hewlett Packard HP 8452A diode array spectrometer. Nuclear magnetic resonance spectra (^{1}H NMR) were obtained either on a BRUKER AC-200 (200MHz), on a 300 MHz Varian-Gemini (300MHz), or in a BRUKER AC-400 (400MHz) spectrometer. In ^{1}H NMR description, the hydrogen number reference is made to the carbon or heteroatom to which the hydrogen is bonded. Mass spectra (FAB) were determined on a VG7070E magnetic sector double focusing mass spectrometer, using fast atom bombardment

with Xenon and a 3-NOBA matrix. Gas chromatography (GLC) was made on a PYE UNICAM model PU 4500 chromatograph, using a split inlet (split ratio = 1/200) and a flame ionisation detector (FID), with an BD-WAX capillary column (JW Scientific Inc, 30m x 0.53mm, stationary phase thickness =1μm); the carrier gas was nitrogen at 5 mL/min and the oven was set isothermally at 100°C. Gel permeation chromatography (GPC) was made with a Knauer HPLC system equipped with a refractive index detector (RI) and fitted with two coupled separating columns: Column 1- PLgel 5μ-500A (Polymer Laboratories, PL); Column 2- PLgel 5μ-10A. Conditions: Eluent: DMF, 1 mL/min; Column oven temperature = 90°C. Fluorescence spectrophotometry studies were made on a Perkin Elmer MPF-43 fluorescence spectrophotometer with emitted light being detected at 425 nm.

III. Chapter 2 experimental details

1. Methods in preparing porphyrins

Method (a).[1] A 250 mL double necked flask was fitted with a reflux condenser and a rubber septum. Into the flask was placed the required aldehyde (20 x 10^{-3} moles) in a mixture of acetic acid (70 mL) and nitrobenzene (30 mL). The reaction mixture was heated to reflux and then pyrrole was added (1.34 g; 20 x 10^{-3} moles). The reaction mixture was refluxed for one hour and, after this period of time, the heating was turned off. The reaction mixture was allowed to cool overnight and then filtered through a glass frit funnel (10-15μ). The crystalline residue was washed with methanol (3 x 15 mL) and dried. In some experiments, no porphyrin was obtained, then methanol was added (30-50 mL) to the reaction medium and the resulting solution stored in a refrigerator overnight (12h). After this period, the solution was filtered and the porphyrin collected as a crystalline material.

Method (b).[2] To a 3 L round-bottomed flask, equipped with a magnetic stirrer was added CH_2Cl_2 (2 L) which had been previously passed through an alumina column (activity grade I -10 cm x 5 cm). The solvent was flushed with nitrogen for 15 min. Under nitrogen, the required aldehyde (1.5 x 10^{-2} moles) was added followed by distilled pyrrole (1.5 x 10^{-2} moles). After the solution had homogenised $BF_3.Et_2O$ (45%; 240μL) was added. The reaction mixture was allowed to stand for 3-4 hours. After this period, triethylamine (300μL) and H_2O_2 (8 g of 35% H_2O_2 in 400 mL acetic acid) were added. The solution was stirred for 1-2 hours, with the flask open to the atmosphere. All solvent was evaporated off and the residue was dissolved in a small volume of chloroform. The required porphyrin was passed through flash chromatography column, using chloroform as eluent (alumina activity grade I/II- 15 x 5 cm). The coloured porphyrinic band was collected and the solvent was evaporated.

2. Details and characterisation of porphyrin synthesized

2.1. 5,10,15,20-*Tetrakis*phenylporphyrin (TPP)

Preparation of this porphyrin was by the method (a) (see above), and gave 720 mg (24% yield). $\delta_H(CDCl_3$; 200MHz; $Me_4Si)$, 8.78 [8H, s, β-pyrrolic], 8.16 [8H, m, 2,6-phenyl], 7.65 [12H, m, 3,4,5-phenyl], -2.82 [2H, s, NH]; $\lambda_{max}(CH_2Cl_2)$/nm, (ε, L. mol^{-1}. cm^{-1}) 418 (357393), 514(22985), 546(11561), 586(11221), 644(8862); MS (FAB), $[M+H]^+$, *m/z* 615; Found: C, 85.8; H, 4.9; N, 9.0. $C_{44}H_{30}N_4$ requires C, 86.0 ; H, 4.9 ; N, 9.1%.

2.2 5-(4-Vinylphenyl)-10,15,20-*tris*-phenylporphyrin

Preparation of this porphyrin was made by method (a), using 4-vinylbenzaldehyde mixture (≈ 3.0 $x10^{-3}$ moles, 430 mg, see experimental details below) mixed with benzaldehyde (2.89 mL, 2.72 x 10^{-2} moles) and pyrrole (0.03 moles, 2.1 mL) in propionic acid/nitrobenzene (7/3, 200 mL). On filtration, 590mg of crystalline material was isolated (12.8% yield). In an attempt to recover even more porphyrinic material from the reaction medium, methanol was added and the solution refrigerated overnight. On filtration a big amount of a brown-solid was isolated. This product showed porphyrin-like visible spectrum but was not further characterized. TLC analysis of the crystalline material (silica gel; $CHCl_3$ as eluant) showed that the reaction product was a mixture of mainly TPP and 5-(4-vinylphenyl)-10,15,20-*tris*-phenylporphyrin. Analysis by mass spectrometry suggested that the relative proportions of the porphyrins was 9/1. A small amount of purified vinylporphyrin was isolated by preparative TLC for purposes of characterization, under conditions similar to those described in Section IV-2.3, for the isolation of 5-(2-methoxyphenyl)-10,15,20-*tris*-phenylporphyrin. $\delta_H(CHCl_3$; 200MHz; $Me_4Si)$, 8.91 [2H, s, β-pyrrolic], 8.84 [6H, s, β-pyrrolic], 8.25 [8H, m, 2,6-phenyl], 7.77 [12H, m, 3,4,5-phenyl], 6.69 [1H, dd, H—C=, J_1 = 10 Hz, J_2 = 18 Hz], 5.78 [1H, d, =CH, J = 17 Hz], 5.48 [1H, d, =CH, J = 17 Hz], -2.33 [2H, s, NH]; $\lambda_{max}(CH_2Cl_2)$/nm, (ε, L. mol^{-1}. cm^{-1}) 418(265054), 514(20518), 550(11301), 586(10424), 644(8010), MS (FAB), $[M+H]^+$, *m/z* 641.

2.2.1 4-Vinylbenzaldehyde

The preparation of 4-vinylbenzaldehyde was effected by a Wittig reaction, between methyltriphenylphosphonium bromide and terephthaldehyde.[3]

Methyltriphenylphosphonium bromide (0.02 mole, 7.15g), potassium carbonate (3.5g) and terephthaldehyde (0.02 mole, 2,68g) were dissolved in 1,4-dioxane (20 mL) containing water (0.3 mL) in a 100 mL flask equipped with a magnetic stirrer and a reflux condenser. The reaction mixture was stirred and refluxed for 4.5 h. The reaction mixture was then evaporated and chromatographed on a silica-gel G-60 (15 x 5 cm), using as eluant a mixture of hexane/CH_2Cl_2 (1/1). The first band collected gave 860 mg of 4-vinylbenzaldehyde. δ_H($CDCl_3$; 200MHz; Me_4Si), 9.96 [1H, s, COH], 7.80 [2H, d, aromatic C(2,6)H, J = 14 Hz], 7.50 [2H, d, aromatic C(3,5)H, J = 14 Hz], 6.75 [1H, q, $\underline{C}H=CH_2$], 5.89 [1H, d, $CH=\underline{C}H_2$, J = 18 Hz], 5.40 [1H, d, $CH=\underline{C}H_2$, J = 10 Hz].

2.3. 5,10,15,20-*Tetrakis*heptylporphyrin

This porphyrin was obtained as a secondary product in the synthesis of 5-(2,6-dimethoxyphenyl)-10,15,20-*tris*-heptylporphyrin, described in Section IV. 3.1. δ_H($CHCl_3$; 200MHz; Me_4Si), 9.42 [8H, s, β-pyrrolic], 4.89 [8H, t, J = 10 Hz, α-CH_2], 2.47 [8H, m, β-CH_2], 1.76 [8H, m, γ-CH_2], 1.51 [8H, m, δ-CH_2], 1.28 [8H, m, ε-CH_2], 1.25 [8H, m, ζ-CH_2], 0.86 [9H, m, -CH_3], -2.66 [2H, s, NH]; λ_{max}(CH_2Cl_2)/nm, (ε, L. mol^{-1}. cm^{-1}) 418(304881), 486(3284), 520(11321), 556(8327), 600(3757), 658(6036); MS (FAB), $[M+H]^+$, *m/z* 703; Found: C, 81.2; H, 10.2; N, 7.7; $C_{48}H_{70}N_4$: requires: C, 81.0 ; H, 10.0 ; N, 8.0%.

2.4. 5-(2,6-Dimethoxyphenyl)-10,15,20-*tris*-heptylporphyrin

Details of the synthesis and characterization of this compound are described in Section IV-3.1.

2.5. 5,10,15,20-*Tetrakis*(2,6-dichlorophenyl)porphyrin (TDCPP)

Preparation of this porphyrin was effected either by method (a) or method (b). Method (a) gave 240mg (4.5% yield); method (b) gave 840mg (25% yield). δ_H($CDCl_3$; 200MHz; Me_4Si), 8.63 [8H, s, β-pyrrolic], 7.69 [12H, m, 3,4,5-phenyl], -2.59 [2H, s, NH]; λ_{max}(CH_2Cl_2)/nm, (ε, L. mol^{-1}. cm^{-1}) 418(357393), 512(4351), 588(1563), 658 (907), 456(826); MS (FAB), $[M+H]^+$, *m/z* 887-905 (Cl isotopes); Found: C, 59.4; H, 2.5; N, 6.3; $C_{44}H_{22}N_4Cl_8$: requires: C, 59.4 ; H, 2.5; N, 6.3%.

2.6. 5,10,15,20-*Tetrakis*(2,6-dichloro-3-chlorosulphophenyl)porphyrin

A 100 mL flask was fitted with a reflux condenser. Into the flask was placed TDCPP (200mg; 2.25 x 10^{-4} moles) and chlorosulphonic acid (12 mL, 2.1 x 10^{-3} moles). The mixture was stirred and heated in an oil bath at 90-100°C for 2 h. After this period of time the reaction mixture was cooled and ice was added to destroy the excess of chlorosulphonic acid. To the reaction medium was added $CHCl_3$ (30 mL) and the organic layer was separated. Purification of the porphyrin effected by chromatography on silica-gel (G-60; 20 cm x 3 cm), using $CHCl_3$ as eluant. The first band, corresponding to unreacted TDCPP was set aside. The second band gave 280mg of the required porphyrin (93% yield); $\delta_H(CHCl_3$; 200MHz; $Me_4Si)$, 8.64 [8H, s, β-pyrrolic], 8.63 [4H, d, 3-phenyl, J = 8 Hz], 8.05 [4H, d, 4-phenyl, J = 8 Hz], -2.48 [2H, s, NH]; $\lambda_{max}(CHCl_3)$/nm, (relative %) 382(64), 424 (100), 516 (8).

2.7. 5,10,15,20-*Tetrakis*(2,6-dichloro-3-sulphophenyl)porphyrin (TDCPPS)

To a 100 mL round bottowed flask, equipped with a condenser was added 5,10,15,20-*tetrakis*(2,6-dichloro-3-chlorosulphonylphenyl)porphyrin (200 mg) and distilled water (10 mL). The mixture was refluxed for 24 h., cooled and acetone (30 mL) was added to give 88 mg of crystalline porphyrin sulphonic acid (85% yield). $\delta_H(CD_3OD$; 200MHz; $Me_4Si)$, 9.07 [8H, s, β-pyrrolic], 8.70 [4H, d, 3-phenyl, J = 9 Hz], 6.94 [4H, d, 3-phenyl, J = 9 Hz]; $\lambda_{max}(H_2O)$/nm (ε, L. mol^{-1}. cm^{-1}) 412(310629), 513(14500), 579(6328), 634(1678); Found: C, 39.5; H, 2.8; N, 3.8; $C_{44}H_{22}N_4S_4O_{12}Cl_8$. $8H_2O$: requires: C, 39.0; H, 2.8 ; N, 4.1%.

3. Metallation of porphyrins

Metallation was effected by reaction with a salts of the required metal, by any of the methods described below. In those cases, where iron(II) salts were used, the metallation reaction was done under nitrogen to avoid oxidation to iron(III).

3.1. Water-soluble porphyrins

To a 100 mL flask fitted with a condenser was added the required porphyrin (4-5 x 10^{-5} moles), an excess of the required metal salt (2x, 1.0 x 10^{-4} moles) and distilled water (20 mL). The whole was refluxed for 24-72 h. The end of reaction was determined by visible spectroscopy by observing the disappearance of the Q free base porphyrin bands. The water was evaporated under reduced pressure and the residue was dissolved in distilled water (2 mL). This solution was passed through a Sephadex G15 column (25 x 3.5cm) using water as eluant. The large second band was collected; it corresponded to the required metalloporphyrin. Finally, the water was evaporated from the eluate as before, and the metalloporphyrin was dissolved in a minimum amount of methanol and then precipitated by addition of acetone.

3.2. Water-insoluble porphyrins

To a 100 mL flask fitted with condenser was added the required porphyrin (5.0 x10^{-5} moles), an excess of the required metal salt (2x, 1.0 x 10^{-4} moles) and dimethylformamide (DMF; 40 mL). The whole was heated to 130°C for 12-24 h. The end of reaction was determined by visible spectroscopy, as before. The DMF was evaporated under reduced pressure and the metalloporphyrin purified by chromatography (silica-gel; 10 x 3 cm) using $CHCl_3$ as eluant.

4. Details and characterization of metalloporphyrins

4.1. Iron(III) 5,10,15,20-*tetrakis*phenylporphyrin chloride (3a)

Preparation of this metalloporphyrin was effected by the method described in Section 3.2 above, using $FeCl_2.4H_2O$. After workup, 29 mg of crystalline material was obtained (83% yield). $\lambda_{max}(CH_3OH)$/nm, (ε, L. mol^{-1}. cm^{-1}) 414

(166446), 530(10459); MS (FAB), M^+, *m/z* 668; Found: C, 74.8; H, 3.9; N, 7.8. $C_{44}H_{28}N_4FeCl$ requires C, 75.1 ; H, 4.0 ; N, 8.0%.

4.2. Manganese(III)-5,10,15,20-*tetrakis*phenylporphyrin chloride (3b)

Preparation of this metalloporphyrin was made by the method described in Section 3.2 above, using $MnCl_2.4H_2O$. After workup, 30 mg of crystalline material were obtained (89% yield). $\lambda_{max}(CH_3OH)$/nm, (ε, L. mol^{-1}. cm^{-1}) 467(140741), 564(14444), 599(10370); MS (FAB), M^+, *m/z* 667; Found: C, 75.4; H, 4.1; N, 7.7. $C_{44}H_{28}N_4MnCl$ requires C, 75.2 ; H, 4.0 ; N, 8.0%.

4.3 Iron(III) 5-(4-vinylphenyl)-10,15,20-*tris*-phenylporphyrin chloride

Preparation of this metalloporphyrin was made by the method described in Section 3.2 above, using $FeCl_2.4H_2O$. After workup, 25 mg of crystalline material was obtained (70% yield). Since this compound was prepared as a mixture with FeTPP (see Section 2.2) no further characterization was made.

4.4. Manganese(III) 5-(4-vinylphenyl)-10,15,20-*tris*-phenylporphyrin chloride

Preparation of this metalloporphyrin was made by the method described in Section 3.2 above, using $MnCl_2.4H_2O$. After workup, 30 mg of crystalline material was obtained (82% yield). Since this compound was prepared as a mixture with FeTPP (see Section 2.2) no further characterization was made.

4.5. Iron(III) 5,10,15,20-*tetrakis*heptylporphyrin chloride (4a)

Preparation of this metalloporphyrin was made by the method described in Section 3.2 above, using $FeCl_2.4H_2O$. After workup, 29 mg of crystalline material was obtained (78% yield). $\lambda_{max}(CH_3OH)$/nm, (ε, L. mol^{-1}. cm^{-1}) 416(115556), 332(24444), 536(10622); MS (FAB), M^+, *m/z* 756; Found: C, 72.8; H, 8.9; N, 7.1. $C_{48}H_{68}N_4FeCl$ requires C, 72.8 ; H, 8.7 ; N, 7.1%.

4.6. Manganese(III) 5,10,15,20-*tetrakis*heptylporphyrin chloride (4b)

Preparation of this metalloporphyrin was made by the method described in Section 3.2 above, using $MnCl_2.4H_2O$. After workup, 35 mg of crystalline material was obtained (87% yield). $\lambda_{max}(CH_3OH)$/nm, (ε, L. mol^{-1}. cm^{-1}) 472(123658), 581(14557), 617(17520); MS (FAB), $[M+H]^+$, *m/z* 755; Found: C, 70.6; H, 8.9; N, 7.0. $C_{48}H_{68}N_4FeCl$ requires C, 71.1 ; H, 8.5 ; N, 6.9%.

4.7. Iron(III) 5-(2,6-dimethoxyphenyl)-10,15,20-*tris*-heptylporphyrin chloride (5a)

Preparation of this metalloporphyrin was made by the method described in Section 3.2 above, but using 5 x 10^{-6} moles of porphyrin with $FeCl_2.4H_2O$. After workup, 3.7 mg of crystalline material was obtained (90% yield). $\lambda_{max}(CH_3OH)$/nm, (ε, L. mol^{-1}. cm^{-1}) 418(124352), 538(12222); MS (FAB), M^+, *m/z* 785.

4.8. Manganese(III) 5-(2,6-dimethoxyphenyl)-10,15,20-*tris*-heptylporphyrin chloride (5b)

Preparation of this metalloporphyrin was made by the method described in Section 3.2 above, but using 5 x 10^{-6} moles of porphyrin with $MnCl_2.4H_2O$. After workup, 3.0 mg of crystalline material was obtained (73% yield). $\lambda_{max}(CH_3OH)$/nm, (ε, L. mol^{-1}. cm^{-1}) 480(124797), 590(2128), 630(2310); MS (FAB), M^+, *m/z* 783.

5. Metal complexes of 5,10,15,20-*tetrakis*(2,6-dichlorophenyl)porphyrin (2)

5.1. Iron(III) 5,10,15,20-*tetrakis*(2,6-dichlorophenyl)porphyrin chloride (2a)

Preparation of this metalloporphyrin was effected by the method described in Section 3.2 above, using TDCPP (40mg; 4.5 x 10^{-5} moles) and $FeCl_2.4H_2O$. After workup, 32mg of the required crystalline product was obtained (61% yield). $\lambda_{max}(CH_2Cl_2)$/nm, (ε, L. mol^{-1}. cm^{-1}), 414(117815), 332(31045), 586(7347), MS

(FAB), M^+, *m/z* 944; Found: C, 54.0; H, 2.1; N, 5.7. $C_{44}H_{20}N_4Cl_8FeCl$ requires C, 54.0 ; H, 2.1; N, 5.7%.

5.2. Manganese(III) 5,10,15,20-*tetrakis*(2,6-dichlorophenyl)porphyrin chloride (2b)

Preparation of this metalloporphyrin was effected by the method described in Section 3.2 above, using $MnCl_2.4H_2O$. After workup, 38mg of the required crystalline product was obtained (80% yield). $\lambda_{max}(CH_3OH)$/nm, (ε, L. mol^{-1}. cm^{-1}) 478(140612), 584(2504); MS (FAB), M^+, *m/z* 943; Found: C, 54.1; H, 2.2; N, 5.7. $C_{44}H_{20}N_4Cl_8MnCl$ requires C, 54.0 ; H, 2.1 ; N, 5.7%.

5.3. Cobalt(III) 5,10,15,20-*tetrakis*(2,6-dichlorophenyl)porphyrin chloride (2c)

Preparation of this metalloporphyrin was effected by the method described in Section 3.2 above, using TDCPP (40mg, 4.5 x 10^{-5} moles) and $CoCl_2.6H_2O$. After workup, 32 mg of the required crystalline product was obtained (73% yield). $\delta_H(CDCl_3$; 200MHz; $Me_4Si)$, 9.43 [8H, s, β-pyrrolic], 7.75 [12H, m, phenyl]; $\lambda_{max}(CH_2Cl_2)$/nm, (ε, L. mol^{-1}. cm^{-1}) 412(208114), 530(3880); MS (FAB), M^+, *m/z* 947; Found: C, 55.7; H, 3.5; N, 5.9. $C_{44}H_{20}N_4Cl_8CoCl$ requires C, 55.8 ; H, 2.1 ; N, 5.9%.

5.4. Molybdenum, 5,10,15,20-*tetrakis*(2,6-dichlorophenyl)porphyrin chloride[4]

To a 50 mL fask fitted with condenser, was added TDCPP (4.5 x 10^{-5} moles) in a mixture of decalin (10 mL) and hexadecane (10 mL). The mixture was heated to 200°C in an oil bath and an excess of $Mo(CO)_6$ (25x, 300mg; 1.14 x 10^{-3} moles) was added. This solution was refluxed for 12 h, after which, decalin was removed by evaporation under reduced pressure and the reaction product was purified by flash chromatography, using CH_2Cl_2 as eluant. $\lambda_{max}(CH_2Cl_2)$/nm, (ε, L. mol^{-1}. cm^{-1}) 416(73552), 516(1604), 640(2562); MS (FAB), M^+ peaks at 1253, 1165, 1119, 1029. No satisfactory CHN analysis was obtained. The results indicate that a mixture of several unknown compounds had been obtained. Under these circunstances, this mixture was not used in the peroxidase-like activity measurements.

6. 5,10,15,20-*Tetrakis*(2,6-dichloro-3-sulphophenyl) porphyrin (TDCPPS) metal complexes (1a-d)

6.1. Iron(III) 5,10,15,20-*tetrakis*(2,6-dichloro-3-sulphophenyl)porphyrin chloride (1a)

Preparation of this metalloporphyrin was effected by the method described in Section 3.1 above, using TDCPPS (50mg; 4.13 x 10^{-5} moles) and $FeCl_2.4H_2O$. After workup, 33mg of crystalline material was obtained (62% yield). $\lambda_{max}(H_2O)$/nm, (ε, L. mol^{-1}. cm^{-1}) 396(104325), 508(24538); Found: C, 35.6; H, 2.5; N, 3.9; $C_{44}H_{20}N_4S_4O_{12}Cl_8FeCl$. $10H_2O$: requires: C, 35.7; H, 2.7; N, 3.8%.

6.2. Manganese(III) 5,10,15,20-*tetrakis*(2,6-dichloro-3-sulphophenyl) porphyrin chloride (1b)

The procedure adopted was the described in Section 3.1 above, using TDCPPS (50mg; 4.13 x 10^{-5} moles) and $MnCl_2.6H_2O$. After workup, 41 mg of crystalline material was obtained (71% yield). $\lambda_{max}(H_2O)$/nm, (ε, L. mol^{-1}. cm^{-1}) 464(169760), 560(34667); Found: C, 37.7; H, 2.5; N, 4.1; $C_{44}H_{20}N_4S_4O_{12}Cl_8MnCl$. $6H_2O$: requires: C, 37.6 ; H, 2.3 ; N, 4.0%.

6.3. Cobalt(III) 5,10,15,20-*tetrakis*(2,6-dichloro-3-sulphophenyl)porphyrin chloride (1c)

The procedure adopted was the described in Section 3.1 above, using TDCPPS (50mg; 4.13 x 10^{-5} moles) and $CoCl_2.6H_2O$. After workup, 34mg of crystalline material was obtained (63% yield). $\delta_H(D_2O$; 200MHz;$CH_3OH)$, 9.36 [8H, s, β-pyrrolic], 8.50 [4H, d, 3-phenyl, J = 8 Hz], 8.05 [4H, m, 4-phenyl]; $\lambda_{max}(H_2O)$/nm, (ε, L. mol^{-1}. cm^{-1}) 430(241801), 546(27933); Found: C, 37.5; H, 2.6; N, 3.2; $C_{44}H_{20}N_4S_4O_{12}Cl_8CoCl$. $6H_2O$: requires: C, 37.5 ; H, 2.3 ; N, 4.0%.

6.4. Molybdenum 5,10,15,20-*tetrakis*(2,6-dichloro-3-sulphophenyl) porphyrin chloride[4] (1d)

The preparation of this metal complex involved reaction of the more hydrophobic 5,10,15,20-*tetrakis*(2,6-dichloro-3-chlorosulphonylphenyl)porphyrin with $Mo(CO)_6$, followed by hydrolysis of the chlorosulphonylphenyl groups.

In a 50 mL fask fitted with a condenser, a solution of TDCPPS (30mg; 2.5 x 10^{-5} moles) in decalin (10 mL) was refluxed. An excess of $Mo(CO)_6$ (45x, 300mg; 1.14 x10^{-3} moles) was added and the solution was refluxed for further 3 h. After this period, decalin was removed by evaporation under vacuum and distilled water (30 mL) and sodium chloride (200 mg) were added. After refluxing this solution for 24 h., workup gave the required metalloporphyrin as described in Section 2.7 of this Chapter; (22 mg; 61% yield). $\lambda_{max}(H_2O)$/nm, (ε, L. mol^{-1}. cm^{-1}) 414(107458), 516(25751), 655(28960); Found: C, 36.9; H, 3.0; N, 3.3; $C_{44}H_{20}N_4S_4O_{12}Cl_8MoCl.6H_2O$: requires: C, 36.5; H, 2.2; N, 3.9%.

7. Preparation and characterization of polymers

7.1. General procedure for the preparation of co-poly(4-styrene sulphonic acid, sodium salt, 2-vinylnaphthalene) polymers (PSSS-VN, 6);[5,6] co-poly(4-styrene sulphonic acid, sodium salt, styrene) polymers (PSSS-S, 7) and co-poly(4-styrene sulphonic acid, sodium salt, 9-vinylanthracene) polymers (PSSS-VA, 8)

To a 100 mL flask, equipped with a magnetic stirrer, was added DMSO (45 mL) and the hydrophobic monomer (in this case, 2-vinylnaphthalene; 2.9g, 0.019 moles), together with 4-styrene sulphonic acid, sodium salt (3.88g, 0.019 moles) and azoisobutironitrile (AIBN, 150 mg, 9.14 x 10^{-4} moles). The mixture was flushed with nitrogen for 15 min. and then the flask was closed with a rubber septum to maintain the nitrogen atmosphere. The mixture was heated at 60° C and stirred for 20 h. After this time, 1-butanol (30-40 mL) was added to precipitate the polymer, which was filtered off under vacuum and washed with three portions of diethylether (30 mL). The residue was dried in a vacuum oven at 40°C overnight.

7.1.1. Co-poly(4-styrene sulphonic acid, sodium salt, 2-vinylnaphthalene) (initial molar ratio of hydrophilic monomer to hydrophobic monomer used in the preparation of the co-polymer = **50/50% molar**) (**6a**)

Average molecular weight, Mw = 19684, polydispersity = 1.86 (GPC); Found: C, 64.3; H, 5.9; S, 10.0. $(C_{20}H_{17}SO_3Na)_n$ requires C, 66.7; H, 4.8 ; S, 8.9%.

7.1.2. Co-poly(4-styrene sulphonic acid, sodium salt; 2-vinylnaphthalene) (66/33% molar) (6b)

Average molecular weight, Mw = 20675, polydispersity = 1.95 (GPC); Found: C, 53.3; H, 4.9; S, 11.2. $(C_{28}H_{24}S_2O_6Na_2)_n$ requires C, 59.4 ; H, 4.3; S, 11.3%.

7.1.3. Co-poly(4-styrene sulphonic acid, sodium salt, 2-vinylnaphthalene) (33/66% molar) (6c)

Average molecular weight, Mw = 22229, polydispersity = 1.91 (GPC); Found: C, 68.7; H, 5.7; S, 6.9. $(C_{32}H_{27}SO_3Na)_n$ requires C, 74.7; H, 5.3; S, 6.2%.

7.1.4. Co-poly(4-styrene sulphonic acid, sodium salt; 2-vinylnaphthalene) (80/20% molar) (6d)

Average molecular weight, Mw = 18491, polydispersity = 1.48 (GPC); Found: C, 48.1; H, 4.7; S, 11.3. $(C_{44}H_{38}S_4O_{12}Na_4)_n$ requires C, 54.0 ; H, 3.9; S, 13.1%.

7.1.5 Co-poly(4-styrene sulphonic acid, sodium salt; styrene) (50/50% molar) (7a)

Average molecular weight, Mw = 6095, polydispersity = 2.08 (GPC); Found: C, 56.7; H, 5.4; S, 12.1. $(C_{16}H_{15}SO_3Na)_n$ requires C, 61.9 ; H, 4.9 ; S, 10.3%.

7.1.6 Co-poly(4-styrene sulphonic acid, sodium salt; styrene) (66/33% molar) (7b)

Average molecular weight, Mw = 19122, polydispersity = 1.85 (GPC); Found: C, 64.3; H, 5.9; S, 10.0. $(C_{24}H_{23}SO_3Na)_n$ requires C, 69.6 ; H, 5.6 ; S, 7.7%.

7.1.7 Co-poly(4-styrene sulphonic acid, sodium salt; styrene) (33/66% molar) (7c)

Average molecular weight, Mw = 1565, polydispersity = 2.36 (GPC); Found: C, 52.9; H, 5.2; S, 13.5. $(C_{24}H_{23}S_2O_6Na_2)_n$ requires C, 55.7 ; H, 4.5 ; S, 12.4%.

7.1.8. Co-poly(4-styrene sulphonic acid, sodium salt; 9-vinyl anthracene) (50/50% molar) (8a)

Average molecular weight, Mw = 1716, polydispersity = 1.06 (GPC); Found: C, 47.2; H, 3.7; S, 12.3. $(C_8H_7SO_3Na)(C_{16}H_{12})$ requires C, 70.2; H, 4.7; S 7.8%. Analysis suggest a composition close to $(C_8H_7SO_3Na)_7(C_{16}H_{12})$; C, 52.5; H, 3.7; S 13.6%.

7.1.9. Co-poly(4-styrene sulphonic acid, sodium salt; 9-vinyl anthracene) (66/33% molar) (8b)

Average molecular weight, Mw = 1736, polydispersity = 1.08 (GPC), (Found: C, 46.4; H, 3.7; S, 13.0. $(C_8H_7SO_3Na)_2(C_{16}H_{12})$ requires C, 62.3; H, 4.3; S 10.4%. Analysis suggest a composition close to $(C_8H_7SO_3Na)_7(C_{16}H_{12})$; C, 51.8; H, 3.7; S 13.8%.

7.1.10. Co-poly(4-styrene sulphonic acid, sodium salt; 9-vinyl anthracene) (33/66% molar) (8c)

Average molecular weight, Mw = 1446, polydispersity = 1.12 (GPC); Found: C, 44.5; H, 3.5; S, 11.7. $(C_8H_7SO_3Na)(C_{16}H_{12})_2$ requires C, 78.2; H, 5.1; S 5.2%. Analysis suggest a composition close to $(C_8H_7SO_3Na)_5(C_{16}H_{12})$; C, 51.8; H, 3.7; S 13.8%.

7.2. Procedure for the preparation of co-poly(4-styrene sulphonic acid, sodium salt; 2-vinylnaphthalene) polymers containing different amounts of pyridine units (initial molar ratios of hydrophilic monomer to hydrophobic monomer used in the preparation of the co-polymer ≈ 66/33% molar) (10)

To a 100 mL flask, equipped with a magnetic stirrer, was added DMSO (45 mL), 2-vinylnaphthalene (0.7g, 4.75 x 10^{-3} moles), 4-stryrene sulphonic acid (1.94g, 5 x 10^{-3} moles), azoisobutironitrile (150 mg, AIBN, 9.14 x 10^{-4} moles) and the required amount of vinylpyridine. The mixture was flushed with nitrogen for 15 min. and then the flask was closed with a rubber septum to maintain the nitrogen atmosphere. The mixture was heated at 60° C and stirred for 20 h. The workup for polymer isolation was the same as described in section 7.1.

7.2.1. Co-poly(4-styrene sulphonic acid, sodium salt; 2-vinylnaphthalene; vinyl pyridine) (≈ 63/33/4% molar)(10a)

The procedure used was the described above, using approximatelly 4% molar of vinyl pyridine (45mg, 4.28 x 10^{-4} moles). Average molecular weight, Mw = 5018, polydispersity = 3.04 (GPC), (Found: C, 53.0; H, 5.2; S, 12.2; N, 0.6. $(C_8H_7SO_3Na)_{64}(C_{16}H_{12})_{33}(C_7H_7N)_3$ requires C, 62.9; H, 4.3; S 10.1, N, 0.2%. Analysis suggest a composition close to $(C_8H_7SO_3Na)_{18}(C_{16}H_{12})_4(C_7H_7N)_2$; C, 56.3; H, 4.0; S 12.2; N, 0.6%.

7.2.2 Co-poly(4-styrene sulphonic acid, sodium salt; 2-vinylnaphthalene; vinylpyridine) (≈ 62/31/7% molar) (10b)

The procedure used was the described above, using approximately 7% molar of vinyl pyridine (120 mg, 1.14 x 10^{-3} moles). Average molecular weight, Mw = 5076, polydispersity = 2.61 (GPC), (Found: C, 54.7; H, 5.2; S, 11.7; N, 0.6. $(C_8H_7SO_3Na)_{62}(C_{16}H_{12})_{31}$ $(C_7H_7N)_7$ requires C, 63.0; H, 4.3; S 10.0, N, 0.5%. Analysis suggest a composition close to $(C_8H_7SO_3Na)_{18}(C_{16}H_{12})_5(C_7H_7N)_2$; C, 57.8; H, 4.1; S 11.7; N, 0.6%.

7.3. Procedure for the preparation of co-poly(4-styrene sulphonic acid, sodium salt; 2-vinylnaphthalene; 5-(4-vinylphenyl)-10,15,20-*tris*-phenylporphyrin metal complex) polymers (9)

The preparation of these polymers required the preparation of the iron and manganese complexes of 5-(4-vinylphenyl)-10,15,20-*tris*-phenylporphyrin, described in Section 4.3 and Section 2.2 of this Chapter.

To a 50 mL flask, equipped with a magnetic stirrer, was added DMSO (10 mL), 2-vinylnaphthalene, (60mg, 3.89 x 10^{-4} moles), 4-styrene sulphonic acid sodium salt (100mg, 4.5 x 10^{-4} moles), 5-(4-vinylphenyl)-10,15,20-*tris*-phenylporphyrin metal complex mixture (approximately 3.0 x 10^{-5} moles, 80mg) and azoisobutyronitrile (20mg, 1.22 x10^{-4} moles). The mixture was flushed with nitrogen for 15 min. and then the flask was closed with a rubber septum to maintain the nitrogen atmosphere. The mixture was heated at 60°C and stirred for 20 h. After this time, the solution volume was reduced to 1-2 mL by reduced pressure evaporation of DMSO and then ethyl ether was added to precipitate the required polymer. This was collected in a small glass sintered funnel, washed with

$CHCl_3$ to remove the excess of TPP metal complex and dried in a vacuum oven (40°C) overnight.

7.3.1. Co-poly(4-styrene sulfonic acid, sodium salt; 2-vinylnaphthalene, Iron(III) 5-(4-vinylphenyl)-10,15,20-*tris*-phenylporphyrin chloride) (9a)

Average molecular weight, Mw = 3384 , polydispersity = 1.95 (GPC), porphyrin content (measured by visible spectrophotometry, at the Soret wavelength and using FeTPP ε value) = 0.5% (w/w); Found: C, 49.2; H, 3.8; N, 1.4. Analysis suggest a average composition close to $(C_8H_7SO_3Na)_{14}(C_{16}H_{12})_{1.3}$ $(C_{46}H_{30}N_4FeCl)$; C, 55.3; H, 3.7; N, 1.4%.

7.3.2. Co-poly(4-styrene sulfonic acid, sodium salt; 2-vinylnaphthalene, manganese(III) 5-(4-vinylphenyl)-10,15,20-*tris*-phenylporphyrin chloride) (9b)

Average molecular weight, Mw = 1982 , polydispersity = 1.37 (GPC); porphyrin content (measured by visible spectrophotometry, at the Soret wavelength and using the ε value for MnTPP) = 0.6% (w/w). No satisfactory elemental analysis was obtained for this polymer.

8. Procedure for the preparation of Merrifield naphthyl-ether modified polymers (11)[6]

To a 100 mL flask equipped with magnetic stirrer and condenser, was added 2-naphthol (6 meq; 6 x 10^{-3} moles, 865mg), potassium t-butoxide (3.0g, 2.67 x 10^{-2} moles) and DMF (50 mL). After heating to reflux start, Merrifield resin (5g; 1 meq Cl/g) was added and the whole was refluxed for 24 h. After this period, the solvent was evaporated and the residue was thoroughly washed with $CHCl_3$ and MeOH. On drying, the naphthyl-ether modified Merrifield polymer was obtained (5.70g; 99% yield).

8.1. Preparation of napthyl-ether Merrifield modified polymer with co-adsorbed iron(III) 5,10,15,20-*tetrakis*phenylporphyrin chloride (11a)

To a 25 mL flask fitted with magnetic stirrer, was added the naphthoxy-modified polymer (prepared as above; 250mg) in CH_2Cl_2 (20 mL) containing FeTPPCl (15mg; 2.0 x 10^{-5} moles). The solution was stirred overnight, in a flask open to air. After this period, the polymer was filtered off and washed with a small portion of CH_2Cl_2 (20 mL) to remove excess of metalloporphyrin. The polymer was dried in a vaccum oven overnight at 40°C.

Evaluation of the amount of co-adsorbed metalloporphyrin was made by quantifying the metal content in the polymer through atomic absorption spectrophotometry after ashing the dry polymer. Two portions of the porphyrinic polymer (accurately weighed; 120-130mg) and one blank polymer (porphyrin free) were weighed on to a previously calcinated ceramic crucible and then heated to 500°C for 4-8 h in a furnace, after which the residual ash became white. The crucible was allowed to cool and the ash was dissolved in a HNO_3 solution (50 mL, 50% v/v). To assist dissolution of ash, the solution was heated on a steam bath for 30 min. The solution was then filtered and adjusted to 100 mL in a volumetric flask. The solution, together with a set of iron standards in nitric acid was examined in an atomic absorption spectrophotometer. From the amount of iron, the calculated amount of iron porphyrin was found to be 0.66% (w/w).

8.2 Preparation of napthyl-ether Merrifield modified polymer with co-adsorbed manganese(III) 5,10,15,20-*tetrakis*phenylporphyrin chloride (11b)

This polymer was prepared by the method just described in the preceding Section, but using MnTPPCl in place of the iron complex. The amount of co-adsorbed metalloporphyrin was found to be 0.51% (w/w).

9. Procedure for the preparation of chitin polymers co-adsorbed with metal complexes of 5,10,15,20-*tetrakis*phenylporphyrin (12)[6]

To a 50 mL flask fitted with a stopper and magnetic stirrer, was added chitin (100mg) and the required metalloporphyrin (usually 30 mg) plus $CHCl_3$ (30 mL). This mixture was stirred for 24 h. at room temperature. After this time, the polymer was filtered off and the residue was washed thoroughly with $CHCl_3$ until

the washings became colourless. The coloured residue was dried in a vacuum oven at 40°C overnight.

The metalloporphyrin content in these polymers was determined by desorbing the metalloporphyrin from the polymer into methanol, followed by visible spectrophotometry; the amount of porphyrin was determined from the Soret wavelength. A sample of the metalloporphyrin-modified chitin (30mg) was washed with pure methanol until this became colourless. The combined washings were collected and its volume adjusted to a final volume of 250 mL in a volumetric flask. The absorption at the Soret band was determined by visible spectroscopy.

9.1. Iron(III) 5,10,15,20-*tetrakis*phenylporphyrin chloride in chitin (12a)

Metalloporphyrin content = 12% w/w

9.2. Manganese(III) 5,10,15,20-*tetrakis*phenylporphyrin chloride in chitin (12b)

Metalloporphyrin content = 10% w/w

9.3. Cobalt(III) 5,10,15,20-*tetrakis*phenylporphyrin chloride in chitin (12c)

Metalloporphyrin content = 11% w/w

10. Measurements of peroxidase-like activity of the various polymer preparations

The peroxidase-like activity assay of the systems developed with simple metalloporphyrins or with the porphyrins connected to a polymers structure was determined by using 2,2'-azino-*bis*(3-ethylbenzthiazoline-6-sulfonic acid) (ABTS) as the substrate and H_2O_2 as the oxygen donor, in phosphate buffer (pH 6). The conditions were similar to those described for the biological peroxidase assay[7] (see below and also Section 2.1.1, Chapter 2).

10.1. General method for assessing peroxidase-like activity

Into a glass spectrophotometer cell (10mm path length) were pipetted 2 mL of the solution for which the peroxidase activity was to be measured (a peroxidase, a metalloporphyrin or a metalloporphyrin/polymer solution in a suitable buffer, usually an pH 6 aqueous phosphate buffer; 0.144 g $Na_2HPO_4.2H_2O$ + 0.798 g KH_2PO_4 in 100 mL water)[7] containing ABTS (200μL of a 2.0 x 10^{-2} mol.L^{-1} stock solution; final concentration in test 1.7 x 10^{-3} mol.L^{-1}). At time zero, H_2O_2 (200μL of a 10^{-2} mol.L^{-1} stock solution; final concentration in test 8.3 x 10^{-4} mol.L^{-1}) was added to the ABTS/porphyrin solution and the resulting oxidation of ABTS was monitored by observing the increases in absorbance on bands for $ABTS^{\cdot+}$ at either 420 nm (ε = 29000 mol^{-1}.L.cm^{-1})[8] or 660 nm (ε = 12000 mol^{-1}.L.cm^{-1})[7]. Visible spectra were usually taken at minute intervals, or other adequate time interval to suit the observed activity.

Kinetic parameters were determined by plotting the values of the observed increase in $ABTS^{\cdot+}$ concentration *versus* time, and adjusting a linear curve to fit the points. The slope of the line was divided by the metalloporphyrin concentration, to give a normalised initial rate constant for $ABTS^{\cdot+}$ formation (k'), where k' referred to a rate constant per mole of added porphyrin.

10.2. Horseradish peroxidase assay

Horseradish peroxidase (HRP, Fluka, 731 U/mg; 5mg) was dissolved in a phosphate buffer (prepared as described in the precedent section; pH 6; 10 mL) in a volumetric flask to give a concentration of 1.12 x 10^{-5} mol.L^{-1}. This stock solution was diluted in 1:100 for the final working solution (final concentration = 1.12 x 10^{-7} mol.L^{-1}). The peroxidase activity of HRP was determined with this last

solution as described in the preceding section by monitoring the oxidation of ABTS.

10.3. Peroxidase-like assay of water-soluble metalloporphyrin

The required amount of water-soluble metalloporphyrin was weigh out and dissolved in phosphate buffer (pH 6) in order to prepare a working solution having a concentration of approximately 3.0×10^{-6} mol.L^{-1} (volume = 100 mL). The activity was determined as described in Section 10.1 above. Before addition of H_2O_2, a visible spectrum was recorded to determine the metalloporphyrin concentration, using ε values previously determined, for the normalisation purposes referred in Section 10.1.

10.4. Peroxidase-like assay of metalloporphyrins carried in amphiphilic co-polymers 6a-d, 7a-c, 8a-c, 9a,b

10.4.1 Preparation of amphiphilic polymer solutions

To an Erlenmeyer (2 L), was added phosphate buffer (1 L; pH 6) and the required polymer (200mg). The mixture was heated to 60°C, with continuous stirring to dissolve the polymer, after which the mixture was cooled and filtered through a membrane filter (Teflon; 20μm) under vacuum (13 mmHg).

10.4.2 Metalloporphyrin insertion in amphiphilic polymers

The required metalloporphyrin (3×10^{-6} moles, $\approx$ 3 mg) was dissolved in DMF (1 mL). The required polymer solution (usually 1 L) was placed in a beaker (2 L) and under continued stirring, the porphyrin solutions in DMF was injected through a syringe into the whole was stirred for one h. After this time filter, the solution was filtered through a membrane filter (Teflon; 20μm) under vacuum (13 mmHg). Before measuring peroxidase-like activity, visible spectroscopy was used to quantify the amount of metalloporphyrin that had been "inserted" into the polymer microdomains.

The ABTS peroxidase-like activity was then determined using these solutions by the procedures described in Section 10.1 above.

10.5. Peroxidase-like assay of amphiphilic polymers containing covalently linked metalloporphyrins, 10a, 10b

To a 50 mL volumetric flask, was added the required metalloporphyrin containing polymer (10 mg) and phosphate buffer solution (20-30 mL; pH 6). The mixture was agitated to dissolve the solid and adjusted to the required volume. The solution was filtered the solution through a membrane filter (Teflon; 20μm) under vacuum (13 mmHg). Before measuring peroxidase-like activity, a visible spectrum was recorded to quantify the amount of metalloporphyrin present in the polymer.

The peroxidase-like activity was then determined as described in Section 10.1 above.

10.5.1. Peroxidase-like assay of amphiphilic polymers containing covalently linked metalloporphyrins in the presence of exogenous imidazoles

Experiments using added 1- and 2-methyl-imidazoles were made according to those described above, except that different volumes (10-600μL) of a 1- or 2-methyl-imidazole solution in pH 6 phosphate buffer (250 mg/100 mL, 0.122 mol.L^{-1}) was added after recording a visible spectrum to quantify the metalloporphyrin content. In all cases, in the evaluation of kinetic parameters, a normalization was made for the metalloporphyrin concentration, resulting from the dilution of the solution on addition of the imidazoles.

11. Peroxidase-like assay of Merrifield modified resin with co-adsorbed metalloporphyrins (11)

Into a glass spectrophotometer cell (10mm path lengh) was added phosphate buffer (2 mL; pH 6) and the metalloporphyrin/naphthoxy-modified Merrifield polymer (10 mg). The solution was stirred with a Pasteur pipette. To the cell was added ABTS (200μL of the 2 x 10^{-2} mol.L^{-1} stock solution to give a final concentration of 1.7 x 10^{-3} mol.L^{-1}) and, at time zero H_2O_2 (200μL of a 10^{-2} mol.L^{-1} stock solution; final concentration 8.3 x 10^{-4} mol.L^{-1}). The reaction was monitored by observing the increase in the absortion bands of the reaction product ($ABTS^{\cdot+}$; either at 420 or 660 nm). Since the reaction product ($ABTS^{\cdot+}$) tended to acumulate close to the resin, the solution was stirred with a Pasteur pipette prior to each visible scan. The kinetic parameters were evaluated as described in Section 10.1.

12. Peroxidase-like assay of adsorbed metalloporphyrins on chitin (12)

Into a glass spectrophotometer cell (10mm path length) was added phosphate buffer (2 mL; pH 6) and chitin with co-adsorbed metalloporphyrin (5 mg). The solution was stirred and left for 1 hour to wet the polymer. ABTS (200μL of the 2 x 10^{-2} mol.L^{-1} stock solution to gave a final concentration of 1.7 x 10^{-3} mol.L^{-1}) was added to the cell and at time zero H_2O_2 (200μL of the 10^{-2} mol.L^{-1} stock solution; final concentration 8.3 x 10^{-4} mol.L^{-1}) was added. The reaction was monitored by observing the increase in the absorption bands of the reaction product ($ABTS^{\cdot+}$, either at 420 or 660 nm). Since the reaction product tended to acumulate close to the resin, it was stirred before each visible spectral scan. Kinetic parameters were evaluated as described in Section 10.1.

IV. Chapter 3 experimental details

1. Methods for preparing 5-methoxyphenylporphyrins

The porphyrin starting point required for preparing the "sandwich" compounds having an aromatic ring in a close proximity to the porphyrin macrocycle, was in the different cases presented in this work 5-methoxyphenyl-10,15,20-*tris*-phenyl- or 5-methoxyphenyl-10,15,20-*tris*-heptyl-porphyrins. These porphyrins were prepared by the methods described in Section III. 1. (method a), but here the need of having different *meso*-substituents required the use of two different aldehydes in the synthesis of the starting porphyrin. The preparation of porphyrins with more than one aldehyde gives as a reaction product a mixture of different *meso*-substituted porphyrins, from which the required porphyrin was separated by a chromatographic technique. Subsequent synthetic modifications involves the demethylation of the methoxyphenyl groups to give the corresponding hydroxyphenylporphyrins which are then condensed with the required aryl acid chloride to give the final compounds.

2. Preparation of 5-(methoxyphenyl)-10,15,20-*tris*-phenylporphyrins

2.1. 5-(2,4,6-trimethoxyphenyl)-10,15,20-*tris*-phenylporphyrin

Preparation of this porphyrin was effected by the method described in Section III. 1. (Method a), using a mixture of 2,4,6-trimethoxybenzaldehyde (245 mg, 1.25 x 10^{-3} moles) and benzaldehyde (0.38 mL, 3.75 x 10^{-3} moles) in a molar ratio of 1:3, and pyrrole (0.35 mL; 0.5 x 10^{-2} moles). At the end of reaction; methanol (30 mL) was added to assist precipitation of porphyrin, and on cooling and filtration, there was obtained crystalline material (64 mg; 29 % yield). TLC analysis (silica gel, chloroform as eluant) showed that the reaction product was a mixture of TPP and 5-(2,4,6-trimethoxyphenyl)-10,15,20-*tris*-phenylporphyrin. The isolation of the latter was made by column chromatography (20 x 5 cm) on silica-gel S using $CHCl_3$/petroleum ether 40-60 (1/1). TPP eluted as the first band (10 mg) and then the eluant was changed to only $CHCl_3$ to recover a second band corresponding to 5-(2,6-dimethoxyphenyl)-10,15,20-*tris*-phenylporphyrin (70 mg; 5.0% yield); δ_H($CHCl_3$; 200MHz; Me_4Si), 8.79 [2H, ls, β-pyrrolic], 8.77 [6H, ls, β-pyrrolic], 8.18 [6H, m, 2,6-phenyl], 7.71 [12H, m, *meso*-(10,15,20)-3,4,5-phenyl], 6.56 [2H, s, *meso*-(5)-3,5-phenyl], 4.07 [3H, s, *meso*-(5)-4-OCH_3], 3.50 [6H, s, *meso*-(5)-2,6-OCH_3], -2.73 [2H, s, NH]; MS (FAB), $[M+H]^+$, *m/z* 705; Found: C, 80.0; H, 5.3; N, 7.9; calculated for $C_{47}H_{36}N_4O_3$: C, 80.1; H, 5.2; N, 8.0%.

2.2. 5-(2,6-dimethoxyphenyl)-10,15,20-*tris*-phenylporphyrin

Preparation of this porphyrin resulted from a mixture 2,6-dimethoxybenzaldehyde (208 mg; 1.25 x 10^{-3} moles) and benzaldehyde (0.38 mL; 3.75 x 10^{-3} moles) in a molar ratio of 1:3, and pyrrole (0.35 mL; 5.00 x 10^{-3} moles). At the end of reaction, methanol (30 mL) was added to assist precipitation of the product. After filtration, there was obtained 178 mg of crystalline material (14.2% yield). TLC analysis (silica gel; chloroform as eluant) showed that the reaction product was a mixture of TPP and 5-(2,6-dimethoxyphenyl)-10,15,20-*tris*-phenylporphyrin. To isolate the latter, the mixture was chromatographed (20 x 5 cm) on silica-gel S in $CHCl_3$/petroleum ether 40-60 (1/1). TPP was eluted first (100 mg), and then the eluant was changed to only $CHCl_3$ to recover a second band corresponding to the 5-(2,6-dimethoxyphenyl)-10,15,20-*tris*-phenylporphyrin, (71 mg; 5.5 % yield); δ_H($CHCl_3$; 200MHz; Me_4Si), 8.76 [6H, ls (large singlet), β-pyrrolic], 8.75 [2H, ls, β-pyrrolic], 8.16 [6H, m, 2,6-phenyl], 7.69 [12H, m, *meso*-(10,15,20)-3,4,5-phenyl], 6.95 [2H, d, J = 8.5 Hz, *meso*-(5)-3,5-phenyl], 3.51 [6H, s, *meso*-(5)-2,6-OCH_3], -2.74 [2H, s, NH]; MS (FAB), $[M+H]^+$, *m/z* 675; Found: C, 80.5; H, 5.1; N, 8.1; calculated for $C_{46}H_{34}N_4O_2$: C, 81.9; H, 5.1; N, 8.3%.

2.3. 5-(2-methoxyphenyl)-10,15,20-*tris*-phenylporphyrin

Preparation of this porphyrin resulted from a mixture of two aldehydes, 2-methoxybenzaldehyde (510 mg; 1.25 x 10^{-3} moles) and benzaldehyde (1.14 mL; 3.75 x 10^{-3} moles) in a molar ratio of 1:3, and pyrrole (1.5 x 10^{-2} moles, 1.05 mL) in 180 mL of acetic acid/nitrobenzene. After cooled, the reaction mixture was filtrated and 890 mg of crystalline material was obtained (36% yield). TLC analysis (silica-gel, chloroform/petroleum ether (4/6) as eluant) showed that the reaction product was a mixture of TPP, 5-(2,6-dimethoxyphenyl)-10,15,20-*tris*-phenylporphyrin and small amounts of more polar *meso*-substituted porphyrins. To isolate the required porphyrin, 200 mg of the porphyrin mixture was dissolved in a small volume of CH_2Cl_2 and placed as a "line" along the bottom of four to six TLC preparative silica-gel plates (20 x 20 cm), prepared from silica-gel 60 having a thickness of 500 μm. Elution in a TLC developing chamber was done with a mixture of $CHCl_3$/petroleum ether (3/7) giving excellent separation of reaction products. The TLC band corresponding to the target porphyrin (the second) was carefully scraped into a glass funnel, and finally the porphyrin was recovered by elution with $CHCl_3$/MeOH to give 74 mg of the required compound (13% yield); δ_H($CHCl_3$; 200MHz; Me_4Si), 8.82 [6H, ls, β-pyrrolic], 8.79 [2H, d, J = 4 Hz, β-pyrrolic], 8.20 [6H, m, 2,6-phenyl], 8.00 [1H, d, J = 7.3 Hz, *meso*-(5)-3-phenyl],

7.75 [12H, m, *meso*-(10,15,20)-3,4,5-phenyl], 7.33 [1H, t, J = 7.5 Hz, *meso*-(5)-4-phenyl], 3.57 [3H, s, *meso*-(5)-2-OCH_3], -2.75 [2H, s, NH]; MS (FAB), $[M+H]^+$, *m/z* 645; Found: C, 82.9; H, 5.0; N, 8.3; calculated for $C_{45}H_{32}N_4O$: C, 83.8; H, 5.0; N, 8.7%.

3. Preparation of 5-(methoxyphenyl)-10,15,20-*tris*-heptylporphyrins

These porphyrins were prepared by the same methods as described in Section IV. 2.1, but modifications were made to the isolation procedures because, in these case, the porphyrins proved to be difficult to precipitate from the reaction medium, even on addition of methanol and refrigeration. To overcome this problem, all of the solvents were evaporated from the reaction medium and the residue was chromatographed on alumina to give the required porphyrin.

3.1. 5-(2,6-dimethoxyphenyl)-10,15,20-*tris*-heptylporphyrin

Preparation of this porphyrin was effected as before (Section III. 1., Method a), using a mixture 2,6-dimethoxybenzaldehyde (7.5×10^{-3} moles, 1.25 g) and octanal (2.25×10^{-2} moles, 3.5 mL), in a molar ratio of 1:3, and pyrrole (3.0×10^{-2} moles, 2.1 mL) in 200 mL of acetic acid/nitrobenzene (7/3). After cooling the reaction mixture, acetic acid was distilled off on a evaporator and the nitrobenzene was removed by steam distillation to yield a black residual material. This residue was dissolved with stirring in the minimum amount of CH_2Cl_2 and placed at the top of a chromatography column (20 x 6 cm, alumina activity grade 0). CH_2Cl_2 was used as eluant. All porphyrinic material (violet band) was collected and the solvent was removed, to yield 374 mg of crystalline material (6.7% yield). TLC analysis (silica gel, CH_2Cl_2/petroleum ether (1/1) as eluant) showed that the reaction product was a mixture of 5,10,15,20-*tetrakis*heptylporphyrin, 5-(2,6-dimethoxyphenyl)-10,15,20-*tris*-heptylporphyrin and small quantities of more polar porphyrins. To isolate the 5-(2,6-dimethoxyphenyl)-10,15,20-*tris*-heptylporphyrin, a second chromatographic column was prepared (25 x 6 cm, packed with silica gel 60 in CH_2Cl_2/petroleum ether (1/1)). The first band was eluted with the column filling solvent to yield 259 mg of 5,10,15,20-*tetrakis*heptylporphyrin (4.6% yield); a second band was eluted with pure CH_2Cl_2, giving 80 mg of the target porphyrin (1.4% yield); δ_H($CHCl_3$; 300MHz; Me_4Si), 9.51 [2H, d, J = 5.0 Hz, β-pyrrolic], 9.47 [2H, d, J = 5.0 Hz, β-pyrrolic], 9.33 [2H, d, J = 4.7 Hz, β-pyrrolic], 8.75 [2H, d, J = 4.8 Hz, β-pyrrolic], 7.73 [1H, t, J = 8.5 Hz, 4-phenyl], 7.02 [2H, d, J = 8.5 Hz, 3,5-phenyl], 4.99 [2H, t, J = 8.7 Hz, *meso*-(15)-α-CH_2], 4.91 [4H, t, J = 7.8 Hz, *meso*-(10,20)-α-CH_2], 3.51 [6H, s, -OCH_3], 2.52 [6H, m, β-CH_2], 1.81 [6H, m, γ-CH_2], 1.54 [6H, m, δ-CH_2], 1.36 [6H, m, ε-CH_2], 1.26 [6H, m, ζ-CH_2], 0.91 [9H, m, -CH_3], -2.56 [2H, s, NH]; MS (FAB), $[M+H]^+$ m/z 741; λ_{max}(CH_2Cl_2)/nm, (ε, L. mol^{-1}. cm^{-1}) 302(15770), 346(19629), 364(23793) 418(482589), 518(18351), 552(10354), 598(5806), 654(7216); Found: C, 79.9; H, 9.1; N, 7.4; calculated for $C_{49}H_{64}N_4O_2$: C, 79.4; H, 8.7; N, 7.6%.

3.2 5-(2-methoxyphenyl)-10,15,20-*tris*-heptylporphyrin

Preparation of this porphyrin was effected as in Section 3.1 but using a mixture of 2-methoxybenzaldehyde (3.75×10^{-3} moles, 0.51 g) and octanal (1.13×10^{-2} moles, 1.75 mL), in a molar ratio of 1:3, and pyrrole (1.5×10^{-2} moles, 1.05 mL) in 100 mL of acetic acid/nitrobenzene (7/3). Workup gave 510 mg total of porphyrinic material (19% yield). To separate the required 5-(2-methoxyphenyl)-10,15,20-*tris*-heptyl-porphyrin, a chromatographic column was used (25 x 6 cm, silica gel 60) using CH_2Cl_2/petroleum ether 3/1 as eluant. The first band eluted was 5,10,15,20-*tetrakis*heptylporphyrin, the second was the required porphyrin, 60 mg (2.3% yield); δ_H($CHCl_3$; 200MHz; Me_4Si), 9.43 [4H, m, β-pyrrolic], 9.27 [2H, d, J = 5.5 Hz, β-pyrrolic], 8.67 [2H, d, J = 5.0 Hz, β-pyrrolic], 7.88 [1H, d, J = 7.0 Hz, 3-phenyl], 7.68 [1H, t, J = 7.0 Hz, 4-phenyl], 7.27 [1H, d, J = 7.0 Hz, 6-phenyl], 7.10 [1H, m, 5-phenyl], 4.84 [6H, m, α-CH_2], 3.50 [3H, s, -OCH_3], 2.15 [8H, m, (β–) + γ-CH_2], 1.70 [8H, m, δ-CH_2], 1.32 [8H, m, ε-CH_2], 1.24 [8H, m, ζ-CH_2], 0.90 [9H, m, -CH_3], -2.64 [2H, s, NH]; MS (FAB), $[M+H]^+$, *m/z* 711; Found: C, 81.2; H, 8.8; N, 7.7; calculated for $C_{48}H_{62}N_4O$: C, 81.1; H, 8.8; N, 7.9%.

4. Preparation of 5-(hydroxyphenyl)-10,15,20-*tris*-phenylporphyrins

Singly substituted methoxyphenyl porphyrins were demethylated using hydrobromic acid, under conditions similar to but modified from those described in the literature,[9] to yield the corresponding hydroxyphenylporphyrins.

4.1. General method for porphyrin demethylation

To a 50 mL flask fittted with a magnetic stirrer and condenser, was added the required methoxylated porphyrin (100 mg), glacial acetic acid (10 mL) and aqueous 48% HBr solution (10 mL). The mixture was refluxed for 5 h. On cooling; ammonium hydroxide (25%, aqueous solution) was added until the porphyrinic material turned brown-violet. The porphyrin precipitate was filtered off, washed with water and then with methanol and dried. Purification of the reaction product was by silica-gel column chromatography (10 x 3cm, silica gel 60) with $CHCl_3$ as eluant for the mono-hydroxyphenylporphyrins, and with $CHCl_3$/ethylether (50/50) for the more polar di- and trihydroxyphenyl substituted porphyrins. Usually the first eluted band, corresponded to a small quantity of unreacted starting material and was discarded. The solvent was evaporated from the eluate and the porphyrin was recrystalised from CH_2Cl_2/MeOH, in air for 48-60h.

5. Preparation of 5-(hydroxyphenyl)-10,15,20-*tris*-phenylporphyrins

5.1. 5-(2,4,6-trihydroxyphenyl)-10,15,20-*tris*-phenylporphyrin

This porphyrin was made from 5-(2,4,6-trimethoxyphenyl)-10,15,20-*tris*-phenylporphyrin (47 mg; 6.67 x 10^{-5} moles) by the method just described, to give 35 mg of the required compound (78% yield); δ_H($CHCl_3$; 300MHz; Me_4Si), 8.83 [8H, m, β-pyrrolic], 8.15 [6H, m, 2,6-phenyl], 7.68 [12H, m, 3,4,5-phenyl], 5.85 [2H, s, *meso*-(5) 3,5-phenyl], -2.79 [2H, s, NH]; Found: C, 74.9; H, 5.7; N, 6.5; calculated for $C_{44}H_{30}N_4O_3.3H_2O$: C, 73.7; H, 5.1; N, 7.8%.

5.2 5-(2,6-dihydroxyphenyl)-10,15,20-*tris*-phenylporphyrin

Preparation of this porphyrin was made from 5-(2,6-dimethoxyphenyl)-10,15,20-*tris*-phenylporphyrin (32 mg; 4.75 x 10^{-5} moles) by the method above, to give 25 mg of the required compound (80% yield); $\delta_H(CHCl_3$; 200MHz; $Me_4Si)$, 8.92 [2H, d, J= 2.2 Hz, β-pyrrolic], 8.85 [6H, m β-pyrrolic], 8.21 [6H, m, 2,6-phenyl], 7.78 [12H, m, 3,4,5-phenyl], 7.51 [1H, t, J = 9 Hz, *meso*-(5)-4-phenyl], 6.98 [2H, d, J = 9 Hz, *meso*-(5)-3,5-phenyl], -2.70 [2H, s, NH]; $\lambda_{max}(CH_2Cl_2)$/nm, (ε, L. mol^{-1}. cm^{-1}) 250(16649), 256(17502), 264(15797), 306(10097), 416(285671), 512(10187), 548(4039), 586(3590), 644(1885); MS (FAB), $[M+H]^+$, *m/z* 647; Found: C, 77.8; H, 5.0; N, 7.2; calculated for $C_{44}H_{30}N_4O_2.2H_2O$: C, 77.4; H, 5.0; N, 8.2%.

5.3 5-(2-hydroxyphenyl)-10,15,20-*tris*-phenylporphyrin

Preparation of this porphyrin was made from 5-(2-dimethoxyphenyl)-10,15,20-*tris*-phenylporphyrin (100 mg; 1.55 x 10^{-4} moles) by the method above, to give 67 mg of the required compound (69% yield); $\delta_H(CHCl_3$; 300MHz; $Me_4Si)$, 8.88 [2H, ls, β-pyrrolic], 8.86 [6H, ls, β-pyrrolic], 8.21 [6H, m, *meso*-(10,15,20)-2,6-phenyl], 7.99 [1H, dd, J_1 = 6.0 Hz, J_2 = 1.6 Hz, *meso*-(5)-3-phenyl], 7.77 [12H, m, *meso*-(10,15,20)-3,4,5-phenyl], 7.72 [1H, t, J = 5.5 Hz, *meso*-(5)-5-phenyl], 7.36 [1H, d, J = 8.0 Hz, *meso*-(5)-4-phenyl], 7.34 [1H, t, J = 8.0 Hz, *meso*-(5)-5 -phenyl], -2.77 [2H, s, NH]; MS (FAB), $[M+H]^+$, *m/z* 631; Found: C, 83.0; H, 4.8; N, 8.4; calculated for $C_{44}H_{30}N_4O$: C, 83.8; H, 4.8; N, 8.9%.

6. Preparation of 5-(hydroxyphenyl)-10,15,20-*tris*-heptylporphyrins

6.1 5-(2,6-dihydroxyphenyl)-10,15,20-*tris*-heptylporphyrin

Preparation of this porphyrin was by the method above but, using 5-(2,6-dimethoxyphenyl)-10,15,20-*tris*-heptylporphyrin (100 mg; 1.35 x 10^{-4} moles) and yielded 42 mg (44% yield) of the final compound. Difficulties were found in characterization this porphyrin, due to its instability (see Chapter 5, Section 2). However, successfull further transformations of this compound were made immediately after their synthesis and these derivatives gave good analyses.

6.2 5-(2-hydroxyphenyl)10,15,20-*tris*-heptylporphyrin

Preparation of this porphyrin was made from 5-(2,6-dimethoxyphenyl)-10,15,20-*tris*-heptylporphyrin (100 mg; 1.41 x 10^{-4} moles) by the method in Section 4.1 above, to give 70 mg of the required compound (66% yield); δ_H($CHCl_3$; 200MHz; Me_4Si), 9.51 [2H, d, J = 4.4 Hz, β-pyrrolic], 9.47 [2H, d, J= 5.5 Hz, β-pyrrolic], 9.38 [2H, d, J= 5.5 Hz, β-pyrrolic], 8.80 [2H, d, J= 5.5 Hz, β-pyrrolic], 7.94 [1H, d, J= 7.7 Hz, 3-phenyl], 7.71 [1H, t, J = 7.7 Hz, 4-phenyl], 7.36 [1H, d, J = 7.7 Hz, 6-phenyl], 7.32 [1H, t, J = 7.7 Hz, 6-phenyl], 4.88 [6H, m, (10,15,20)-α-CH_2], 2.49 [6H, m, (10,15,20)-β-CH_2], 1.78 [6H, m, (10,15,20)-γ-CH_2], 1.52 [6H, m, (10,15,20)-δ-CH_2], 1.34 [12H, m, (10,15,20)-ε– + ζ-CH_2], 0.90 [9H, m, -CH_3], -2.68 [2H, s, NH]; MS (FAB), $[M+H]^+$, *m/z* 697; Found: C, 81.0; H, 9.0; N, 7.6; calculated for $C_{47}H_{60}N_4O$: C, 81.0; H, 8.7; N, 8.0%.

7. Preparation of porphyrins substituted with aromatic rings (tolyl, naphthyl, anthranyl)

The hydroxyphenyl porphyrins prepared earlier were condensed with acid chlorides (4-toluic acid chloride, 2-naphthoic acid chloride and 9-anthranoic acid chloride) to yield the required esters.

7.1. General methods for condensation of hydroxyphenylporphyrins with acid chlorides

Method (a). To a 50 mL flask fitted with magnetic stirrer and condenser was added the required hydroxyphenylporphyrin (50 mg; $\approx 8.5 \times 10^{-5}$ moles) in $CHCl_3$ (10 mL), an excess of the required acid chloride (3 equivalent for each hydroxy group, 2.6×10^{-4} moles/-OH) in $CHCl_3$, and triethylamine (150μL). The mixture was refluxed for 24-48 h. and was checked for completion by TLC (CH_2Cl_2 as eluant). On completion, the volume of reaction was reduced to about 5 mL and this concentrate was placed on the top of a chromatographic column (15 x 3 cm, silica-gel 60) and eluted with CH_2Cl_2. The required porphyrin ester was collected as the first band. A final purification was usually effected by precipitation from a CH_2Cl_2/MeOH mixture (1/1; 30mL), in a rotary evaporator. The flask was left in air in order to cool by CH_2Cl_2 evaporation. The compound was finally isolated by filtration and dried in air.

Method (b). To a 50 mL flask, fitted with magnetic stirrer and vacuum pump adapter, was added 50 mg of the required hydroxyphenylporphyrin and an excess (3 equivalent for each hydroxy group) of the required acid chloride (appropriate to 2-naphthoic acid chloride and 9-anthranoic acid chloride). The flask was connected to a vacuum water pump to remove gaseous HCl as it formed and heated in an oil bath at 140°C. The reaction remains under this conditions for 1-2 h. The reaction was checked for completion by TLC (CH_2Cl_2 as eluant). After cooling; the mixture was solubilized in 5 mL of dichoromethane, neutralized with triethylamine (2-3 drops) and the bulk mixture was chromatographed (15 x 3 cm, silica-gel 60 in CH_2Cl_2). The porphyrin ester was eluted as the first band. A final purification was usually effected by precipitation from a CH_2Cl_2/MeOH mixture (1/1; 30mL), in a rotary evaporator. The flask was left in air in order to cool by CH_2Cl_2 evaporation. The compound was finally isolated by filtration and dried in air.

8. Preparation of 5-(2-[4-oxycarbonyltoluene]phenyl)-10,15,20-*tris*-phenyl porphyrins

8.1. 5-(2,6-*bis*-(2-oxycarbonyltoluene)phenyl)-10,15,20-*tris*-phenyl porphyrin (4)

This porphyrin was made by method (a) described above, using 5-(2,6-dihydroxyphenyl)-10,15,20-*tris*-phenylporphyrin (30 mg; 4.39 x 10^{-5} moles) and gave 21 mg of the required compound (54% yield); δ_H($CDCl_3$; 200MHz; Me_4Si), 9.01 [2H, d, J = 4.4 Hz, β-pyrrolic], 8.81 [2H, d, J = 4.4 Hz, β-pyrrolic], 8.78 [4H, m, β-pyrrolic], 8.15 [7H, m, *meso*-(5)-4-phenyl + *meso*-(10,15,20)-2,6-phenyl], 7.75 [12H, m, *meso*-(10,15,20)-3,4,5-phenyl], 7.33 [2H, d, *meso*-(5)-3,5-phenyl], 6.75 [2H, d, J = 7.7 Hz, 3,5-tolyl], 6.25 [2H, d, J = 7.7 Hz, 2,6-tolyl], 1.76 [6H, s, -CH_3 tolyl], -2.89 [2H, s, NH]; λ_{max}(CH_2Cl_2)/nm, (ε, L. mol^{-1}. cm^{-1}) 244(34769), 308(9842), 370(16262), 418(287527), 514(12142), 548(4599), 590(3863), 644(2208); MS (FAB), $[M+H]^+$, *m/z* 883; Found: C, 80.9; H, 4.8; N, 6.2; calculated for $C_{60}H_{42}N_4O_4$: C, 81.6; H, 4.8; N, 6.3%.

8.2 5-(2-[4-oxycarbonyltoluene]phenyl)-10,15,20-*tris*-phenylporphyrin (3)

Preparation of this porphyrin was made by method (a) described above, using 5-(2-hydroxyphenyl)-10,15,20-*tris*-phenylporphyrin (10 mg; 1.58 x 10^{-5} moles) and gave 6.2 mg of the required compound (52% yield); δ_H($CDCl_3$; 200MHz; Me_4Si), 8.92 [2H, d, J = 5.5 Hz, β-pyrrolic], 8.85 [2H, d, J = 2.2 Hz, β-pyrrolic], 8.82 [4H, m, β-pyrrolic], 8.18 [7H, m, *meso*-(5)-3-phenyl + *meso*-(10,15,20)-2,6-phenyl], 7.76 [12H, m, *meso*-(10,15,20)-3,4,5-phenyl], 6.89 [2H, d, J = 7.7 Hz, 3,5-tolyl], 6.34 [2H, d, J = 7.7 Hz, 2,6-tolyl], 1.80 [3H, s, -CH_3 tolyl], -2.84 [2H, s, NH]; λ_{max}(CH_2Cl_2)/nm, (ε, L. mol^{-1}. cm^{-1}) 244(29699), 308(13462), 348(17227), 368(22705), 418(410001), 512(17022), 514(17265), 548(6757), 590(5350), 644(3196); MS (FAB), $[M+H]^+$, *m/z* 749; Found: C, 83.9; H, 4.9; N, 7.2; calculated for $C_{52}H_{36}N_4O_2$: C, 83.2; H, 4.9; N, 7.5%.

9. Preparation of 5-(2-[4-oxycarbonyltoluene]phenyl-10,15,20-*tris*-heptyl-porphyrins

9.1. 5-(2,6-*bis*-[4-oxycarbonyltoluene]phenyl)-10,15,20-*tris*-heptyl-porphyrin (2)

Preparation of this porphyrin was made by method (a) described above, using freshly made 5-(2,6-dihydroxyphenyl)-10,15,20-*tris*-heptylporphyrin (16 mg; 2.14 x 10^{-5} moles) to gave 10 mg of the target compound (50% yield); δ_H($CDCl_3$; 300MHz; Me_4Si), 9.49 [2H, d, β-pyrrolic], 9.44 [2H, d, β-pyrrolic], 9.16 [2H, d, J = 5.1 Hz, β-pyrrolic], 8.96 [2H, d, J = 5.1 Hz, β-pyrrolic], 7.96 [1H, t, J = 8.1 Hz, 4-*meso*-phenyl], 7.72 [2H, d, J = 8.1 Hz, *meso*-3,5-phenyl], 6.70 [2H, d, J = 8.7 Hz, 3,5-tolyl], 6.19 [2H, d, J = 8.5 Hz, 2,6-tolyl], 4.96 [2H, m, (15)-α-CH_2], 4.89 [4H, t, (10,20)-α-CH_2], 2.70 [2H, m, (15)-β-CH_2], 2.44 [4H, m, (10,20)-β-CH_2], 1.70 [6H, s, -CH_3 tolyl], 1.53 [12H, m, (10,15,20)-γ; δ-CH_2], 1.36 [6H, m, (10,15,20)-ε-CH_2], 0.91 [9H, m, (10,15,20)-CH_3], -2.74 [2H, s, NH]; λ_{max}(CH_2Cl_2)/nm, (ε, L. mol^{-1}. cm^{-1}) 304(13805), 350(17539), 366(20893), 418(278821), 486(4803), 518(15588), 552(9286), 596(6190), 654(6708); MS (FAB), $[M+H]^+$, *m/z* 950; Found: C, 79.2; H, 7.6; N, 5.4; calculated for $C_{63}H_{72}N_4O_4$: C, 79.7; H, 7.6; N, 5.9%.

9.2. 5-(2-[4-oxycarbonyltoluene]phenyl)-10,15,20-*tris*-heptylporphyrin (1)

Preparation of this porphyrin was made by method (a) described above, using 5-(2-hydroxyphenyl)-10,15,20-*tris*-heptylporphyrin (23 mg; 3.24 x 10^{-5} moles) to gave 10 mg of the required compound (38% yield); δ_H($CDCl_3$; 300MHz; Me_4Si), 9.50 [2H, d, J = 4.9 Hz, β-pyrrolic], 9.46 [2H, d, J = 4.7 Hz, β-pyrrolic], 9.36 [2H, d, J = 4.8 Hz, β-pyrrolic], 8.86 [2H, d, J = 4.8 Hz, β-pyrrolic], 8.09 [1H, d, J = 5.9 Hz, 3-*meso*-phenyl], 7.87 [1H, t, J = 7.4 Hz, *meso*-phenyl], 7.75 [1H, d, J = 8.4 Hz, *meso*-phenyl], 7.64 [1H, t, J = 7.6 Hz, *meso*-phenyl], 6.86 [2H, d, J = 8.1 Hz, 3,5-tolyl], 6.29 [2H, d, J = 8.1 Hz, 2,6-tolyl], 4.97 [2H, t, J = 8.0 Hz, (15)-α-CH_2], 4.90 [4H, t, J = 7.8 Hz, (10,20)-α-CH_2], 2.47 [6H, m, (10,15,20)-β-CH_2], 1.78 [6H, m, (10,15,20)-γ-CH_2], 1.75 [3H, s, -CH_3 tolyl], 1.51 [6H, m, (10,15,20)-δ-CH_2], 1.34 [6H, m, (10,15,20)-ε-CH_2], 1.26 [6H, m, (10,15,20)-ζ-CH_2], 2.47 [9H, m, (10,15,20)-CH_3],-2.70 [2H, s, NH]; λ_{max}(CH_2Cl_2)/nm, (ε, L. mol^{-1}. cm^{-1}) 244(24251), 284(10495), 304(10495), 350(13654), 366(16711), 418(305328), 486(2751), 518(11616), 552(6623), 596(3668), 654(4381); MS (FAB), $[M+H]^+$, *m/z* 815; Found: C, 80.4; H, 8.5; N, 6.5; calculated for $C_{55}H_{66}N_4O_2$: C, 81.0; H, 8.2; N, 6.9%.

10. Preparation of 5-[2-oxycarbonylnaphthalene]phenyl-10,15,20-*tris*-phenyl-porphyrins

10.1. 5-(2,4,6-*tris*-[2-oxycarbonylnaphthalene]phenyl)-10,15,20-*tris*-phenyl-porphyrin (9)

Preparation of this porphyrin was made by the method (b) described in Section 7.1, using 5-(2,4,6-trihydroxyphenyl)-10,15,20-*tris*-phenylporphyrin (100 mg; 1.40 x 10^{-4} moles) to gave 70 mg of the required compound (45% yield); δ_H($CDCl_3$; 300MHz; Me_4Si), 9.20 [2H, d, J = 5.0 Hz, β-pyrrolic], 9.00 [1H, s, (4)–8–naphthyl], 8.89 [2H, d, J = 5.0 Hz, β-pyrrolic], 8.76 [4H, m, β-pyrrolic], 8.19 [1H, d, J = 9.0 Hz, (4)–naphthyl], 8.13-7.90 [10H, m, (4)–naphthyl + *meso*-(10,15,20)-6-phenyl], 7.72 [14H, m,(4)–naphthyl + *meso*-(10,15,20)-6-phenyl], 7.24 [2H, d, J= 6.3 Hz, 1-naphthyl], 7.10-6.96 [8H, m, 3,4,5,8-naphthyl], 6.72 [2H, t, J= 6.5 Hz, 6-naphthyl], 6.20 [2H, d, J = 6.7 Hz, 7-naphthyl], -2.80 [2H, s, NH]; λ_{max}(CH_2Cl_2)/nm, (ε, L. mol^{-1}. cm^{-1}) 274(41879), 284(45767), 294(39759), 342(22088), 370(24562), 420(462220), 514(18908), 548(7598), 590(6043), 644(3357); MS (FAB), $[M+H]^+$, *m/z* 1125; Found: C, 81.4; H, 4.2; N, 4.8; calculated for $C_{77}H_{48}N_4O_6$: C, 82.2; H, 4.3; N, 4.8%.

10.2 5-(2,6-*bis*-[2-oxycarbonylnaphthalene]phenyl)-10,15,20-*tris*-phenyl-porphyrin (8)

Preparation of this porphyrin was made by the method (b) described in Section 7.1 above, using 5-(2,6-dihydroxyphenyl)-10,15,20-*tris*-phenylporphyrin (100 mg; 1.46 x 10^{-4} moles) to gave 63 mg of the required compound (45% yield); δ_H($CDCl_3$; 300MHz; Me_4Si), 9.11 [2H, d, J = 4.8 Hz, β-pyrrolic], 8.86 [2H, d, J = 4.8 Hz, β-pyrrolic], 8.75 [2H, d, J = 4.9 Hz, β-pyrrolic], 8.72 [2H, 2, J = 4.7 Hz, β-pyrrolic], 8.05 [6H, d, J = 9.6 Hz, *meso*-(10,15,20)-2,6-phenyl], 7.89 [2H, d, 8-naphthyl (see Chapter 3)], 7.15 [2H, d, J = 8.4 Hz, naphthyl], 7.89 [2H, d, J = 8.0 Hz, *meso*-(5)-3,5-phenyl], 7.73 [12H, m, *meso*-(10,15,20)-3,4,5-phenyl], 7.22 [2H, d, J= 8.4 Hz, 1-naphthyl], 7.09-6.99 [6H, m, 4,5,8-naphthyl], 6.96 [2H, s, 3-naphthyl], 6.74 [2H, t, J = 8.2 Hz, 6-naphthyl], 6.26 [2H, d, J = 8.1 Hz, 7-naphthyl], -2.84 [2H, s, NH]; λ_{max}(CH_2Cl_2)/nm, (ε, L. mol^{-1}. cm^{-1}) 222(5093), 254(5093), 283(33658), 374(23014), 418(217122), 515(18843), 548(8918), 589(8127), 646(6257); MS (FAB), $[M+H]^+$ *m/z* 955; Found: C, 83.0; H, 4.7; N, 5.4; calculated for $C_{66}H_{42}N_4O_4$: C, 83.0; H, 4.4; N, 5.9%.

10.3 5-(2-[2-oxycarbonylnaphthalene]phenyl)-10,15,20-*tris*-phenyl-porphyrin (7)

Preparation of this porphyrin was made by method (b) described in Section 7.1, using 5-(2-hydroxyphenyl)-10,15,20-*tris*-phenylporphyrin (70 mg; 1.11 x 10^{-4} moles) to gave 60 mg of the required compound (69% yield); δ_H($CDCl_3$; 300MHz; Me_4Si), 8.97 [2H, d, J = 4.8 Hz, β-pyrrolic], 8.85 [2H, d, J = 4.9 Hz, β-pyrrolic], 8.79 [4H, m, β-pyrrolic], 8.27 [1H, d, J = 7.6 Hz, *meso*-(5)-3-phenyl], 8.19 [6H, m, *meso*-(10,15,20)-2,6-phenyl], 8.05 [1H, d, J = 5.9 Hz, *meso*-(5)-6-phenyl], 7.89 [2H, m, *meso*-(5)-4,5-phenyl], 7.75 [12H, m, *meso*-(10,15,20)-3,4,5-phenyl], 7.24 [1H, s, 1-naphthyl], 7.10-6.98 [4H, m, 3,4,5,6-naphthyl], 6.80 [1H, t, J= 6.9 Hz, 7-naphthyl], 6.40 [1H, d, J = 8.1 Hz, 8-naphthyl], -2.81 [2H, s, NH]; λ_{max}(CH_2Cl_2)/nm, (ε, L. mol^{-1}. cm^{-1}) 272(18085), 284(18995), 294(16954), 370(19309), 418(321331), 514(14207), 548(5808), 590(4490), 646(3116); MS (FAB), $[M+H]^+$, *m/z* 785; Found: C, 83.3; H, 4.5; N, 6.8; calculated for $C_{55}H_{36}N_4O_2$: C, 84.2; H, 4.6; N, 6.8%.

11. Preparation of 5-(2-[2-oxycarbonylnaphthalene]phenyl)-10,15,20-*tris*-heptylporphyrins

11.1 5-(2,6-*bis*-[2-oxycarbonylnaphthalene]phenyl)-10,15,20-*tris*-heptyl-porphyrin (6)

This porphyrin was made by method (b), described in Section 7.1, using freshly prepared 5-(2,6-dihydroxyphenyl)-10,15,20-*tris*-heptylporphyrin (20 mg; 2.68 x 10^{-5} moles) to yield 12 mg of the required compound (44% yield); δ_H($CHCl_3$; 300MHz; Me_4Si), 9.4 [2H, d, J = 4.9Hz, β-pyrrolic], 9.38 [4H, m, β-pyrrolic], 9.05 [2H, d, J = 4.0Hz, β-pyrrolic], 8.03 [1H, t, J = 7.8Hz], 7.89 [2H, d, J = 8.4Hz, 3,5-phenyl], 7.26 [2H, d, J = 9.0Hz, 3,3'-naphthyl], 7.15 [2H, d, naphthyl], 7.05-6.86 [8H, m, naphthyl], 6.63 [2H, m, 7,7'-naphthyl], 6.05 [2H, dd, 8,8'-naphthyl], 4.93 [2H, m, *meso*-(15)-α-CH_2], 4.83 [4H, m, *meso*-(10,20)-α-CH_2], 2.49 [2H, m, *meso*-(15)-β-CH_2], 2.34 [4H, m, *meso*-(10,20)-β-CH_2], 1.75 [6H, m, γ-CH_2], 1.50 [12H, m, δ– + ε-CH_2], 1.24 [6H, m, ζ-CH_2], 0.91 [9H, m, -CH_3], -2.66 [2H, s, NH]; λ_{max}(CH_2Cl_2)/nm, (ε, L. mol^{-1}. cm^{-1}) 274(15680), 284(15680), 294(15680), 326(11892), 342(14050), 370(15041), 418(256817), 486(2889), 518(10837), 554(6809), 596(3788), 656(4148); MS (FAB), $[M+H]^+$, *m/z* 1022; Found: C, 80.8; H, 7.0; N, 5.4; calculated for $C_{69}H_{72}N_4O_4$: C, 81.1; H, 7.1; N, 5.5%.

11.2 5-(2-[2-oxycarbonylnaphthalene]phenyl)-10,15,20-*tris*-heptyl-porphyrin (5)

Preparation of this porphyrin was made by method (b) described in Section 7.1, using 5-(2-hydroxyphenyl)-10,15,20-*tris*-heptylporphyrin (30 mg; 4.30 x 10^{-5} moles) to yield 15 mg of the required compound (40% yield); $\delta_H(CHCl_3$; 300MHz; Me_4Si), 9.49 [2H, d, J = 4.8Hz β-pyrrolic], 9.44 [2H, d, J = 4.7Hz β-pyrrolic], 8.91 [2H, d, J = 4.8Hz β-pyrrolic], 8.21 [1H, d, 3-phenyl], 7.87 [2H, m, 4,5-phenyl], 7.69 [1H, t, J = 7.1Hz, 6-phenyl], 7.18 [1H, d, J = 8.1Hz, 3-naphthyl], 7.03 [2H, m, 4,6-naphthyl], 7.01 [1H, s, 1-naphthyl], 6.95 [1H, d, J = 8.9Hz, 5-naphthyl], 6.69 [1H, t, J = 7.4Hz, 7-naphthyl], 6.26 [1H, d, J = 8.4Hz, 8-naphthyl], 4.95 [2H, t, J = 8.5Hz, *meso*-(15)-α-CH_2], 4.87 [4H, t, J = 8.0Hz, *meso*-(10,20)-α-CH_2], 2.51 [2H, t, *meso*-(15)-β-CH_2], 2.42 [4H, t, J = 7.4Hz, *meso*-(10,20)-β-CH_2], 1.77 [6H, m, γ-CH_2], 1.50 [12H, m, δ– + ε-CH_2], 1.33 [6H, m, ζ-CH_2], 0.90 [9H, m, -CH_3], -2.66 [2H, s, NH]; $\lambda_{max}(CH_2Cl_2)$/nm, (ε, L. mol^{-1}. cm^{-1}) 418(404197), 486(3054), 514(9269), 554(7264), 596(4066), 656(4879); MS (FAB), $[M+H]^+$, *m/z* 851; Found: C, 81.1; H, 7.9; N, 6.2; calculated for $C_{58}H_{66}N_4O_2$: C, 81.8; H, 7.8; N, 6.6%.

12. Preparation of 5-[9-oxycarbonylanthracene]phenyl-10,15,20-*tris*-phenyl-porphyrins

12.1 5-(2,6-*bis*-[9-oxycarbonylanthracene]phenyl)-10,15,20-*tris*-phenyl-porphyrin (13)

This porphyrin was made by method (b) described in Section 7.1, using 5-(2,6-dihydroxyphenyl)-10,15,20-*tris*-phenylporphyrin (30 mg; 2.92 x 10^{-5} moles) and 9-anthracene acid chloride (prepared by overnight reflux of 9-anthracene carboxilic acid (1.5g; 6.8 x 10^{-3} moles) in 30 mL of thionyl chloride, followed by solvent evaporation and driyng under high vaccum) to yield 5 mg of the required compound (16% yield); $\delta_H(CHCl_3$; 200MHz; Me_4Si), 9.12 [2H, d, J= 5.0Hz, β-pyrrolic], 8.90 [2H, d, J= 4.0 Hz, β-pyrrolic], 8.85 [2H, d, J= 4.5 Hz, β-pyrrolic], 8.78 [2H, d, J= 4.4Hz, β-pyrrolic], 8.00-8.15 [7H, m, *meso*-(10,15,20)-2,6-phenyl], 7.67 [10H, m, *meso*-(10,15,20)-3,4,5-phenyl], 7.27 [2H, d, J = 4.1Hz, 1,8-anthranyl], 6.63 [2H, t, J = 6.6Hz, 2,7-anthranyl], 6.09 [2H, d, J = 8.8Hz, 3,6-anthranyl], 5.12 [2H, t, J = 7.8Hz, 4,5-anthranyl], -2.70 [2H, s, NH]; MS (FAB), M^+, *m/z* 1124,[10] $\lambda_{max}(CH_2Cl_2)$/nm, (relative %) 340(14), 358(19), 376(25), 400(47), 418(100), 512(10), 546(5), 586(4), 642(3); no satisfatory CHN analysis was obtained for this compound.[10]

12.2 5-(2-[9-oxycarbonylanthracene]phenyl)-10,15,20-*tris*-phenylporphyrin (12)

This porphyrin was made by method (b) described in the Section 7.1, using 5-(2-hydroxyphenyl)-10,15,20 -*tris*-phenylporphyrin (10 mg; 1.58 x 10^{-5} moles) to gave 4.1 mg of the required compound (29% yield); $\delta_H(CHCl_3$; 200MHz; $Me_4Si)$, 8.90 [2H, d, J= 5.5Hz, β-pyrrolic], 8.83 [4H, m, β-pyrrolic], 8.76 [2H, d, J= 4.4Hz, β-pyrrolic], 8.27 [1H, d, J = 6.8 Hz, *meso*-(5)-3-phenyl], 8.05-8.20 [7H, m, *meso*-(10,15,20)-2,6-phenyl + *meso*-(5)-phenyl], 7.69 [10H, m, *meso*-(10,15,20)-3,4,5-phenyl], 7.27 [2H, d, J = 4.6Hz, 1,8-anthranyl], 6.60 [2H, t, J = 6.6Hz, 2,7-anthranyl], 6.08 [2H, d, J = 8.8Hz, 3,6-anthranyl], 5.10 [2H, t, J = 8.8Hz, 4,5-anthranyl],-2.56 [2H, s, NH]; $\lambda_{max}(CH_2Cl_2)$/nm, (ε, L. mol^{-1}. cm^{-1}) 332(9046); 350(13798), 366(17670), 418(162452), 446(5221), 514(9251), 546(3735), 590(3005), 642(1958); MS (FAB), M^+, *m/z* 835; Found: C, 83.0; H, 4.8; N, 6.4; calculated for $C_{59}H_{48}N_4O_2$: C, 83.9; H, 5.7; N, 6.6%.

13. Preparation of 5-[9-oxycarbonylanthracene]phenyl-10,15,20-*tris*-heptyl-porphyrins

13.1. 5-(2,6-*bis*-[9-oxycarbonylanthracene]phenyl)-10,15,20-*tris*-heptyl-porphyrin (11)

This porphyrin was made by method method (b) described in the Section 7.1, using freshly prepared 5-(2,6-dihydroxyphenyl)-10,15,20-*tris*-heptylporphyrin (20 mg; 2.68 x 10^{-5} moles) to yield 4 mg of the compound (13% yield); $\delta_H(CHCl_3$; 200MHz; $Me_4Si)$, a very weak spetrum was obtained and no assignements could be made; MS (FAB), $[M+H]^+$, *m/z* 1124.

13.2 5-(2-[9-oxycarbonylanthracene]phenyl)-10,15,20-*tris*-heptylporphyrin (10)

This porphyrin was made by method (b) described in Section 7.1, using 5-(2-hydroxyphenyl)-10,15,20-*tris*-heptylporphyrin (21 mg; 2.63 x 10^{-5} moles) to yield 12 mg of the required compound (52 % yield); $\delta_H(CHCl_3$; 300MHz; $Me_4Si)$, 9.54 [2H, d, J = 4.0Hz β-pyrrolic], 9.50 [2H, d, J = 4.1Hz β-pyrrolic], 9.32 [2H, d, J = 4.1Hz β-pyrrolic], 8.90 [2H, d, J = 4.1Hz β-pyrrolic], 8.25 [1H, d, J = 7.7 Hz, 3-phenyl], 7.98 [1H, m, 4-phenyl], 7.87 [1H, d, J = 6.5Hz, 6-phenyl], 7.84 [1H, s, 10-anthranyl (see Chapter 3)], 7.80 [1H, t, J = 7.3Hz, 5-phenyl], 7.27 [2H, d, J = 9.3Hz, 1,8-anthranyl], 6.44 [2H, t, J = 8.0Hz, 2,7-anthranyl], 5.01 [4H, m, 4,5-

anthranyl + *meso*-(15)-α-CH2 (see Chapter 3)], 4.88 [4H, t, J = 7.7Hz, *meso*-(10,20)-α-CH_2], 2.60 [2H, m, (15)-β-CH_2], 2.45 [4H, m, *meso*-(10,20)-β-CH_2], 1.85 [2H, t, J = 6.7Hz, (15)-γ-CH_2], 1.74 [4H, t, J = 7.4Hz, (10,20)-γ-CH_2]; 1.51, 1.40, 1.29 [18H, m, δ– + ε– + ζ-CH_2], 0.93 [3H, t, J = 7.7Hz, -CH_3], 0.93 [3H, t, J = 7.7Hz, *meso*-(15)-CH_3], 0.86 [6H, t, J = 6.7Hz, *meso*-(10,20)-CH_3], -2.48 [2H, s, NH]; $\lambda_{max}(CH_2Cl_2)$/nm, (ε, L. mol^{-1}. cm^{-1}) 308(7611), 346(12017), 398(17424), 418(235382), 484(1602), 518(9515), 552(5094), 596(2987); MS (FAB), $[M+H]^+$, *m/z* 902; Found: C, 86.5 ; H, 7.9 ; N, 7.9; calculated for $C_{62}H_{68}N_4O_2$: C, 82.6; H, 7.6; N, 6.2%.

14. Preparation of metal complexes of porphyrins substituted with aromatic rings (1-13)

In the following sections are presented analytical data relative to the iron complexes of porphyrins (**1-13**). Very small quantities of these compounds were available, frequently in the range of 3-6 mg. This sometimes led to doing only peroxidase-like activity assays instead of expending the material on elemental analysis. For the same reason, the study of peroxidase-like activity for these complexes was restricted almost exclusively to the use of iron as central metal. In the cases, in which larger quantities of porphyrin were available, manganese complexes were also prepared for comparison with the iron complexes.

When attempts were made to metallate the substituted porphyrins (**1-13**) under the conditions used to prepare other metallated porphyrins (Section 3.2 of this Chapter 2) it was clear that this led considerable hydrolysis of the ester linkage. For this reason, a new metallation method was invented, using mild conditions to prevent ester hydrolysis (see below).

14.1. A general method for the metallation of substituted porphyrins (1-13)

To a 50 mL flask fitted with a rubber septum and a magnetic stirrer, was added a porphyrin solution in chloroform (usually 5 mg in 20 mL) and nitrogen was fluxed through the solution for 5 min. via a syringe needle. In a separate 50 mL vessel, methanol (15 mL) was flushed with nitrogen for 15 min. After this, the methanol was saturated with ferrous acetate ($Fe(AcO)_2$; 100 mg) always under nitrogen. Through a syringe, 2 mL of this solution were taken and placed into the first flask containing the porphyrin and the whole was then heated in an oil bath to 50-60°C. The solution was kept at this temperature under nitrogen for 18 h. After this time, all the solvent was evaporated off and the orange ferrous complex was purified on a silica-gel column (15 x 2 cm), using $CHCl_3$ as eluent. The eluted porphyrin still in the eluant solvent was left open to air so as to oxidatively convert the Fe(II) complex to its ferric form (usually dark-brown). This complex was further purified by recrystalisation from CH_2Cl_2/MeOH.

15. Iron complexes of 5-(2-oxycarbonyltoluene)phenyl substituted porphyrins

15.1. Iron(III) 5-(2,6-*bis*-(2-oxycarbonyltoluene)phenyl)-10,15,20-*tris*-phenylporphyrin chloride

This metalloporphyrin was made by the method described just above, from 5-(2,6-*bis*-(2-oxycarbonyltoluene)phenyl)-10,15,20-*tris*-phenylporphyrin (10 mg; 1.13 x 10^{-5} moles) to yield 4 mg of the required compound (36% yield); λ_{max}(MeOH)/nm (ε, L. mol^{-1}. cm^{-1}) 246(43062), 336(25275), 414(204749), 488(9964), 598(4836); MS (FAB), M^+, *m/z* 936.

15.2. Iron(III) 5-(2-[4-oxycarbonyltoluene]phenyl)-10,15,20-*tris*-phenyl-porphyrin chloride

This metalloporphyrin was made by method described in Section 14.1 above, from 5-(2-[4-oxycarbonyltoluene]phenyl)-10,15,20-*tris*-phenylporphyrin (10 mg; 1.34 x 10^{-5} moles) to yield 5 mg of the required complex (45% yield); λ_{max}(MeOH)/nm (ε, L. mol^{-1}. cm^{-1}) 244(58646), 336(20118), 412(210133); MS (FAB), $[M+H]^+$, *m/z* 802.

15.3. Iron(III) 5-(2,6-*bis*-[4-oxycarbonyltoluene]phenyl)-10,15,20-*tris*-heptyl-porphyrin chloride

This metalloporphyrin was made by method described in Section 14.1 above, from 5-(2,6-*bis*-[4-oxycarbonyltoluene]phenyl)-10,15,20-*tris*-heptyl-porphyrin (10 mg; 1.35 x 10^{-5} moles) to yield 5 mg of the required compound (45% yield); λ_{max}(MeOH)/nm (ε, L. mol^{-1}. cm^{-1}) 244(38321), 324(17370), 394(87028), 414(80133),534(7342); MS (FAB), M^+, *m/z* 1002.

15.4. Iron(III) 5-(2-[4-oxycarbonyltoluene]phenyl)-10,15,20-*tris*-heptyl-porphyrin chloride

This metalloporphyrin was made by method described in Section 14.1 above, from 5-(2-[4-oxycarbonyltoluene]phenyl)-10,15,20-*tris*-heptylporphyrin (10 mg; 1.23 x 10^{-5} moles) to yield 7 mg of the required compound (63% yield); λ_{max}(MeOH)/nm (ε, L. mol^{-1}. cm^{-1}) 244(36148), 334(27981), 416(111572), 536(8338), 648(3816); MS (FAB), M^+, *m/z* 904.

16. Metal complexes of 5-[2-oxycarbonylnaphthalene]phenyl substituted porphyrins

16.1. Iron(III) 5-(2,4,6-*tris*-[2-oxycarbonylnaphthalene]phenyl)-10,15,20-*tris*-phenylporphyrin chloride

This metalloporphyrin was made by method described in Section 14.1, from 5-(2,4,6-*tris*-[2-oxycarbonylnaphthalene]phenyl)-10,15,20-*tris*-phenylporphyrin (10 mg; 8.90 x 10^{-6} moles) to yield 6 mg of the required complex (55% yield); λ_{max}(MeOH)/nm (ε, L. mol^{-1}. cm^{-1}) 242(30970), 272(88054), 282(97163), 294(81981), 336(77123), 416(193719), 580(18218); MS (FAB), M^+, *m/z* 1179.

16.2 Iron(III) 5-(2,6-*bis*-[2-oxycarbonylnaphthalene]phenyl)-10,15,20-*tris*-phenylporphyrin chloride

Preparation of this complex was made by the method described in Section 14.1, from 5-(2,6-*bis*-[2-oxycarbonylnaphthalene]phenyl)-10,15,20-*tris*-phenylporphyrin (15 mg; 1.57 x 10^{-5} moles) to yield 14 mg of the required complex (87% yield); λ_{max}(MeOH)/nm (ε, L. mol^{-1}. cm^{-1}) 242(5374), 272(25556), 284(26798), 292(24315), 336(24242), 416(99159), 532(6061), MS (FAB), M^+, *m/z* 1008.

16.3. Manganese(III) 5-(2,6-*bis*-[2-oxycarbonylnaphthalene]phenyl)-10,15,20-*tris*-phenylporphyrin chloride

This metalloporphyrin was made by method described in Section 14.1, from 5-(2,6-*bis*-[2-oxycarbonylnaphthalene]phenyl)-10,15,20-*tris*-phenylporphyrin (15 mg; 1.57 x 10^{-5} moles) to yield 13 mg of the required compound (80% yield); λ_{max}(MeOH)/nm (ε, L. mol^{-1}. cm^{-1}) 282(75654), 380(78263), 400(80871), 422(65219), 468(142960), 558(31305); MS (FAB), M^+, *m/z* 1007.

16.4. Iron(III) 5-(2-[2-oxycarbonylnaphthalene]phenyl)-10,15,20-*tris*-phenylporphyrin chloride

This metalloporphyrin was made by method described in Section 14.1, from 5-(2-[2-oxycarbonylnaphthalene]phenyl)-10,15,20-*tris*-phenylporphyrin (10 mg; 1.27 x 10^{-5} moles) to yield 7 mg of the required complex (63% yield);

λ_{max}(MeOH)/nm (ε, L. mol^{-1}. cm^{-1}) 226(43708), 242(63611), 276(15894), 282(26197), 336(15894), 414(101001), 570(6070); MS (FAB), M$^+$, *m/z* 838.

16.5. Manganese(III) 5-(2-[2-oxycarbonylnaphthalene]phenyl)-10,15,20-*tris*-phenylporphyrin chloride

This metalloporphyrin was made by method described in Section 14.1, from 5-(2-[2-oxycarbonylnaphthalene]phenyl)-10,15,20-*tris*-phenylporphyrin (10 mg; 1.27 x 10^{-5} moles) to yield 5 mg of the required complex (45% yield); λ_{max}(MeOH)/nm (ε, L. mol^{-1}. cm^{-1}) 237(92346), 282(26187), 292(24655), 378(52227), 399(52811), 440(22102), 467(98109), 517(4231), 564(11306), 596(7513), 687(948); MS (FAB), M$^+$, *m/z* 837.

16.6. Iron(III) 5-(2,6-*bis*-[2-oxycarbonylnaphthalene]phenyl)-10,15,20-*tris*-heptylporphyrin chloride

This metalloporphyrin was made by method described in Section 14.1, using 5-(2,6-*bis*-[2-oxycarbonylnaphthalene]phenyl)-10,15,20-*tris*-heptyl-porphyrin (21 mg; 2.06 x 10^{-5} moles) to yield 9 mg of the required complex (40% yield); λ_{max}(MeOH)/nm (ε, L. mol^{-1}. cm^{-1}) 272(21478), 284(23695), 294(20246), 322(15813), 338(15074), 416(84915), 532(6946); MS (FAB), M$^+$, *m/z* 1077.

16.7. Manganese(III) 5-(2,6-*bis*-[2-oxycarbonylnaphthalene]phenyl)-10,15,20-*tris*-heptylporphyrin chloride

This metalloporphyrin was made by method described in Section 14.1, from 5-(2,6-*bis*-[2-oxycarbonylnaphthalene]phenyl)-10,15,20-*tris*-heptylporphyrin (5 mg; 4.9 x 10^{-6} moles) to yield 4.8 mg of the complex (82% yield); λ_{max}(MeOH)/nm (ε, L. mol^{-1}. cm^{-1}) 270(37753), 284(40318), 294(35508), 340(33104), 380(42722), 402(41921), 422(38554), 470(86967), 568(11863), 608(11141); MS (FAB), M$^+$, *m/z* 1076.

16.8 Iron(III) 5-(2-[2-oxycarbonylnaphthalene]phenyl)-10,15,20-*tris*-heptyl-porphyrin chloride

This metalloporphyrin was made by method described in Section 14.1, from 5-(2-[2-oxycarbonylnaphthalene]phenyl)-10,15,20-*tris*-heptylporphyrin (20 mg;

2.39 x 10^{-5} moles) to yield 21 mg of the required complex (93% yield); λ_{max}(MeOH)/nm (ε, L. mol^{-1}. cm^{-1}) 238(112253), 270(20084), 282(20994), 292(19902), 328(19781), 416(96987), 532(7888); MS (FAB), M^+, *m/z* 904.

16.9 Manganese(III) 5-(2-[2-oxycarbonylnaphthalene]phenyl)-10,15,20-*tris*-heptylporphyrin chloride

This metalloporphyrin was made by method described in Section 14.1, from 5-(2-[2-oxycarbonylnaphthalene]phenyl)-10,15,20-*tris*-heptylporphyrin (20 mg; 2.35 x 10^{-5} moles) to yield 15 mg of the required complex (68% yield); λ_{max}(MeOH)/nm (ε, L. mol^{-1}. cm^{-1}) 281(22820), 341(26350), 379(40968), 401(39107), 443(20067), 470(63927), 526(5366), 574(8199), 610(7880); MS (FAB), M^+, *m/z* 903.

17. Metal complexes of 5-[9-oxycarbonylanthracene]phenyl substituted porphyrins

17.1. Iron(III) 5-(2,6-*bis*-[9-oxycarbonylanthracene]phenyl)-10,15,20-*tris*-phenylporphyrin chloride

This metalloporphyrin was made by method described in Section 14.1 above, from 5-(2,6-*bis*-[9-oxycarbonylanthracene]phenyl)-10,15,20-*tris*-phenylporphyrin (5 mg; 4.98 x 10^{-6} moles) to yield 2 mg of the required compound (36% yield); λ_{max}(MeOH)/nm (ε, L. mol^{-1}. cm^{-1}) 254, 336, 414 (48567), 548, 614; MS (FAB), M^+, *m/z* 1111; weak spectrum, showing some unknow contaminant peaks.

17.2. Iron(III) 5-(2-[9-oxycarbonylanthracene]phenyl)-10,15,20-*tris*-phenylporphyrin chloride

This metalloporphyrin was made by method described in Section 14.1 above, from 5-(2-[9-oxycarbonylanthracene]phenyl)-10,15,20-*tris*-phenylporphyrin (5 mg; 5.92 x 10^{-5} moles) to yield 3 mg of the required compound (54% yield); λ_{max}(MeOH)/nm (ε, L. mol^{1}. cm^{-1}) 254(36388), 336(16540), 414(41085), 548(16540), 614(1852); MS (FAB), M^+, *m/z* 888.

17.3. Iron(III) 5-(2,6-*bis*-[9-oxycarbonylanthracene]phenyl)-10,15,20-*tris*-heptylporphyrin chloride

This metalloporphyrin was made by method described in Section 14.1 above, from 5-(2,6-*bis*-[9-oxycarbonylanthracene]phenyl)-10,15,20-*tris*-heptyl-porphyrin (9 mg; 1.0 x 10^{-4} moles) to yield 9 mg of the required complex (89% yield); λ_{max}(MeOH)/nm (ε, L. mol^{-1}. cm^{-1}) 254(91143), 334(24267), 416(66962), 504(5952), 634(2289); MS (FAB), M^+, *m/z* 954.

V. Chapter 4 experimental details

1. Measurement of peroxidase-like activity of metal complexes of porphyrins (1-13)

The peroxidase-like activity assay of the systems of metalloporphyrins containing covalently attached aromatic rings was examined using 2,2'-azino-*bis*(3-ethylbenzthiazoline-6-sulfonic acid) (ABTS) as substrate and H_2O_2 as the oxygen donor, under conditions similar to those described for water soluble metalloporphyrins (Section IV. 10.3, in this Chapter), with exception that the solvent was, in this case, a "buffered" methanolic solution (See Chapter 4, Section II 1.5).

1.1. General method for the determination of the peroxidase-like activity with ABTS

1.1.1. Preparation of a "buffered" methanolic solution

To a 400 mL beaker with magnetic stirring was added pure methanol (250 mL) and and anhydrous sodium acetate (250 mg). A glass electrode from a previously calibrated pH meter was immersed in the solution. The salt dissolved on stirring and then glacial acetic acid was added dropwise until the solution reached a pH of 6.

1.1.2. Peroxidase-like activity assay

Metalloporphyrin solutions were made by dissolving the required metallo-porphyrin (2-3 mg) in methanol and diluting this solution 1:10 with the "buffered" methanol (see Section 1.1.1 just above). The final concentrations of metalloporphyrins in these solutions were usually in the range of 3-27 x 10^{-6} $mol.L^{-1}$. In each case, more precisely determined value was obtained by visible spectrophotometry at the Soret wavelength. The peroxidase activity was measured with ABTS as described in Section III. 10.1.

2. General method for the determination of the peroxidase-like activity with guaiacol

Metalloporphyrin solutions were made in "buffered" methanol as in Section 1.1.2. just above. Into a glass cuvette (10mm path length) were pipetted solutions of metalloporphyrin (2 mL buffered solution) and guaiacol (200μL of a 5.0 x 10^{-3} mol.L^{-1} solution). The solution was homogenized by stirring it with a pipette. At zero time, H_2O_2 (200μL of the 10^{-2} mol.L^{-1} stock solution) was added to the solution. The reaction was monitored by measuring the increase in absorbance for the reaction products, which are guaiacol dimers and oligomers, at 470 nm (ε = 2,6 x 10^4 mol^{-1}.L.cm^{-1}).[8] Kinetic parameters were determined by plotting the values of the reaction product concentration against time. A linear curve fitting procedure was used and the observed slope value was divided by the molar metalloporphyrin content in solution, as before.

3. General method for the determination of the monooxygenase-like activity with cyclooctene

The system used for the determination of the monooxygenase-like activity using metalloporphyrins with covalently linked aromatic rings was realised by simply exchanging for cyclooctene guaiacol in the procedure for examining peroxidase-like for guaiacol (Section 2). The course of reaction was analysed by injection, at a regular intervals, sample aliquots of the reaction solution into a GC system. This last was set isothermically at 100°C. Cyclooctene epoxide formation was monitored, using an authentic standard. The concentration of the epoxide was plotted against time to determine the initial rate of formation of cyclooctene epoxide. This initial rate was divided by the molar amount of metalloporphyrin present in the solution, as determined by visible spectrophotometry at the Soret wavelength.

VI. Chapter 5 experimental details

1. Determination of the isolated yield of formation of porphyrin in the Rothemund/Adler synthesis of TDCPP in the presence of nitrobenzene

To a 100 mL double necked flask, equipped with reflux condenser and a rubber septum, was added a solution of nitrobenzene in glacial acetic acid (40 mL; 2.9 mol.L^{-1}) and 2,6-dichlorobenzaldehyde (0.88g; $5x10^{-3}$ moles). The mixture was set to reflux. Distilled pyrrole (0,34g; $5x10^{-3}$ moles) was then added at zero time. Every 3 min. (for 15 min.), small aliquots of the reaction medium were withdrawn through a 10 cm needle syringe so as to transfer the whole amount of solution for a small vessel. Using a 10μL syringe, 1μL of the solution was loaded into a silica TLC plate. The organic acid on the TLC plates was neutralized with ammonia vapour and then dried under a flow of nitrogen. Elution of the TLC plates was effected with $CHCl_3$ and these were dried after the end of a suitable period of elution. The TLC band corresponding to porphyrin was carefully scraped into a visible spectrometer cell and 3 mL of chloroform (previously neutralised by passsage through an alumina column) were added to the cell, the contents of which were mixed carefully. The absorbance of the solution at the Soret wavelength (418 nm) was recorded and the amount of porphyrin was calculated from its ε value.

2. Determination of kinetic parameters in the oxidative conversion of *tetrakis*(4-methoxyphenyl)porphyrinogen to porphyrin, in the presence of nitroarenes

2.1. Preparation of porphyrinogen

Method (a). *Tetrakis*(4-methoxyphenyl)porphyrinogen was prepared by reduction of the corresponding porphyrin.[12] *Tetrakis*(4-methoxyphenyl) porphyrin (0.5g; 6.81 x 10^{-4} moles) was dissolved in a mixture of glacial acetic acid (50 mL) and trifluoroacetic acid (2.5 mL) and transfered to a 50 mL flask. The solution was degassed by refluxing it under nitrogen. After cooling to room temperature; zinc dust (2.5 g; 3,8 x 10^{-1} moles) was added and the solution was stirred for 1 h. To determine when reaction was complete, visible spectra of aliquots were recorded until there were no longer any bands in the region 400-600 nm.

Method (b). CH_2Cl_2 (1 L; previously neutralised through a neutral alumina column) was placed in a flask (2 L) and degassed with nitrogen for 30 min. 2,6-dichlorobenzaldehyde (1.3g; 7.42 x 10^{-3} moles) was added, followed by distilled pyrrole (0.7g; 1.0 x 10^{-2} moles) and BF_3. Et_2O (45%; 118 μL). The reaction mixture was left under nitrogen for 6 h. After this time, NEt_3 (300 μL) was added to neutralise the Lewis acid. For reactions that required porphyrinogen dissolved in acetic acid, addition of 50 mL of acetic acid, previously degassed with nitrogen, was made at this stage. Evaporation of all CH_2Cl_2 under nitrogen resulted in a porphyrinogen solution in the acetic acid or in a residue of solid porphyrinogen.

2.2. Oxidation of *tetrakis*(4-methoxyphenyl)porphyrinogen

2.2.1. Under anaerobic conditions

In each of five 5 cm diameter test tubes, each equipped with a small magnetic stirrer, was placed one of the following nitroarenes: nitrobenzene (**1**), 1,4-dinitrobenzene (**2**), 4-nitroaniline (**3**), 4-nitrobenzoic acid (**4**), 4-nitroanisole (**5**) (1.5 x 10^{-3} moles each). In addition, another "blank" tube was used in which there was no nitroarene. The tubes were closed with a rubber septa and nitrogen was passed through each tube for 5 min. by the use of inlet and outlet syringe needles. After withdrawing the needles, the tubes were heated to 90°C in a bath oil, under nitrogen. A filtered (Teflon; 0.45μm) porphyrinogen solution (50 mL) was prepared as described in Section 2.1; method (a). To each tube was added porphyrinogen solution (10 mL at 40-50°C), through a syringe needle (at all times avoiding contact with air). Stirring was started at zero time. Using a syringe, 25 μL of each solution were removed and dissolved in $CHCl_3$ (3 mL; containing 13 mL of NEt_3 per litre of $CHCl_3$). The visible spectra were recorded and the absorbances were used to calculate the concentrations of porphyrin and porphodimethene from known ε values.[11-13]

2.2.2. Under aerobic conditions

The procedure is the same as that described in the Section 2.2.1, except that the five test tubes were always open to air.

3. Oxidation of *tetrakis*(2,6-dichlorophenyl)porphyrinogen

To a 100 mL double necked flask, equipped with reflux condenser was added glacial acetic acid (40 mL) and the required amount of one of the following nitroarenes: nitrobenzene (**1**), 1,4-dinitrobenzene (**2**), 4-nitroaniline (**3**), 4-nitrobenzoic acid (**4**) so as to obtain solutions with a concentration of 0.15 mol.L^{-1} (in 50 mL). The solutions were warmed to 90°C. A blank flask was prepared containing no nitroarenes. Porphyrinogen solution (10 mL; prepared by method (b) in acetic acid medium) was added and the whole was allowed to react for 4 h. After this time, each solution was cooled and the acetic acid was removed by rotary evaporation. When using nitrobenzene, this was removed by steam distillation. The black residue from each reaction was dissolved in a minimum of chloroform and run on an alumina column prepared (activity 0; 15 x 3 cm). The porphyrinic products were collected by elution with chloroform (the presence of porphyrin was checked by the Soret band). The solvent was evaporated from the eluate and the residual porphyrin was dried under vacuum and weighed. The determination of the proportions of chlorin and porphyrin was determined by ^{1}H NMR integration of the -NH pyrrolic protons near δ = -2. Average values of three determinations were used.

4. Detection of hydrogen peroxide during the oxidation of *tetrakis*-(2,6-dichlorophenyl)porphyrinogen

A porphyrinogen solution (10 mL; prepared by method (b) of Section 2.1, in 50 mL of dichloromethane) was placed in a 50 mL round flask fitted with a magnetic stirrer. The solvent was evaporated off under nitrogen atmosphere to leave a residue. Separately, two portions of acetic acid (10 mL), one containing 0.15 mol.L^{-1} of nitrobenzene, were warmed to 90°C. The acetic acid solutions were transfered to the flasks containing the solid porphyrinogen and stirring was started (zero time). The solid solubilized readily. At regular intervals, 10 μL samples of the reaction solution were taken and added to a fluorimeter cell filled with a luminol solution (3 mL; 100 μmol.L^{-1}) in *tris*(hydroxymethyl)methylamine buffer (0.1 mol.L^{-1}, pH = 8.6). To this solutionm was added a peroxidase solution (100μL; 1 mg/ mL) and the emitted fluorescent light was recorded in a fluorescence spectrophotometer.[14] Light emission was recorded until a maximum value was clearly definable. Previous calibration of the analytical method was done using a known aqueous H_2O_2 solution (20μmol.L^{-1}).

VII. Notes and References

1. J. M. T. B. Varejao, M.Sc. Thesis, Universidade de Coimbra, Coimbra, 1990; A. M. d'A. Rocha Gonsalves, Jorge M. T. B. Varejão and M. M. Pereira, *J. Het. Chem.*, 1991, **28**, 635 .

2. J. S. Lindsey, H. C. Hsu and I. C. Schreiman; *Tetrahedron Lett.*, 1986, **41**, 4969, J. S. Lindsey, I. C. Schreiman, H. C. Hsu, P. C. Kearney, and A. M. Marguerettaz; *J. Org. Chem.*, 1987, 52, 827; J. S. Lindsey and R. W. Wagner, *J. Org. Chem.*, 1989, **54**, 828.

3. Y. Le Bigot, M. Delmas and A. Gaset, *Synth. Comm.*, 1983, **13**, 177.

4. P. Hoffmann and B. Meunier, *New. J, Chem.* 1992, **16**, 559-561, H. Ledon, B. Mentzen, *Inorgan. Chim. Acta,* 1978, **31**, L393-L394.

5. B. White, P. Johnson and J. E. Guillet, *Polymer Internat.*, 1993, **30**, 401-405; G. J. Vancso, B. R. White and J. E. Guillet, *Europ. Polym. Journal*, 1993, **29**, 751-754; E. Sustar, M. Nowakowska & J. E. Guillet, *J. Photochem. PhotobioL. A Chemistry*, 1992, **63**, 357-365; M. Nowakowska & J. E. Guillet, *Chemistry in Britain*, 1991, **27**, 327-330; M. Nowakowska, B. White, and J. E. Guillet, *Macromolecules*, 1989, **22**, 2317-2324; M. Nowakowska, B. White, and J. E. Guillet, *Macromolecules*, 1988, **21**, 3430-3437;

6. P. A. Stocks, PhD Thesis, The University of Liverpool, 1995.

7. J. Putter and R. Becker in, *Methods of Enzymatic Analysis*, 1985, VoL. 3. Ed. H. U. Bergmeyer, VCH Publications, Weinheim, 286 *et seq.*

8. S. Ozachi and P. R. O. de Montelano, *J. Am. Chem. Soc.,* 1995, **117**, 7056-7064

9. M. Fieser in, *Fieser and Fieser's Reagents for Organic Synthesis*, 1982, VoL. 1, John Wiley and Sons, New York, pag. 480.

10. Despite ^{1}H NMR spectrum shown good agrement with the expected structure, both MS and CHN analysis gives unexpected results (expected mass at m/z = 1055). A possible explanation for this effect considers the stable inclusion of solvent molecules between porphyrin macrocycle and anthranyl ring.

11. A. D. Adler, L. Sklar, F. R. Longo, J. D. Finarelli and M. G. Finarelli; *J. Het. Chem.*, 1968, **5**, 669.

12. D. Dolphin, *J. Het. Chem.*, 1970, **7**, 275.

13. D. W. Thomas and A. E. Martell; *J. Am. Chem. Soc.*, 1956, **78**, 1335.

14. R. B. Herhert, F. G. Holliman and J. D. Kynnerley, *Tetrahedron Lett.*, 1968, **16**, 1907.